5-1989

Characterization of the Emission Properties of Thermographic Phosphors for Use in High Temperature Sensing Applications

Alan Ronald Bugos
University of Tennessee, Knoxville

To the Graduate Council:

I am submitting herewith a thesis written by Alan Ronald Bugos entitled "Characterization of the Emission Properties of Thermographic Phosphors for Use in High Temperature Sensing Applications." I have examined the final electronic copy of this thesis for form and content and recommend that it be accepted in partial fulfillment of the requirements for the degree of Master of Science, with a major in Electrical Engineering.

Michael J. Roberts, Major Professor

We have read this thesis and recommend its acceptance:

Stephen W. Allison, Graham W. Hoffman

Accepted for the Council:
Dixie L. Thompson

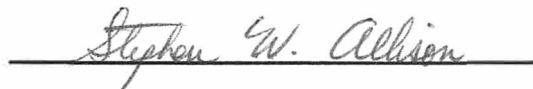Vice Provost and Dean of the Graduate School

(Original signatures are on file with official student records.)
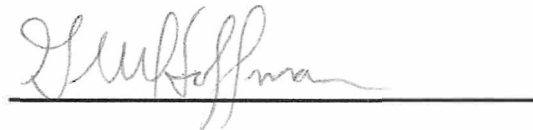
To the Graduate Council:

I am submitting herewith a thesis written by Alan Ronald Bugos entitled "Characterization of the Emission Properties of Thermographic Phosphors for Use in High Temperature Sensing Applications." I have examined the final copy of this thesis for form and content and recommend that it be accepted in partial fulfillment of the requirements for the degree of Master of Science, with a major in Electrical Engineering.

_____
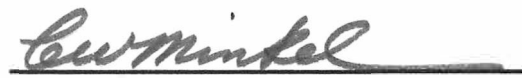
Michael J. Roberts, Major Professor

We have read this thesis
and recommend its acceptance:

_____

_____

Accepted by the Council:

_____

Vice Provost
and Dean of The Graduate School

CHARACTERIZATION OF THE EMISSION PROPERTIES OF THERMOGRAPHIC PHOSPHORS FOR USE IN HIGH TEMPERATURE SENSING APPLICATIONS

A Thesis
Presented for the
Master of Science
Degree
The University of Tennessee, Knoxville

Alan Ronald Bugos
May 1989

DEDICATION

This thesis is dedicated to my father whose engineering footsteps I follow.

ACKNOWLEDGEMENTS

ABSTRACT

Emission properties of fifteen different powder and crystalline thermographic phosphors have been characterized for potential use in high temperature sensing applications. Excitation and emission spectra of these rare-earth activated thermographic phosphors have been measured as a function of temperature using a special mini oven built inside of a fluorescence spectrophotometer. Several of the thermophosphors underwent decay lifetime analysis and were calibrated for use in high temperature measurements.

The excitation spectra taken from room temperature to approximately 400°C, reveal that the phosphors $Y_2O_3:Eu^{3+}$, $YVO_4:Eu^{3+}$, $Ba_3(PO_4)_2:Eu^{2+}$, $LaPO_4:Eu^{3+}$, $LuPO_4:Eu^{3+}$, $YPO_4:Eu^{3+}$, $YVO_4:Dy^{3+}$, $Y_2O_2S:Eu^{3+}$, and $Y_2O_2S:Tb^{3+}$ exhibit a significant temperature-dependent shift in their charge-transfer (C-T) absorption band. In addition, the peak position of the charge-transfer band in the europium-doped orthophosphate crystals is located at higher energies or deeper into the ultraviolet as the cation radius of the host crystal lattice decreases. The experimental results also show that the onset quenching temperature of the orthophosphate phosphors increases as a function of decreasing cation radius. The orthophosphate crystals $YPO_4:Eu^{3+}$, $LuPO_4:Eu^{3+}$, and $LuPO_4:Dy^{3+}$ were found to have high onset quenching temperatures when compared to those of the powder phosphors. Orthophosphate single-crystals may prove to be the phosphor of choice for high temperature measurements ranging from 700°C to 1400°C.

TABLE OF CONTENTS

LIST OF FIGURES

xi

LIST OF TABLES

CHAPTER I

AN INTRODUCTION TO THERMOGRAPHIC PHOSPHORS

Introduction

The word *luminescence* was introduced by E. Wiedemann around 1889 to describe light emission which is not caused solely by the temperature of the material. Luminescent sources may be classified according to the way the source material generates light. Two such classifications are *fluorescence* and *phosphorescence*, which depend solely on the lifetime in the excited state or radiative relaxation time. When the lifetime of the excited state is of the magnitude of approximately 10^{-8} second (or 10 nsec), the phenomenon is usually regarded as *fluorescence*. Therefore in the fluorescence case, the emission of light normally exists only as long as the exciting source is present. If the emission of light persists after the exciting source has been removed, the action is then termed *phosphorescence*. In phosphorescence, the radiative emission of light may continue for seconds, minutes, days, even months after the stimulating source has been removed. With the phosphorescence phenomenon, the electrons are generally stable and in an intermediate state, and gradually they return to their lower states. The processes that control the luminescent behavior are complex and vary widely depending on the type of materials used in the construction of the phosphor.[1]

Phosphors are luminescent compounds that emit either visible, infrared, or in some cases, ultraviolet light when subject to an exciting radiation source. Phosphors consist

of a basic material, such as an oxide, oxysulfide, vanadate, or phosphate, activated by a rare-earth element. Most of the inorganic phosphors used commercially have a crystalline structure and usually behave as insulators. Phosphor excitation can be accomplished in several ways. In cathodoluminescence, the phosphor is exposed to highly energetic electron bombardment in which electron energies may exceed ten kilovolts. This method is typically used in operation of a cathode ray tube. Injection luminescence occurs in semiconductor devices such as light emitting diodes. This technique causes high energy electrons and holes to be swept across a PN junction. When they recombine with majority carriers, photons are emitted. Finally photo- luminescence occurs when the phosphor electrons are optically excited or pumped to higher energy levels and upon relaxation by different processes emit photons.

Rare earth activated phosphors have been the subject of extensive research studies. The luminescent emission of the dopant impurities in a wide variety of host lattice environments has led to the development of phosphors with attractive properties for many varied applications. For example, phosphors have emission properties which make them useful in the development of solid state lasers. Researched and developed primarily for the lighting and display industries, phosphors have found use in hundreds of applications. Fluorescent lamps, cathode ray tubes for oscilloscopes, computers, and televisions, are some common phosphor applications. They are also used in criminology. Current research efforts are being placed on the commercial development of bright phosphors with small particle size for use in high-resolution cathode ray screens.

The fact that phosphor luminescence properties can be influenced by external stimuli such as temperature and pressure, to name a few, make phosphors the subject of study for potential use in temperature sensing applications.

High Temperature Thermophosphor Measurements

All phosphors are affected by temperature in some way. Certain phosphors which are exploited for their temperature characteristics are known as *thermophosphors* or *thermographic phosphors* and have potential application in high temperature luminescent measurement systems. Although thermographic phosphors have been studied for years, there is still much to be learned concerning the characteristics and quantum mechanical mechanisms which make them temperature-sensitive. As new phosphor materials and instrumentation are being developed, more facts are being uncovered regarding thermophosphor emission.

Recent efforts exploit the temperature dependence of fluorescence properties of various thermophosphors for temperature measurement applications on static and dynamic remote surfaces. Demonstrations in the past have shown that remote phosphor thermometry can be used to measure temperatures of gas centrifuge rotors, internal components of a jet turbine engine or rocket engine and other remote, rotating surfaces.[2,3,4] Other applications of the thermophosphor technique can be extended to rotating machinery such as motors and generators, internal combustion engines, and flywheels. The temperature of dynamic surfaces such as projectiles in flight, rail- and coil-gun components and explosive environments are prospective measurement applications. These temperature measurements are often performed optically without touching the surface of interest with any thing other than the thermophosphor. [5,6]

The technique is based on the fact that thermographic phosphors emit strong fluorescence under ultraviolet excitation and that the fluorescence decay lifetime has a logarithmic dependence with temperature. The temperature dependence arises from phonon-induced nonradiative relaxation processes which compete with radiative

processes. The fluorescence intensity and lifetime decreases abruptly with rising temperature at the onset of the temperature range where nonradiative processes begin to dominate. As a result of these lifetime decay measurements, thermophosphors are calibrated for use in temperature measuring systems. Several of the most common thermographic phosphors used in temperature measurements are Y_2O_3:Eu^{3+}, YVO_4:Eu^{3+}, La_2O_2S: Eu^{3+} and Y_2O_2S:Tb^{3+}. Figure 1-1 shows four phosphor calibration curves for three of the most reliable thermophosphors.
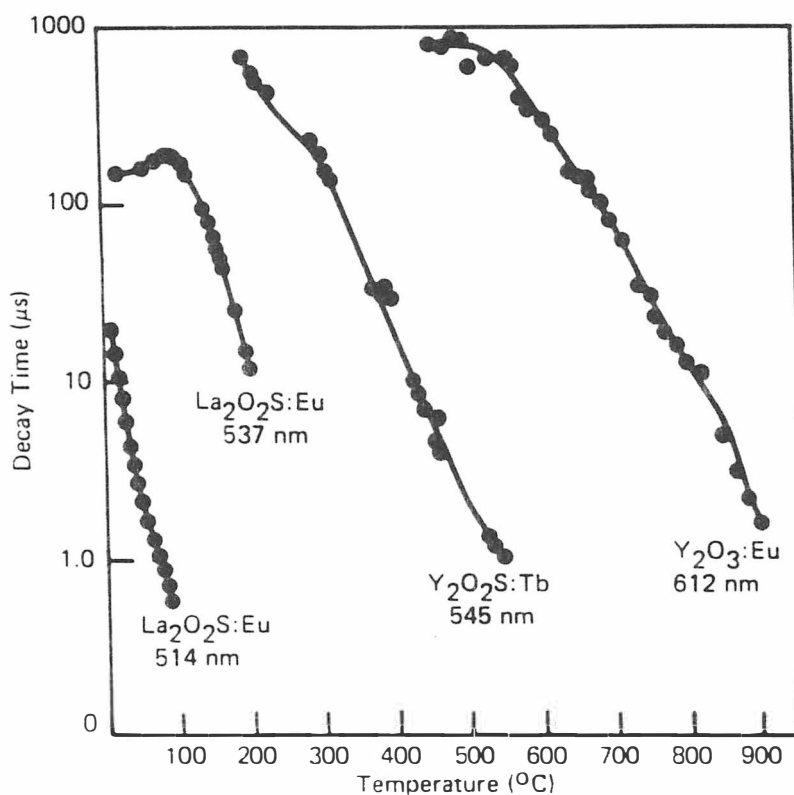
Figure 1-1. Calibration curves for several thermographic phosphors.

It is interesting to note that by selection of the proper emission lines, these three phosphors provide for a temperature measurement range from 0°C to 1200°C.

The advantages of high temperature measurements that incorporate thermographic phosphor techniques are many. Since the method can be performed remotely, it is useful in hazardous, noisy, and explosive environments. Optical temperature methods based on thermophosphors, are essentially immune to electrical interference and have a wide temperature sensing range. With current state-of-the-art electronic equipment, measurements can be made at a rate of 5000 times per second. Finally since phosphor thermometry is a non-contact method, it is useful in static or dynamic surfaces, confined areas or rotating surfaces where measurements with conventional temperature transducers such as thermocouples can not be made.

In other research efforts, it has been shown that certain charge-transfer states and spectral bands of most europium-doped phosphors shift as a function of temperature.[7,8,9,10,11] Fluorescent spectral line shift phenomena can also be exploited for use in high temperature measurements and can be used to support theories which explain the quantum electronic mechanisms of exponential decay lifetimes. Characteristics of thermophosphors are still being carefully investigated and new phosphor powders and crystals are undergoing testing and calibration for potential thermometry applications.

The focus of this thesis is twofold. First, the investigations of the luminescent spectra of thermophosphors measured as a function of temperature will be summarized and second, the results of an experimental study of the decay lifetimes of several temperature-dependent phosphors will be presented. It is believed that this effort specifically records for the first time, phosphor excitation spectra, measured as function of increasing temperature ranging from ambient to 450°C.

In the pages that follow, characteristics of the emission properties of thermographic

phosphors will be investigated in finer detail. Particular attention will be given to important information and observations that may have influence on or application to high temperature measurements.

Chapter II gives some details on the theory of thermographic phosphors and how the theory is related to the research efforts of this thesis. Spectroscopy of rare-earth activated phosphors will be discussed along with the origin of the fluorescence spectrum. Details of the temperature dependence of thermographic phosphors will be given. Particular attention will be given to the role of the charge-transfer state and its relationship to thermophosphor quantum mechanisms.

Chapter III is a very detailed discussion of the experimental configurations, methods and procedures used in the investigation of thermophosphor emission properties. Specific details are given about the acquisition of excitation and emission spectra for phosphors at room temperature and measurements of spectra as a function of increasing temperature. Equally important is a complete description of the methods and equipment used in obtaining lifetime decay data of the thermographic phosphors research. Details of the instrumental errors and random errors in data acquisition are given. The fluorescence spectrophotometer has been investigated for chart recorder reproducibility and xenon lamp spectra are presented along with a description of correcting obtained spectra for variations in lamp intensity. A new method of defining the onset quenching temperature from a phosphor lifetime calibration curve using a computer program is presented and discussed in detail. A discussion of experimental results follows in Chapter IV.

Spectra obtained at room and elevated temperatures are presented in detail along with decay lifetime calibration data. Chapter V summarizes the experimental results and presents improvements to experimental methods and suggests several possible thermophosphor experiments for future research.

CHAPTER II

THERMOGRAPHIC PHOSPHOR THEORY

Several theoretical aspects related to the quantum mechanical nature of thermographic phosphors will be discussed in the following pages. The origin of the fluorescence spectrum is described along with specific transitions of phosphors researched in this work. The phosphor Y_2O_3:Eu^{3+} which has been intensively studied in the past, will be used as an example for descriptive purposes. Particular attention will be given to the temperature dependence of thermophosphors and the charge transfer state and its role in the luminescence process.

Spectroscopy of Rare-earth Doped Materials

Rare-earth ions incorporated into a host crystal lattice structure when properly excited, exhibit sharp-line emission spectra. This means a large fraction of their fluorescent output is concentrated into a few narrow-band emission lines. In addition, one may see broad bands in both absorption and excitation spectra, usually in the ultraviolet. The emission lines are typically associated with the inner 4f transitions of the ions themselves while the bands may result from the dopant ion interactions with the host lattice.

Origin of the Fluorescence Spectrum

The discussion will begin with a description of the transitions in a two level quantum system. The system may be excited to the higher levels by acquiring energy, for example via collision or light absorption. The downward relaxation that occurs from this state is due either to nonradiative relaxation or spontaneous emission of electromagnetic or fluorescent radiation. Photons are emitted as the electrons give up their energy on the downward transitions from higher energy levels. The total relaxation rate γ_{total} on any given transition will be the sum of the radiative decay rate γ_{rad} and the nonradiative decay rate γ_{nr}. Therefore,

$$\gamma_{total} = \gamma_{rad} + \gamma_{nr}. \tag{1.1}$$

Above the onset quenching temperature of the phosphor, the nonradiative decay rate becomes appreciable and increases with temperature. In most cases, the nonradiative transition rate is generally not directly measureable. The intrinsic lifetime τ_j is equal to $1/\gamma_{rad}$ at all temperatures. This is measured when $\gamma_{total} = \gamma_{rad}$ or when γ_{nr} is approximately zero. The fluorescence lifetime τ_{fl} or τ_{total} is given as $1/\gamma_{total}$ and is actually measured experimentally. The lifetime τ_j of an upper level can be measured by observing the fluorescent emission from the upper level E_j to any other lower level E_i immediately after a short pulse of exciting radiation is subject to the sample material. The measured intensity $I_{fl}(t)$ of the fluorescent emission on a specific $j \rightarrow i$ transition is given by

$$I_{fl}(t) = \text{const.} \times e^{-t/\tau_{total}} = \text{const.} \times e^{-t\gamma_{total}}. \tag{1.2}$$

Therefore, the measured intensity should decrease, decay, or relax in an exponential manner. The same result is achieved in terms of population difference by considering the transient response of a two-level atomic system. The transient solution to the rate equation for $t > t_0$ is

$$\Delta N(t) = \Delta N_{ss} + [\Delta N(t_0) - \Delta N_{ss}] \exp [-(2W_{12} + 1/T_1)(t - t_0)], \qquad (1.3)$$

where ΔN_{ss} is the steady-state value of ΔN, $\Delta N(t_0)$ is the initial population difference, and W_{12} is an applied signal or driving function. If the applied signal or driving function W_{12} is not present, such as when the excitation is turned off, the population $\Delta N(t)$ will then relax from its initial population value $\Delta N(t_0)$ to its thermal-equilibrium population value ΔN_0. This relaxation will therefore be a decaying exponential function with an exponential time constant T_1. The time constant T_1 is generally equivalent to the population recovery or energy decay times t or γ^1 used in other analyses. [12]

The energy level diagram shown in Figure 2.1 helps to further explain the band theory of a basic phosphor. The diagram shows the valence band, conduction band, and the forbidden gap, also known as the band gap. The band gap separates the tightly bound valence band electrons from the free electron conduction band level. When an electron is excited into the conduction band, it may wander about before becoming trapped in a potential well just below the conduction band minimum. It may also make a radiative transition back to the valence band ground state emitting a photon in the process. Traps are thought to be defects in the crystal lattice structure. The electron, once trapped will remain for a time determined by the depth of the trap and the subsequent excitations the trapped electron experiences. However if the electron escapes from the trap back into the conduction band, it may become retrapped or possibly be returned through a radiative
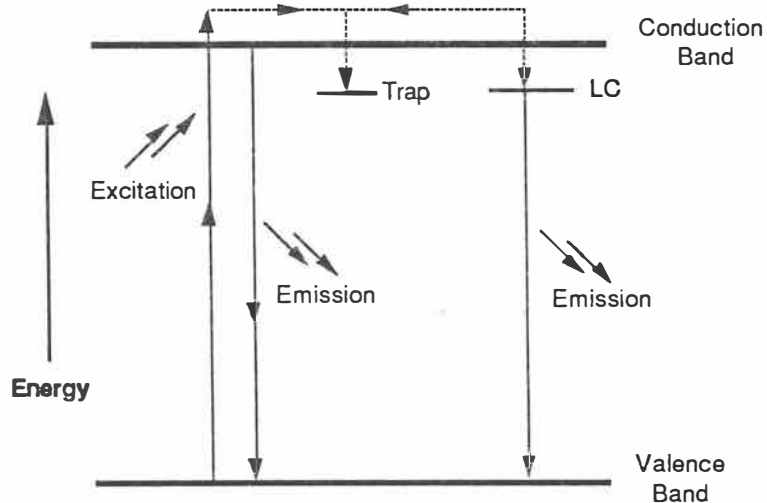
Figure 2-1. Simplified energy level diagram.

process to the ground state. In many phosphors, the excited electron makes radiative transitions to luminescence centers (LC) located in the band gap rather than return to the valence band. The term luminescence center refers to any atom, ion or group of atoms which assist in the luminescence process. Such luminescence centers in phosphors are the rare-earth activators.[13]

Activator ions, such as Eu^{3+}, Pr^{3+}, Gd^{3+}, Sm^{3+}, and Tm^{3+}, may be excited by the transfer of energy from the host lattice. Figure 2-2 shows the positions in energy of a number of the excited states of these and other rare-earth ions of the lanthanide series.[14] Certain absorption band regions are indicated, together with the environments in which they were observed. The arrows indicate known excitation transfer interactions resulting in sensitized fluorescence.
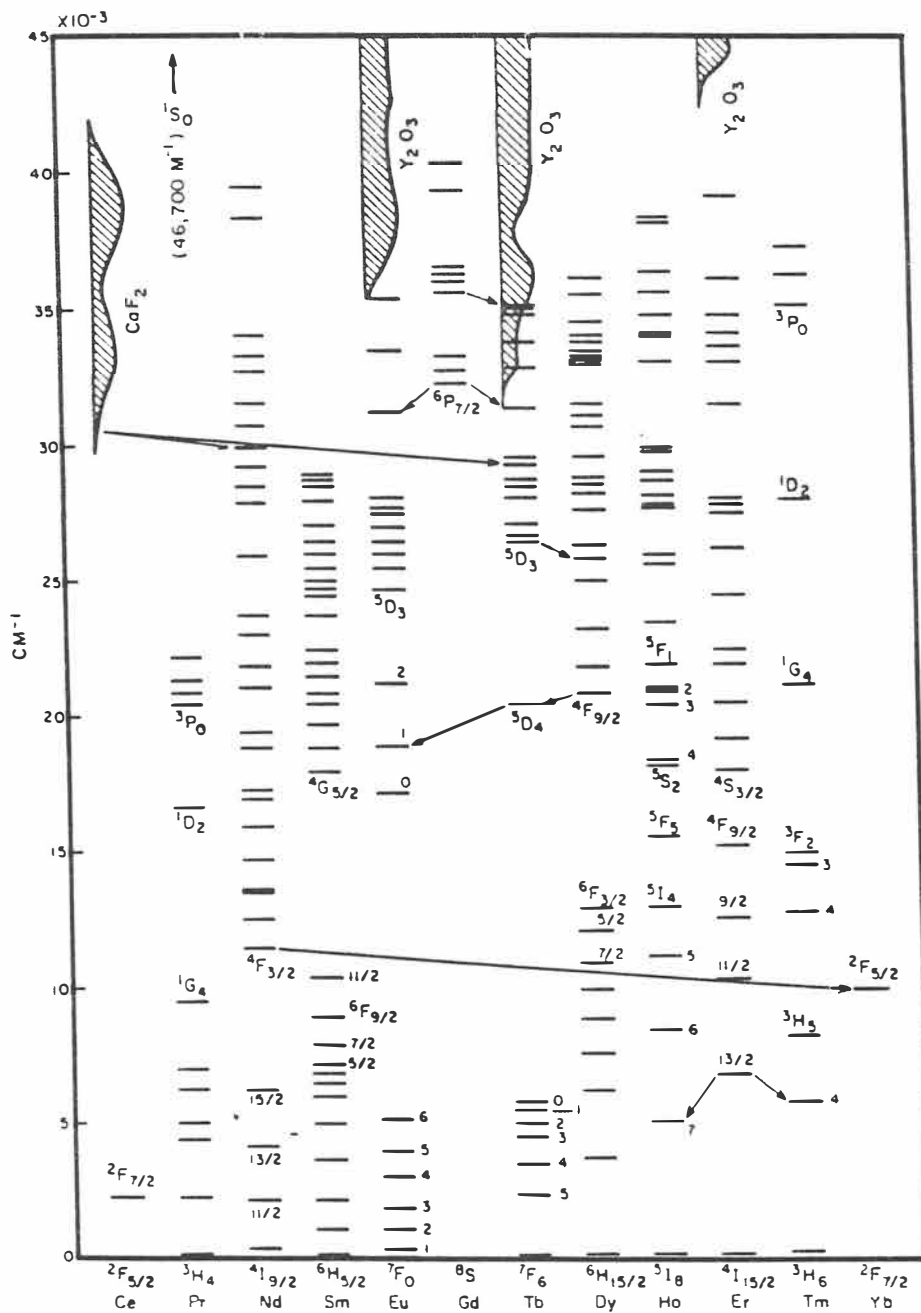
FROM "LUMINESCENCE OF INORGANIC SOLIDS" GOLDBERG, ed., ACADEMIC PRESS 1966.

Figure 2-2. Energy levels of the lanthanides.

When a phosphor or other luminescent substance emits light, it gives, in most cases, an emission according to a fundamental law known as *Stokes' Law*. This law states that the wavelength of the emission λ_{EM} is always greater than the wavelength of the exciting source λ_{EX}.

Visible spectroscopy utilizes the principle of excitation of the electrons in a molecule. Energy differences exist between the ground state and the excitation state of the electrons. When the various wavelengths of radiation from, for instance, a spectrophotometer correspond with the energy differences of the electron states, energy is removed from the optical beam. These appear as absorption peaks or bands at those particular wavelengths. The amount of absorption is proportional to the concentration of the activator in the sample.

Fluorescence spectroscopy uses the principle of excitation of electrons in a molecule. Besides measuring energy absorption from a ground state to an excitation state (excitation spectrum), fluorescence spectroscopy analyzes energy in the form of light given off by a molecule in returning from an excitation state to a ground state (emission spectrum). The excitation energy is composed of electronic and vibrational energy, while the emission energy is only the electronic energy (light is not emitted by vibrational energy). Therefore the emission energy will always be less than the excitation energy, causing the emission spectrum to appear at longer wavelengths than the excitation spectrum.

The emission spectrum is a plot of emission intensity as a function of the emission wavelength for a particular excitation wavelength. The excitation spectrum is a plot of emission intensity as a function of the excitation wavelength for a particular emission wavelength. In other terminology, it is a plot of the energy absorbed by the phosphor as a function of the excitation wavelength.

Role of the Charge-Transfer State (CTS)

A charge-transfer transition is an electronic transition between the states of the activator ion and the surrounding ligands. In an oxide such as yttrium oxide, a charge-transfer can be thought of by removing an electron off a neighboring oxygen ion and placing it in an empty europium orbital. In this particular scenerio, the resultant is the formation of an Eu^{2+} ion. When the electron leaves the Eu^{2+} ion and returns back to the oxygen, it leaves the Eu^{3+} ion in an excited state which lead to the production of the Eu^{3+} emission. Struck and Fonger describe this excitation into the charge-transfer state of Eu^{3+} as leading to the partial dissociation of the charge-transfer state into divalent europium and a free hole which may subsequently trapped.[15] This effect of charge-transfer state dissociation may lead to decreased emission or quenching of the phosphor fluorescence.

In the case of the host lattice Y_2O_3, with an impurity ion of Eu^{3+}, a charge-transfer takes place between the oxygen-dominated lattice and the Eu^{3+} ion. As determined from absorption spectrum, this charge-transfer band would be observed at approximately 260 nm. Figure 2-3 shows the position of the Y_2O_3 charge-transfer state with respect to the 4f states of the Eu^{3+} activator in its normalized configuration coordinate diagram. Similarly, Figure 2-4 shows the position of the La_2O_2S charge-transfer state with respect to the 4f states of the Eu^{3+} dopant ion in its normalized configuration coordinate diagram. Other phosphors such as some of the oxysulfides can exhibit two charge-transfer bands since charge-transfer transitions occur between Eu^{3+} and both oxygen and sulfur. The phosphors $Y_2O_3S:Eu^{3+}$, $La_2O_2S:Eu3+$, and $Y_2O_3S:Pr$ may show double charge-transfer bands in their absorption spectra. The appearance of a charge-transfer band is generally governed by two factors, the willingness of a dopant ion to accept another electron and
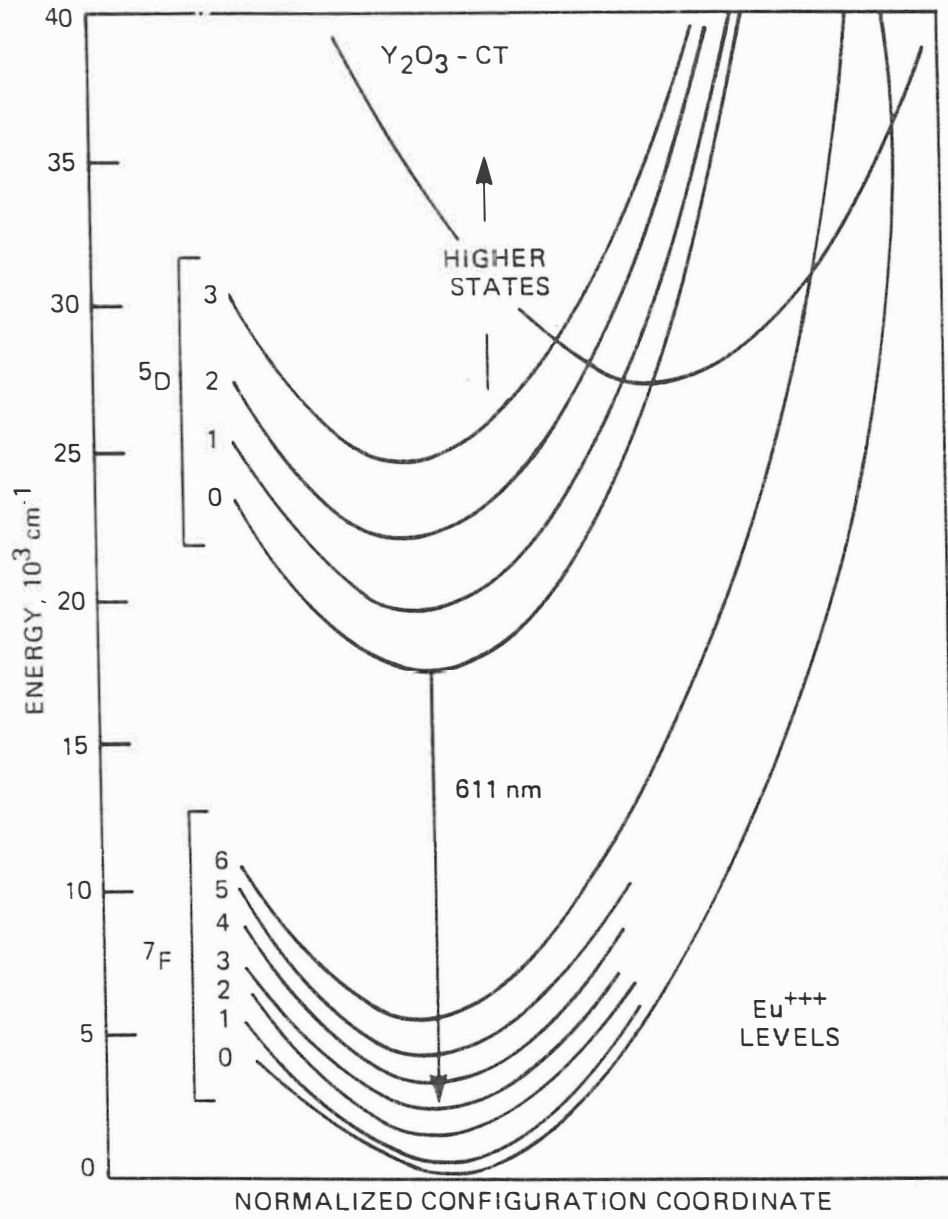
Figure 2-3. Energy levels in Eu^{3+} with the charge-transfer state in Y_2O_3.
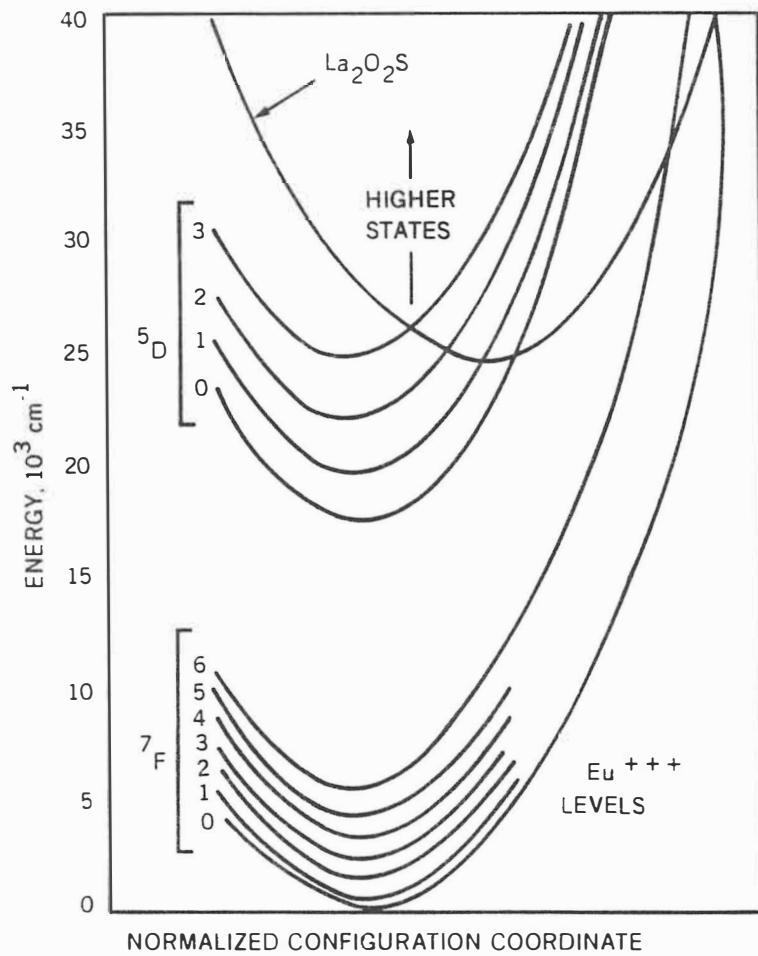
Figure 2-4. Energy levels in Eu^{3+} with the charge-transfer state in La_2O_2S.

the willingness of the neighboring host to donate an electron. A study by Ozawa shows that it is possible for the charge-transfer band to partially overlap the host lattice absorption band.[16] Although excitation into the host absorption band results in a large amount of fluorescence, many researchers prefer to take advantage of the charge-transfer state excitation which is efficient at 337 nm. The 337 nm line is commonly produced by a nitrogen laser.

Temperature Dependence of Thermographic Phosphors

Interaction of the charge-transfer transition with those of the 4f levels of Eu^{3+} is primarily responsible for the temperature quenching of the europium luminescence. The temperature dependence and thermal quenching of the ^5D emission of Eu^{3+} has been studied by Fonger and Struck.[17] A simplified description of the results of their work will be discussed with the use of several configuration coordinate diagrams. Figure 2-5 shows a configuration coordinate diagram at low temperature. The lowest vibrational levels of the 4f ground state (^7F), the 4f excited state (^5D), and the charge-transfer state can be occupied at relatively low temperatures. Excitation of the charge-transfer state ($0 \Rightarrow 1$) is followed by a rapid relaxation into the lower vibrational levels of the charge-transfer state ($1 \Rightarrow 2$). The energy is then channeled to the lowest vibrational levels in the excited 4f configuration ($2 \Rightarrow 3$). This is known as direct feeding of the charge-transfer state to the ^5D states. Further relaxation to the 4f ground state ($3 \Rightarrow 0$) produces the optical transition which is observed as 4f fluorescence. Nonradiative relaxation may occur from ($1 \Rightarrow 3$) and ($2 \Rightarrow 3$) which at low temperatures is usually quite small. Therefore there may be some lattice quenching at lower temperatures due predominatly to the nonradiative effects.
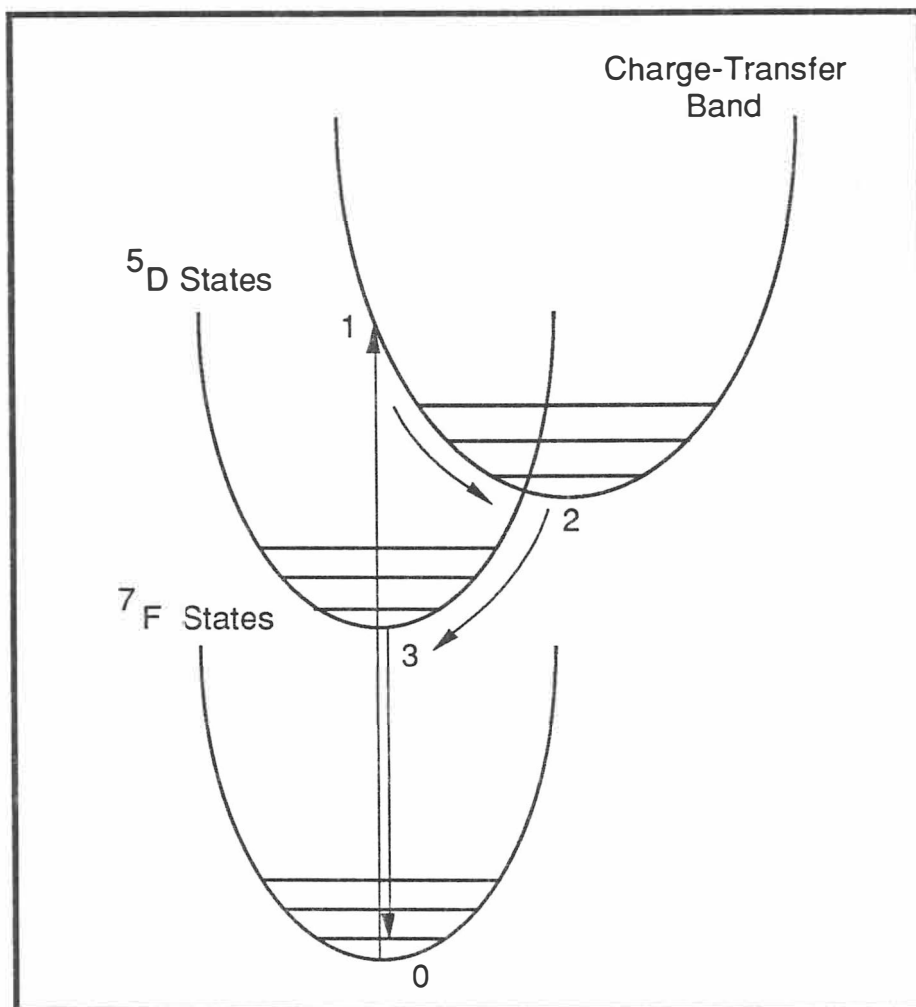
Figure 2-5. Configuration coordinate diagram at low temperature.

At higher temperatures, more vibrational levels for each of the states can be occupied. The Boltzmann distributions of electrons are shifted and the vibronic levels become thermally populated in both the 4f states and the charge-transfer states. Figure 2-6 shows a configuration coordinate diagram at high temperature. Excitation of the charge-transfer state ($0 \Rightarrow 1$), followed by rapid relaxation into the lower vibrational levels of the charge-transfer state ($1 \Rightarrow 2$) occurs similar to lower temperatures. Since the higher vibronic levels of the 4f excited states are now thermally populated, this leads to energy transfer back to the charge-transfer state ($3 \Rightarrow 2$). The energy which was transferred from the charge-transfer state to the ^5D state is now transferred back into the charge-transfer state. This can occur in both directions ($2 \Leftrightarrow 3$). And since this energy is transferred back into the charge-transfer state, it is no longer available for luminescence. The result is an observed decrease in emission intensity and reduced fluorescence lifetime. The phenomenon in which electrons bleed off from the charge-transfer state back to the lattice is the known as phono-coupling. This largely nonradiative process gives rise to thermal quenching.

Struck and Fonger determined that ^5D_j populations ($j = 0,1,2,3$) were quenched to the charge-transfer state in the order $^5D_3$, $^5D_2$, and $^5D_1$ as the temperature increased. These results were based on emission intensity measurements on the dominant fluorescence lines of the ^5D_j levels in $La_2O_2S:Eu^{3+}$ and $Y_2O_2S:Eu^{3+}$ as a function of temperature.[18] This can be seen once again by recalling Figure 2-4.

An interesting phenomenon detailed by Struck and Fonger occurs at higher temperatures when an electron from an neighboring oxygen ion fills the hole left by the electron that transferred to create the Eu^{2+} ion.[15] This formation of the Eu^{2+} ion leaves a free hole which upon recombination with other electrons gives rise to emission created through the recombination of the Eu^{2+} - hole. This recombination may explain the
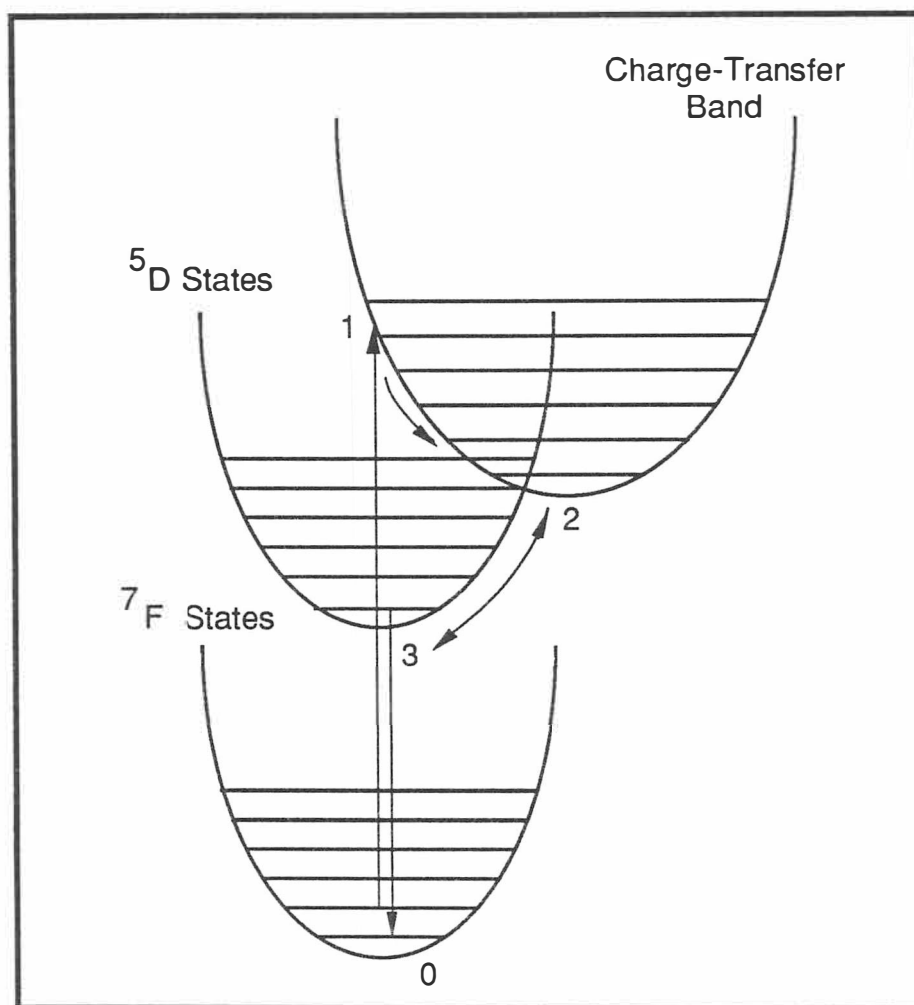
Figure 2-6. Configuration coordinate diagram at high temperature.

non-exponential effects that may occur in the Eu^{3+} fluorescence at higher temperatures, specifically above the onset of emission quenching.

Quenching of Emission

For some phosphors, the fluorescence intensity slowly increases with increasing temperature, reaches a maximum, and then decreases. This behavior arises from a competition of an increasing absorption for the exciting radiation and thermal quenching of the emitted radiation. The decrease in fluorescence intensity beyond the onset of quenching is usually logarithmic. In a study by Haake [19], he shows that the initial slow increase of fluorescence intensity as temperature increases is strongly dependent on the thickness of the sample considered. The phosphors used in his study were manganese-doped magnesium fluorogermanate. Thin samples, for example those in which the penetrating exciting radiation is not absorbed completely, in comparison with thick samples exhibit a steeper slope and a maximum at higher temperature. If the phosphor is in powder form, the average particle size also influences the slope.

Quenching of Emission Intensity

Quenching of the emission intensity at higher temperatures can be explained simply as a redistribution of electron population densities. These population densities are described by Boltzman's relationship of electron distributions. At higher temperatures, phonon-induced nonradiative relaxation begins to dominate. There are fewer electrons in the higher energy states available for de-excitation. At the onset of temperature quenching, a larger number of electrons are transferred back into the charge-transfer state

making them unavailable for luminescence. Therefore the intensity of the fluorescence should decrease significantly with increasing temperatures above quenching onset.

Quenching of Lifetime Decay

The variation in exponential lifetime decay with temperature is due to the presence of the charge-transfer states in the host lattice. The fluorescence is produced by radiative de-excitations of the dopant activators. However, the presence of the charge transfer state governs the fraction of radiative to non-radiative decay that can occur and as a result the overall exponential lifetime decay will change. As described previously in this section, the fact that electrons are transferred back to the charge-transfer band results in a reduction of energy available for fluorescence thereby making fluorescence lifetimes shorter.

Spectral Temperature Dependence

The spectral shift of the ultraviolet band in europium-doped phosphors when measured as a function of increasing temperature should theoretically shift to lower energies. This phenomenon will only occur in the excitation spectrum, particularly in the charge-transfer absorption bands of Eu^{3+} activated phosphors. At any temperature, the nuclei of the phosphor are constantly in motion and under normal excitation, the charge-transfer band is created by electron transfer between the oxygen-dominated lattice and the activator ion. As the temperature of the phosphor increases, vibronic levels of the 4f excited states will fill up. Since the higher vibronic levels of the 4f excited states are now thermally populated, this leads to a lower excitation energy because the excitation

transition starts at a higher level in the 4f vibrational ground states (^{7}F). The transition has a lower difference in excitation energy from the 4f ground state to the 4f excited states and therefore requires lower optical absorption energy. This in turn leads to a decrease in absorption energy and a charge-transfer band shift towards the red should be evident in the excitation spectra when measured as a function of increasing temperature. Results of the excitation spectra measured as a function of increasing temperature are presented in Chapter IV.

Role of the Structure and CTS in Quenching Onset

In this section, the effects of the cation radius within the host crystal lattice are presented. A short discussion on the importance of the position of the charge-transfer state with respect to the onset quenching temperature follows.

Effect of the Cation Radius in the Host Crystal Lattice

A paper by Ropp [20] discusses the coupling between the charge transfer and ^{5}D states of the trivalent rare earths. The separation or overlap of the intershell (4f-5d) and charge transfer spectra of the trivalent rare earths depend upon properties of the host crystal lattice, not upon the activator rare earths themselves. Charge transfer energy positions can be related to (a) symmetry of neighboring atoms around the central rare earth, (b) degree of polarizability of these neighboring atoms, and (c) the amount of covalency in the structural bonding. An example indicates that when sulfur was added to a Y_2O_3 host (doped with trivalent europium) to form a new host lattice of Y_2O_3S the

observed charge transfer band appears at lower energies in the excitation spectra. The effects of the host cation radius can be exploited to create phosphors with charge transfer band at specific energy locations.

Position of the CTS with Respect to the Onset Quenching Temperature

The energy or position of the charge-transfer transition relative to the ground state affects the onset of quenching temperature of phosphors. The contribution to the charge-transfer energy from the host depends mainly upon the polarizability of the nearby anions. Blasse and Hoefdraad have studied the position of the charge-transfer band of Eu^{3+} and the effects of the ionic radius of the relevant host ion.[21,22] They conclude that (a) the charge-transfer band position varies as a function of the host lattice, and (b) the variation in VIII coordinations is proportional to the Eu-O distance and with increasing bond length the charge-transfer band shifts to lower energies. Their data place the position of $ScPO_4:Eu^{3+}$ (≈ 48 kK) at a higher energy when compared to $LaPO_4:Eu^{3+}$ (37 kK). Thus, for a given dopant ion, the charge-transfer band shifts to lower energies as the cation radius increases.

Rare-earths are suited for high temperature measurements since the optical transitions occur between the energy levels of the 4f states. Since the lattice-dopant ion coupling is small for the 4f states, many processes which contribute to the onset of temperature quenching of emission occur at relatively high temperatures. Furthermore, reduction of the lattice-ion coupling should yield an increase in onset quenching temperatures which can be observed in lifetime decay calibration. Exploiting the knowledge of the effect of a decrease in host-ion bonding and applying it to thermographic phosphor measurements may show interesting results.

Several orthophosphate single crystal phosphors are being investigated in this work for charge-transfer band location and lifetime decay calibration. These phosphors have potential use in high temperature sensing applications. More importantly, these orthophosphates have been fabricated with various host lattice structures and are all trivalent europium-doped with the same activator concentrations. Details of their constituents and fabrication are presented further in this document. Table 2-1 compares the host cation radii of the available orthophosphate crystals.

Table 2-1. Comparison of the ionic radii of several orthophosphate phosphors.

Orthophosphate Phosphor	Cation Radius
Europium-doped Lanthanum Phosphate	1.061 Å
Europium-doped Yttrium Phosphate	0.893 Å
Europium-doped Lutetium Phosphate	0.850 Å
Europium-doped Scandium Phosphate	0.730 Å

Source: CRC Handbook of Physics

It is seen that lanthanum has a cation radius of 1.061Å whereas yttrium has a cation radius of 0.893Å. The cation radii of lutetium and scandium are even smaller. Therefore two aspects should be evident in the results of excitation spectra and lifetime decay analysis of these orthophosphates. First, it should be observed that the position of the

charge-transfer band in the absorption spectra will be located at higher energies or optically, deeper into the ultraviolet as the cation of the host crystal decreases. For example, the peak position of the charge-transfer band in lanthanum phosphate should be located at lower energies than the peak position of the charge-transfer band in yttrium phosphate. Secondly, an increase in the onset of temperature quenching should be observed in the phosphors which host a smaller cation radius. For example, the onset quenching temperature for lutetium phosphate should be higher than the onset quenching temperature for lanthanum and yttrium phosphate. Details of the results of the spectral and lifetime decay measurements are discussed in Chapter IV.

CHAPTER III

EXPERIMENTAL METHODS AND PROCEDURE

Complete details of the experimental methods and procedures used to obtain excitation and emission spectra at room and elevated temperatures, and lifetime decay calibration measurements are presented in the following pages. A brief discussion of thermographic phosphor materials compares and contrasts properties of the powder phosphors with those of the single crystal orthophosphate phosphors. Orthophosphate crystal structure and fabrication are also discussed. Systematic and experimental complications, error measurement, and error correction are presented for excitation and emission spectra and for lifetime decay measurements. A new method of defining and calculating the onset quenching temperature from a phosphor lifetime calibration curve using a computer program is presented and discussed in detail.

Thermographic Phosphor Materials

Luminescent phosphor materials used in this research are categorized into two types, polycrystalline granular powder phosphors (referred to as powders) and single crystal orthophosphate crystals. Each phosphor consists of a host crystal lattice structure which is doped with one of several rare-earth activator elements. Typically found in the powder phosphors is an oxygen-dominated crystal lattice structure with compounds such as the metal oxides, oxysulfides, vanadates, fluorogermanates, and phosphates being combined

with element such as yttrium, lanthanum, magnesium and many other similar elements. The orthophosphate crystals usually consist of an oxygen-dominated phosphate lattice structure with the addition of a lanthanide element such as lanthanum, cerium, praseodymium, and so forth.

The lighting and display industries use a variety of rare-earth doped phosphors for various applications. There are literally hundreds of different host crystal lattice/dopant ion combinations that are and can be manufactured by these phosphor companies. Chemicals and materials used for the production of commercially-produced and specialty phosphors are well documented by the industry, in particular Sylvania Chemical and Metallurgical Division of GTE Products Corporation.[23]

General information on all of the thermographic phosphors researched for spectral and emission properties is shown in Table 3-1. All of the fifteen powder and crystal phosphors were analyzed spectroscopically by their excitation and emission spectra measured both at room temperature and as a function of increasing temperature. Tabulated are the number and type of spectra taken for each phosphor sample. The table also describes peak emission color, the phosphor manufacturer, the lot number, phosphor type, lifetime data availability, and other pertinent information concerning any of the phosphors characterized.

Phosphor Powders

The powder phosphors used in spectral and lifetime experiments were manufactured commercially by GTE-Sylvania Chemical and Metallurgical Division, USR Optronix, and AESAR. Samples of the phosphors were either purchased from or donated by the manufacturer or obtained from other research laboratories currently involved in thermo-

Table 3-1. Tabulated information on thermographic phosphors researched for spectral and emission properties.

Phosphor	Excitation Spectrum (Room Temp.)	Emission Spectrum (Room Temp.)	Excitation Spectrum (Elevated Temp.)	Emission Spectrum (Elevated Temp.)	Powder or Crystal	Emission Color	Lifetime Data	Manufacturer	Lot No.	Type	Other Information
Yttrium Vanadate Dysprosium-doped	1	2	1	1	Powder	Yellowish	Yes	Sylvania	2370	DL79-5	
Yttrium Oxide Dysprosium-doped	1	1	1	1	Powder	Pink-red	No	AESAR	—	—	Y2O3 99.9% Dopant3% wt
Lutetium Phosphate Dysprosium-doped	1	2	2	1	Crystal	Yellow	Yes	ORNL Solid State Div.	—	—	
Lanthanum Phosphate Europium-doped	1	1	1	1	Crystal	Red	Yes	ORNL Solid State Div.	—	—	60g PbHPO$_4$ 3.5g La2O3 0.0175g Eu2O3
Lutetium Phosphate Europium-doped	1	1	1	1	Crystal	Red	Yes	ORNL Solid State Div.	—	—	60g PbHPO$_4$ 3.5g Lu2O3 0.0175g Eu2O3
Yttrium Phosphate Europium-doped	1	1	1	1	Crystal	Red	Yes	ORNL Solid State Div.	—	—	60g PbHPO$_4$ 3.5g Y2O3 0.0175g Eu2O3
Yttrium Oxide Europium-doped	1	1	2	1	Powder	Red	Yes	Sylvania	46	—	
Yttrium Vanadate Europium-doped	2	1	2	1	Powder	Bright red	No	Sylvania	QRX-383	1120	
Barium Phosphate Europium-doped	1	1	1	1	Powder	Blue	No	Sylvania	—	215	Photocopy phosphor
Lanthanum Oxysulfide Europium-doped	3	2	1	1	Powder	Orange	Yes	USR Optonix	1459-8	P-22	1% dopant
Yttrium Oxysulfide Europium-doped	2	2	1	1	Powder	Red	No	Sylvania	YOX-165	1150	
Yttrium Oxide Gadolinium-doped	1	1	1	1	Powder	Purple (UV)	No	Sylvania	RY93-82	2650	
Magnesium Fluorogermanate Manganese-doped	2	3	1	1	Powder	Red	No	Sylvania	YMX-75	2361	
Yttrium Oxysulfide Praseodymium-doped	1	1	1	1	Powder	Green/Yellow	No	USR Optonix	104	GRE3911	
Yttrium Oxysulfide Terbium-doped	1	3	1	3	Powder	Blue-white	Yes	Sylvania	HS98-60	1840	
Magnesium Oxide	2 charts	Magnesium Oxide with UV Filter		2 charts	Powder	- none -	No	Buehler Chemical	1309-48	CSA	99.999% pure

phosphor work. These inorganic phosphors have typical application in cathode-ray tubes, photocopy and UV-emitting lamps, fluorescent sign tubes, x-ray intensifying screens, electroluminescent devices, tagging and identification, and high-pressure mercury vapor lamps to name a few. Europium-doped yttrium oxide with its characteristic red emission can be found in color television tubes as a tri-phosphor component, whereas terbium-doped lanthanum oxysulfide is used in monochromatic green data display screens.

Available in technical information bulletins published by phosphor chemical manufacturers are typical optical properties such as fluorescence color, peak emission wavelength, line or band width, color coordinates, relative CR brightness, and decay or persistence classification. Typical physical properties of commercially-made phosphors such as body color, particle size, bulk density, material density, and other useful information are available to researchers in published technical literature.[24] Some of the commercially-made phosphors contain impurities and oftentimes gives rise to unknown spectral lines in emission spectra. Therefore further chemical analysis may be necessary to completely understand the fluorescent results.

Eleven polycrystalline phosphor powders were researched for spectral shifts in their charge-transfer absorption bands and of these eleven powders, two of the phosphors underwent decay lifetime calibration for potential use in high temperature sensing applications. These phosphor powders include dysprosium-doped yttrium vanadate and yttrium oxide, europium-doped yttrium oxide, yttrium vanadate, barium phosphate, lanthanum oxysulfide, and yttrium oxysulfide, gadolinium-doped yttrium oxide, manganese-doped magnesium fluorogermanate, praseodymium-doped yttrium oxysulfide, and terbium-doped yttrium oxysulfide.

Orthophosphate Crystals

Single crystals are generally thought to be better host structures for thermographic phosphor work than polycrystalline granular powders. Several reasons are noted for this hypothesis. Single crystal phosphors can be grown under carefully monitored conditions which should result in lower surface and internal impurity levels that those found in polycrystalline powder form. Using x-ray diffraction analysis, single crystal lattice parameters can be measured with greater accuracy. Crystals can be cut and polished to meet higher optical standards and specifications which may help eliminate optical alignment errors in the measurement system. Typically the lattice spacing and general structure of a single crystal is quite regular, therefore analysis and modeling of the quantum physics of the de-excitation process can be more easily performed. It can be seen that single crystals, as compared to granular polycrystalline powders, offer more opportunity for quantitative analysis and structural control for use in thermometry measurements.

Several single crystal orthophosphate samples were obtained from the Solid State Physics Division of Oak Ridge National Laboratory. The mineral monazite, a mixed lanthanide orthophosphate (from the lanthanide series La, Ce, Nd,...) exhibits characteristics that make analogs of this substance attractive for potential employment as hosts for the containment of radioactive nuclear waste. These research investigations of nuclear waste containment and management by the Solid State Division of ORNL are well documented.[25,26]

Since many of these orthophosphate crystals are doped with rare-earth activators, they exhibit strong fluorescence of varied wavelengths. Of particular interest to thermographic phosphor measurements are the europium and dysprosium-doped

orthophosphate crystals which display bright visible orange-red and yellow fluorescence under ultraviolet excitation.

An orthophosphate is defined as a molecular compound which contains the PO_4 radical, for example lanthanum orthophosphate $LaPO_4$. Construction of an orthophosphate begins with an oxide such as Lu_2O_3 and combines it with lead hydrogen phosphate. The chemical equation of the reaction of these two compounds is given as

$$Lu_2O_3 + 4PbHPO_4 \Rightarrow Pb_2P_2O_7 + 2PbO + 2H_2O + 2LuPO_4 \qquad (3.1)$$

which yields lead pyrophosphate, lead oxide, water and the orthophosphate. With the addition of another oxide to the reaction equation which contains the dopant ion, a doped orthophosphate can be formed. For example, the addition of europium oxide, lutetium oxide, and lead hydrogen phosphate will eventually form an europium-doped lutetium orthophosphate crystal.

Four orthophosphate crystals were researched for spectral shifts in their charge-transfer absorption bands and underwent decay lifetime calibration for potential use in a high temperature measurement system. These orthophosphates include single crystals of europium-doped lanthanum, yttrium and lutetium phosphate and dysprosium-doped lutetium phosphate.

Crystal Lattice Structure

At elevated temperatures, the lanthanide orthophosphates (LnPO4 with Ln = La, Ce, Pr, ..., Lu) crystallize into two different structural classes. Orthophosphates of the first half of the lanthanide transition series ($LaPO_4$ through $GdPO_4$) crystallize in the

monoclinic form, while orthophosphates of the second half of the series (TbPO$_4$ through LuPO$_4$) crystallize with the tetragonal structure. It is important to note that even though ScPO$_4$ and YPO$_4$ are not included in the lanthanide transition series, they also have tetragonal crystal structures. The monoclinic lanthanide orthophosphate form is a direct structural analog of the natural mixed rare-earth mineral monazite, while the tetragonal form is the structural analog of the minerals, zircon and xenotime.[27,28] Therefore, of the orthophosphate host crystals researched, YPO$_4$ and LuPO$_4$, have tetragonal crystal symmetry whereas LaPO$_4$ is of the monoclinic structural form.

Although the physical structure of orthophosphate crystals is quite complex, the fundamental properties of both pure and rare-earth-doped phosphates have been investigated by utilization of techniques such as optical absorption spectroscopy, Rutherford backscattering, x-ray diffraction, and Raman spectroscopy. In particular, electron paramagnetic resonance (EPR) spectroscopy has been used to determine the site symmetries and valence states for a number of impurities in both single crystal and polycrystalline samples of orthophosphates. Structural investigations of LaPO$_4$, YPO$_4$ and LuPO$_4$ crystals using EPR spectroscopy and other techniques have been exhaustively researched and are well documented in other publications.[26,29]

Crystal Fabrication

Doped single crystals of LaPO$_4$, YPO$_4$, and LuPO$_4$ were grown at the Solid State Division of ORNL using a flux technique by first reacting the host material and dopant oxides with lead hydrogen phosphate in covered, tight-fitting platinum crucibles. Trivalent europium and dysprosium dopants were added in the form of the oxides, Eu$_2$O$_3$ and Dy$_2$O$_3$. As a result, the crystals in their final form, are either europium- or

dysprosium-doped. After 16 hours in a high temperature furnace at approximately 1360°C, the crucibles were slowly cooled at a rate of approximately 1°C/h to 900°C and then, directly to room temperature. Following the subsequent cooling to room temperature, the resulting single crystals were removed from the solidified lead pyrophosphate flux by boiling in concentrated nitric acid for approximately three weeks. [28] The freed crystals appear translucent with a very slight white color. However, some of the crystals exhibit a slight grayish color due to minute amounts of the flux material still embedded in its structure. Further optical clarification of the crystals can be achieved by continued boiling in the nitric acid bath.

For example, the orthophosphate phosphor $LuPO_4:Eu^{3+}$ was grown with the following initial constituents:

$$60g \ PbHPO_4$$
$$3.5g \ Lu_2O_3$$
$$0.0175g \ Eu_2O_3$$

where the ratio of the weight of Eu_2O_3 to the weight of Lu_2O_3 gives the dopant percentage by weight. For this particular orthophosphate the dopant level is 0.5% by weight. Dopant levels of phosphors are also commonly given in atomic percent. However in this work, dopant levels are given in percentage by weight. Constituents of each orthophosphate crystal are given by formula and weight in grams and can be found in Table 3-1. An electron photomicrograph of the single crystal $LaPO_4:Eu^{3+}$ is shown in Figure 3-1 and details some of its surface features.
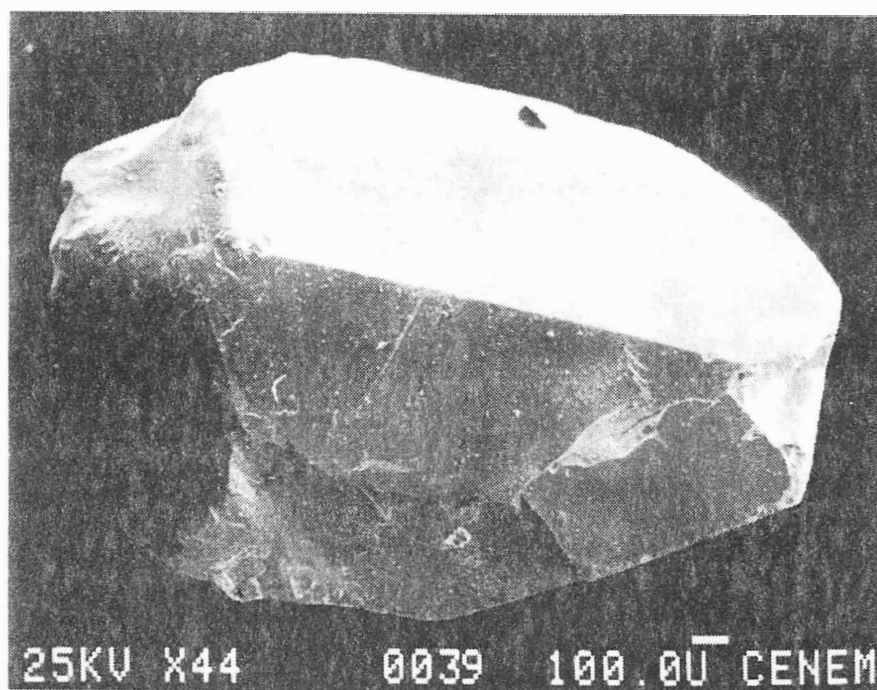
Figure 3-1.   SEM photograph of the $LaPO_4$:Eu^{3+} single crystal phosphor.

Excitation and Emission Spectra at Room and Elevated Temperatures

Excitation and emission spectra were obtained at room and elevated temperatures using the experimental configuration shown in Figure 3-2. A Perkin-Elmer 650-10S fluorescence spectrophotometer was used along with its built-in, high-intensity xenon lamp as an excitation source. The model XBO 150 watt source is a short arc xenon lamp manufactured by Osram Incorporated. A miniature oven was constructed of high temperature ceramic brick material and was designed to fit inside the internal housing of the fluorescence spectrophotometer. The ceramic brick pieces were joined together and cemented with Sauereisen No. 75 high temperature electrical refractory cement.

In addition to the ceramic material, the oven consists of a diffusion-pump cartridge heating element controlled by an adjustable AC power supply and has a maximum output temperature of approximately 500°C. A Keithley 173A digital voltmeter is connected to the output of the AC power supply and is used to monitor the voltage to the oven heating element. The oven temperature has been roughly calibrated to its input AC voltage. Since there is no feedback output from the thermocouple, the operator must set a voltage value and monitor the oven temperature until the desired temperature is reached.

The mini oven also features quartz optical ports through which excitation radiation is incident upon the crystals and its fluorescence observed through the exit port by a photomultiplier tube. Dimensions of these SupraSil quartz optical windows are 1 mm in thickness and 31.75 mm in diameter and are essentially UV transparent. A Wahl type K thermocouple calibrated with NBS standards was mounted in the mini oven and placed approximately 1-2 mm in front of the crystal sample to monitor its temperature.

A cross-sectional top view of the ceramic oven used for the high temperature spectral
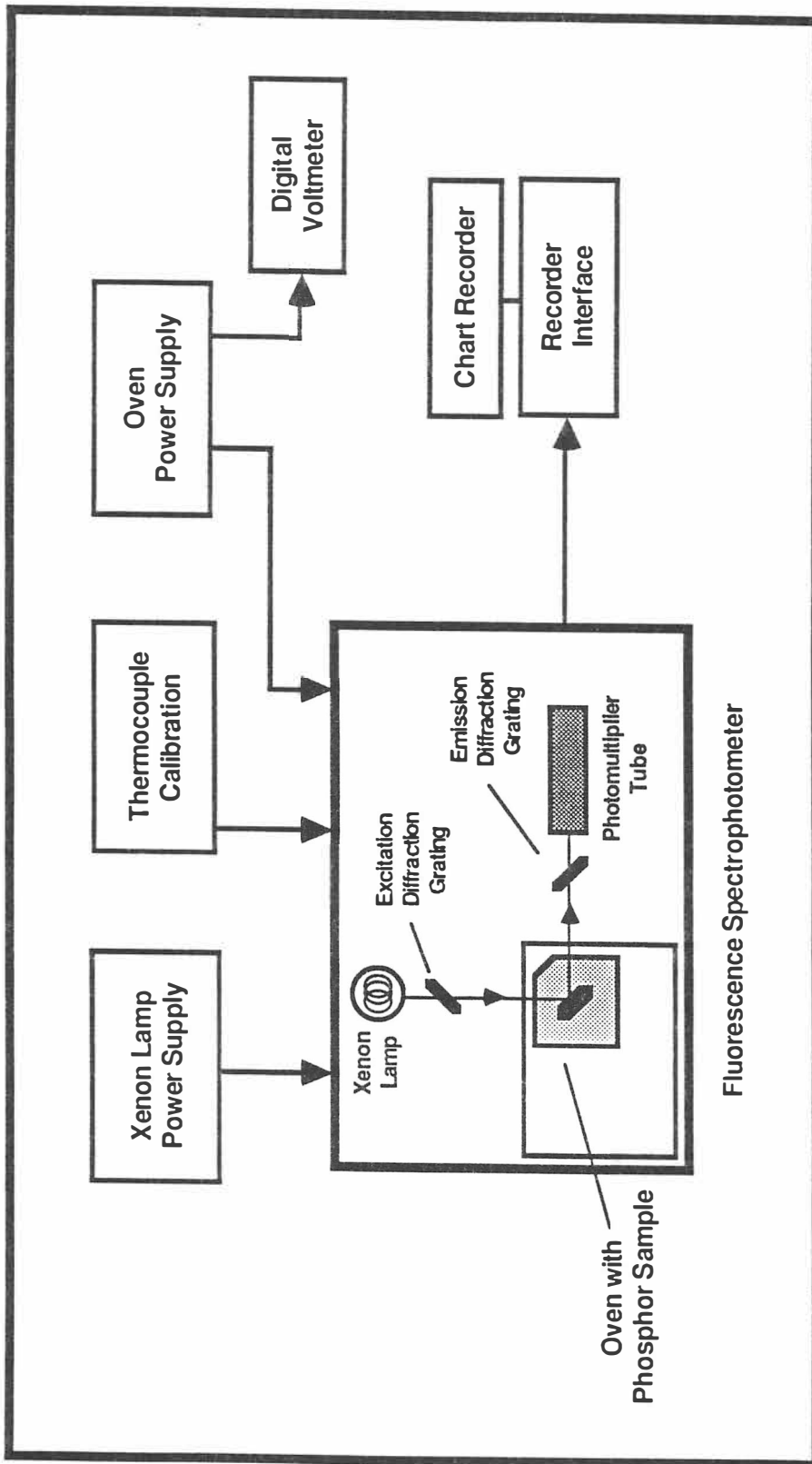
Figure 3-2. Experimental configuration for obtaining excitation and emission spectra at elevated temperatures.

characterization is shown in Figure 3-3 and reveals the major components of the oven.

The dimensions of the high temperature ceramic oven are shown in Figure 3-4. The oven has an overall length of 130 mm, width of 108 mm, and height of 100 mm. A Helma solid sample cell holder was used to hold all of the powders and crystals for room temperature spectra measurements. This cell contains a metal cavity for the sample and is covered with a 12 mm SupraSil II quartz window. The holder mounts in the housing of the spectrophotometer and positions the sample cell at a 60° angle to the excitation beam. A special ceramic holder was constructed for each powder and crystal phosphor sample under high temperature measurement and was carefully positioned inside the cavity of the mini oven. The holder consists of a 40x15x10 mm piece of ceramic material with a small 10x6x4 mm hole near its bottom in which the powders and crystals are placed. Covering the crystals is a 1 mm thick quartz window cemented in place with Sauereisen No. 75 cement. A diagram for the ceramic holder used to hold the orthophosphate crystals is shown Figure 3-5.

The powder phosphors are usually packed into their ceramic holders and then soaked with pure ethanol. The ethanol helps to coagulate the powder, keeping it from falling out of the holder and thereby eliminating the need for a quartz window cover. Since the phosphor crystals are held in their ceramic holders with a quartz window, it may be possible that optical coupling between the excitation source, the phosphor sample, and the photomultiplier will be reduced slightly. The two quartz windows of the oven will also reduce the excitation and emission radiation slightly.

Excitation and emission wavelengths for each spectrum varied from 220.0 nm continuously up to 800.0 nm which is the range of the spectrophotometer. The operator of the spectrophotometer has several options or settings to choose from, although most setting remained fixed throughout the majority of the measurements.
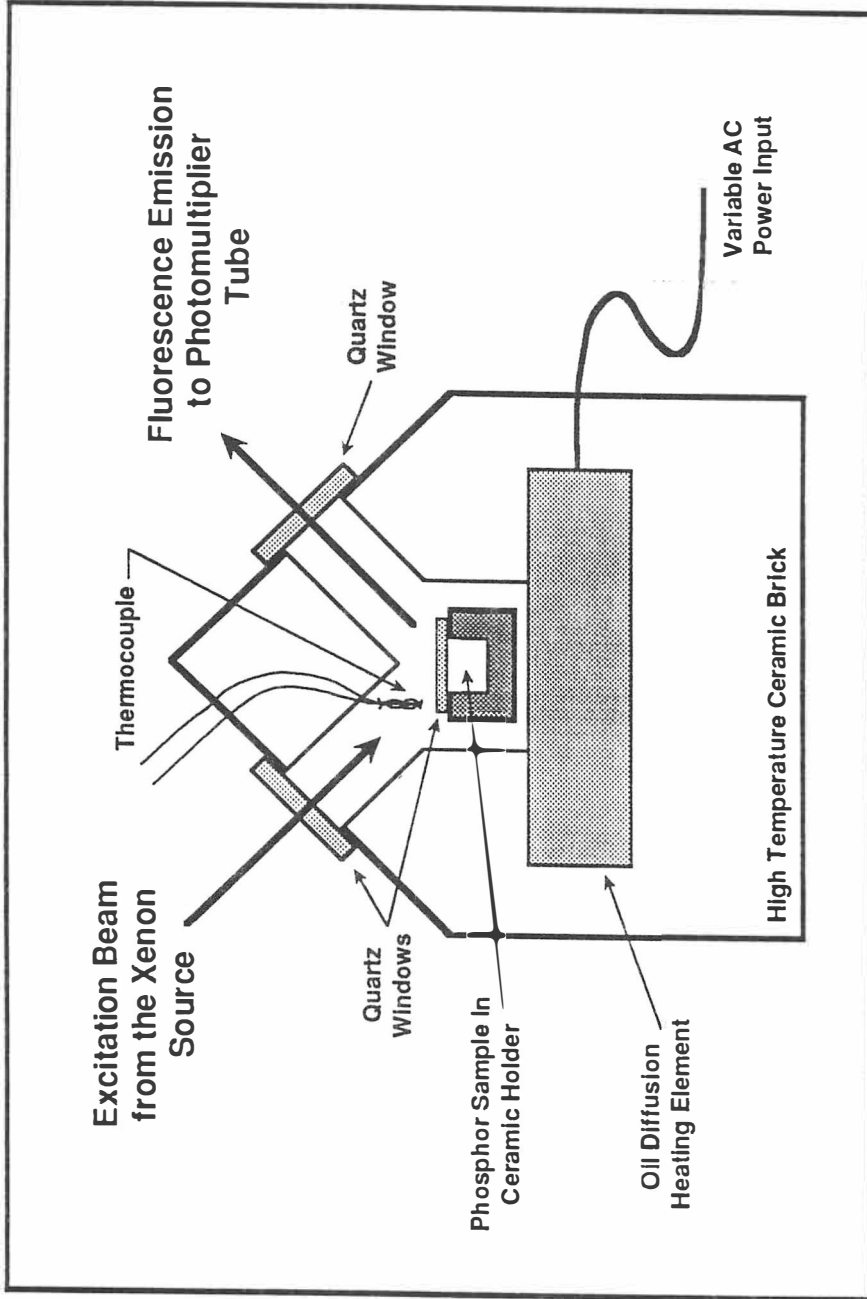
Figure 3-3. Cross-sectional top view of the ceramic oven used for high temperature spectral characterization of thermographic phosphors.
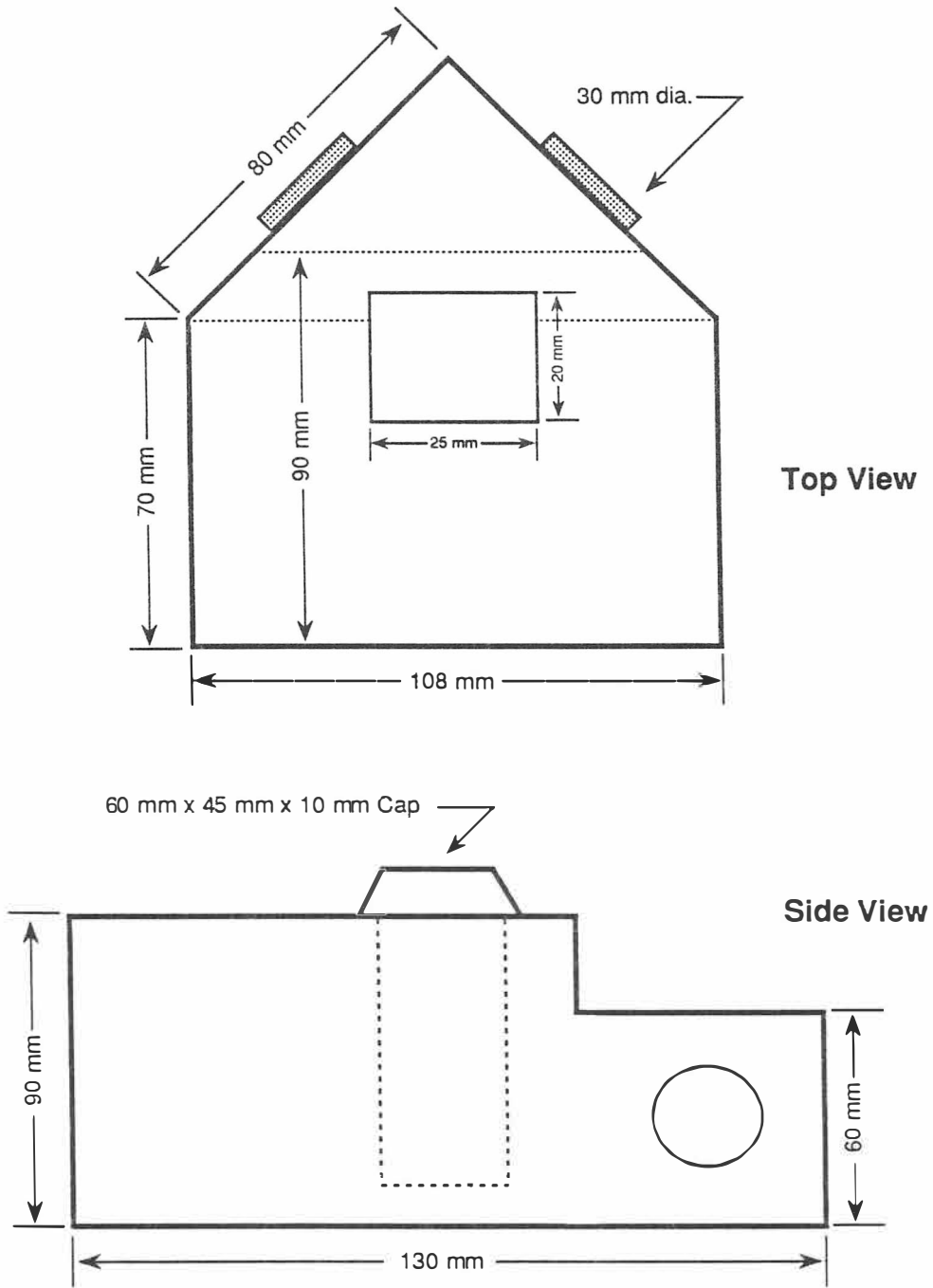
Figure 3-4. High temperature ceramic oven dimensions.
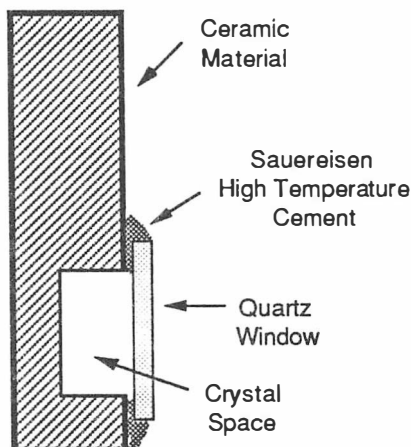
Figure 3-5. Ceramic sample holder for the orthophosphate crystals.

Photomultiplier sensitivity ranges from 0.1 to 30 with increments available in one tenths. The gain of the Hamamatsu R372F photomultiplier tube in the spectrophotometer was set to normal unless specified on the spectrum label. Spectrophotometer response and mode were set to normal. The scan speed has a range of 15 to 240 nanometers per minute however most spectrum scans were obtained at 30 nm/min. Excitation and emission bandpass slits have widths ranging from 1 nm to 25 nm. The majority of spectra were obtained with excitation and emission bandpass slit widths set to 1 nm. The spectrophotometer has a wavelength resolution of less than or equal to 1.5 nm and a wavelength accuracy of ± 2 nm or better.

Spectra obtained for each phosphor sample were plotted on Gould Accuchart recording paper with an Perkin Elmer/Hitachi Model 057 X-Y chart recorder. The chart recording paper measures 11 inches by 16 inches and is marked in 1 mm increments. A Perkin Elmer 650-10 X-Y Recorder Interface was used to drive the chart recorder. The recorder interface scan mode was set to λ to correlate the movement of the x-axis with

the wavelength of the spectrophotometer. The reset button was used to reposition the chart pen to the starting point of the x-axis so that another scan can be run. The pen setting on the chart recorder set to "auto" so that when an excitation or emission scan was run, the pen was raised from and lowered to the chart paper automatically. The chart hold setting was set "on" to firmly hold the chart recording paper in place. The X and Y range setting on the chart recorder were used to scale the acquired spectrum so that it would fit on the recording chart paper. These range settings were adjusted for each spectrum. Figure 3-6 show a sample label that is attached to each spectrum chart. This label is used to preserve important information about each phosphor spectrum including spectrophotometer settings so that spectra may be reproduced easily in the future.

Sample __$LuPO_4{:}Eu^{3+}$__

Date __Nov. 10, 1988__

Init. __A.R.B__

Temp. __300 °C__

Bandpass EX __1 nm__

EM __1 nm__

Scan __30__

Sens. __10.4__

X = X5   Y = X2

Spectrum Type __EMISSION__

@ Wavelength __395 nm EX__

Gain __Norm__

Mode __Norm__

Resp. __Norm__

Filter __- None -__

☐ Sample cell   ■ Temp.

Figure 3-6.   Label attachment for each spectrum chart.

The procedure of obtaining a typical excitation spectra will be described. The powder or crystal phosphor is placed carefully in its appropriate holder and placed into the cavity of the mini oven. The oven was then aligned with the excitation beam. The

excitation grating was slowly rotated while watching the phosphor sample for bright fluorescence. This was done if the emission lines of the phosphor were unknown. The emission grating was set near the wavelength of the visually-detected emission and the sample compartment lid was closed. The emission and excitation gratings were slowly rotated until the chart recorder pen reached its peak intensity value (maximum photomultiplier signal) and still remained in the range of the chart recorder y-axis. This was done mainly by trial and error to achieve the maximum intensity value. Other spectrophotometer settings were adjusted accordingly, in particular the photomultiplier tube sensitivity. After the peak emission line is found, the emission grating remains fixed. The excitation grating is set to 220.0 nm and the spectrophotometer rotates the excitation grating to excite the phosphor usually through a range of wavelengths starting from 220.0 nm and ending with 600.0 nm. The result of this procedure produces an excitation spectrum. After a few test scans are completed and the final spectrophotometer settings are verified, excitation spectra are taken at room temperature and then at elevated temperatures. Temperatures within the oven range from roughly 20°C up to 450°C. Care was taken to allow for temperature within the oven to stabilize. Each excitation or emission spectrum was recorded on a separate chart for each temperature point. The emission spectrum is recorded using the same procedure however the excitation wavelength remains fixed while the emission grating rotates through a selected range of wavelengths. It is usually not necessary to have to readjust the photomultiplier sensitivity when acquiring the emission spectrum.

The excitation and emission wavelengths for each spectrum were analyzed using hand-calculated graphical methods. All wavelength measurements are given in nanometers. The charts were proportionally scaled and for some of the phosphors, significant changes in wavelength were measured at the peak of the charge-transfer

absorption bands. The spectral charts for each phosphor at different temperatures were then compiled on a light table by hand tracing each with multicolored pencils. This results in a one-page excitation or emission spectra which displays all of the spectral lines for each temperature measured. Details of any significant charge-transfer spectral shifts and changes in intensity and wavelength can be compared and contrasted from the one-page chart. The spectral charts found in the following pages of this thesis are only graphical representations of the actual spectra and are solely used for neat and orderly presentation of data and results. Using a DEST optical scanner in conjunction with an Apple Macintosh computer, each chart was digitized and store on computer disks. The digitized spectra charts were then used as background templates for Adobe Illustrator 88, an program which traces a template and produces high-quality graphical output. The graphs produced with Adobe Illustrator 88 were printed on an Apple LaserWriter Plus high-resolution printer.

Two other final details regarding spectrophotometer measurements should be discussed at this time. It was mentioned earlier that the Helma solid sample cell was mounted at 60° with respect to the excitation beam. Since the excitation beam maybe partially reflected (specular light) from the surface of the sample cell, a portion of the excitation light may enter the emission monochromator. Also second order excitation may enter the emission monochromator, interfering with spectral measurements. For example if the excitation wavelength is on the order of 220 to 300 nm, it is possible that a second order line will be observed by the emission monochromator in the 400 to 600 nm range. An ultraviolet filter was used to help reduce or eliminate second order effects in the spectra obtained.

Since the mini oven is in close proximity to the photomultiplier tube of the spectrophotometer, it is suspected that blackbody background radiation or thermal heating

may be a contributing factor affecting the spectral results, especially at higher temperatures. This complication is discussed later in this chapter.

UV Filter Characteristics

An ultraviolet filter was normally used in the measurement of excitation and emission spectra at room temperature. The primary purpose of the filter was to reduce or eliminate the second order excitation lines sometimes reflected from the surface of the Helma solid sample cell holder. The ultraviolet filter was placed inside the sample compartment of the spectrophotometer in front of the photomultiplier tube. This filter has a cutoff wavelength of 400.0 nm as shown in the reflectance spectrum of magnesium oxide of Figure 3-7. The reflectance spectrum of magnesium oxide was also used to characterize the spectral output of the the xenon lamp of the spectrophotometer and is discussed in the following section. The emission spectrum of the filter was also acquired and shows a small amount of fluorescence located at 518.0 nm when excited with 300 nm. This spectrum was taken at a photomultiplier tube sensitivity of 30. Figure 3-8 shows the emission spectrum of the filter with first and second order excitation lines whereas Figure 3-9 shows the essentially the same emission spectrum but with the reflected excitation lines removed.

Fluorescence Spectrophotometer Intensity Correction Spectra

A short discussion of spectrophotometer intensity correction is necessary and a method for obtaining corrected spectra is presented. It should be noted that the output of the Perkin-Elmer 650-10S fluorescence spectrophotometer is not corrected for variations
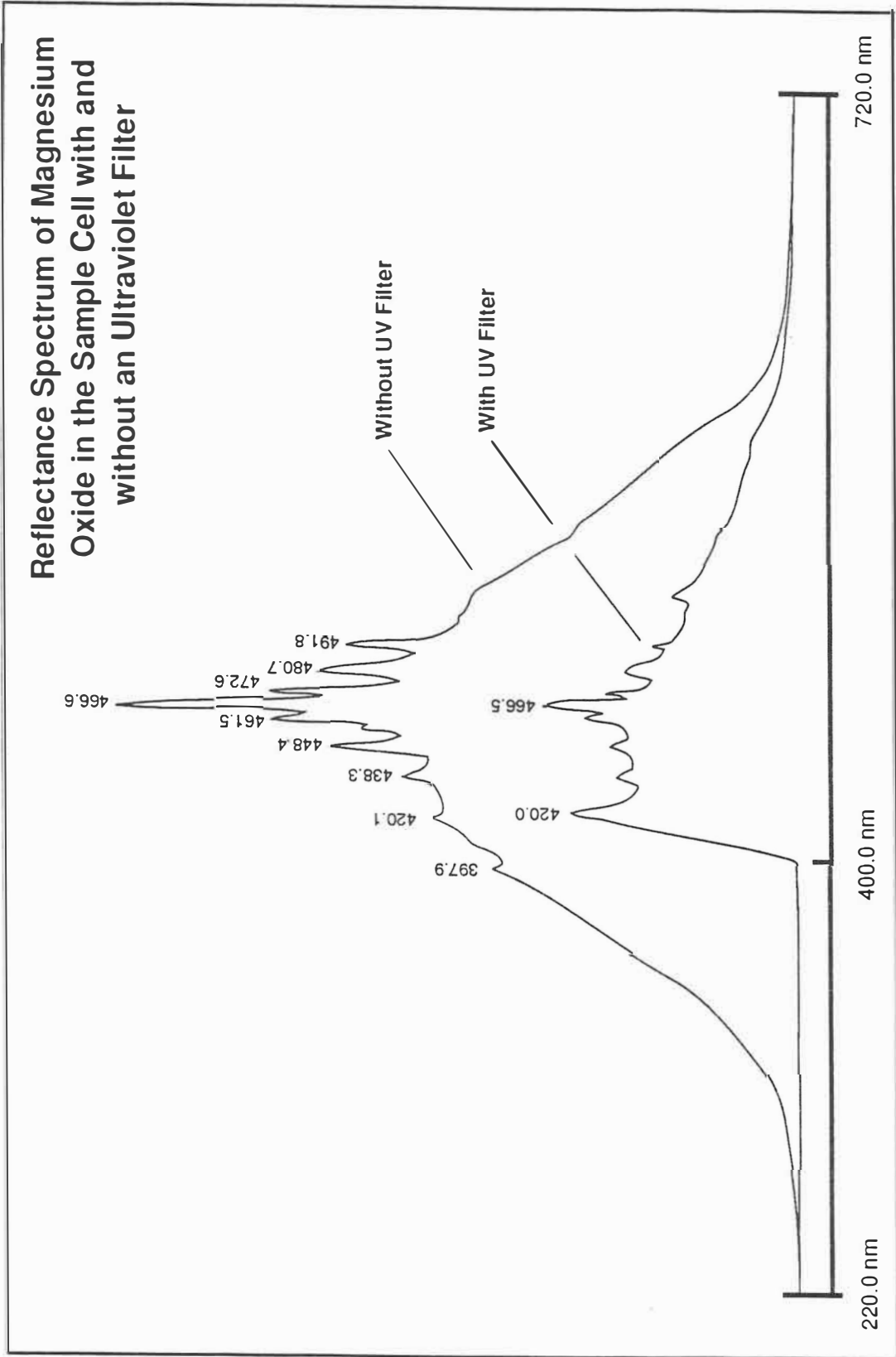
Figure 3-7. Reflectance spectrum of magnesium oxide in the sample cell with and without an ultraviolet filter.
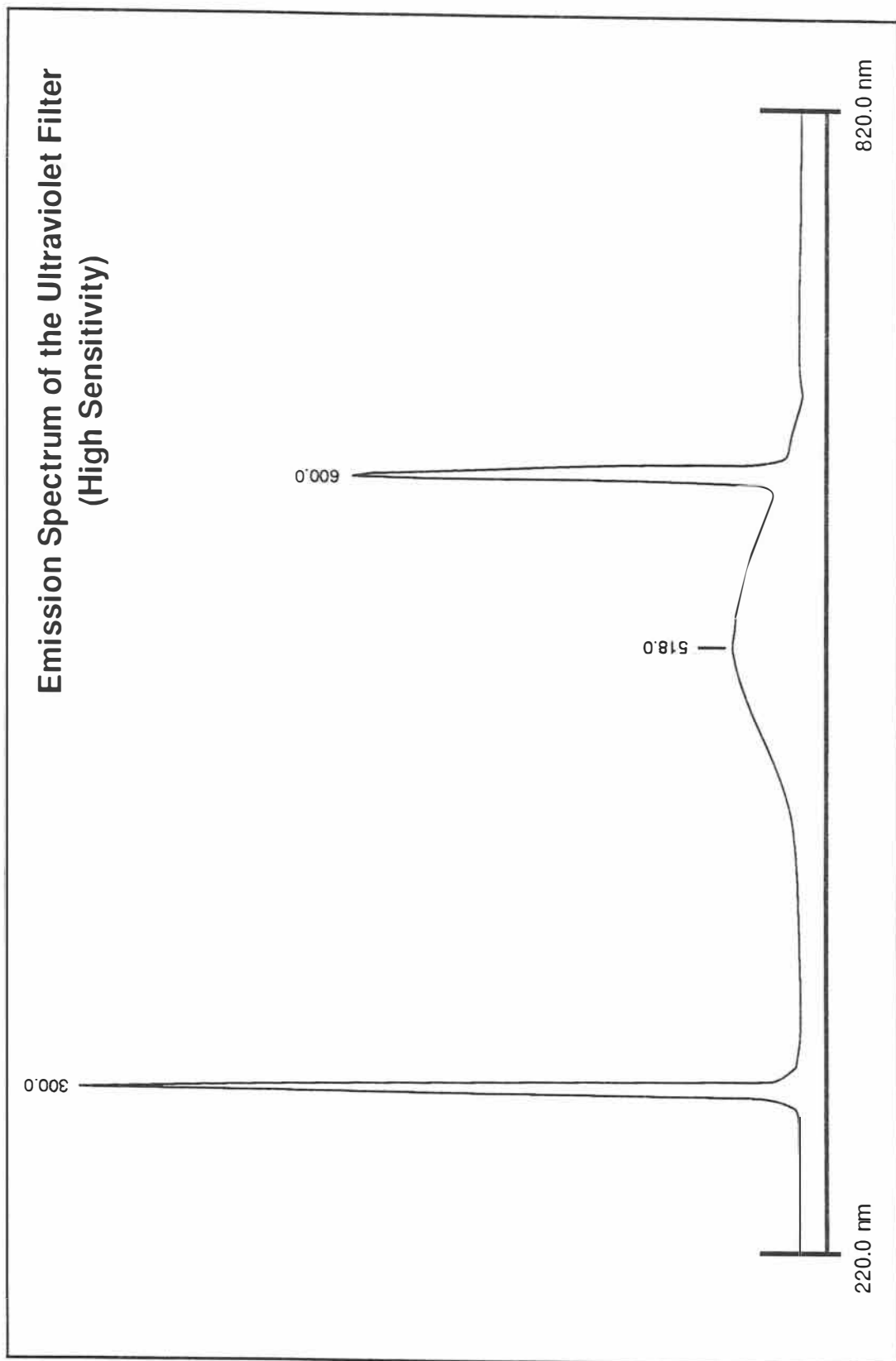
Figure 3-8. Emission spectrum of the ultraviolet filter (high sensitivity).

Figure 3-9. Emission spectrum of the ultraviolet filter without the 1st and 2nd (300.0 nm and 600.0 nm) order lines.

in source intensity and photomultiplier spectral responsivity. Most of the current state-of-the-art fluorescence spectrophotometers have built-in computer correction for both the xenon lamp intensity and photomultiplier spectral responsivity and the result is true corrected spectral output. These spectrophotometers have two detectors, one which monitors the xenon lamp intensity spectrum and the other which is used to collect the fluorescence spectrum. Since a computer collects the spectral waveforms, which are usually displayed on a high-resolution screen, it can easily run the waveforms through a correction algorithm thereby producing the corrected spectra.

Ideally, one would like the intensity of the excitation source to be flat across the spectrum of wavelengths of interest. However this is usually not the case since most broadband lamps contain spectral peaks at various wavelengths. This usually calls for correction of peak variations. The correction of intensity variations of the xenon source can be made by dividing the spectra obtained by the xenon lamp spectra. The correction of spectral variations in the photomultiplier tube can be made by dividing the spectra obtained by its spectral responsivity curve. These corrected spectra are then multiplied by the measured excitation or emission spectrum to obtain a corrected measurement.

A reflectance spectrum of 99.99% pure magnesium oxide powder was actually used to obtain a spectrum of the 150 Watt OSRAM high-pressure xenon lamp used in the Perkin Elmer spectrophotometer. Figures 3-10 shows the reflectance spectrum of magnesium oxide when placed in the Helma sample cell with a quartz window. Figure 3-11 shows the reflectance spectrum of magnesium oxide when placed in ceramic holder without a quartz window. The reflectance spectrum of magnesium oxide is generally straight (or flat) for all wavelengths of light since it is a pure reflector.

This was done to verify any changes in the reflectance spectrum due to effects of the quartz window in the Helma sample cell. A comparison of the two spectra shows almost
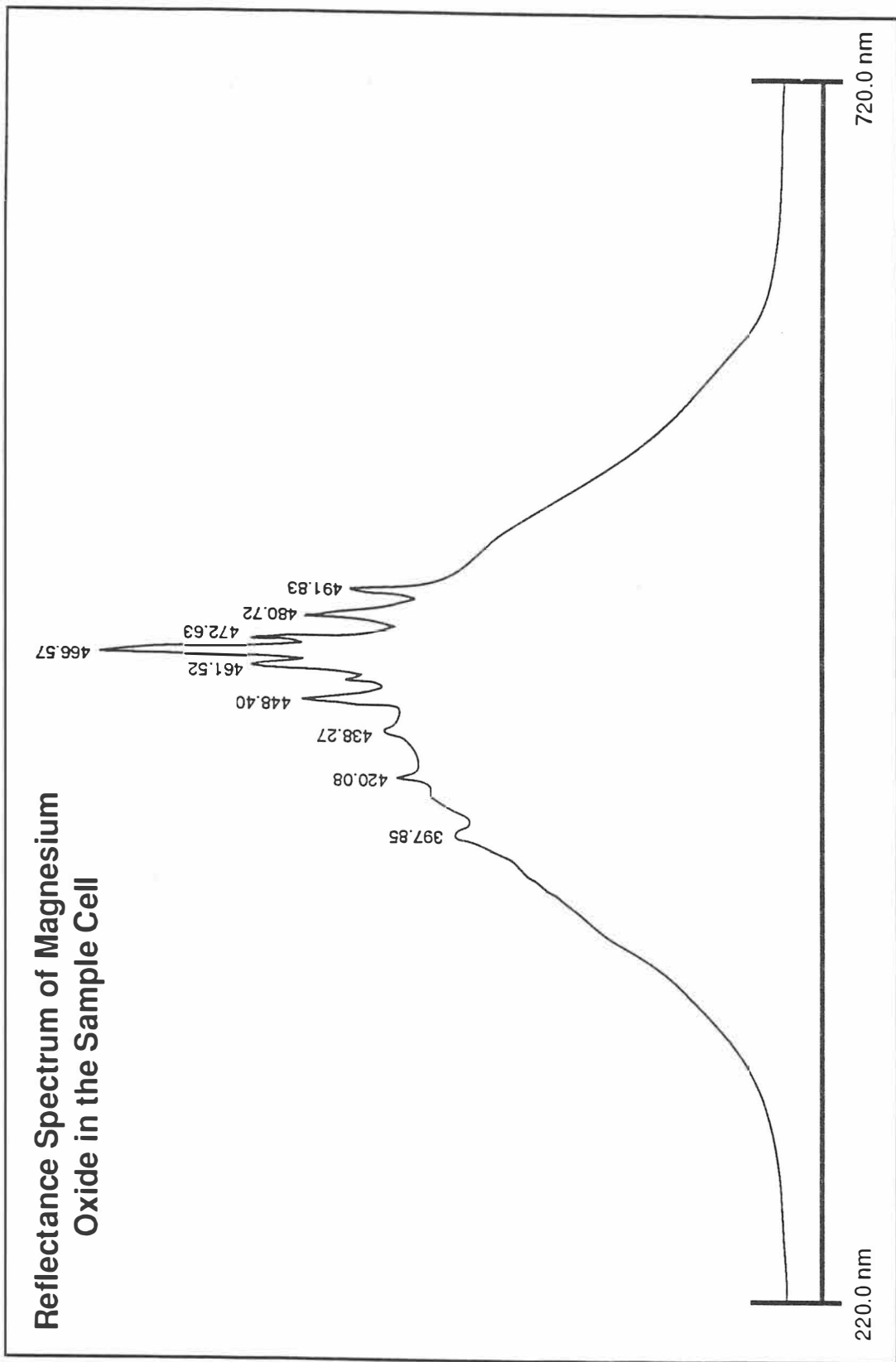
Figure 3-10. Reflectance spectrum of magnesium oxide in the sample cell.

50
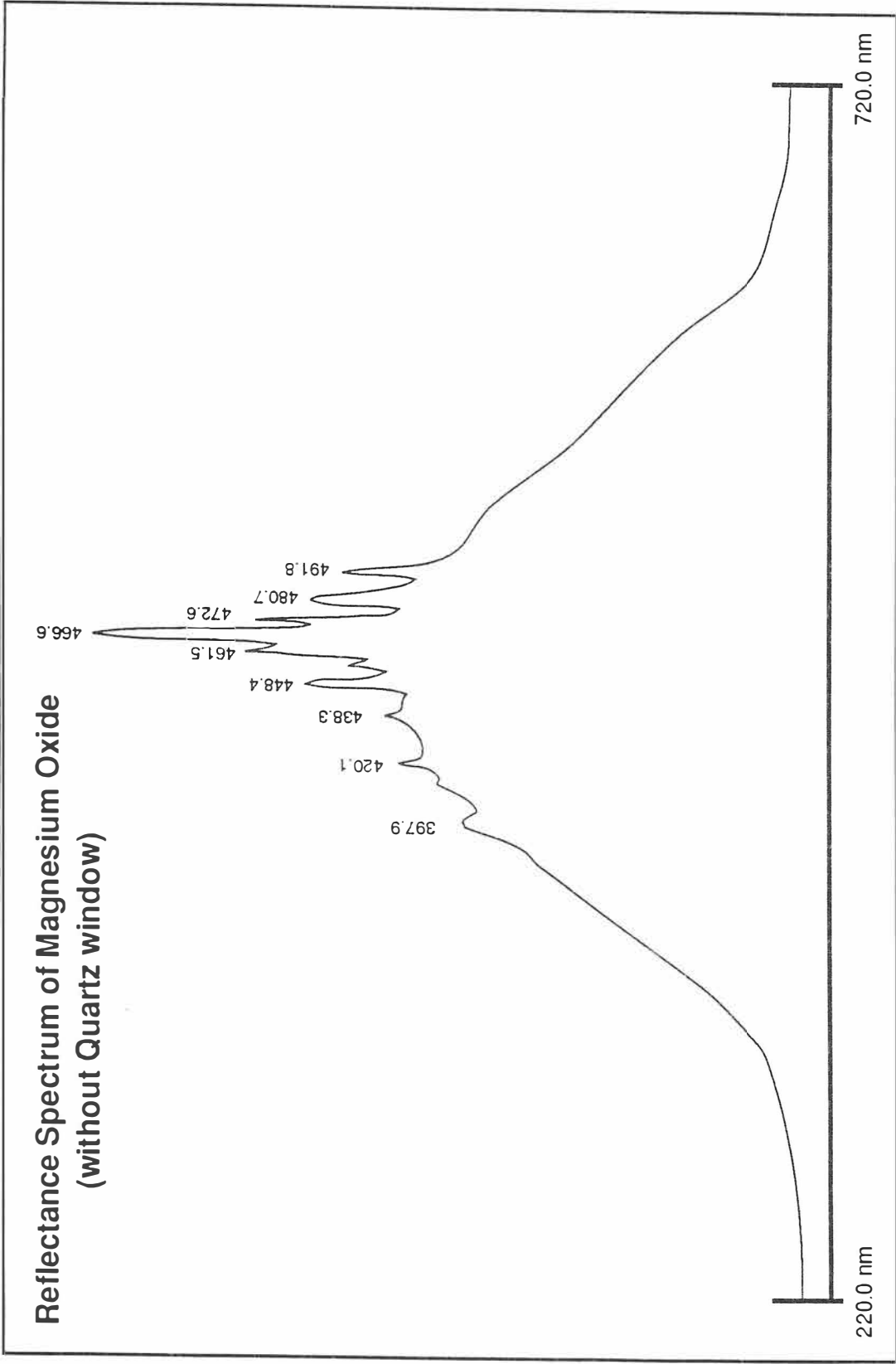
Figure 3-11. Reflectance spectrum of magnesium oxide (without quartz window).

identical peaks, both in intensity height and wavelength peak position. More importantly the reflectance spectra characterize the spectral output of the xenon lamp and it can be easily seen that there is wide variation in its intensity. Prominent peaks in the spectrum are found at approximately 397.85, 420.08, 438.27, 448.40, 461.52, 466.57, 472.63, 480.72, and 491.83 nm. The spectral radiant distribution of the same xenon lamp was obtained from the OSRAM corporation and can be found in Appendix A of this document. Prominent peaks in the OSRAM spectrum are found near 397, 420, 438, 450, 462, 467, 473, 480, and 492 nm which compares favorably to the reflectance spectra shown in Figures 3-10 and 3-11. Once the xenon lamp spectrum is known it can be used to correct for variations in its intensity with respect to the acquired spectra.

Intensity correction of the spectra obtained with the Perkin Elmer 650-10S fluorescence spectrophotometer could be a time-consuming task. One could use a computer to digitize the spectra of the xenon lamp and photomultiplier tube response and store the waveforms in memory. Likewise all acquired spectra could be digitized and stored in the computer. Using certain software packages, the waveforms could be divided and multiplied accordingly until corrected spectra are obtained, analyzed, and printed. Other techniques are probably available to achieve the same results but may hardly be worth the effort.

Therefore, the spectra presented in Chapter IV have not been corrected for variations in the excitation source or photomultiplier output. However, the need for intensity corrected spectra is not of great importance to this work since the spectral work focuses mainly on the wavelength-dependence or the wavelength peak position(s) of each spectrum. The spectra presented in this thesis work, when compared to similar spectra produced by other researchers, may exhibit slightly different intensity values for the same spectral peak or band.

Fluorescence Spectrophotometer Reproducibility

A simple statistical study was performed to analyze the reproducibility of a spectrophotometer spectral scan and to obtain a level of uncertainty in the measurement. Random errors only are presented and are due mainly to the inconsistency of the x-axis or wavelength drive motor train in the X-Y chart recorder. Other random errors may be due to operator error in resetting the excitation or emission grating dials to their proper wavelength values prior to recording a spectra, or fluctuations in the timing signals from the spectrophotometer to the X-Y chart recorder interface. Most importantly, this analysis will provide useful information as to the reproducibility of fluorescence spectra as the wavelength peaks of the spectra shift due to random errors.

The sample mean, sample variance, sample standard deviation and mean value of the sample standard deviation of the complete spectra were measured for selected fluorescence peaks of the emission spectra of $La_2O_2S:Eu^{3+}$. The arithmetic mean or average of ungrouped data for a sample is given by

$$A = \frac{\sum_{i=1}^{n} X_i}{n}$$

(3.2)

where n is the number of observations in the sample, X_i is the observed individual sample value (or peak value of a $La_2O_2S:Eu^{3+}$ fluorescence lines in this case), and A is the sample mean or mean value of the fluorescence peak.[30] The sample variance, s^2, is given by

$$s^2 = \frac{\sum_{i=1}^{n} (X_i - A)^2}{n - 1}$$

(3.3)

where the numerator is the summation of the squared deviations between each observed sample value X_i, and the sample mean A. The standard deviation s, is given by

$$s = \sqrt{\frac{\sum_{i=1}^{n}(X_i - A)^2}{n - 1}}$$

(3.4)

which is the positive square root of the variance. The standard deviation is noted as the most important calculation since it is a measure of the dispersion of the sample data from the sample mean. The more the sample data are dispersed, the higher will be the value of the standard deviation from the sample mean. The mean value of the variance of all spectral data or for all of the sample data for all six peaks is denoted by the variable M_{VAR}, is given by

$$M_{VAR} = \frac{\sum_{j=1}^{m} s_j^2}{m}$$

(3.5)

whereas the mean value of the standard deviation between all of the spectral data denoted by the variable M_{SD} is given by

$$M_{SD} = \frac{\sum_{j=1}^{m} s_j}{m}$$

(3.6)

where m is the number of samples or the number of fluorescence peaks in the $La_2O_2S:Eu^{3+}$ spectrum which was analyzed.

Using the $La_2O_2S:Eu^{3+}$ test phosphor in the spectrophotometer, 20 identical spectra (hence n = 20) were acquired, each on a separate chart. The excitation wavelength remained fixed at 345 nm while the emission wavelength began at 520 nm and ended at

640 nm for each scan. The scan speed was set at 30 nm/min and the x-axis range was increased to X5 to allow for finer resolution of the peaks. Six major fluorescence peaks (hence m = 6) were analyzed for their sample mean, variance, and standard deviation. A graphical representation of the compiled spectra for the $La_2O_2S:Eu^{3+}$ test phosphor is shown in Figure 3-12 and gives the sample mean, variance, and standard deviation values for each peak.

Table 3-2 shows a complete breakdown of the data for all 20 charts and also includes the sample mean, variance, and standard deviation values for each of the six peaks. All wavelength values are given in nanometers.

All calculations were done with a Macintosh computer using a spreadsheet program. It can be seen that the standard deviation for Peaks 1 through 6 are 0.510298, 0.476363, 0.457333, 0.277901, 0.310476, and 0.340925 nanometers respectively. Peak 1 had the largest amount of data dispersion whereas Peak 4 had the least. The standard deviation versus the mean wavelength of several emission peaks of $La_2O_2S:Eu^{3+}$ is shown in Figure 3-13.

The mean value of the standard deviation for all of the spectral data was found to be 0.395549333 nm. Therefore for this chart recorder and spectrophotometer, the dispersion of data as a function of wavelength may vary on the average of approximately 0.4 nm per spectral scan.

Using the Emission Spectrum of Europium-doped Lanthanum Oxysulfide to Analyze the Chart Recorder Reproducibility

Peak 1

A – 539.3046
SD – 0.510298
Var.= 0.260404

Peak 2

A – 556.5278
SD – 0.476363
Var.= 0.226922

Peak 3

A – 586.3972
SD – 0.457333
Var.= 0.209154

Peak 4

A – 594.1380
SD – 0.277901
Var.= 0.077229

Peak 5

A – 614.7954
SD – 0.310476
Var.= 0.096395

Peak 6

A – 623.4369
SD – 0.340925
Var.= 0.116230

520.0 nm

640.0 nm
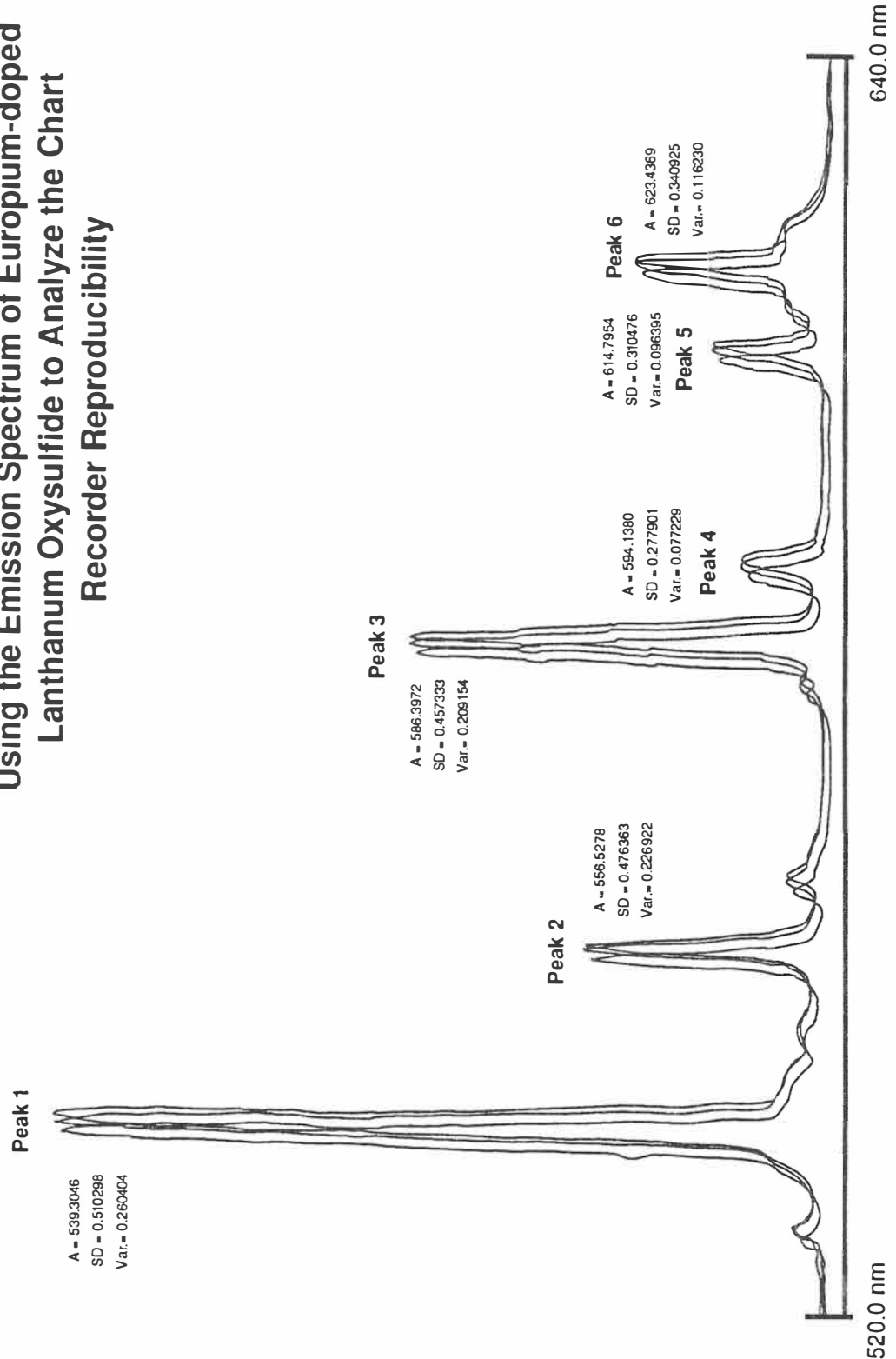
Figure 3-12. Emission spectra of europium-doped lanthanum oxysulfide for analysis of chart recorder reproducibility.

Table 3-2. Spectrophotometer reproducibility data.

Chart	Peak 1	Peak 2	Peak 3	Peak 4	Peak 5	Peak 6
Chart 1	539.5349	556.6777	586.5781	594.1528	614.4850	623.4551
Chart 2	539.0955	556.3819	586.3317	593.9698	614.8744	623.7186
Chart 3	538.8629	556.1204	586.4214	594.2475	614.7157	623.1438
Chart 4	538.5994	555.7988	585.5978	593.5975	614.3969	622.9966
Chart 5	539.9993	557.1988	587.1978	594.3975	614.9968	623.5965
Chart 6	539.0635	556.3211	586.4214	594.0468	614.7157	623.7458
Chart 7	539.2965	556.9849	586.5327	594.3719	614.8744	623.1156
Chart 8	539.4702	556.5563	586.3576	593.9073	614.9669	623.7086
Chart 9	539.9667	557.1381	586.8885	594.2762	614.6423	623.4276
Chart 10	539.6689	556.9536	586.7550	594.3046	615.1656	623.7086
Chart 11	538.8314	556.0601	585.7095	593.9232	614.3573	622.7713
Chart 12	539.5993	556.7988	586.5978	594.3975	615.1968	623.7965
Chart 13	540.3322	557.0764	586.9767	594.5515	614.8837	623.6545
Chart 14	539.8662	557.1237	587.0234	594.6488	615.5184	623.9465
Chart 15	539.6656	556.9231	586.2207	594.2475	615.1171	623.5452
Chart 16	538.9369	556.2791	586.3787	594.1528	614.8837	623.6545
Chart 17	538.9262	556.2416	586.4430	594.0940	614.6309	623.4899
Chart 18	538.5235	555.8389	585.8389	593.6913	614.6309	623.0872
Chart 19	538.7994	555.7988	585.9978	593.9975	614.3969	622.7966
Chart 20	539.0541	556.2838	585.6757	593.7838	614.4595	623.3784
Mean	539.3046	556.5278	586.3972	594.1380	614.7954	623.4369
Standard Deviation	0.510298	0.476363	0.457333	0.277901	0.310476	0.340925
Variance	0.260404	0.226922	0.209154	0.077229	0.096395	0.116230
All wavelength values given in nanometers.						
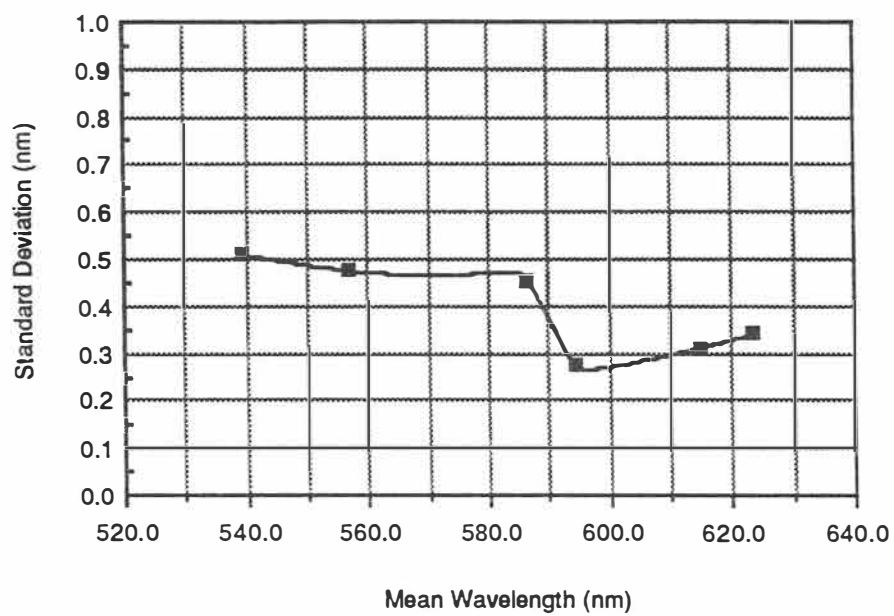
Figure 3-13. The standard deviation versus the mean
wavelength of several emission peaks of $La_2O_2S:Eu^{3+}$.

Decay Lifetime Measurements

The laser-induced fluorescence of thermographic phosphors provides a remote, non-contact method of of making high temperature measurements as describe previously. Certain temperature-dependent emission lines are selected for each phosphor and are analyzed by their exponential lifetime decays at specific temperatures. The fluorescence lifetime normally exhibits a logarithmic dependence above the onset quenching temperature of the phosphor. Europium- and dysprosium-doped phosphors have been considered in this work. Specifically, single crystals of $LaPO_4:Eu^{3+}$, $YPO_4:Eu^{3+}$, $LuPO_4:Eu^{3+}$, and $LuPO_4:Dy^{3+}$ where examined along with $YVO_4:Dy^{3+}$ and $Y_2O_2Eu^{3+}$ powders. Lifetime measurements of $YVO_4:Dy^{3+}$ powder were performed in the Precision Measurements Laboratory of the Department of Nuclear Engineering and Engineering Physics at The University of Virginia. All other lifetime measurements were made at the laboratories of the Applied Technology Division of the Oak Ridge National Laboratory in Oak Ridge, Tennessee.

The following two sections give details of the experimental configurations and methods used for making lifetime decay measurements. It should be noted that lifetime decay data for the $Y_2O_2:Eu^{3+}$ powder was not acquired as part of this research and is presented only for comparison to other phosphor lifetime measurements. The experimental configuration for $Y_2O_2:Eu^{3+}$ is described by Cates [6] and is very similar to the apparatus used in the Precision Measurements Laboratory at The University of Virginia.

Experimental Lifetime Method for $YVO_4:Dy^{3+}$

Lifetime decay measurements of the fluorescence of $YVO_4:Dy^{3+}$ were acquired using the experimental configuration shown in Figure 3-14. The measurements system utilizes a PRA nitrogen laser as an excitation source which operates at 16 kilovolts and with a 7.9 Hz repetition rate. The phosphor sample was stimulated with ultraviolet radiation at 337 nm, a primary line generated by the nitrogen laser. The Type 2370 $YVO_4:Dy^{3+}$ phosphor was obtained from Sylvania Electrochemical Division and exhibits light green-yellow fluorescence color under laser excitation. Strong fluorescence of $YVO_4:Dy^{3+}$ was observed at 485 nm and 575 nm in which the emission wavelengths were selected with a Jarrell-Ash Model 82010 monochromator. The excitation slit was set at 2000 micron while the emission slit was set at 1750 micron. An EMI photomultiplier tube was used to detect the fluorescence at the exit slit of the monochromator. The photomultiplier tube was adjusted to - 1.1 kilovolts provided by an ORTEC high-voltage power supply. The photomultiplier tube output was connected to a Tektronix 7854 digitizing oscilloscope with the vertical 7A26, horizontal 7B85, and horizontal 7B87 modules installed. The signal input was terminated with 50 Ω and 2 kΩ terminators. A Compaq DeskPro 286 computer was interfaced to the oscilloscope with the GPIB bus and was used to primarily analyze and store the acquired lifetime signals on disk. A single fiber optic cable was used to transfer laser light into a Lindberg high temperature oven whereas a bundled two cable fiber was used to collect fluorescence and transfer in to the monochromator input aperture. The hard clad silica optical fiber used in the experiment was Type 1-076, manufactured by Ensign-Bickford Optics and was polished at both ends. The fiber has a cladding diameter of 1040 μm and a core diameter of 1005 μm.
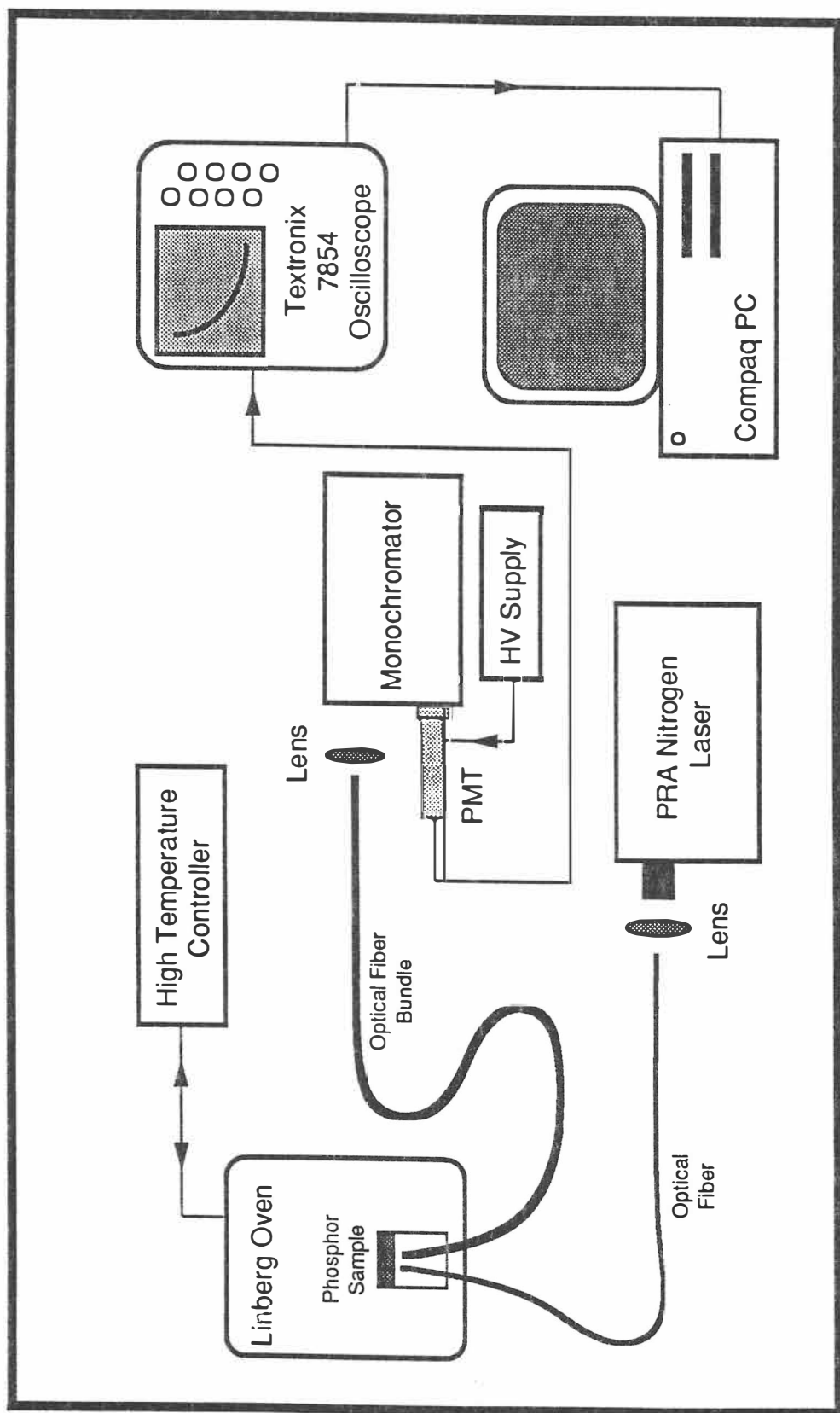
Figure 3-14. Experimental configuration for lifetime decay measurements of dysprosium-doped yttrium vanadate.

A ceramic holder was constructed for the $YVO_4:Dy^{3+}$ phosphor which was carefully placed and aligned in the oven. Under 337 nm laser excitation, a fluorescence signal was observed and then optimized for the 575nm emission line on the monochromator. Fluorescence from the phosphor was very bright. The 575nm line appears to have a higher intensity and yields a larger signal than that of the 485nm emission line. Data were initially taken at room temperature, 300°C and 350°C until all of the signal was lost due to thermal quenching and the burning of the fiber cladding in the oven. It was first thought that the fibers had simply become misaligned, however at closer inspection, it was seen that the fiber ends which were placed in the oven had actually blackened. The oven was shut down and the fibers were realigned but still no signal was observed so they were removed and inspected. The fiber ends were repolished but still there was a significant loss in light propagation down the fiber. Finally the damaged ends were stripped of the jacket covering, recleaved and polished. Another fiber was stripped, cleaved, and polished and it was combined together with the other emission fiber in order to double the fluorescence intensity detected by the monochromator. This technique worked well since the observed signal was rather large in intensity.

Lifetime data were taken at room temperature, 150, 200, 250, 300, 350, 360, 370, 380, 390, and 400°C. The laser was shut off after each lifetime signal was acquired and digitized, in order to save nitrogen gas. However the settings on the laser were marked to give approximately the same power settings. The repetition rate as mentioned before was fixed at 7.9 Hz and was not changed during experimentation. All exponential lifetime signals were acquired using the DECAY program and were stored on computer disk for future analysis. Several of the lifetime waveforms (the exponential signal and its logarithm) were photographed with the oscilloscope camera. This was done to observe any non-exponential effects in the lifetime signal.

Studies aimed at identifying the systematic errors associated with a laboratory-grade version of this type of phosphor-based thermometry system have been well documented and are summarized by Gillies.[31]   In addition, estimates for the lifetime errors were taken from a comprehensive study by Dowell [32] and the Lindberg oven temperature measurement uncertainty is estimated as 10°C as an upper bound as documented in a calibration study by Lutz.[33] Complete results of the lifetime decay analysis of YVO_4:Dy^{3+} are presented in detail and can be found in Chapter IV.

Experimental Lifetime Method for the Orthophosphate Crystals

Fluorescent decay lifetime measurements of the single crystal orthophosphates were made using a rather elaborate experimental configuration which is shown in Figure 3-15. The fluorescence of all orthophosphate samples was stimulated with a tunable laser system operating within a range of 394 to 397 nm.   For all lifetime measurements, the excitation wavelength was set to approximately 395 nm.   The creation of a 395 nm excitation line from a Nd:YAG laser was performed in a interesting way and will be described in the following two paragraphs.

A Quanta Ray DCR Nd:YAG pulsed laser operated with 1064 nm output. This 1064 nm beam (infrared) was input to a Quanta Ray Model HG-2 crystalline harmonic generator where its second harmonic line of 532 nm (green) was selected. A Quanta Ray HG-2 Crystal Temperature Controller was used to keep the harmonic generator crystals warm and at a constant temperature. The fundamental beam and the second harmonic was separated using a Quanta Ray PHS-1 Prism Harmonic Separator. The separated

63
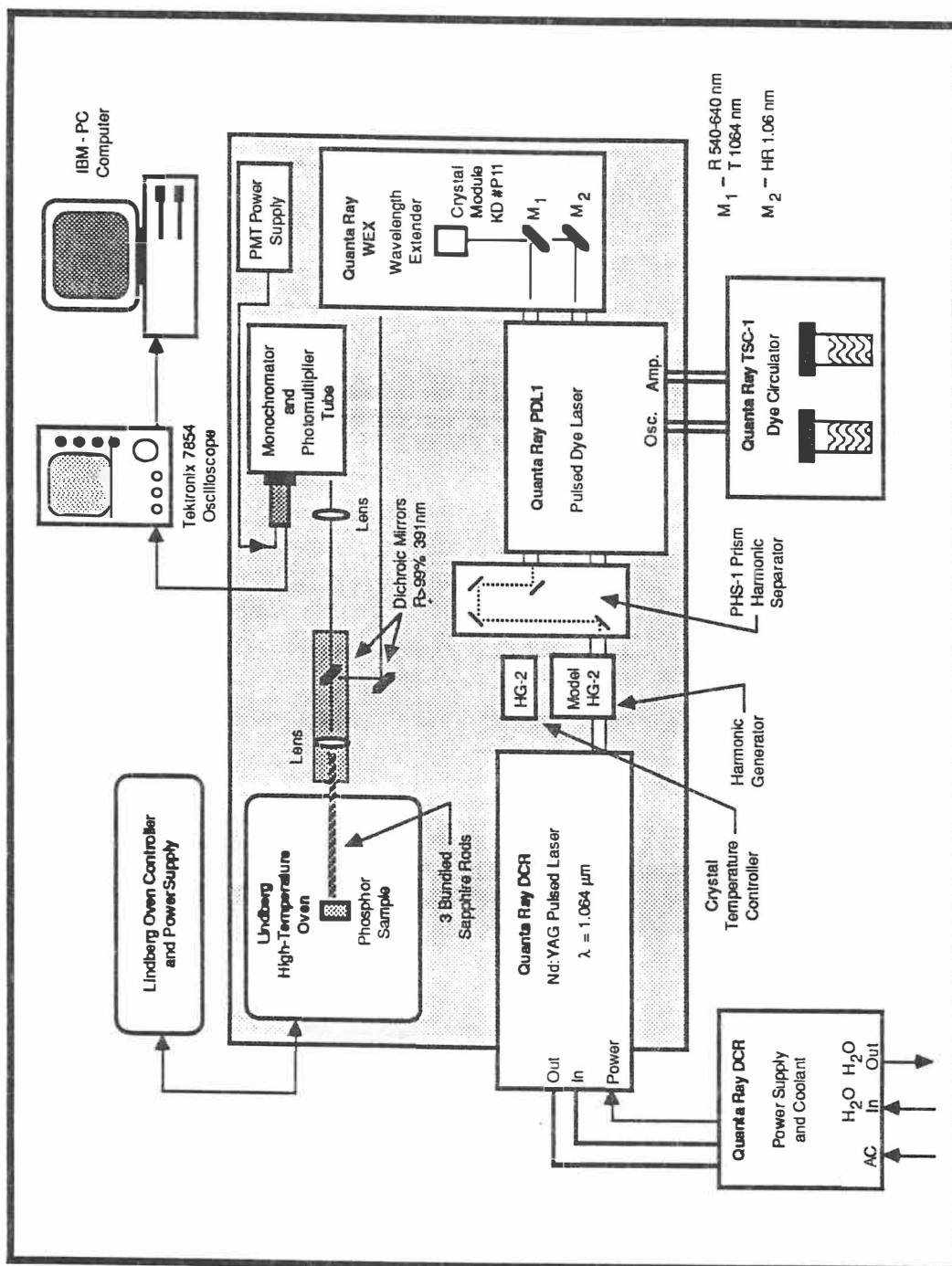
Figure 3-15. Experimental configuration for obtaining exponential lifetime data of several orthophosphate crystals.

fundamental and second harmonic beams were sent to the Quanta Ray PDL1 pulsed dye laser. The 532 nm line was used to pump an DCM red laser dye which was tuned to 628.2 nm whereas the 1064 nm line passes through the dye laser cavity.

The DCM dye was dissolved in optical-grade methanol and mixed in different concentrations for use in the oscillator and amplifier cuvettes of the dye laser. DCM which is manufactured by Exciton Incorporated, was selected because of its high tuning efficiency peak located at 640 nm. A Quanta Ray TSC-1 Dye Circulator was used to continuously circulate the laser dye throughout the oscillator and amplifier cuvettes. The 1064 nm and 628.2 nm lines are directed to the input apertures of the Quanta Ray WEX wavelength extender. A nonlinear process known as sum-frequency mixing occurs in the crystal at sufficiently high powers in which a photon is created with an energy equal to the sum of the input photons. The WEX system uses two dichroic mirrors to combine the two beams and a crystal module which contains a KDP No.11 crystal. The equation describing the sum-frequency mixing is given by

$$\frac{1}{\lambda_{WEX}} = \frac{1}{\lambda_{Laser}} + \frac{1}{\lambda_{Dye}}$$

(3.7)

where λ_{Laser} is the wavelength of the fundamental laser beam, λ_{Dye} is the operating wavelength of the dye laser and λ_{WEX} is the output or generated wavelength of the wavelength extension system. Substitution of the operating wavelengths of the experimental configuration into Equation 3.7 gives the following relationship

$$\frac{1}{395\,nm} = \frac{1}{1064\,nm} + \frac{1}{628.2\,nm}$$

(3.8)

where the 395 nm beam is actually the sum of the reciprocals of the 1064 nm and 628.2

nm lines. Therefore the output of the WEX yields the 395 nm excitation line. A schematic diagram for generating a 395 nm laser line from a 1.064 µm Nd:YAG laser using the previously described technique is shown in Figure 3-16.

The 395 nm beam was guided with planar dichroic mirrors to a short focussing lens which focussed the radiation into a bundle of three 1 mm diameter sapphire rods. Sapphire rods were chosen for their ability to transfer ultraviolet light without significant losses and for their resistance to the high temperatures generated by the oven. The dichroic mirrors used have a reflectance greater than 99% at a wavelength of 391 nm. The sapphire bundle transfers the excitation light through a small hole in the oven to the non-fluorescing ceramic sample holder which is firmly mounted inside of a Lindberg high temperature oven. The temperature of the Lindberg oven was controlled by an external control unit and has a maximum internal operating temperature of 1200°C. The fluorescence from the orthophosphate crystals was collected once again by the sapphire rods and transferred the phosphor luminescence to the entrance aperture of a McKee-Peterson quarter meter monochromator (f/8) which selects the emission wavelength. A convex lens was used to couple the fluorescence into the monochromator. The fluorescence signal was acquired by a highly-sensitive RCA photomultiplier tube which is displayed on a Tektronix 7854 digitizing oscilloscope. This particular photomultiplier tube was modified by EG&G Corporation of Las Vegas in which the dynode was optimized for linear output at higher output currents. This change allows for a larger dynamic range, increased linearity, higher output currents and most important, increased sensitivity. A EG&G ORTEC Model 456 high voltage power supply provides -2.5 kilovolts to the photomultiplier tube. Five hundred and 2 kilohm terminators were used to terminate the input signal to the oscilloscope. The oscilloscope is triggered by a 10 Hz signal from the Nd:YAG laser. An IBM AT computer is attached via an IEEE 488

66
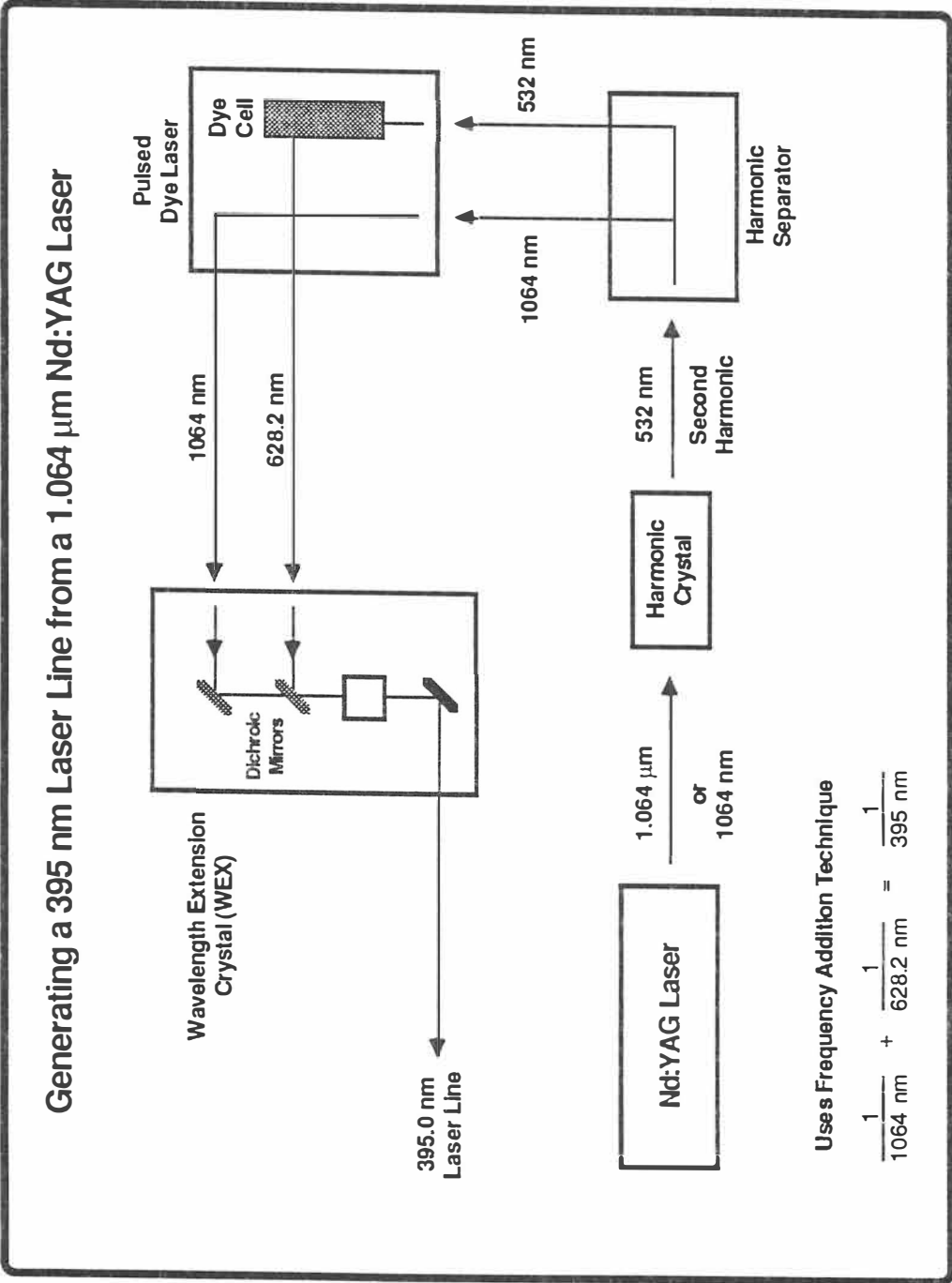
Figure 3-16. Technique for the generation of a 395 nm laser line from a 1064 nm Nd:YAG laser.

parallel bus (GPIB) and is used to store and analyze the digitized waveforms and lifetime measurements.

Most of the lifetime measurements were taken with the Nd:YAG laser set to approximately 60 Joules/pulse on the oscillator and 70 Joules/pulse on the amplifier, however higher amplifier power settings were used at higher calibration temperatures to increase the amount of fluorescence. The Quanta Ray DCR power supply provides high voltage and filtered coolant water necessary to the operation of the Nd:YAG laser. The laser flashlamp coolant water is pumped at approximately 2 gallons per minute.

Lifetime measurements for $LaPO_4:Eu^{3+}$, $YPO_4:Eu^{3+}$, and $LuPO_4:Eu^{3+}$ were made at emission wavelengths of 593.8, 593.5, and 593.0 nm respectively whereas the measurements for $LuPO_4:Dy^{3+}$ were made at 574.4 nm. A typical lifetime measurement of an orthophosphate is obtained by first positioning the ceramic crystal holder in the oven and aligning it with the sapphire rod bundle. While the oscilloscope is being observed, the holder can be translated and rotated slightly in the oven to find the optimum fluorescence signal. Likewise the grating of the dye laser can be turned to achieve the most efficient excitation wavelength. The coupling lens in front of the monochromator is positioned for maximum signal. It may also be necessary to adjust the emission wavelength and entrance aperture slit of the monochromator. Hence these procedures can be used for "tuning up the system optics". Amplitude and timebase settings are adjusted accordingly so that a good exponential signal is viewed on the screen of the oscilloscope.

A program called EXP.PRO was written for the oscilloscope to analyze the exponential fluorescence signal and a listing of the programming commands can be found in Appendix B. The oscilloscope utilizes its own unique programming language developed by Tektronix. The algorithm begins by initializing the proper amplifier and timebase plug-in modules. One hundred samples of the background are taken with the

laser excitation blocked, allowing the photomultiplier tube to detect ambient light and optical background noise (blackbody radiation from the oven in some cases) in the surrounding measurement environment. With the Nd:YAG laser in full operation, the program takes 100 samples of the fluorescence signal. The background signal is then subtracted from the acquired fluorescence signal and smoothed with a built-in waveform smoothing algorithm. A single cursor appears allowing the operator to set its value to the maximum value of the smoothed fluorescence waveform. This maximum value is multiplied by 1/exp (or 2.718281828). It should be noted that this operation is analogous to taking 36.8% of the maximum value. The first cursor is then set to the 1/exp point while a second cursor remains at the maximum value point. The lifetime is therefore given as the time between the maximum value and 36.8% (1/exp) of the maximum value.

The 1/exp criterion was used for all of the orthophosphate lifetime measurements and was chosen mainly to assure consistency in data acquisition, especially if the lifetime decay is not first-order exponential. The method helps to eliminate the ambiguity in placing the cursors on the acquired waveform thereby allowing for increased coherence between lifetime measurements of the samples.

During lifetime measurements it was sometimes necessary to adjust the monochromator aperture slits, the Nd:YAG laser power settings, and the amplifier and time-base settings on the oscilloscope to allow for the best resolution of a fluorescence signal on the oscilloscope. A background signal was always taken after each minor readjustment to the system to account for any optical noise changes in the nearby environment. Each of the raw lifetime decay signals were transferred to the IBM AT computer via the GPIB bus and were archived on disk for future analysis. The computer also has the capability to transfer the digitized waveform stored on disk back to the oscilloscope for comparison to similar acquired data. In addition to storing lifetime

signals on computer disk, oscilloscope photographs were taken of the acquired fluorescence signal superimposed on its logarithm to show any non-exponential effects in the measurement. At higher temperatures, the exponential decay signal may begin to change from a first order exponential into second- or third-order exponential making the logarithm slightly non-linear. Therefore, the more non-linear the logarithm of the raw exponential signal is, the more difficult it will become to accurately measure the lifetime from its slope.

A few other less important points about this particular lifetime experimental configuration should be mentioned. There is some concern about the bundled sapphire rods used to couple excitation and emission light into and out of the oven. It is suspected that systematic losses are most prominent at this point of the measurement system and other ways of coupling light should be investigated for future experimentation. It was interesting to note the accuracy and consistency of the 1/exp criterion (for calculating the lifetime of the phosphor) used in the Oak Ridge Applied Technology Division laboratory when compared to the DECAY program used in the Precision Measurements Laboratory of the University of Virginia. Most of the lifetime values were held to within +/-4 microseconds. In addition, the Lindberg oven temperature measurement uncertainty is estimated as 10°C as an upper bound as found in the study performed by Lutz.[33] Estimates for the lifetime errors were not analyzed. Complete results of the lifetime decay analysis of the orthophosphate crystals can be found in Chapter IV.

Background Blackbody Radiation and Thermal Leakage Effects

Blackbody radiation is normally generated by the heating elements found in the mini oven of the fluorescence spectrophotometer and in the Lindberg oven used for lifetime

decay experiments. Particularly above 700°C, blackbody radiation effects on the photomultiplier tube can be a complication in the measurement of spectra or lifetime decay. In lifetime measurements ranging from 300°C to 900°C, the blackbody background is collected by the photomultiplier tube and sampled by the digitizing oscilloscope. This background signal is then subtracted from the acquired fluorescence signal before the lifetime is analyzed. However at temperatures above 900°C, blackbody radiation becomes so intense that it makes it difficult to extract the fluorescence signal from the collected signal. In addition, since the blackbody is everpresent and behaves like a DC signal, it tends to saturate the photomultiplier tube, making the lifetime measurement even more difficult.

In regard to the phenomenon of thermal leakage, it is uncertain at this time exactly what effects the mini oven inside the fluorescence spectrophotometer has on the system optics and photomultiplier tube. Since the ceramic oven is not absolutely insulated, thermal energy does escape into the sample chamber and its surrounding environment and heats the area near the photomultiplier tube of the spectrophotometer. The temperature of the photomultiplier window was measured using an Omega HH-99A digital thermometer with a type-K (chromel-alumel) thermocouple. At an oven temperature of 350°C, the surface in front of the photomultiplier tube window was measured to be approximately 42°C. This measured temperature is high enough to possibly cause the photomultiplier to produce an inaccurate reading. A recent study has documented the effects of increased temperatures on photomultiplier tubes.[34] An increase in temperature can cause an increase in photomultiplier tube dark current, which reduces the signal to noise ratio of the instrument. The results of this study may help explain the decrease in luminescent intensity of the phosphor excitation and emission spectra taken at temperatures above 200°C.

In addition, at temperatures near 350°C, the background blackbody radiation emitted from the heating element of the mini oven tends to dominate the observed fluorescence, making it difficult to discern and detect. Therefore it is possible that at temperatures greater than 400°C, the blackbody radiation effects may completely dominate the fluorescence in this type of measurement system. On the other hand, it may also be possible that the fluorescence is being quenched at these temperatures and shows up in the spectral plots as a reduction of the fluorescence intensity peaks.

Background blackbody radiation may be reduced significantly with a fluorescence spectroscopy system that utilizes a pulsed, tunable dye laser excitation source. It may also be necessary to cool the photomultiplier tube with liquid nitrogen in an attached chamber or to use an internally-mounted fan to circulate and cool the air near the photomultiplier tube housing. Lifetime decay configurations may someday include mechanical choppers or liquid crystal display optical windows to help eliminate or reduce the amount of blackbody that reaches the photomultiplier tube. Further experimentation and several methods of reducing the effects of thermal leakage and background blackbody radiation are presented and discussed in Chapter V.

Temperature Cycling Behavior

Temperature cycling experiments detail any change in fluorescence under repeated large temperature excursions. In many aspects, temperature cycling is similar to signal and lifetime reproducibility. The need for these data is most useful to applications which utilize the thermophosphor technique. Some temperature cycling work has been done in the past with $La_2O_2S:Eu^{3+}$ phosphors.[4] Fluorescence variation can possibly occur from

dopant ion concentration changes by ion drift or migration within the lattice, from a host lattice structure configuration change, or even a chemical breakdown of the phosphor compound. These effects were not characterized as part of this research but should be investigated in future thermophosphor work for both the powder and orthophosphate phosphors.

Calculation of the Onset Quenching Temperature

The onset quenching temperature of thermographic phosphors can now be easily determined with the use of a computer program developed as part of this thesis project. Using the method of best-fit or linear regression, two equations linearly approximate the lifetime calibration curve (data) of a thermographic phosphor and determine the initial point of temperature dependence. This point is actually the intersection of the two lines. A graphical representation of this method is shown in Figure 3-17.

The method is used to define a consistent and mathematically simple criteria for onset quenching temperature. In the past, the onset quenching temperature point was graphically estimated at the knee of the calibration curve but was never quantified. Several other criteria were considered for onset quenching temperature such as taking the temperature point which is 10% of the maximum value of the lifetime, graphically analyzing of the curve, or using any other statistically measured value which may be fitted consistently to the "knee" of the lifetime calibration curve.

Using the linear best-fit relationship between two sets of n data which include the points (x_1, y_1), (x_2, y_2), $\cdots$, (x_n, y_n), the equation for the line of
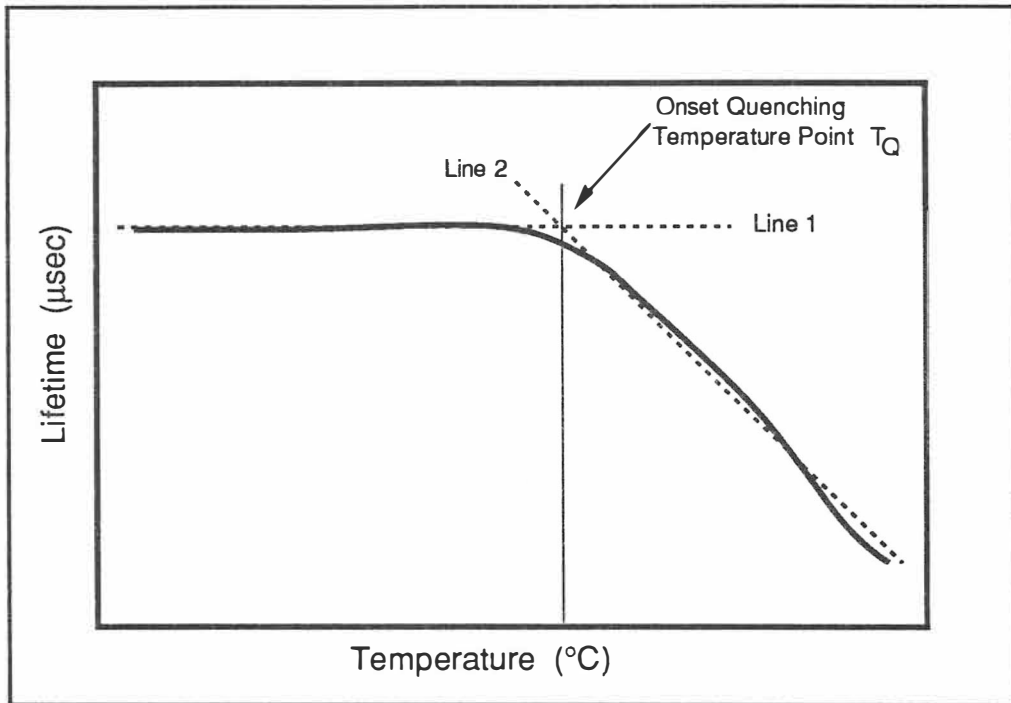
Figure 3-17. Method used for determining the onset

quenching temperature of a thermographic phosphor.

best-fit is given as

$$y_i = mx_i + b \tag{3.9}$$

where the slope of the line m and y-intercept b are given by

$$m = \frac{n \sum_{i}^{n} x_i y_i - \sum_{i}^{n} x_i \sum_{i}^{n} y_i}{n \sum_{i}^{n} x_i^2 - \left(\sum_{i}^{n} x_i\right)^2}$$

$$\tag{3.10}$$

$$b = \frac{\sum_{i}^{n} y_i \sum_{i}^{n} x_i^2 - \sum_{i}^{n} x_i \sum_{i}^{n} x_i y_i}{n \sum_{i}^{n} x_i^2 - \left(\sum_{i}^{n} x_i\right)^2}.$$

(3.11)

Consequently the line of best-fit is also defined as the line which minimizes the sum

$$\sum_{i=1}^{n} \left| y_i - (mx_i + b) \right|.$$

(3.12)

This sum is the total of the lengths (if all lengths are considered to be nonnegative) of the vertical distances from the data points to the best-fit line.[35] Since a typical lifetime decay curve consists of two near linear data regions, two linear equations can be written

$$y = m_1 x + b_1$$

(3.13)

$$y = m_2 x + b_2$$

(3.14)

where Equation 3.13 describes the equation of the line for the data that is not temperature-dependent and Equation 3.14 represents the equation of the line for the temperature-dependent part of the calibration curve. In order to find the intersection points (x, y) of the two lines, one may use Cramer's rule and determinants. The solution to the x-value point or the onset quenching temperature point T_Q can be found by solving

$$x = \frac{\begin{vmatrix} 1 & b_1 \\ 1 & b_2 \end{vmatrix}}{\begin{vmatrix} 1 & m_1 \\ 1 & m_2 \end{vmatrix}}$$

(3.15)

which can be reduced to

$$T_Q = x = \frac{|b_2 - b_1|}{|m_2 - m_1|}.$$

(3.16)

Similarly the lifetime value at the onset quenching temperature point can be found using the same methods but solving for the y-value of the two linear equations.

The theory as described above was developed into a menu-driven computer program which is used to determine the onset quenching temperature given a lifetime calibration curve. The original computer program, named CALQUEN.BAS Version 1.00, was written 'in Microsoft BASIC for any personal computer that will run MS-DOS. However, the program code can be simply converted to run on any other machine such as an Apple Macintosh or DEC VAX. A complete program listing of CALQUEN.BAS can be found in Appendix C.

Using the program is easy. The main menu allows the user to input lifetime data manually, input data stored in an external data file, obtain help with the program, or quit the program. If data are input manually, the program has an option which will allow the user to store data to disk for later use. The program constantly checks and reports input and file-handling errors and has a built-in option which will print data to a line printer for data input verification. It should be noted that all data files should include the filename extension .DAT, which must be included when the program requests a filename. The extension must be typed as part of the filename since the program will not append this

extension. Perhaps future versions of this program will allow for more elaborate data structures and filename variables. The calculations section of the program linearly fits the data, calculates the slope m and y-intercept of each line and reports a temperature value for the onset quenching point of the phosphor being analyzed. The user once again has the option to proceed with more calculations and/or obtain a complete printout of the results of the analysis. Results of this computer analysis of the onset quenching temperature are described later in Chapter IV.

CHAPTER IV

DISCUSSION OF RESULTS

Excitation and Emission Spectra at Room and Elevated Temperatures

The excitation and emission spectra of fifteen powder and crystalline phosphors were measured at room temperature and at elevated temperatures ranging from approximately 22°C to 400°C. The experimental apparatus described in Chapter III was used to acquire this spectral data. In particular, these phosphors are activated with the rare-earth elements dysprosium, europium, gadolinium, manganese, praseodymium, and terbium. Observations of the experimental results show that certain absorption lines in the excitation spectra of both phosphors are temperature-dependent.

In the excitation spectra taken from room temperature to approximately 400°C, the phosphors $Y_2O_3:Eu^{3+}$, $YVO_4:Eu^{3+}$, $Ba_3(PO_4)_2:Eu^{2+}$, $LaPO_4:Eu^{3+}$, $LuPO_4:Eu^{3+}$, $YPO_4:Eu^{3+}$, $YVO_4:Dy^{3+}$, $Y_2O_2S:Eu^{3+}$, and $Y_2O_2S:Tb^{3+}$ exhibit a significant temperature-dependent shift in their charge-transfer absorption band. The majority of these phosphors are europium-doped in which their charge-transfer shift is much larger than the other two phosphors doped with dysprosium and terbium. In general, the charge-transfer band of these particular phosphors exhibits a shift towards the red (or to lower energies) with an increase in temperature. Graphs of the peak charge-transfer wavelength versus temperature for several of the europium-doped phosphors show that this temperature-dependent shift is linear.

In light of the theoretical discussion of Charter II, one possible factor that may be

causing this shift is the increased crystal lattice spacing between the host crystal and the dopant europium (or dysprosium and terbium) activator. At elevated temperatures, the charge-transfer band does not actually change itself, however the relative position of the transition from its base ground state to the charge-transfer state has changed. This characteristic is observed as the spectral shift in the charge-transfer absorption band in the excitation spectra. For example, at room temperature, the transition to the charge-transfer state starts from the ground state of the host atom. At a much higher temperature, the transition to the charge-transfer state does not actually start at the ground state (as it did at room temperature) but at a vibrational level higher up on the energy level configuration coordinate diagram.

It was observed that phosphors with charge-transfer bands deeper into the ultraviolet region or located at higher charge-transfer state energies yield higher onset quenching temperatures. The measurement of decay lifetimes for these phosphor provides more evidence on the previous statement and details are discussed further on in this chapter. It was also found that the peak of the charge-transfer band is located at higher energies as a function of the decrease in the cation radius of the host crystal lattice. In particular, the excitation spectra of the europium-doped orthophosphate crystals show the differences of the locations of the charge-transfer bands. The specific locations of the charge-transfer bands in the orthophosphates will be presented later in this chapter.

It was generally observed in both the excitation and emission spectra of the thermophosphors, that the luminescent intensity decreased as the temperature was increased. The charge-transfer bands of the majority of the phosphors also tend to broaden at higher temperatures. Both of these phenomena can be verified through the observation of the phosphor spectra. As previously mentioned in Chapter III, it is suspected that the observed decrease in luminescent intensity may be due to either background blackbody radiation, an increase in the photomultiplier dark current,

quenching of the phosphor, or possibly a combination of these. Future research may help identify the mechanisms which cause this phenomenon to be observed.

One advantage of an increased spectral shift of the charge-transfer absorption band towards the red is that lasers of longer excitation wavelengths can be used to stimulate the fluorescence of the phosphor samples at higher initial temperatures, thus making these lasers useful in high temperature measurement applications. For example, if a particular phosphor has a charge-transfer band located at a peak wavelength of 260 nm at room temperature, one would need a laser operating at 260 nm to obtain maximum absorption by the phosphor during excitation. Lasers with output at this wavelength are generally hard to find. However if the charge-transfer band of this same phosphor is located near 335 nm at a temperature of 800°C, one could use a nitrogen laser operating at 337 nm for the excitation of the fluorescence.

In the pages that follow, can be found the spectra of all the phosphors that were researched as part of this thesis. It should be noted that the spectral results are organized and presented by the dopant element of the phosphor. In some cases where a significant shift of the charge-transfer band is observed, the data for its peak position are presented in tabulated form and graphed.

Dysprosium-doped Yttrium Vanadate (YVO_4:Dy^{3+})

Dysprosium-doped phosphors under excitation exhibit a fluorescence color that appears yellowish-green to the eye. Two strong emission areas are visible in the emission spectra and are centered around 480 nm and 575 nm. This bright emission is mainly due to the $^4F_{9/2}$-$^6H_{15/2}$ transitions for the 480 nm group and $^4F_{9/2}$-$^6H_{13/2}$ for the 575 nm group as described in a study by Blasse.[36]

The excitation and emission spectra of dysprosium-doped yttrium vanadate were measured at room temperature and at elevated temperatures ranging from 26°C to 295°C. The room temperature excitation spectrum for the 571 nm emission line of $YVO_4:Dy^{3+}$ can be found in Figure 4-1. Most of the absorption occurs in the charge-transfer band located at 330.0 nm whereas a smaller absorption peak is found at 364.0 nm. Figure 4-2 shows a room temperature emission spectrum taken under 330 nm excitation. Two fluorescence groups were measured at 481 nm and 570 nm. Figure 4-3 shows the same room temperature emission spectrum in its expanded form to give higher resolution of the two fluorescent groups. Strong lines of emission in this spectrum are found at 473.6, 480.6, 483.3, 570.0, 572.3, and 575.9 nm.

The excitation and emission spectra of $YVO_4:Dy^3$ measured as a function of temperature are shown in Figures 4-4 and 4-5 respectively. There is a significant spectral shift towards the red in the charge-transfer band of the excitation spectra of $YVO_4:Dy^3$. At 26°C the peak of the charge-transfer band is located at 321.2 nm whereas at 295°C it has been relocated to 344.4 nm, an overall shift of 23.2 nm in roughly 270°C. One may notice a second order line located at 286.0 nm in the spectrum of 295°C. It is also interesting to note the broadening of the band along with the decrease in luminescent intensity as the phosphor temperature increases.

The high resolution emission spectra taken measured as a function of temperature shown no significant spectral shifts although there is a reduction of luminescent intensity at a temperature of 250°C. This emission spectrum at 250°C shows two peaks located at 482.5 and 570.0 nm.
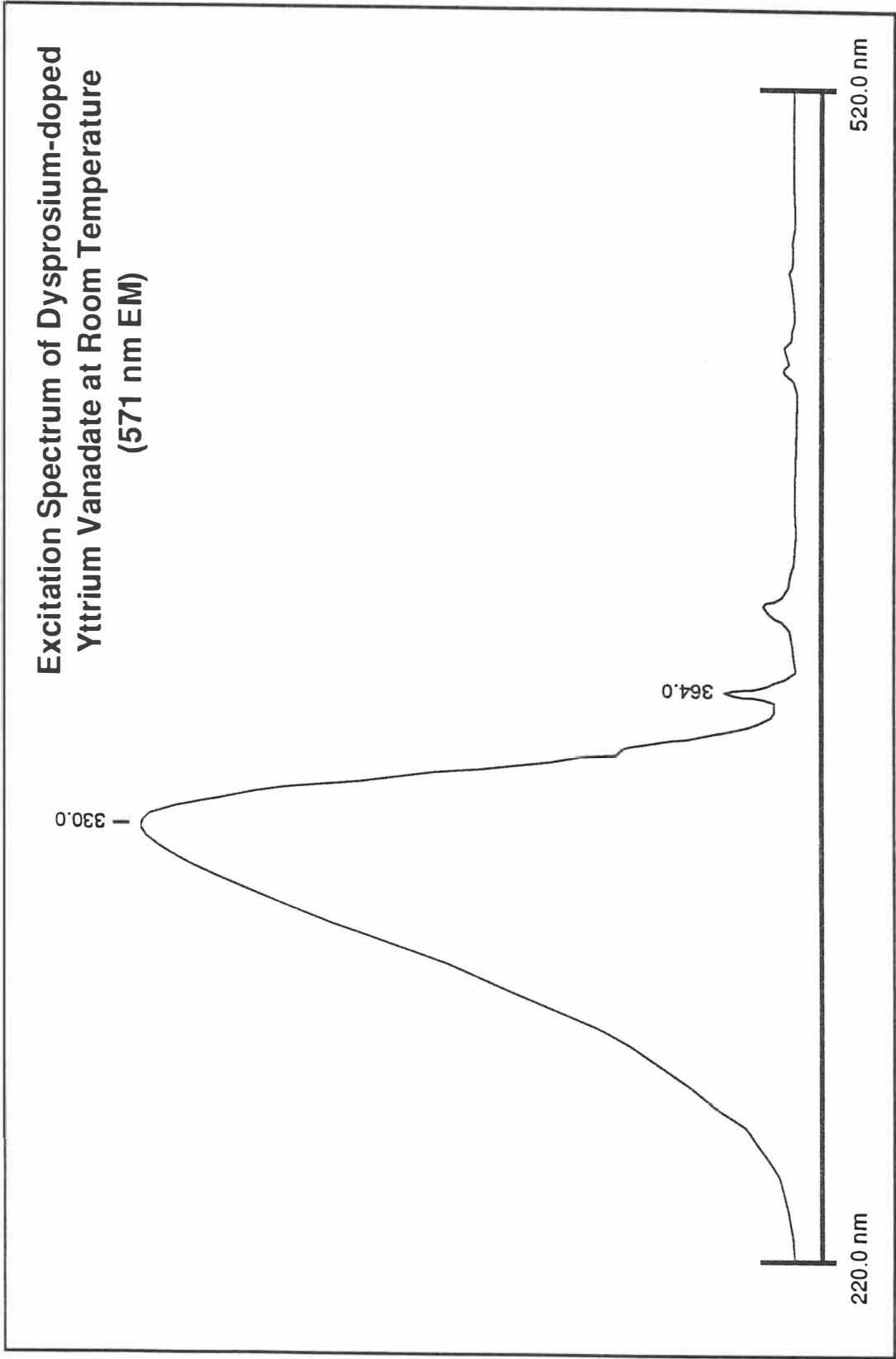
Figure 4-1. Excitation spectrum of dysprosium-doped yttrium vanadate at room temperature (571 nm EM).
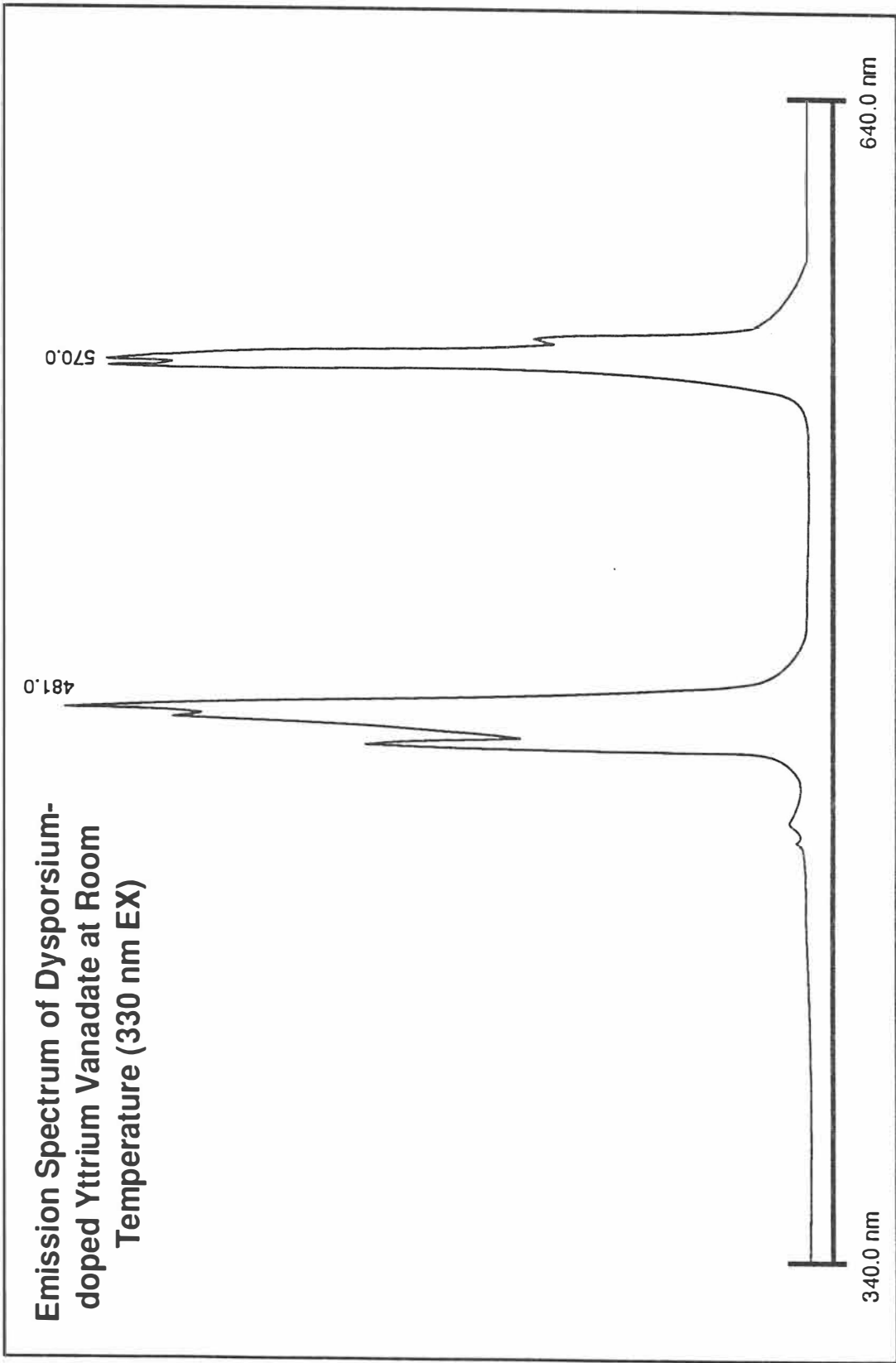
Figure 4-2. Emission spectrum of dysprosium-doped yttrium vanadate at room temperature (330 nm EX).
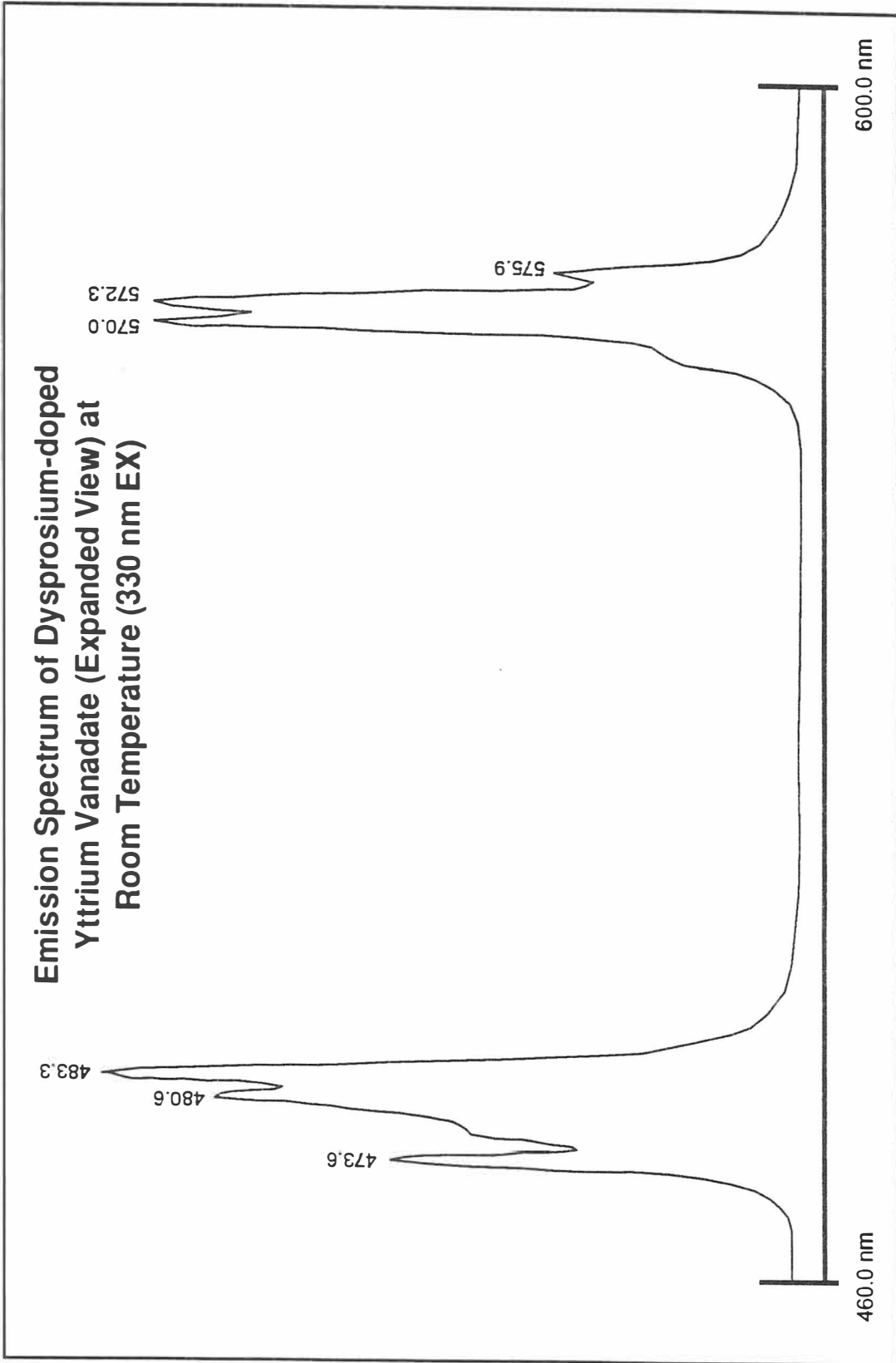
Figure 4-3. Emission spectrum of dysprosium-doped yttrium vanadate (expanded view) at room temperature (330 nm EX).

84
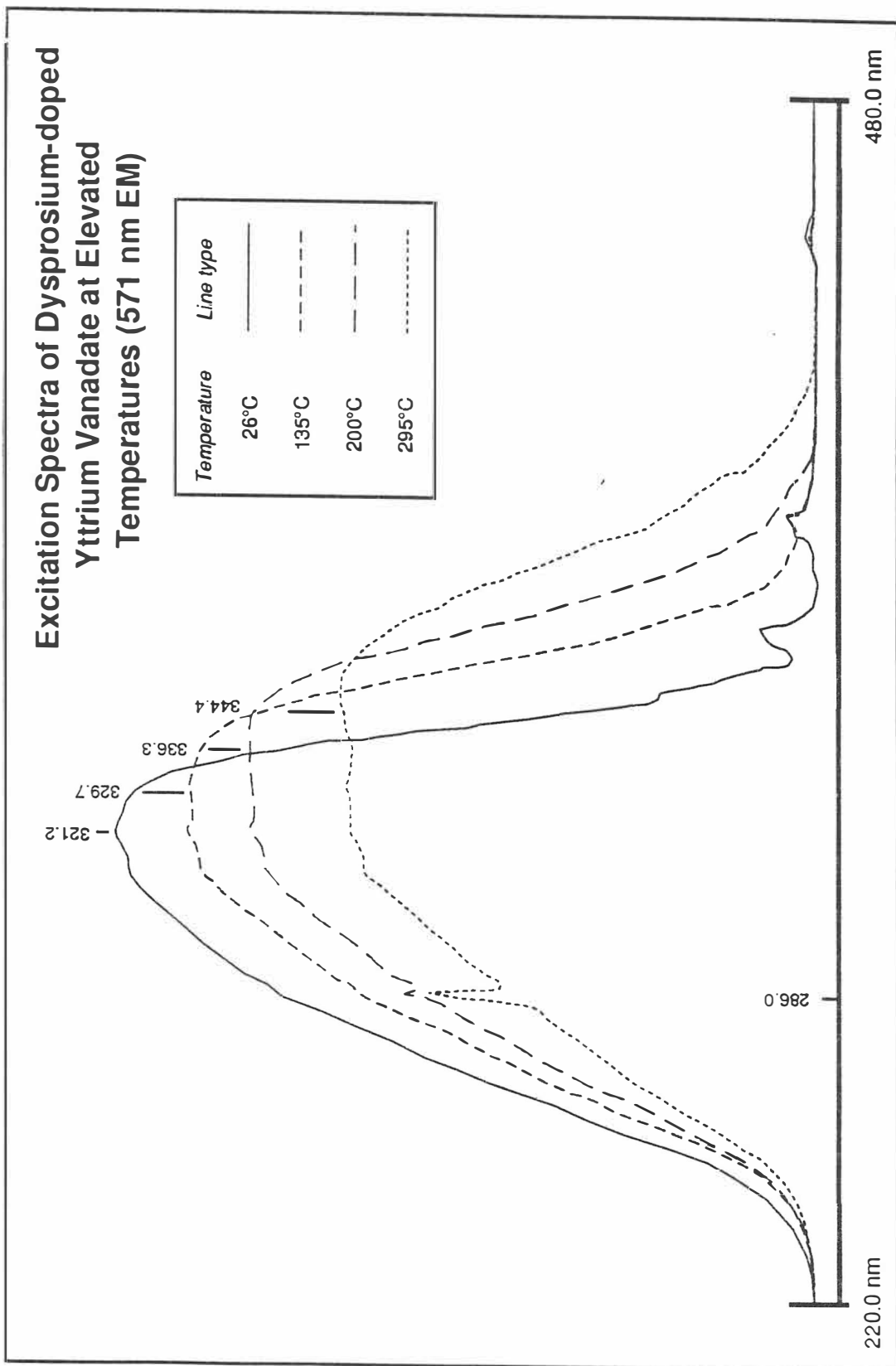
Figure 4-4. Excitation spectra of dysprosium-doped yttrium vanadate at elevated temperature (571 nm EM).
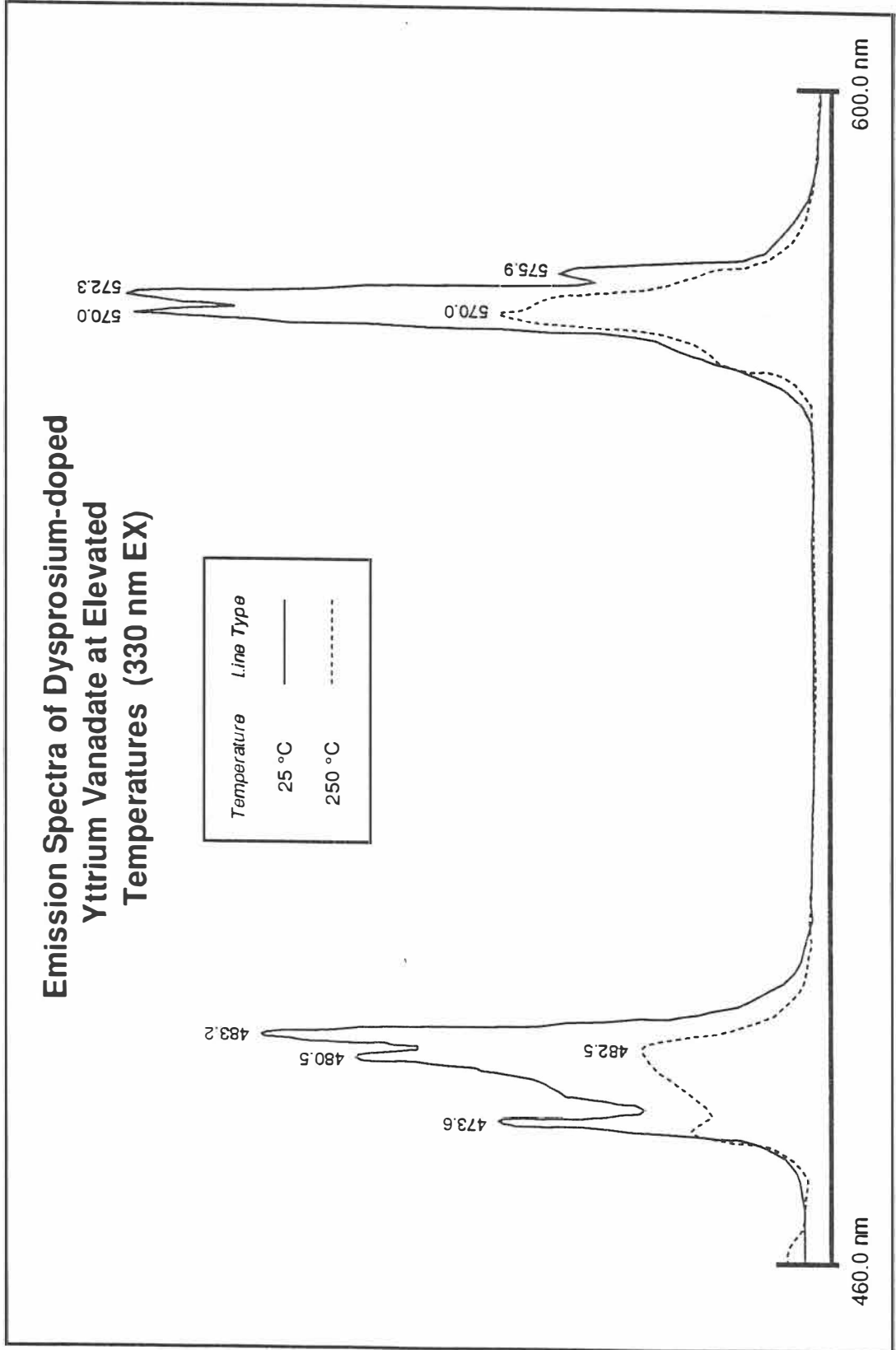
Figure 4-5. Emission spectra of dysprosium-doped yttrium vanadate at elevated temperatures (330 nm EX).

Dysprosium-doped Yttrium Oxide (Y_2O_3:Dy^{3+})

The excitation and emission spectra of dysprosium-doped yttrium oxide were measured at room temperature and at elevated temperatures ranging from 23°C to 350°C. The room temperature excitation spectrum for the 571 nm emission line of Y_2O_3:Dy^{3+} can be found in Figure 4-6. There is no evidence of any major charge-transfer band in this spectrum however there are several other absorption bands which were detected. A strong absorption peak is found at 349 nm whereas other less intense peaks are found at 295, 324, 363, 383, 395, 423, 445, and 454 nm. Figure 4-7 shows a room temperature emission spectrum taken under 349 nm excitation. Two fluorescence groups are located at 485 nm and 571 nm, however unlike the emission spectrum of YVO_4:Dy^{3+}, it is difficult to resolve the other peaks of emission located in the two groups. The 571 nm line should be noted for its strong fluorescence.

The excitation and emission spectra of Y_2O_3:Dy^3 measured as a function of temperature are shown in Figures 4-8 and 4-9 respectively. There is a no significant spectral shift towards the red in any of the peaks of the excitation spectra of Y_2O_3:Dy^{3+}. It may be possible that there are charge-transfer bands located near 240 nm of the spectra however it is unknown at this time if these bands are indeed true charge-transfer bands. Since the spectrophotometer has not been intensity corrected, it may be possible that these bands were not truly resolved. The other peaks of absorption lie at approximately the same location as those in the room temperature spectrum. It is also interesting to note that there is not a drastic reduction in luminescent intensity as the temperature increases which is characteristic of the excitation spectra of most of the other phosphors researched. The emission spectra (with two groups located at roughly 485 nm and 571.0 nm) measured as a function of temperature shown no significant spectral shifts although there is a reduction of luminescent intensity at a temperature of 250°C.

Figure 4-6. Excitation spectrum of dysprosium-doped yttrium oxide at room temperature (571 nm EM).

Figure 4-7. Emission spectrum of dysprosium-doped yttrium oxide at room temperature (349 nm EX).
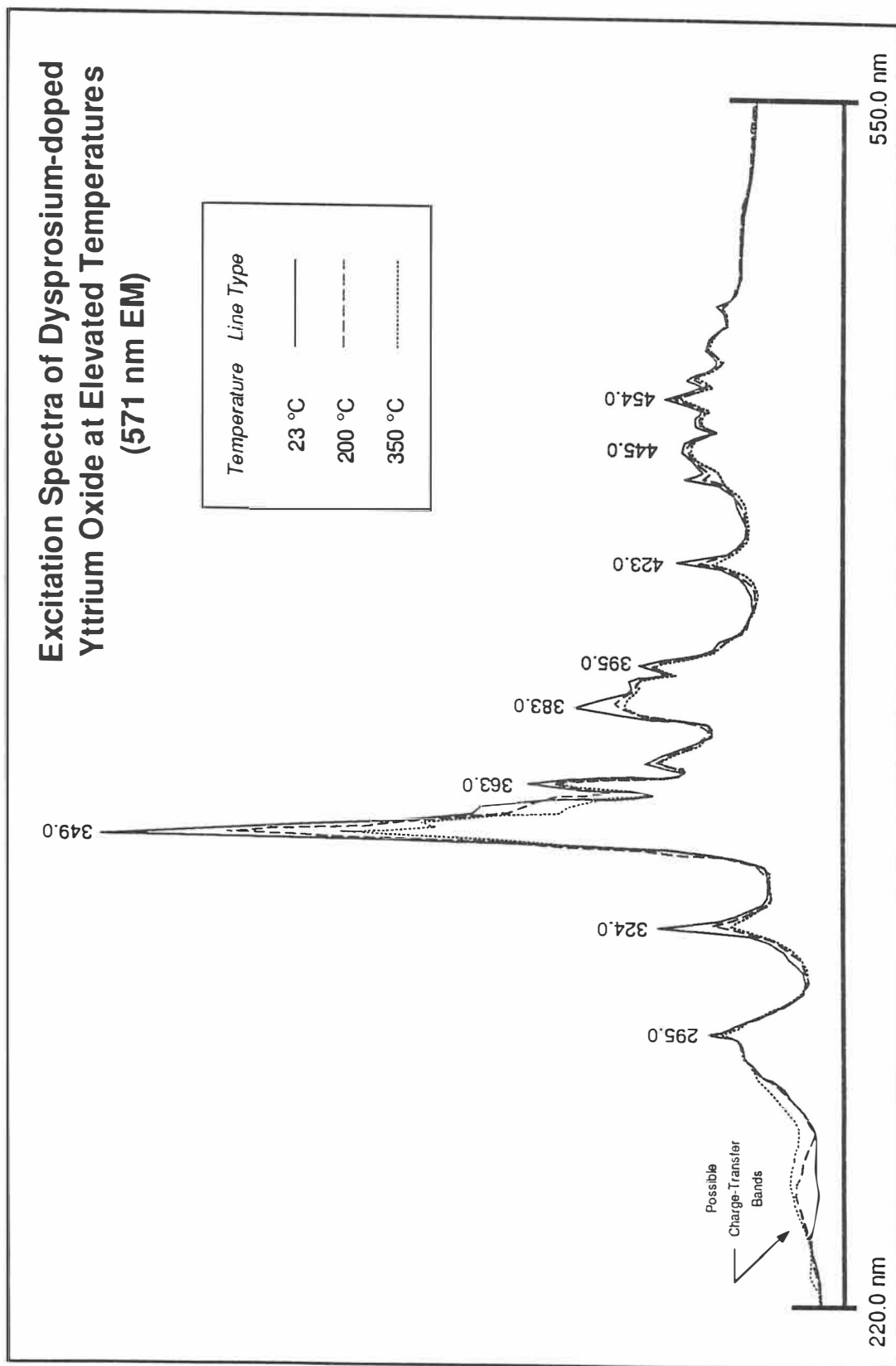
Figure 4-8. Excitation spectra of dysprosium-doped yttrium oxide at elevated temperatures (571 nm EM).
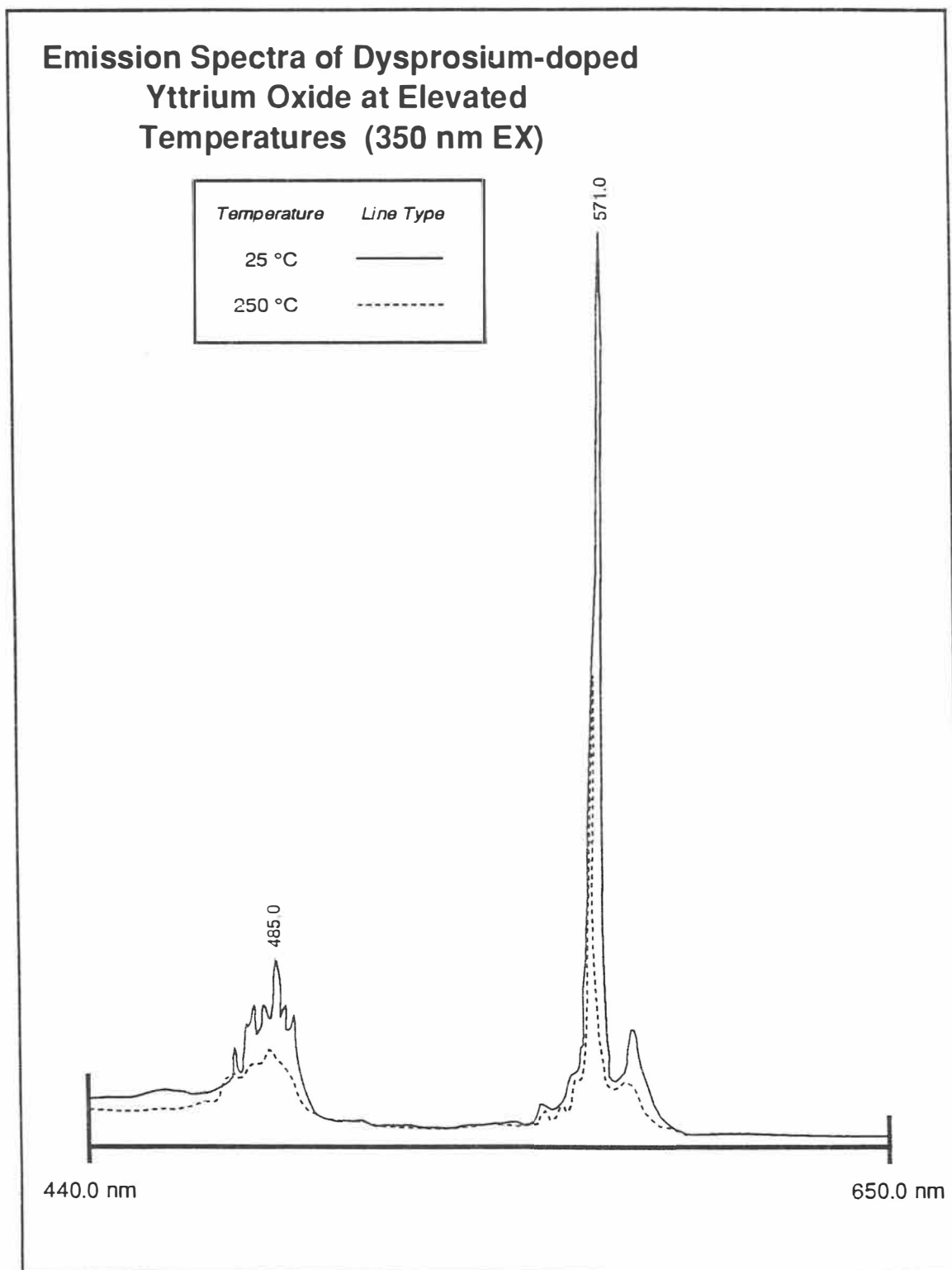
Figure 4-9. Emission spectra of dysprosium-doped yttrium oxide
at elevated temperatures (350 nm EX).

Dysprosium-doped Lutetium Phosphate ($LuPO_4$:Dy^{3+})

The room temperature excitation spectrum for $LuPO_4$:Dy^{3+} is shown in Figure 4-10 and is obtained at an emission wavelength of 573 nm. No charge-transfer band was evident in the spectrum. Strong lines of absorption are located at 327, 353, 361, and 390 while less intense peaks are found at 258, 296, 339, 382, 399, 429, 451, and 474 nm.

The room temperature emission spectrum for $LuPO_4$:Dy^{3+} at 353 nm excitation is shown in Figure 4-11. Two fluorescence groups were measured near 480 nm and 573 nm. The same room temperature emission spectrum shown in Figure 4-12 was expanded to give better resolution of the emission lines within each group. The 480 nm group consists of lines of emission at 475.7, 478.7, 483.1, and 485.8 nm whereas the 575 nm group consists of three emission lines located at 568.3, 572.9, and 578.7 nm.

Excitation spectra of $LuPO_4$:Dy^{3+} taken at elevated temperatures are presented in Figure 4-13 and Figure 4-14 for the 484 nm and 573 nm emission lines respectively. At 484 nm emission, the major lines of excitation are located at 326.5, 352.8, 365.9, and 388.5 nm. Other lesser significant lines of excitation are located at 295.9, 339.2, and 388.5 nm. For emission at 573 nm, the dominant lines of excitation are 327.3, 353.0, 366.7, and 389.9 nm. Other lesser significant lines of excitation are located at 395.0, 428.8, 451.1, and 474.4 nm.

In the excitation spectra at high temperature of an emission wavelength of 484 nm, it can be seen that there is little quenching of fluorescence at 390°C as compared to the 573 nm emission at 285°C where quenching has already begun. It is possible that the 484 nm line of $LuPO_4$:Dy^{3+} may have a higher onset quenching temperature during lifetime decay calibration. The lifetime decay data for $LuPO_4$:Dy^{3+} was taken at an emission wavelength of 575 nm and results of the measurements are presented later in this chapter. In both of the excitation spectra, a charge-transfer band is not visible in the spectral plot.

Figure 4-10. Excitation spectrum of dysprosium-doped lutetium phosphate at room temperature (573 nm EM).
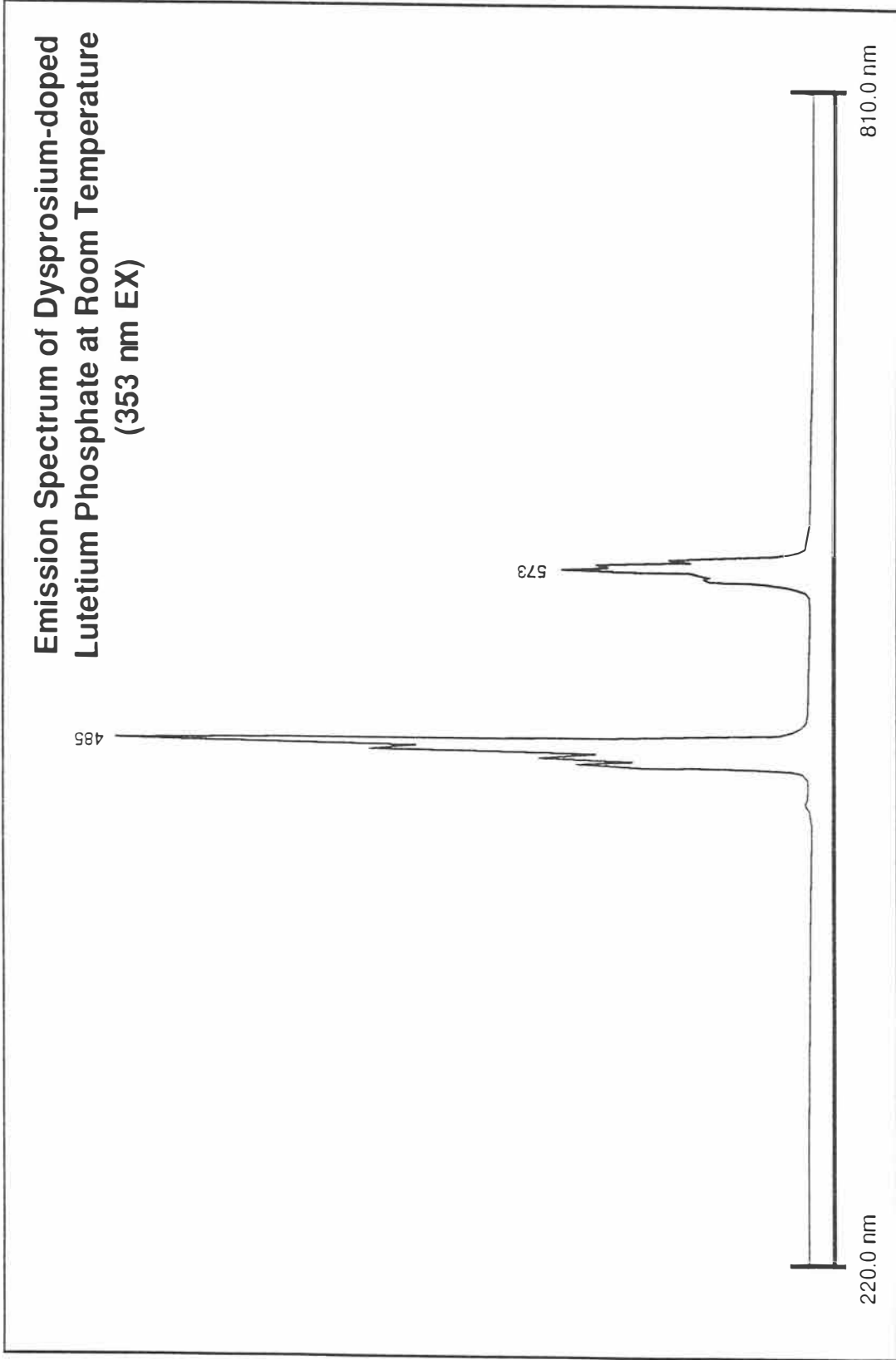
Figure 4-11. Emission spectrum of dysprosium-doped lutetium phosphate at room temperature (353 nm EX).
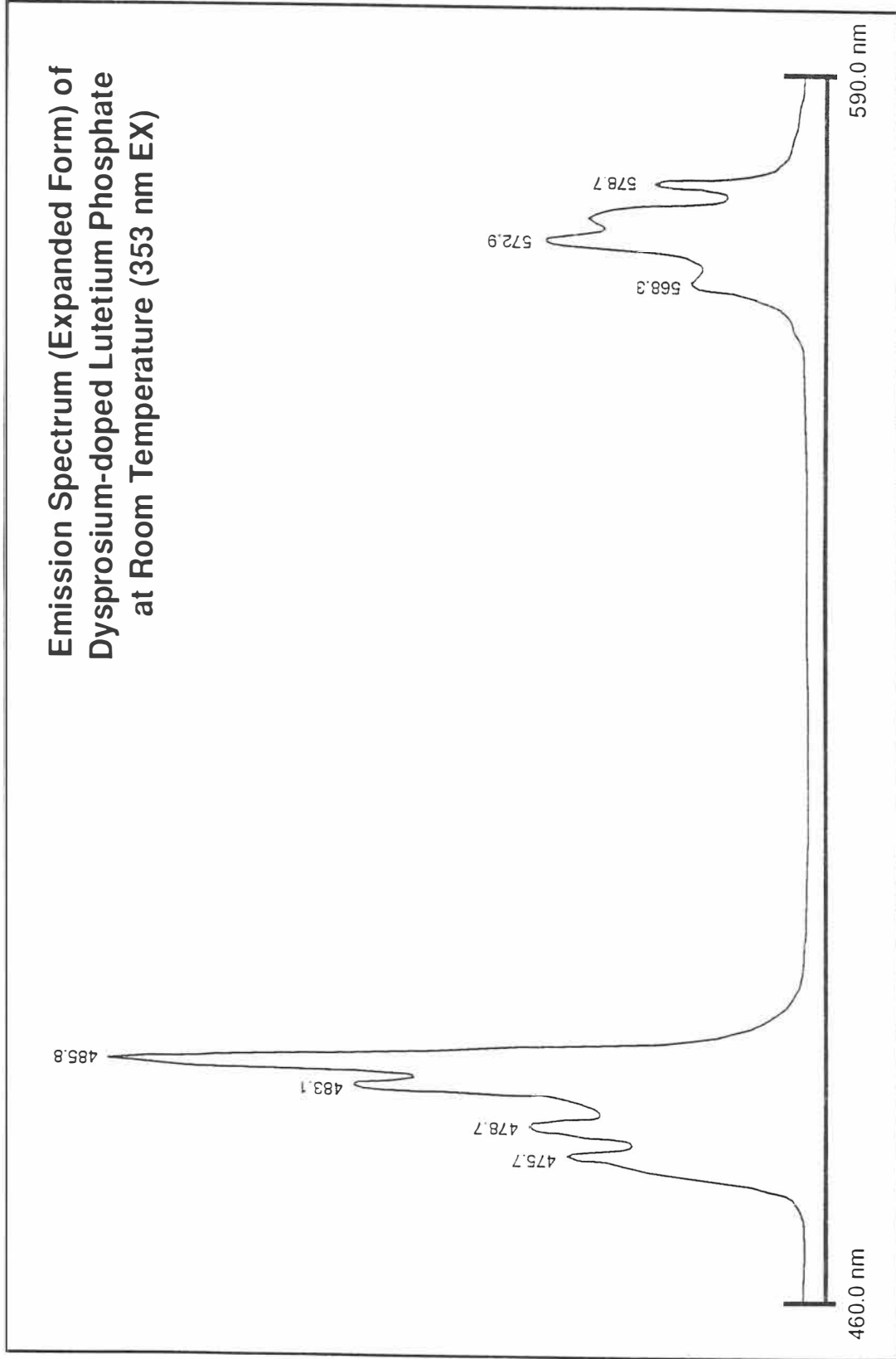
Figure 4-12. Emission spectrum (expanded form) of dysprosium-doped lutetium phosphate at room temperature (353 nm EX).

Figure 4-13. Excitation spectra (expanded form) of dysprosium-doped lutetium phosphate at elevated temperatures (484 nm EM).
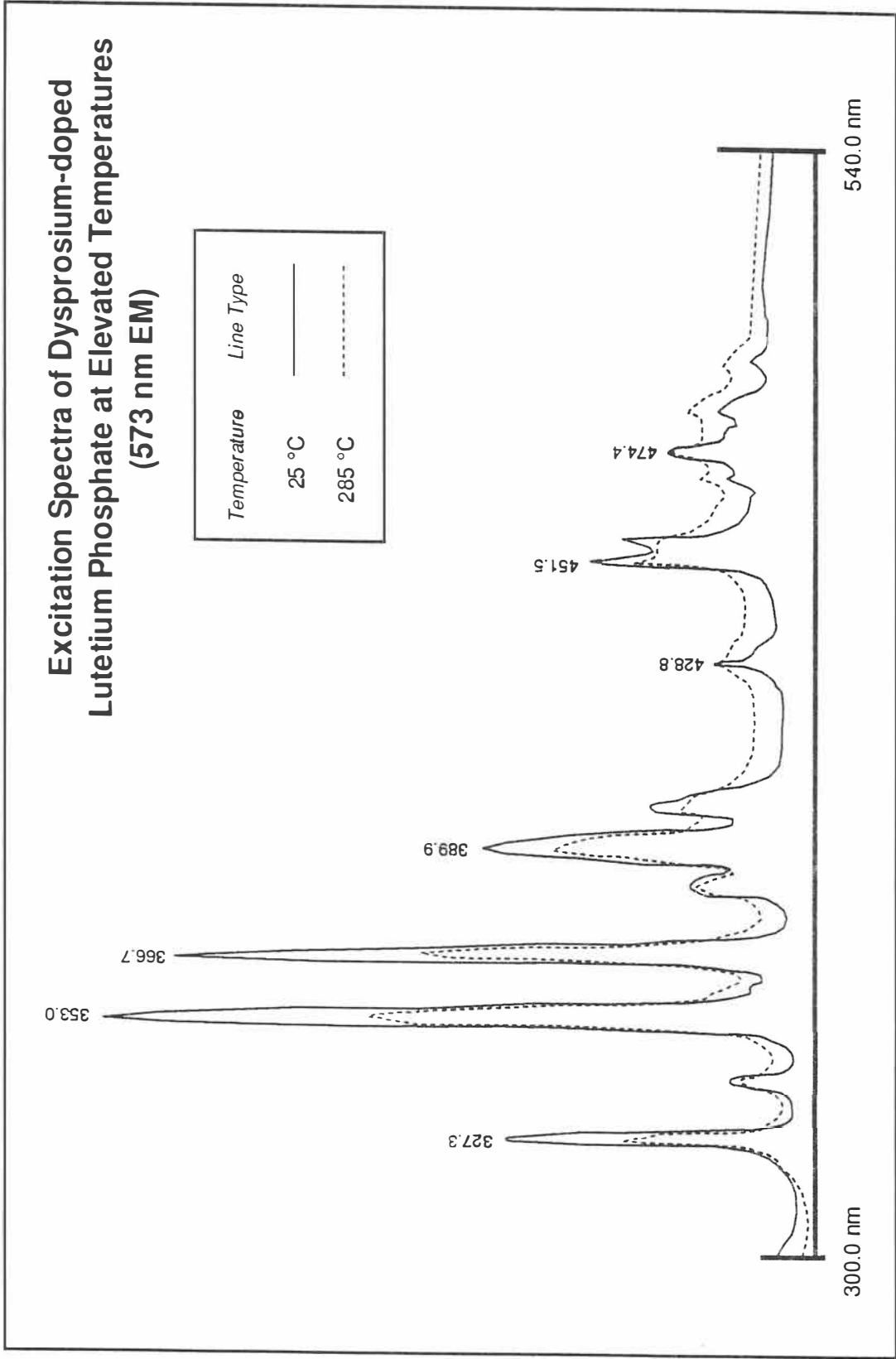
Figure 4-14. Excitation spectra of dysprosium-doped lutetium phosphate at elevated temperatures (573 nm EM).

Emission spectra of $LuPO_4:Dy^{3+}$ acquired at elevated temperatures (25°C and 250°C) are presented in Figure 4-15. Lines of emission are found at 475.5, 478.5, 483.0, 485.8, 568.0, 573.0, and 578.8 nm. It can be seen in these spectra that the emission intensity is still rather strong at the higher temperature. Since the dysprosium ion has no charge-transfer transitions, and the energy gap between the ground state and $^4F_{9/2}$ state is somewhat larger than europium, it is expected that the onset quenching of its luminescence may occur at higher temperatures. For this reason, $LuPO_4:Dy^{3+}$ is of great interest to thermophosphor researchers since it and other dysprosium-doped phosphors may possibly be the thermophosphors of choice for high temperature applications.

Europium-doped Lanthanum Phosphate ($LaPO_4:Eu^{3+}$)

In the excitation spectrum of both orthophosphate phosphors and other Eu^{3+} doped phosphors, a charge-transfer absorption band is usually evident along with several narrower absorption peaks, which are due to atomic transitions within the dopant ion.

Excitation and emission spectra are presented for $LaPO_4:Eu^{3+}$ taken at room temperature and at elevated temperatures. The excitation spectrum of the 590 nm emission line of $LaPO_4:Eu^{3+}$ taken at room temperature (20°C) is shown in Figure 4-16. The peak of the charge-transfer absorption band for this phosphor lies at 280 nm while another prominent atomic transition line lies at 395 nm. Other less important atomic transition peaks lie at 317, 359, and 375 nm. The room temperature emission spectrum for $LaPO_4:Eu^{3+}$ at 280 nm excitation is shown in Figure 4-17. Two strong emission lines are seen at 585 nm and 591 nm and two weaker emission lines are also found at 611 nm and 619 nm.
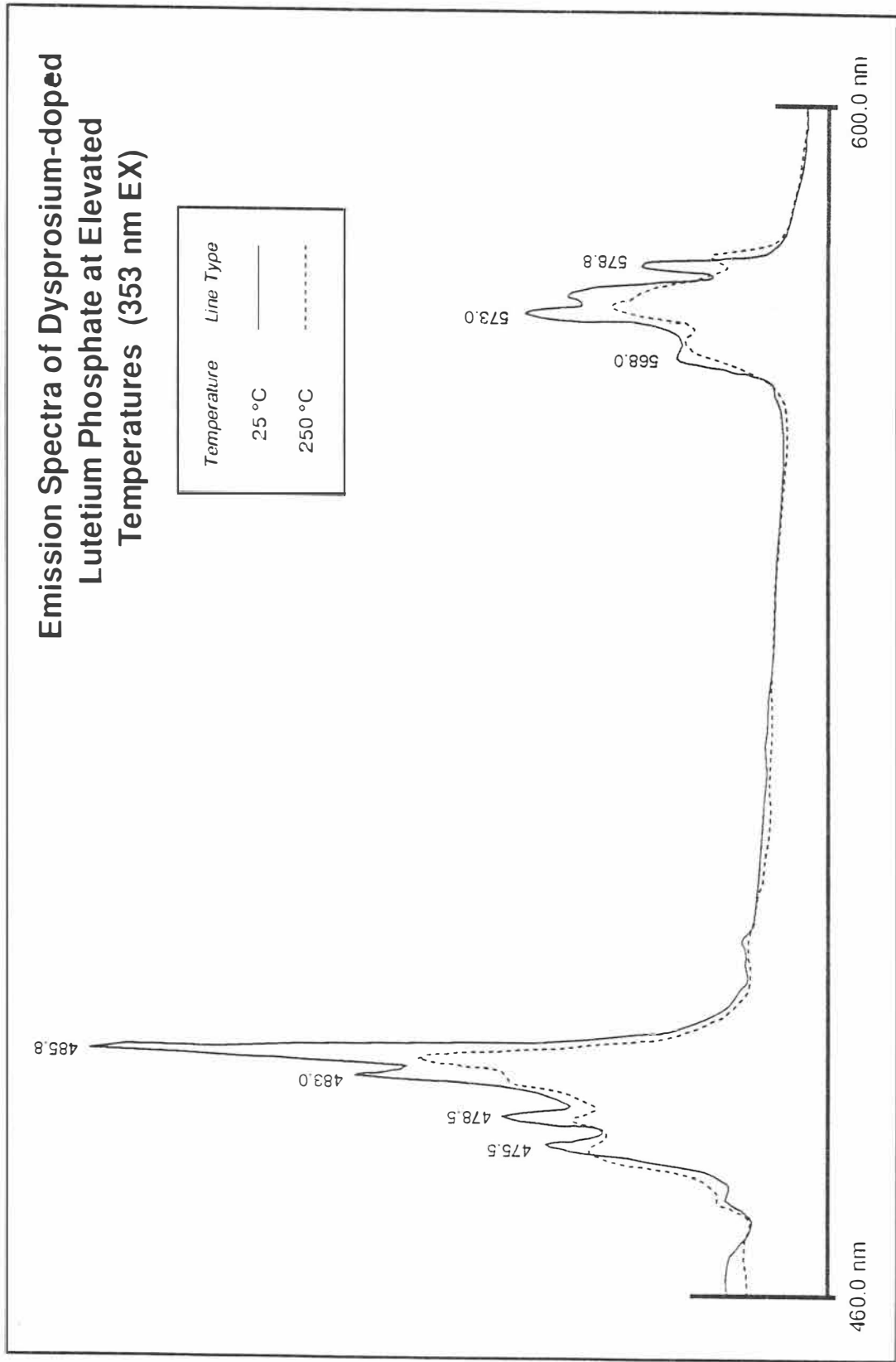
Figure 4-15. Emission spectra of dysprosium-doped lutetium phosphate at elevated temperatures (353 nm EX).
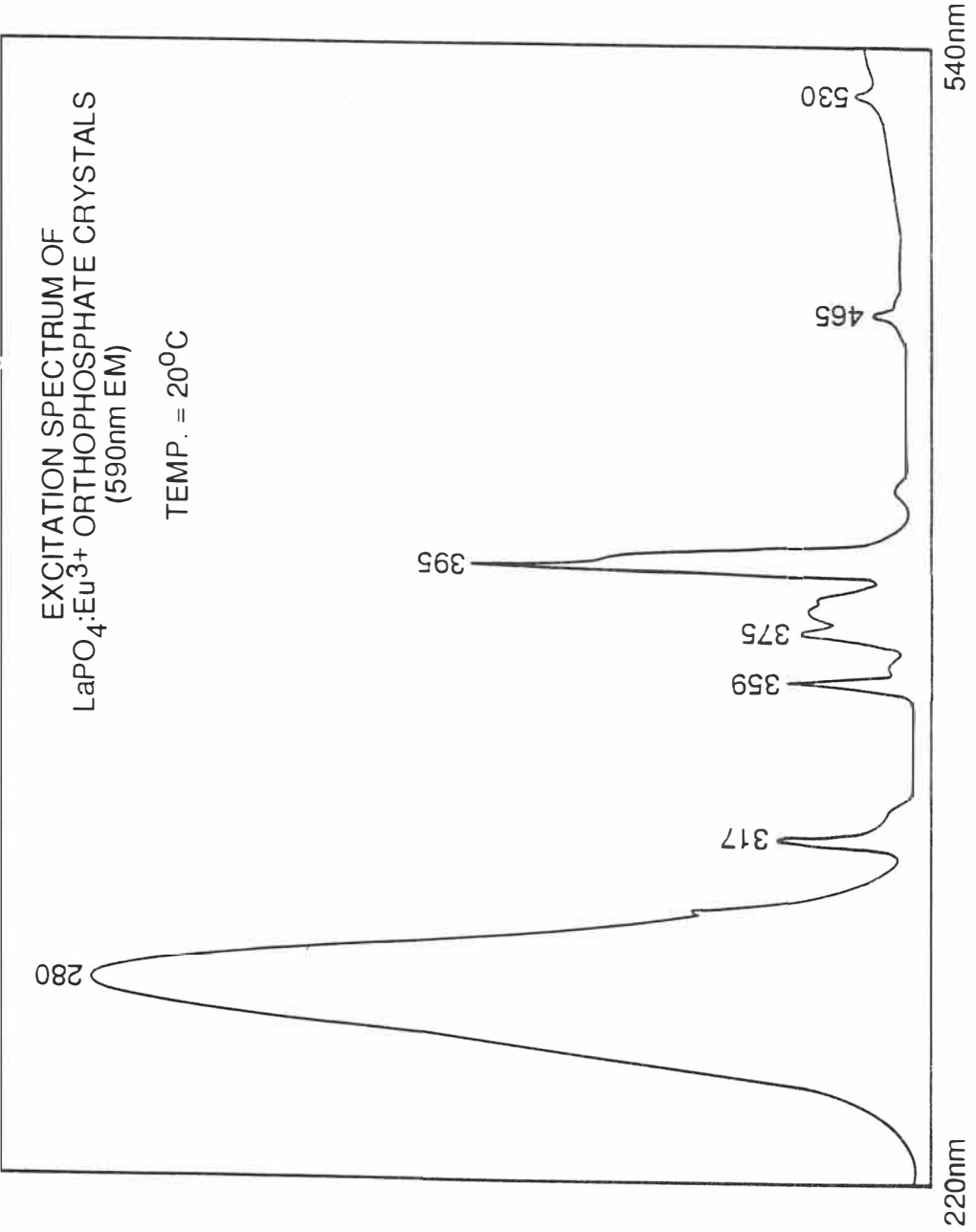
Figure 4-16. Excitation spectrun of europium-doped lanthanum phosphate at room temperaure (590 nm EM).
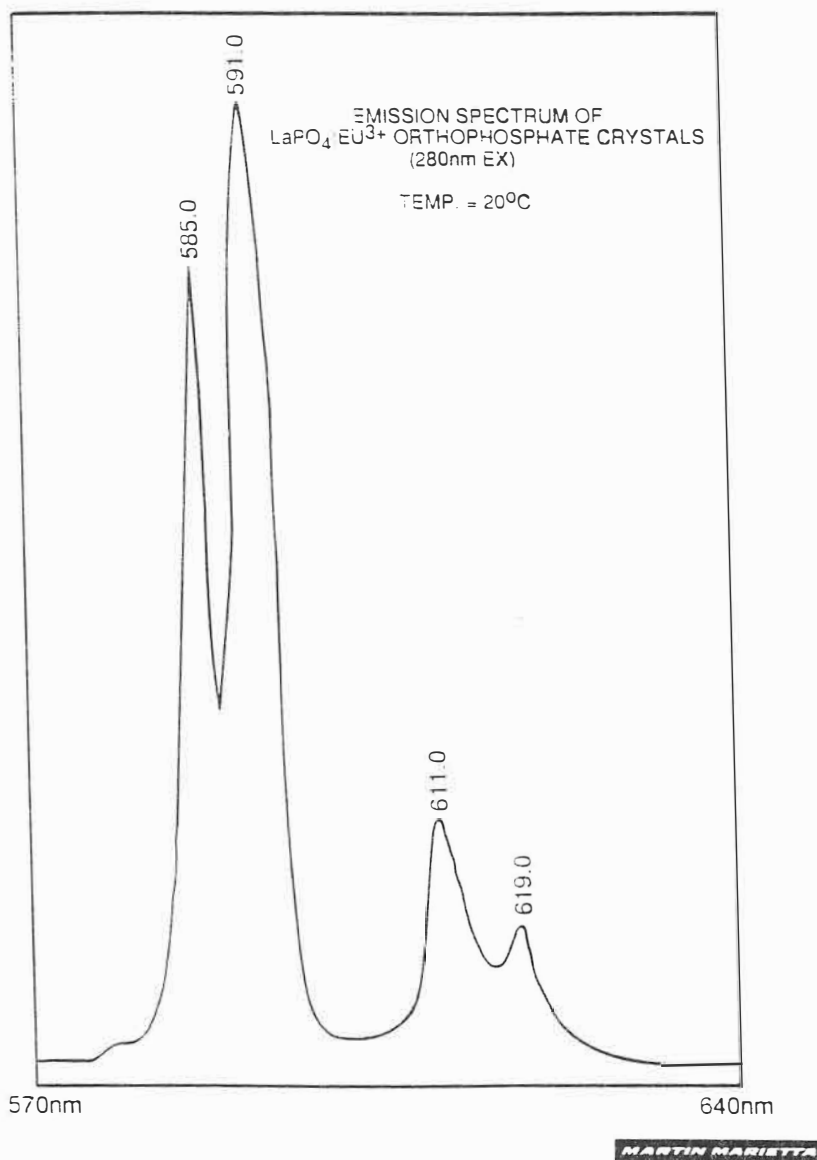
Figure 4-17. Emission spectrum of europium-doped lanthanum

phosphate at room temperature (280 nm EX).

Table 4-1 shows in tabulated form the data for the peak position of the 590 nm charge-transfer bands of the phosphor measured as a function of temperature. Excitation spectra at elevated temperatures for the 590 nm emission line of $LaPO_4:Eu^{3+}$ are displayed in Figure 4-18. The peak of the charge-transfer band shifts from 276.5 nm to 296.2 nm, a difference of 19.7 nm as temperature increases from 25.5°C to 300°C. The difference and minute change of the atomic transition peaks are within the error limits of the instrumentation and do not display any significant temperature-dependent spectral shift. The peak charge-transfer wavelength versus temperature is plotted in the graph of Figure 4-19. It is observed that the spectral shift of the charge-transfer band peak wavelength is linear as a function of the elevated temperature.

The emission spectra of $LaPO_4:Eu^{3+}$ for excitation at 280 nm are shown in Figure 4-20 for increasing temperatures. No distinguishable spectral shifts were observed on the 585 nm or 591 nm emission lines, however it was observed that the peaks decreased in signal intensity as temperature increased.

Table 4-1.Tabulated data for the peak position of the 590 nm charge-transfer bands of europium-doped lanthanum phosphate measured as a function of temperature.

Europium-doped Lanthanum Phosphate	
Temperature (°C)	Wavelength (peak)
25.5	276.5 nm
100.0	283.1 nm
200.0	293.7 nm
300.0	296.2 nm
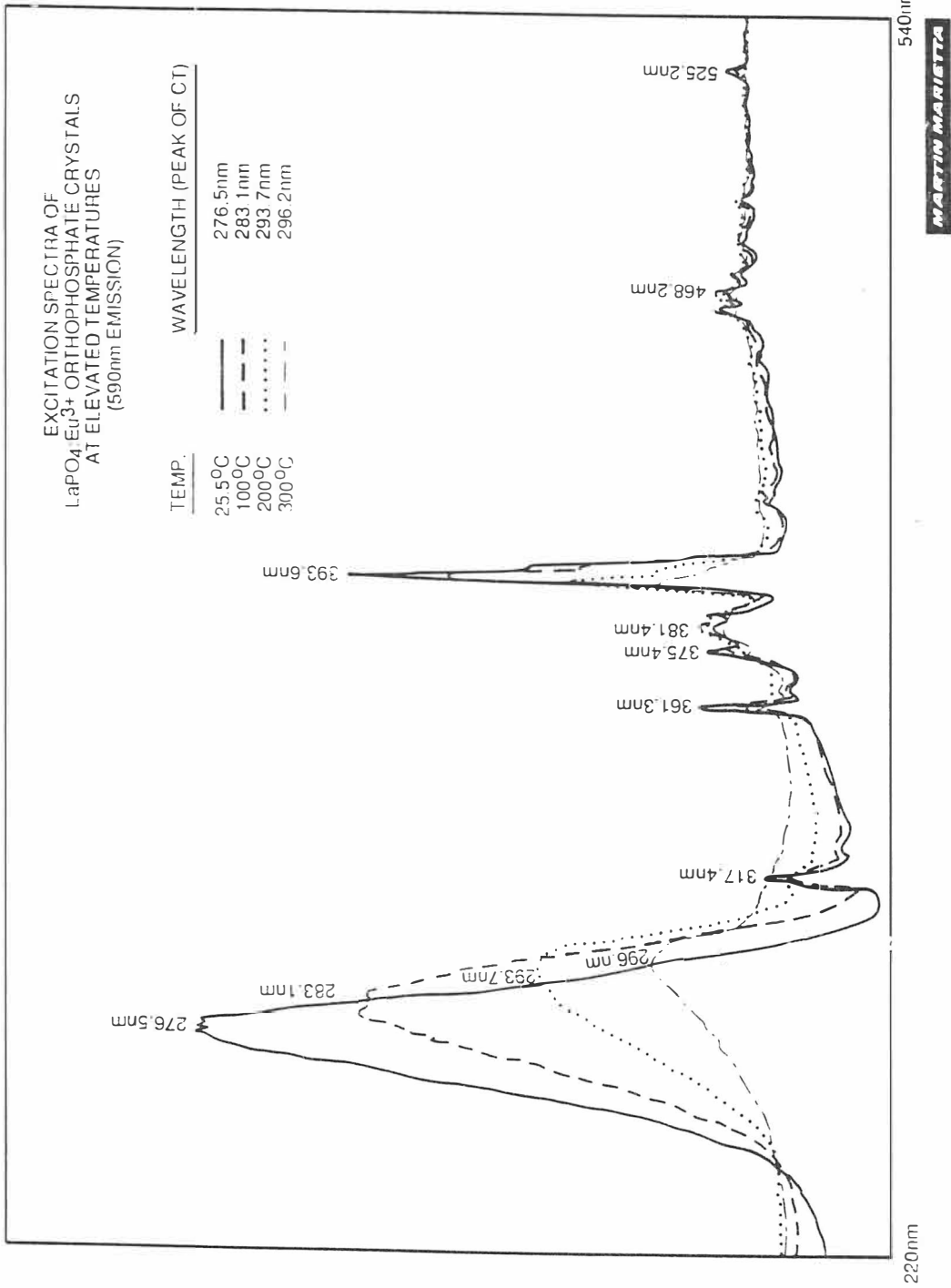
Figure 4-18. Excitation spectra of europium-doped lanthanum phosphate at elevated temperatures (590 nm EM).

Peak C-T Wavelength versus Temperature for Eu-doped LaPO4

$y = 275.6656 + 0.0749x$ $R = 0.97$
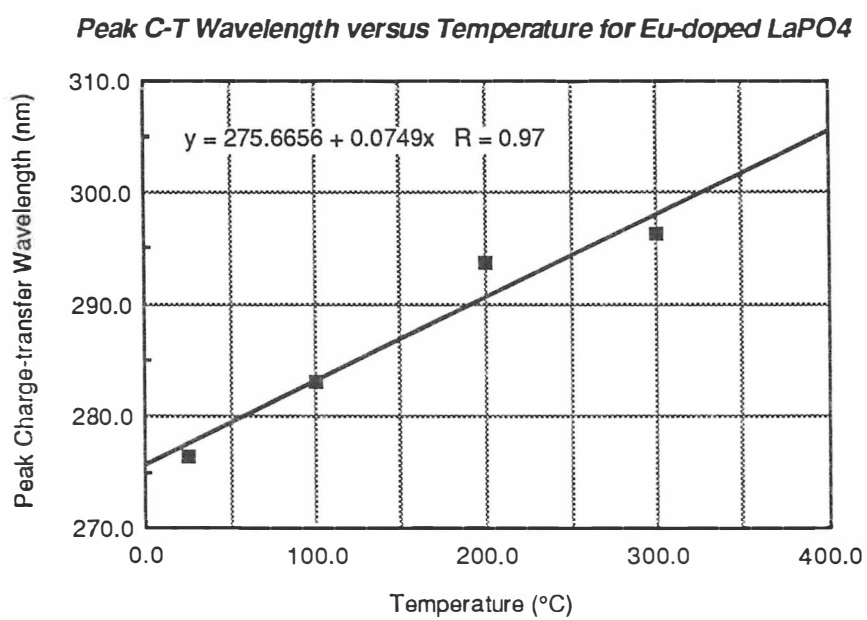
Figure 4-19. Peak charge-transfer wavelength versus temperature for $LaPO_4$:Eu^{3+}.

Figure 4-20. Emission spectra of europium-doped lanthanum

phosphate at elevated temperatures (280 nm EX).

Europium-doped Yttrium Phosphate (YPO_4:Eu^{3+})

Excitation and emission spectra are presented for YPO_4:Eu^{3+} acquired at room temperature and at elevated temperatures. The excitation spectrum of the 592 nm emission line of YPO_4:Eu^{3+} taken at room temperature (26°C) is shown in Figure 4-21. The room temperature charge-transfer band is found at a peak wavelength of 240 nm. A strong absorption band is located at 395 nm while other peaks of lesser intensity were observed at 287, 319, 364, 384, 452, and 467 nm. It is unsure at this time as to why there is a large band observed in the region from 360 to 570 nm.

The room temperature emission spectrum for YPO_4:Eu^{3+} at 396 nm excitation is shown in Figure 4-22. Similar to $LaPO_4$:Eu^{3+}, two strong emission lines are seen at 593 nm and 595 nm and two weaker emission lines are found at 612 nm and 618 nm.

Excitation spectra are presented in Figure 4-23 for YPO_4:Eu^{3+} taken at temperatures ranging from 26°C to 460°C. The peak of the charge-transfer absorption band for this phosphor lies at 239.7 nm while another prominent atomic transition line lies at 395 nm. Other less important atomic transition peaks lie at 318.8, 363.7, 383.9, 451.9 and 467.1 nm. There is a significant spectral shift towards the red in the charge-transfer band of YPO_4:Eu^{3+}. At 26°C the peak of the charge-transfer band is located at 239.7 nm whereas at 460°C it has been relocated to 265.9 nm, an overall shift of 26.2 nm in roughly 434°C. Note the broadening of the charge-transfer band along with an increase in luminescent intensity as the phosphor temperature increases. There is not any noticeable shift in any of the atomic transition lines of this spectra. Table 4-2 shows in tabulated form the data for the peak wavelength position of the charge-transfer bands measured as a function of temperature. The peak charge-transfer wavelength versus temperature is plotted in the graph of Figure 4-24. It is observed that the spectral shift of the charge-transfer band peak wavelength is a linear function of the elevated temperature.

EXCITATION SPECTRUM OF
YPO$_4$:Eu^{3+} ORTHOPHOSPHATE CRYSTALS
(592 nm EM)
TEMP. = 26°C

220nm   570nm

Figure 4-21. Excitation spectrum of europium-doped yttrium phosphate at room temperature (592 nm EM).

107

Figure 4-22. Emission spectrum of europium-doped yttrium phosphate at room temperature (396 nm EX).
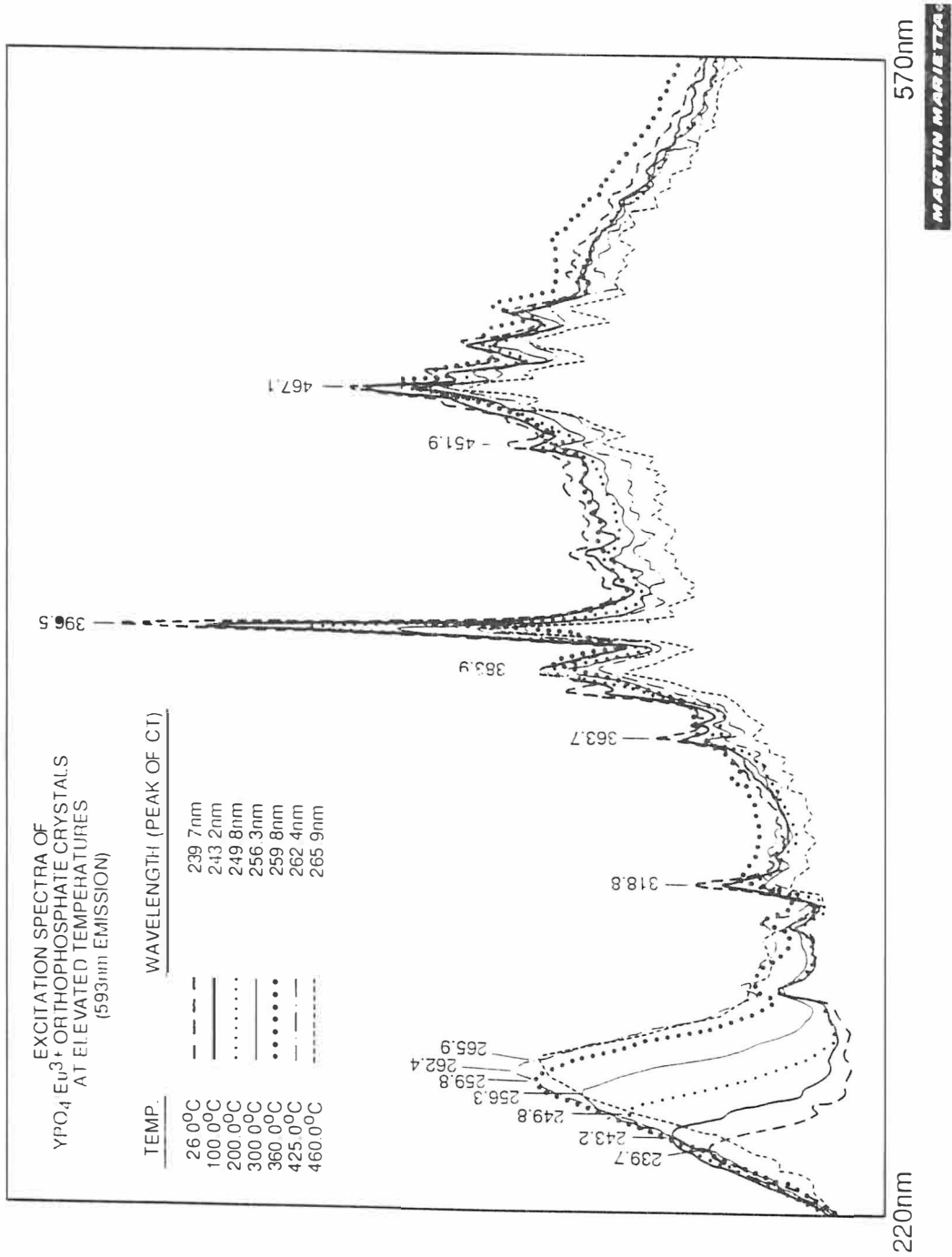
Figure 4-23. Excitation spectra of europium-doped yttrium phosphate at elevated temperatures (593 nm EM).

Table 4-2. Tabulated data for the peak position of the 593 nm charge-transfer bands of europium-doped yttrium phosphate measured as a function of temperature.

Europium-doped Yttrium Phosphate	
Temperature (°C)	*Wavelength (peak)*
26.5	239.7 nm
100.0	243.2 nm
200.0	249.8 nm
300.0	256.3 nm
360.0	259.8 nm
425.0	262.4 nm
460.0	265.9 nm
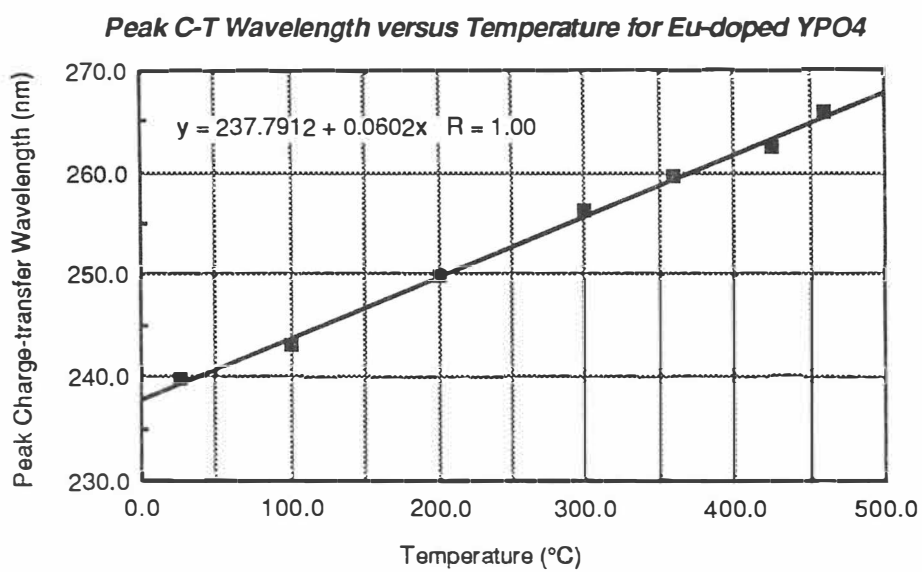
Figure 4-24. Peak charge-transfer wavelength versus temperature for $YPO_4:Eu^{3+}$.

The emission spectra of $YPO_4:Eu^{3+}$ for excitation at 396 nm is shown in Figure 4-25 for increasing temperatures. No distinguishable spectral shifts were observed on the 591.9 nm or 595.0 nm emission lines, however it was observed that the peaks decreased in signal intensity as temperature increased.

Europium-doped Lutetium Phosphate ($LuPO_4:Eu^{3+}$)

Excitation and emission spectra are presented for $LuPO_4:Eu^{3+}$ obtained at room temperature and at elevated temperatures. The excitation spectrum of the 593 nm emission line of $LuPO_4:Eu^{3+}$ taken at room temperature (26°C) is shown in Figure 4-26. The room temperature charge-transfer band is found at a peak wavelength of 227 nm. A very strong absorption band is located at 395 nm while other less intense peaks were observed at 287, 300, 320, 363, 380, 385, 470, and 530 nm.

Five fluorescence lines are found in the $LuPO_4:Eu^{3+}$ room temperature emission spectrum taken at 395 nm excitation as shown in Figure 4-27. This spectrum is very similar to that of $YPO_4:Eu^{3+}$ with the addition of a emission line at 587.7 nm. This additional line may be due to intrinsic host-dopant crystal structure factors however its presence requires further investigation.

Europium-doped lutetium phosphate also shows a significant spectral shift towards the red in its charge-transfer band as temperature is increased. Figure 4-28 displays excitation spectra at elevated temperatures for the 593 nm emission line of $LuPO_4:Eu^{3+}$. The peak position of the charge-transfer absorption band for $LuPO_4:Eu^{3+}$ lies at 227 nm while another strong line of absorption lies at 397 nm. The peak of the charge-transfer band shifts from 228 nm to 243 nm, a difference of 15 nm as temperature increased from 25.0°C to 400°C. The atomic transition peaks show no significant spectral shift. Other less intense atomic transition peaks lie at 280, 300, 320.6, 363.9, 383.9, 418.2, 466.5,
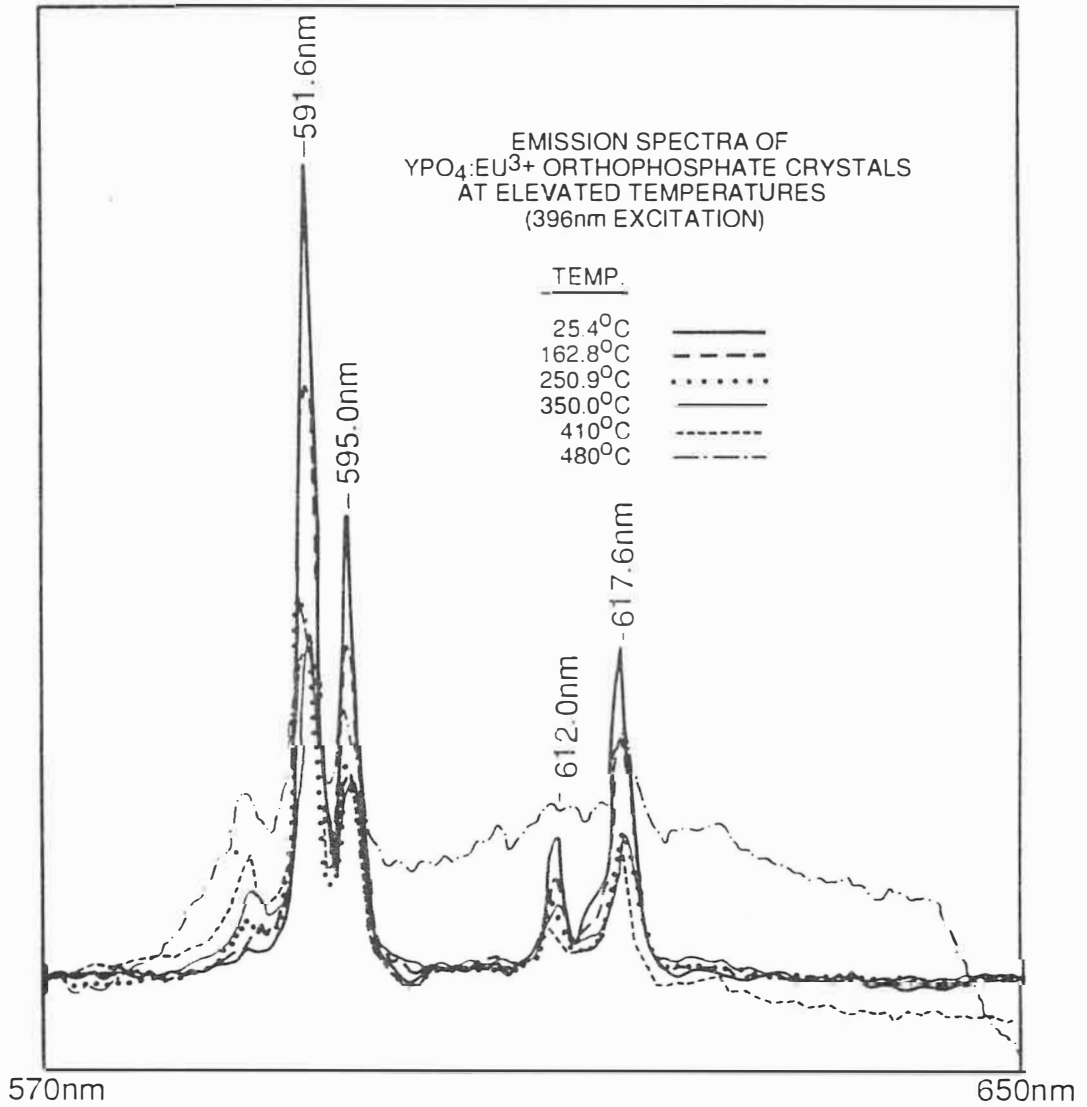
Figure 4-25. Emission spectra of europium-doped yttrium

phosphate at elevated temperatures (396 nm EX).

Figure 4-26. Excitation spectrum of europium-doped lutetium phosphate at room temperature (593 nm EM).
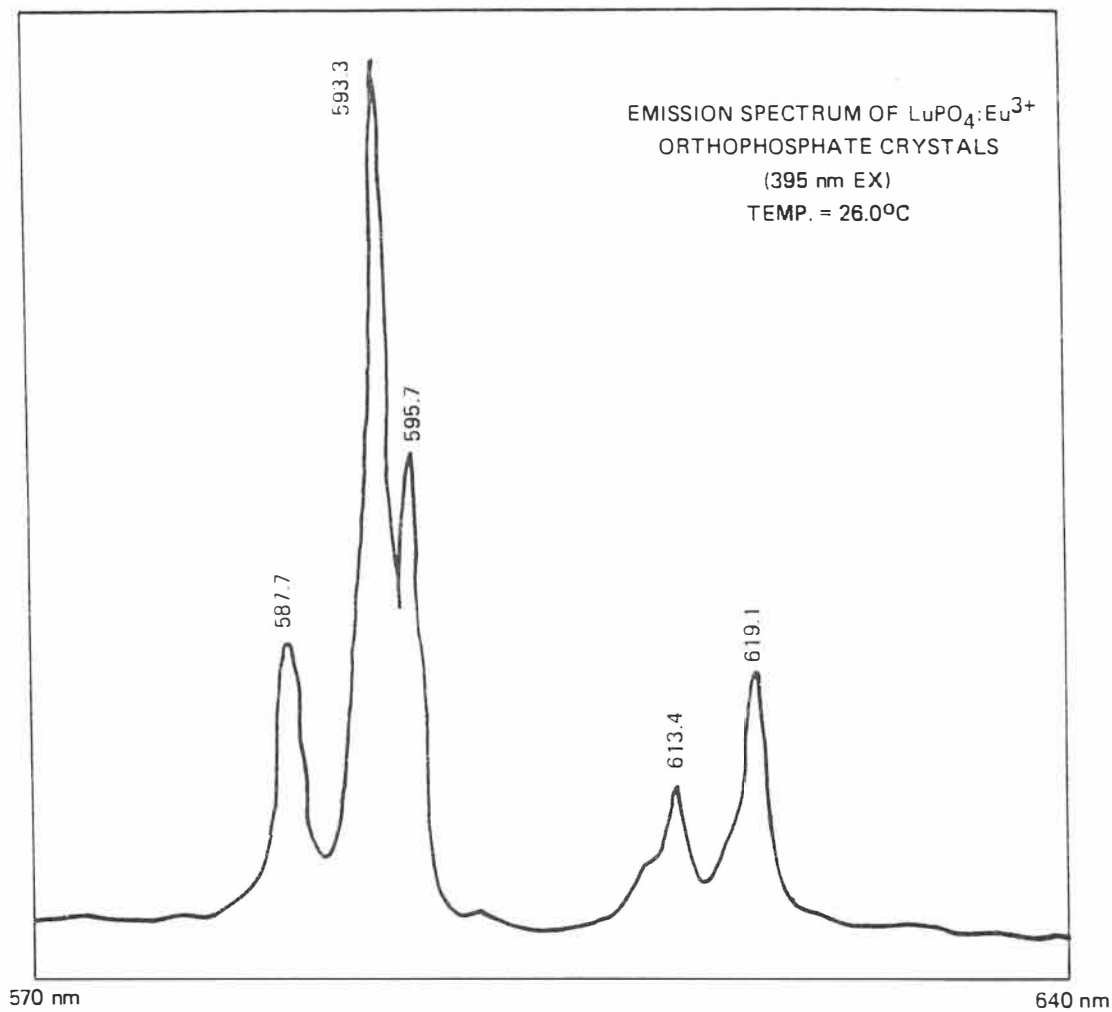
Figure 4-27. Emission spectrum of europium-doped lutetium

phosphate at room temperature (395 nm EX).
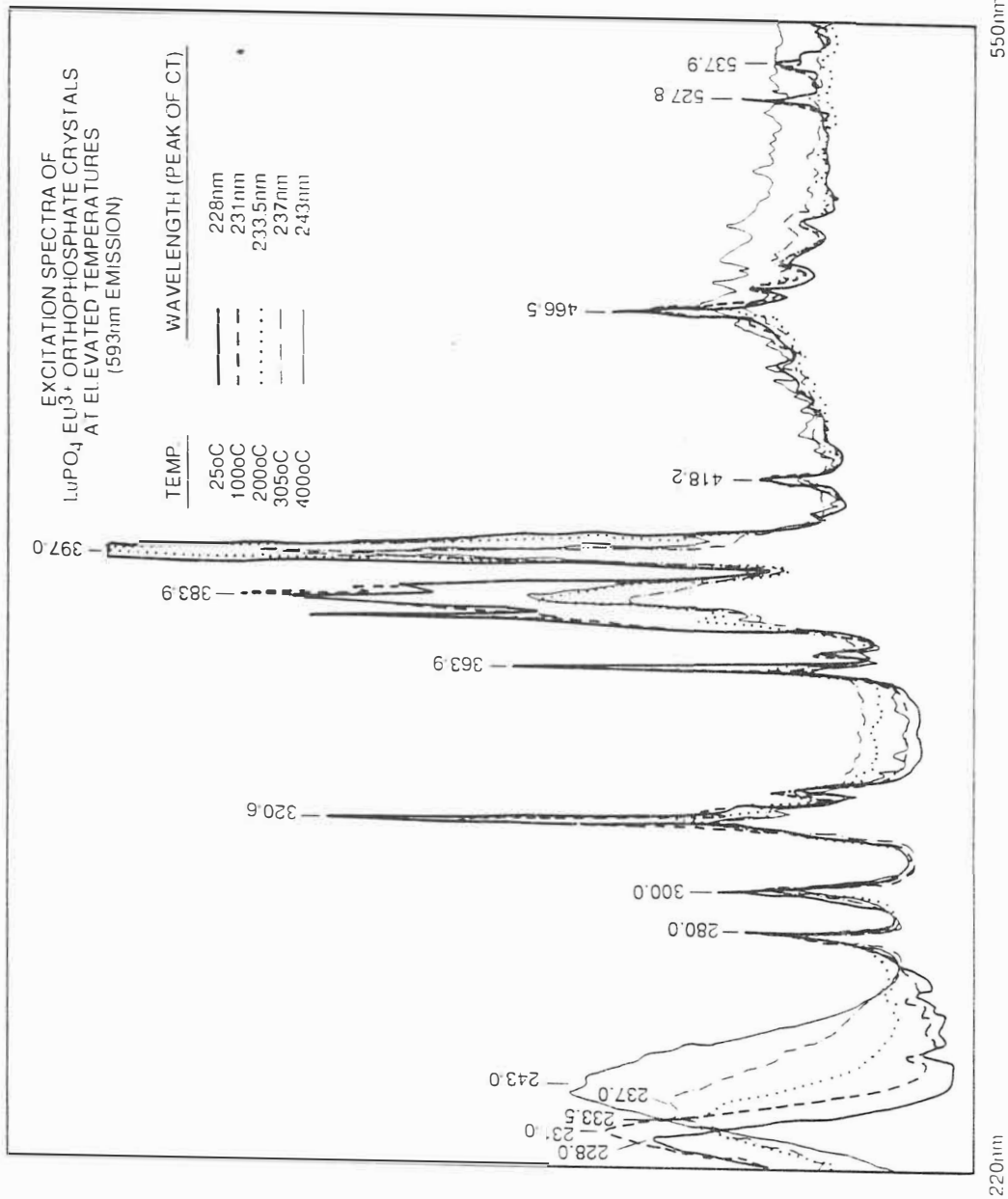
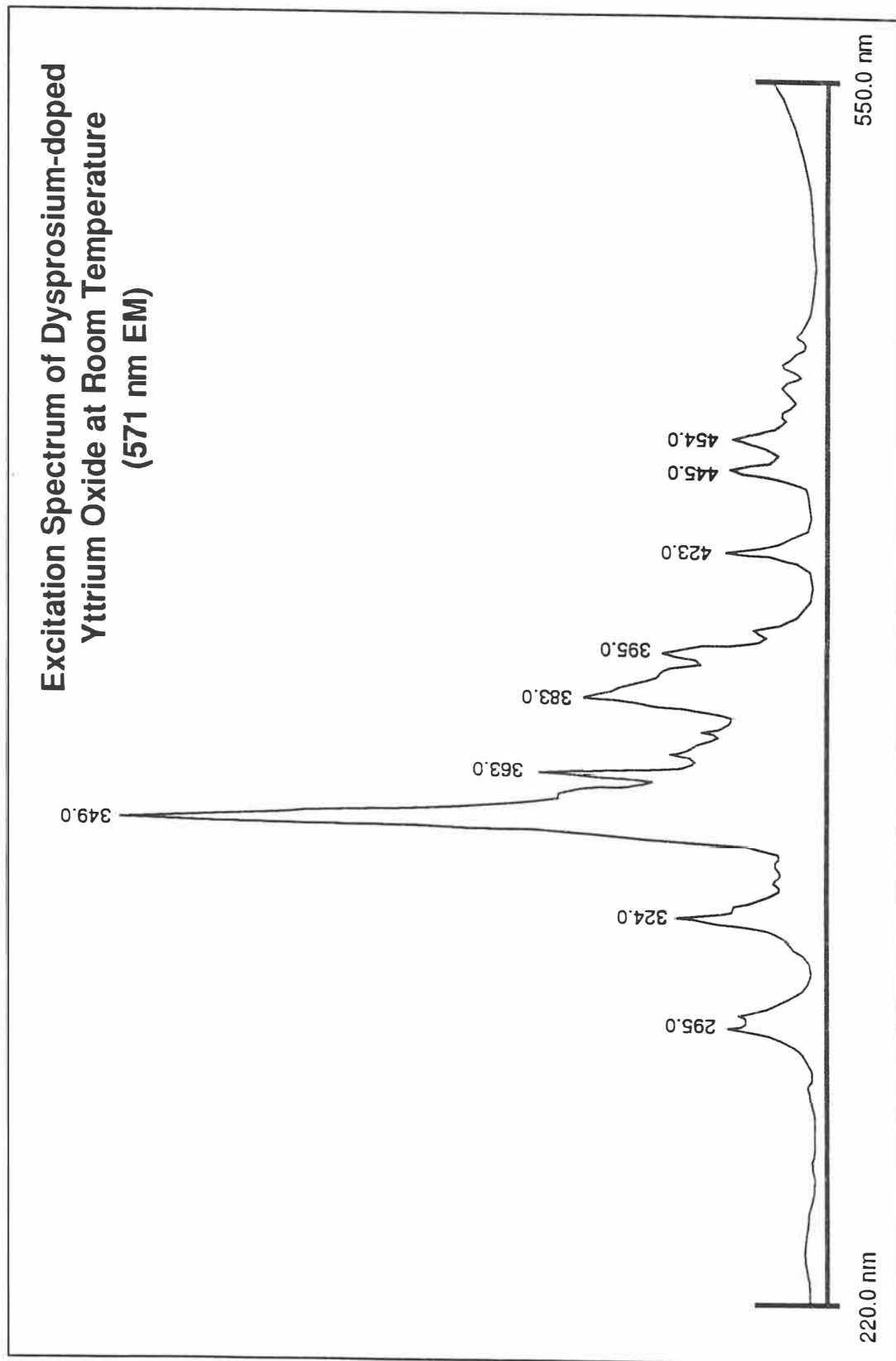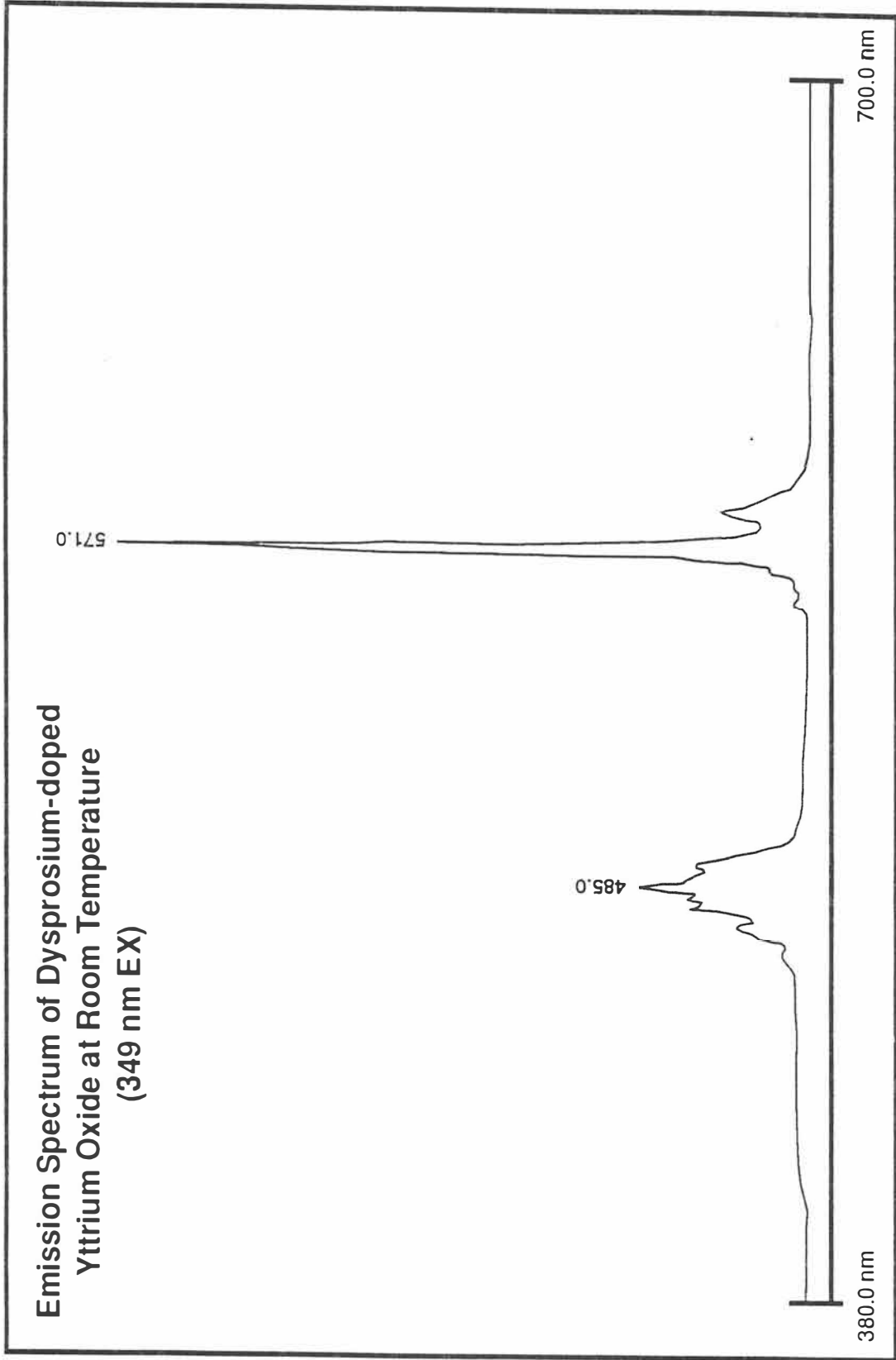Figure 4-28. Excitation spectra of europium-doped lutetium phosphate at elevated temperatures (593 nm EM).

527.8 and 537.9 nm. Table 4-3 shows in tabulated form the data for the peak wavelength position of the charge-transfer bands measured as a function of temperature.

The peak charge-transfer wavelength versus temperature is plotted in the graph of Figure 4-29. Similar to the other orthophosphates, it is observed that the spectral shift of the charge-transfer band peak wavelength is linear as a function of the elevated temperature.

The emission spectra of $LuPO_4:Eu^{3+}$ for excitation at 227 nm is shown in Figure 4-30 for increasing temperatures. No distinguishable spectral shifts were observed for the emission lines. However, unlike the emission spectra taken at temperature for $LaPO_4:Eu^{3+}$ and $YPO_4:Eu^{3+}$, it was observed that the peaks decreased very slightly in signal intensity as temperature increased.

It should be noted that the peak of the charge-transfer band of $LuPO_4:Eu^{3+}$ starts at 228 nm, deeper into the UV region when compared to the peak of the charge-transfer band of $LaPO_4:Eu^{3+}$ which begins at 276.5 nm. The peak of the room temperature charge-transfer band of $YPO_4:Eu^{3+}$ lies at 239.7 nm. This shows that the peak of the charge-transfer band shifts to higher energies with decreasing host cation radius, since lutetium has a cation radius of 0.85 Å compared to yttrium at 0.893 Å and lanthanum at 1.061 Å. Hence the onset quenching temperature of $LuPO_4:Eu^{3+}$ should be significantly higher than that of $LaPO_4:Eu^{3+}$ and this is shown in further lifetime decay results.

Table 4-3. Tabulated data for the peak position of the 593 nm charge-transfer bands of europium-doped lutetium phosphate measured as a function of temperature.

Europium-doped Lutetium Phosphate	
Temperature (°C)	*Wavelength (peak)*
25.0	228.0 nm
100.0	231.0 nm
200.0	233.5 nm
305.0	237.0 nm
400.0	243.0 nm

Peak C-T Wavelength versus Temperature for Eu-doped LuPO4

$y = 226.7302 + 0.0377x \quad R = 0.99$
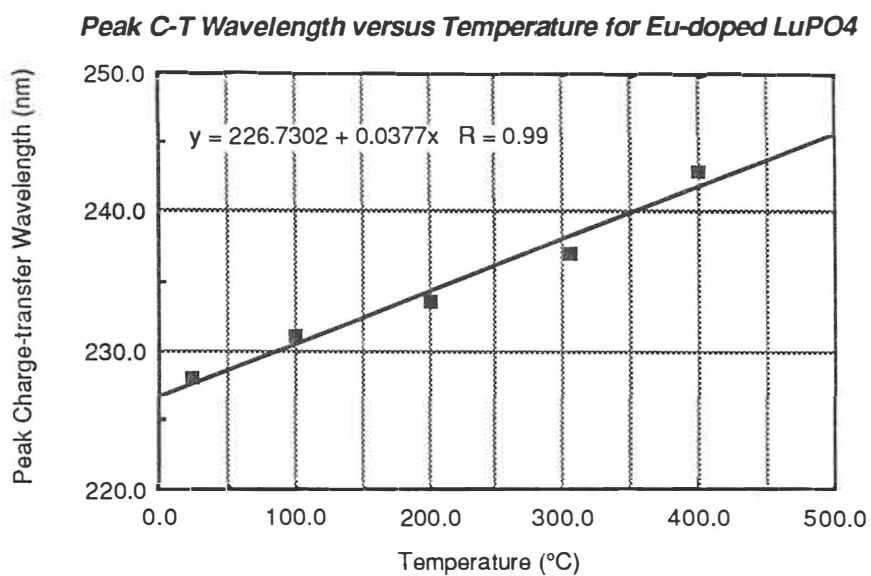
Figure 4-29. Peak charge-transfer wavelength versus temperature for $LuPO_4:Eu^{3+}$.
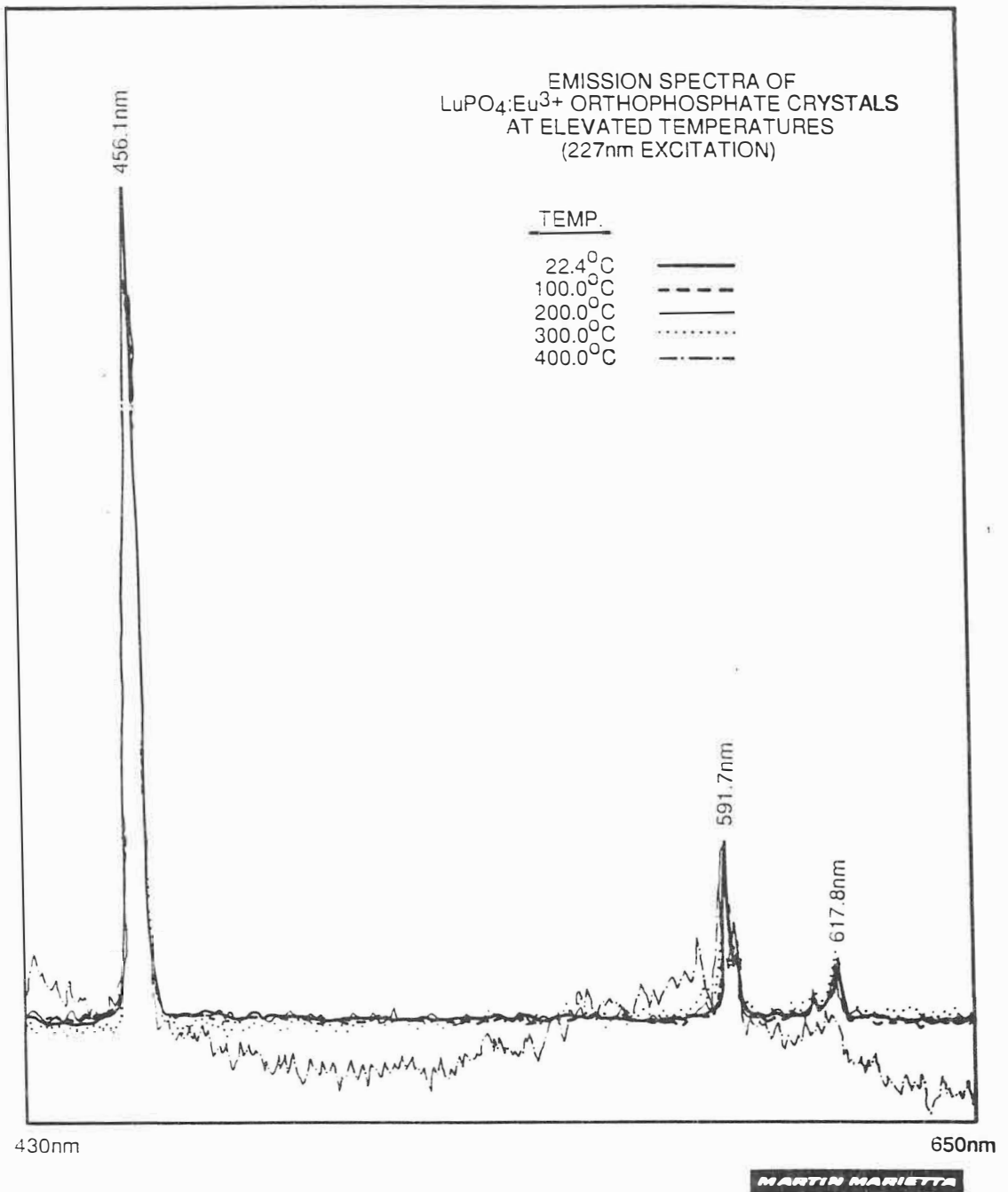
Figure 4-30. Emission spectra of europium-doped lutetium

phosphate at elevated temperatures (227 nm EX).

Europium-doped Yttrium Oxide (Y_2O_3:Eu^{3+})

Of all the thermophosphors researched for broadening effects and absorption band spectral shift, Y_2O_3:Eu^{3+} showed the most significant changes in its peak charge-transfer absorption band position at elevated temperatures. First, the excitation spectrum of the 611 nm emission line of Y_2O_3:Eu^{3+} taken at room temperature is shown in Figure 4-31. The room temperature charge-transfer band is found at a peak wavelength of 267.3 nm. A strong absorption band is located at 466.0 nm while other less intense peaks were observed at 363.2, 383.4, 394.5, and 533.0 nm.

Five fluorescence lines are displayed in the Y_2O_3:Eu^{3+} room temperature emission spectrum taken at 270 nm excitation which is shown in Figure 4-32. The most prominent emission line is located at 611.0 nm whereas other lines are located at 586.0, 593.0, 598.0, and 630.0 nm.

The excitation spectra at increasing temperatures for the 611 nm emission line of Y_2O_3:Eu^{3+} is shown in Figure 4-33. At room temperature (26.6°C), the spectra display a charge-transfer absorption band centered at 267.3 nm and several atomic transition peaks. The strongest atomic emission transitions are found at wavelengths 394.5 ($^7F_0$-$^5L_6$), 466.1 ($^7F_2$-$^5D_2$), and 533.7 nm ($^7F_0$-$^5D_1$). A line at 337 nm marks the point where excitation from a nitrogen laser may be used in a particular temperature sensing application. Figure 4-34 displays an excitation spectrum at elevated temperatures for the 611 nm emission line in Y_2O_3:Eu^{3+} and reveals the charge-transfer absorption peak with increased resolution. Table 4-4 tabulates the peak wavelength position and bandwidth (measured at FWHM) for the 611 nm absorption band in the excitation spectra at their associated temperatures. The charge-transfer absorption band peak wavelength at 26.6°C is 267.3 nm, where at 400°C, the peak wavelength is found at 289.5 nm, a change of 22.2 nm in 373.4°C. Similarly, the bandwidth of the charge-transfer band broadens at

Excitation Spectrum of Europium-doped Yttrium Oxide at Room Temperature (611 nm EM)

230.0 nm

267.3

337 nm Laser Line

363.2

383.4

394.5

466.0

533.0

560.0 nm
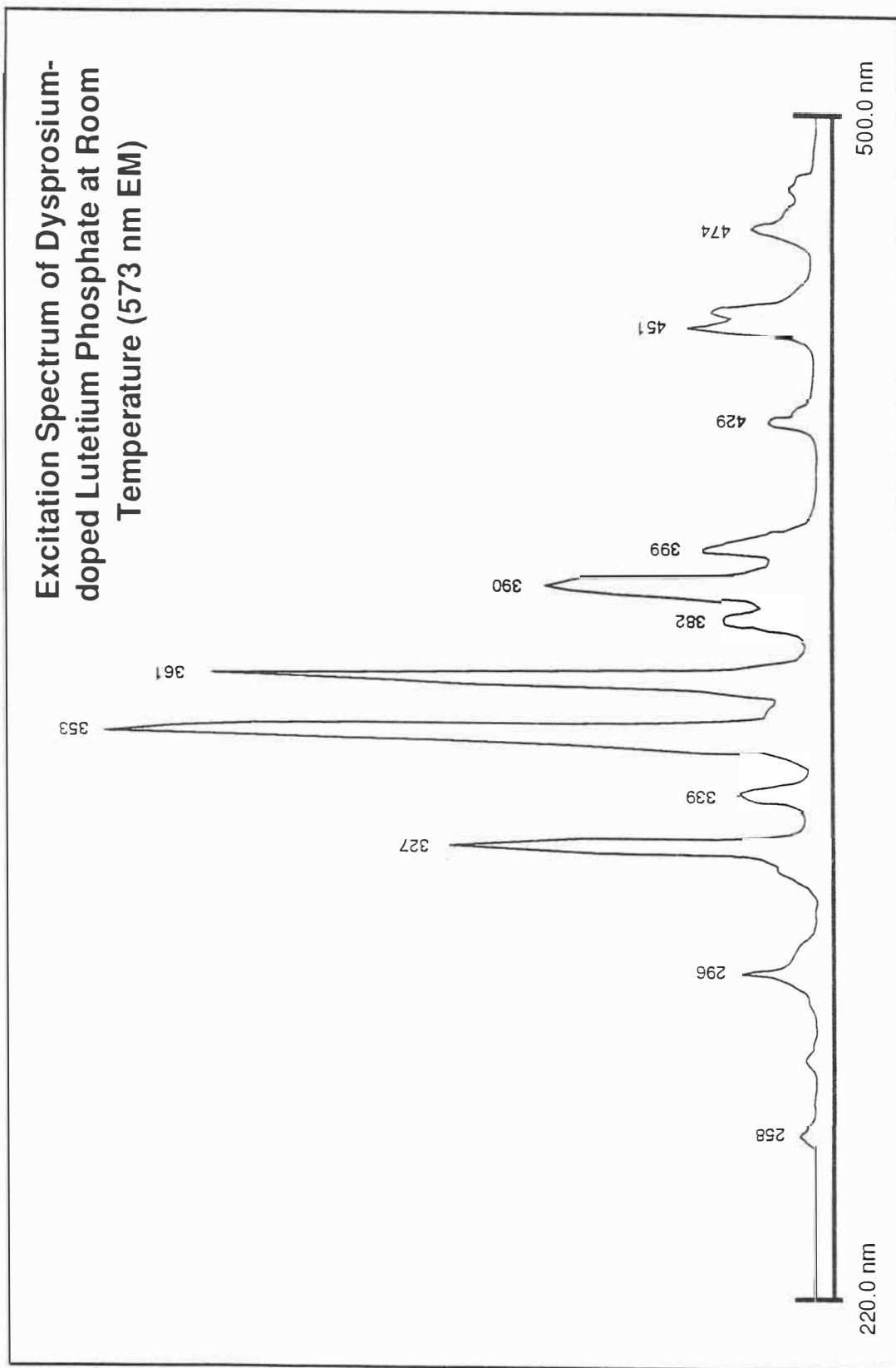
Figure 4-31. Excitation spectrum of europium-doped yttrium oxide at room temperature (611 nm EM).

Figure 4-32. Emission spectrum of europium-doped yttrium oxide at room temperature (270 nm EX).
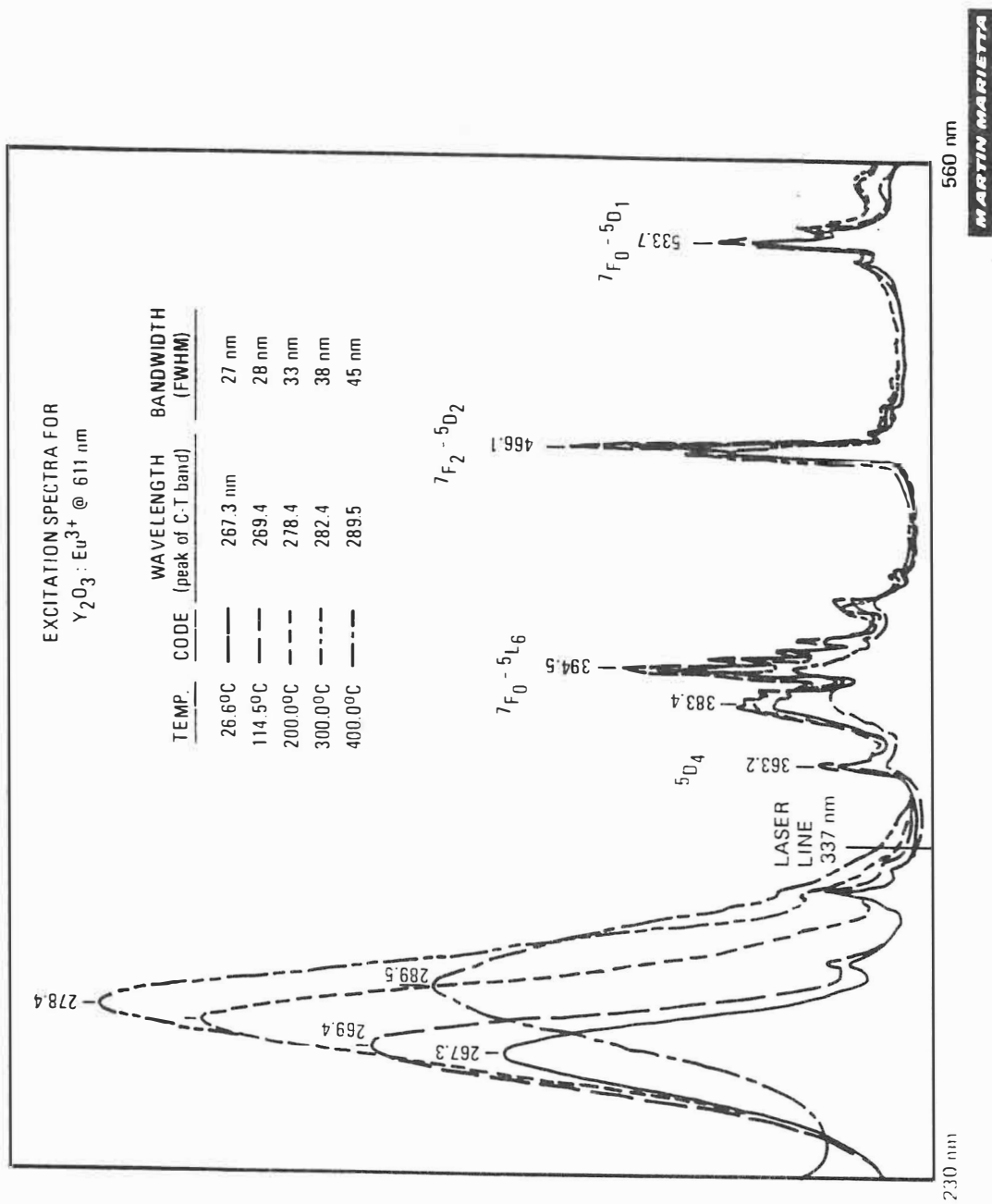
Figure 4-33. Excitation spectra of europium-doped yttrium oxide at elevated temperatures (611 nm EM).
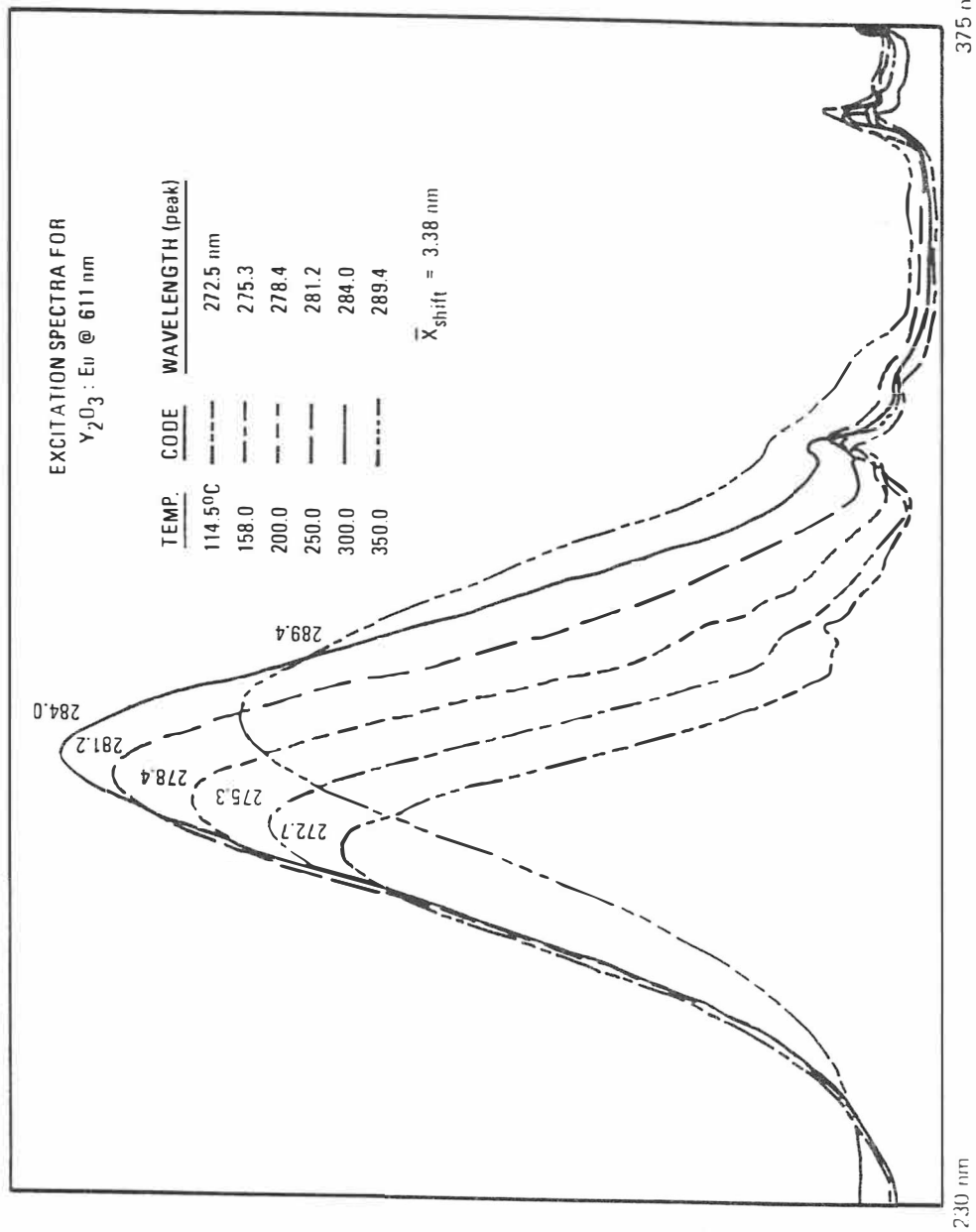
Figure 4-34. Excitation spectra (expanded form) of europium-doped yttrium oxide at elevated temperatures (611 nm EM).

Table 4-4. Tabulated data for the peak position of the 611 nm charge-transfer bands of europium-doped yttrium oxide measured as a function of temperature.

Europium-doped Yttrium Oxide		
Temperature (°C)	Wavelength (peak)	Bandwidth (FWHM)
26.6	267.3 nm	27 nm
114.5	269.4 nm	28 nm
150.0	273.4 nm	31 nm
200.0	278.4 nm	33 nm
250.0	280.5 nm	35 nm
300.0	282.4 nm	38 nm
350.0	285.4 nm	41 nm
400.0	289.5 nm	45 nm

elevated temperatures. It is observed that the atomic transition peaks show no detectable shift to the red with increasing temperatures. Figure 4-35 shows the peak position of the charge-transfer band plotted as a function of increasing temperature. It can be seen from this plot that the spectral shift in this phosphor is linear. An extrapolation of the data, assuming the charge-transfer shift continues in a linear manner, would show the peak position of charge-transfer band to be located at 337 nm near 1200°C. At this point, a nitrogen laser may be most efficient in stimulating the phosphor's luminescence.

The emission spectra of $Y_2O_3:Eu^{3+}$ for excitation at 270 nm is shown in Figure 4-36 for increasing temperatures ranging from 38°C to 386°C. No distinguishable spectral shifts were observed on the 611 nm emission line, however it was observed that the peak, when measured at FWHM, broadened from 9 nm to 21 nm as temperature increased.

Peak C-T Wavelength vs Temperature for Eu-doped Y2O3

$y = 264.6067 + 0.0611x \quad R = 0.99$
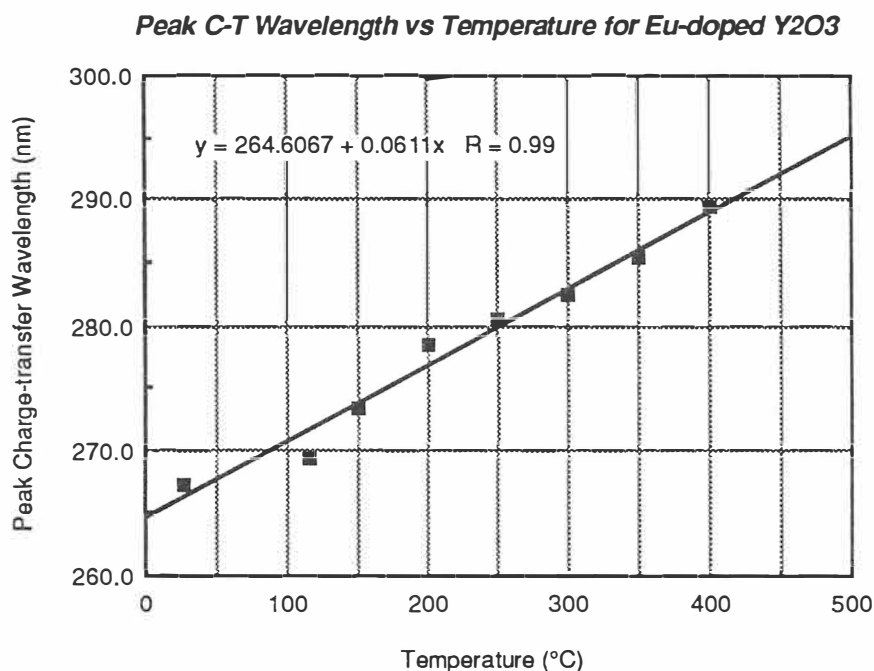
Figure 4-35. Peak position of the charge-transfer band plotted
as a function of increasing temperature.

Figure 4-36. Emission spectra of europium-doped yttrium

oxide at elevated temperatures (270 nm EX).

Europium-doped Yttrium Vanadate (YVO_4:Eu^{3+})

Two different types of YVO_4:Eu^{3+} phosphor were used in this spectral analysis both manufactured by Sylvania. It is not specifically known what chemical differences there may be between the two phosphors, however slightly stronger dopant concentrations, higher purity, or particle size may be certain factors related to their differences.

The room temperature spectrum of Type 1120 YVO_4:Eu^{3+} has a charge-transfer band located at 325.6 nm as shown in Figure 4-37. Other lines of absorption are located at 362.0, 381.0, 394.0, 416.0, and 464.0 nm. The room temperature spectrum of Type 2391 YVO_4:Eu^{3+} has a charge-transfer band located at 321.5 nm as shown in Figure 4-38. Other lines of absorption are found at 394.0 and 464.0 nm.

The room temperature emission spectrum of Type 1120 YVO_4:Eu^{3+} is presented in Figure 4-39 and shows strong fluorescent lines located at 613.4 and 617.4 nm due primarily to the europium activator. Several other less significant emission lines are found at 420.1, 432.2, 449.3, 468.4, 538.9, and 593.3 nm, in which some of their emission may arise from impurities in the phosphor.

Europium-doped yttrium vanadate also shows a significant spectral shift to the red in its charge-transfer absorption band as temperature is increased. The excitation spectra presented for these phosphors were made within a temperature range of 23.0°C to 400°C. Shown in Figure 4-40 is the excitation spectrum of Type 2391 YVO_4:Eu^{3+} at various temperatures for the 619.0 nm emission line. Table 4-5 shows the peak wavelength position and bandwidth for the charge-transfer absorption band in the excitation spectra at their associated temperatures. The absorption band peak wavelength at 23°C is 321.5 nm, where at 400°C, the peak wavelength is found at 368.2 nm, a noticeable change of 46.7 nm in 377°C. Figure 4-41 shows a graph of the peak charge-transfer wavelength position plotted against temperature for Type 2391 YVO_4:Eu^{3+}.
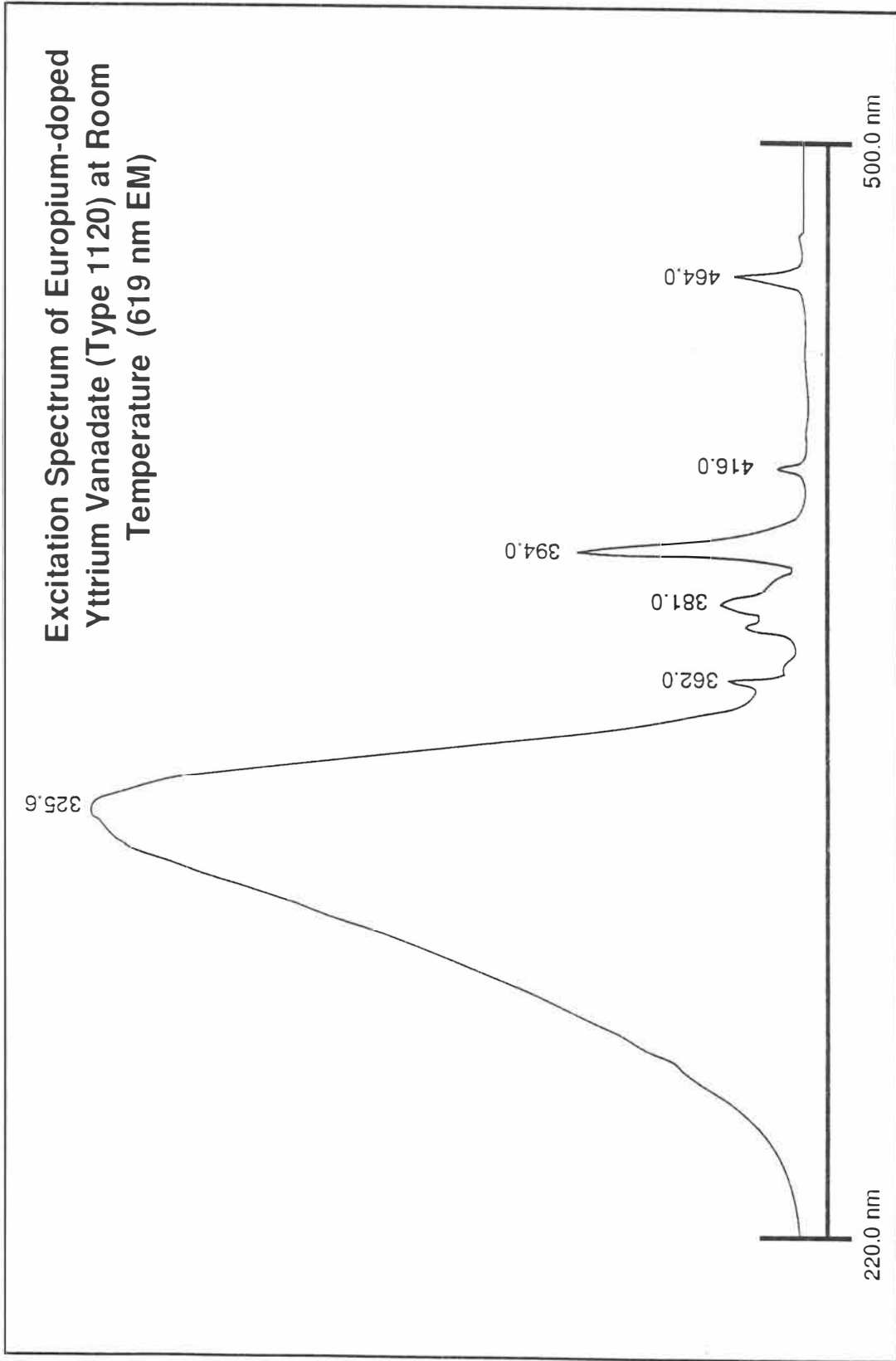
Figure 4-37. Excitation spectrum of europium-doped yttrium vanadate (Type 1120) at room temperature (619 nm EM).
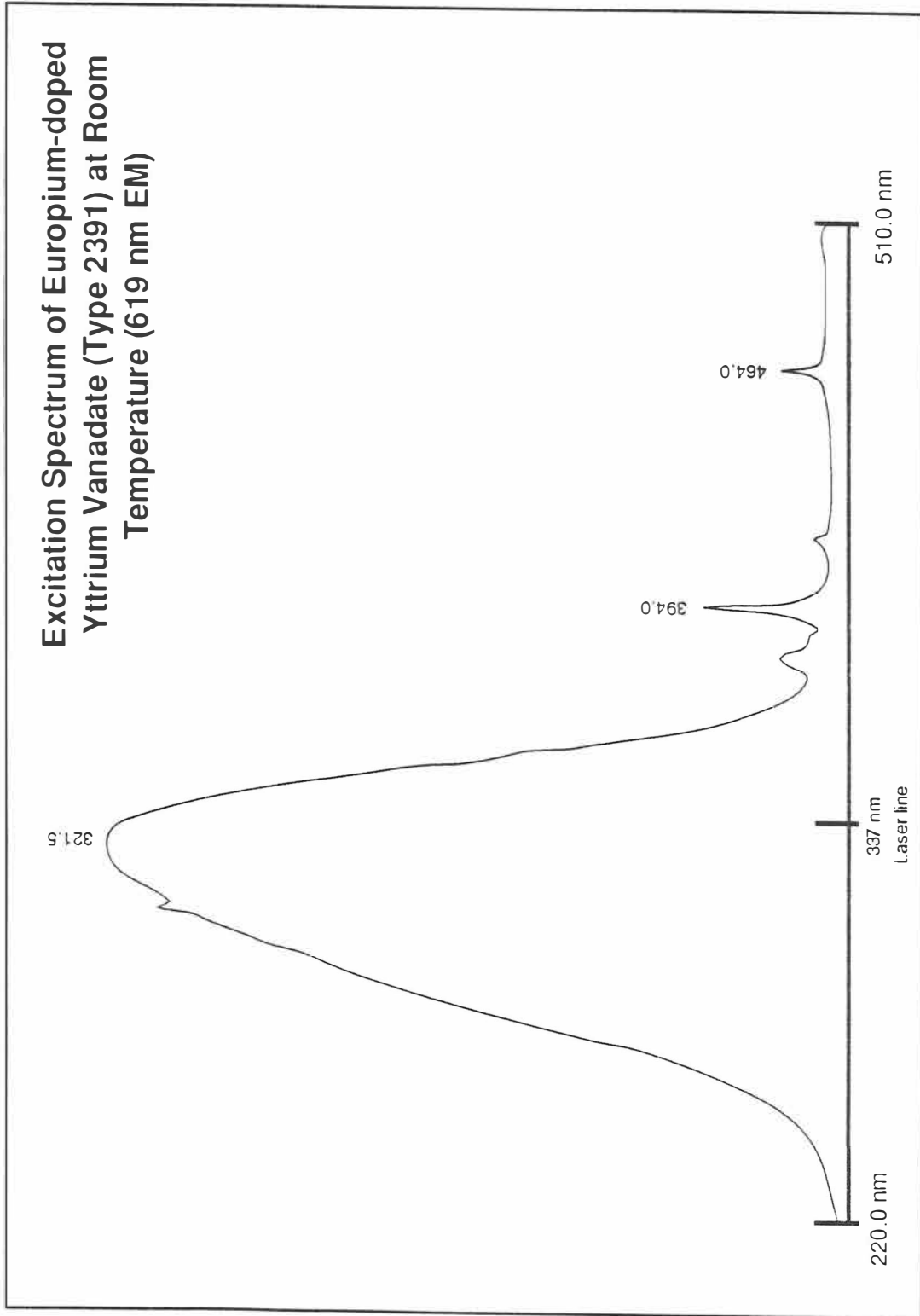
Figure 4-38. Excitation spectrum of europium-doped yttrium vanadate (Type 2391) at room temperature (619 nm EM).
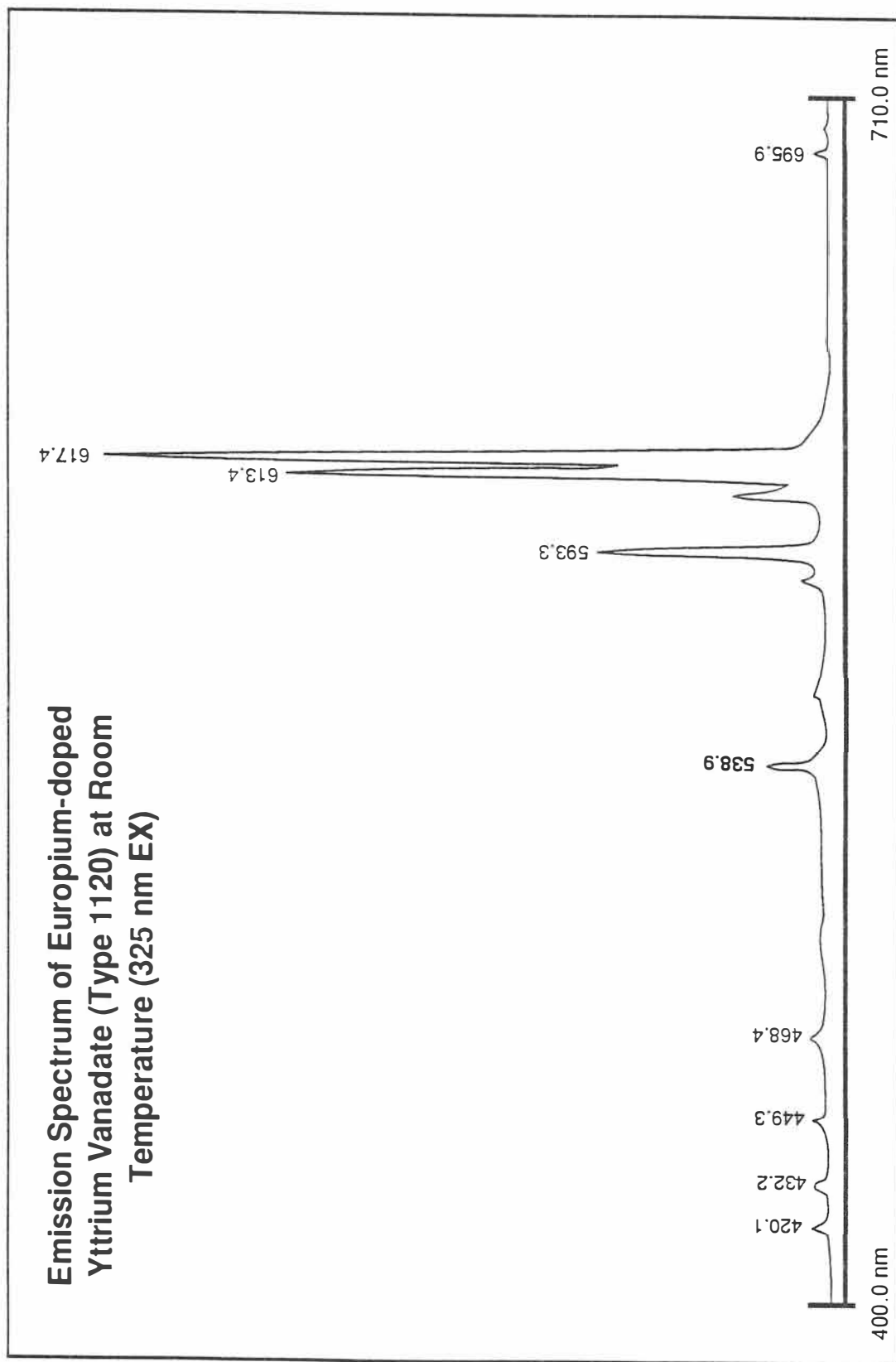
Figure 4-39. Emission spectrum of europium-doped yttrium vanadate (Type 1120) at room temperature (325 nm EM).

Figure 4-40. Excitation spectra of europium-doped yttrium vanadate

(Type 2391) at elevated temperatures (619 nm EM).

Table 4-5. Tabulated data for the peak position of the 619 nm charge-transfer bands of europium-doped yttrium vanadate measured as a function of temperature.

Europium-doped Yttrium Vanadate		
Temperature (°C)	Wavelength (peak)	Bandwidth (FWHM)
23.0	321.5 nm	63.0 nm
77.0	326.5 nm	66.0 nm
100.0	329.6 nm	70.0 nm
150.0	335.6 nm	77.0 nm
200.0	343.6 nm	83.0 nm
255.0	348.6 nm	89.0 nm
300.0	353.2 nm	91.0 nm
370.0	357.2 nm	93.0 nm
400.0	368.2 nm	76.0 nm

Peak C-T Wavelength versus Temperature for Eu-Doped YVO4

$y = 318.3781 + 0.1166x \quad R = 0.99$
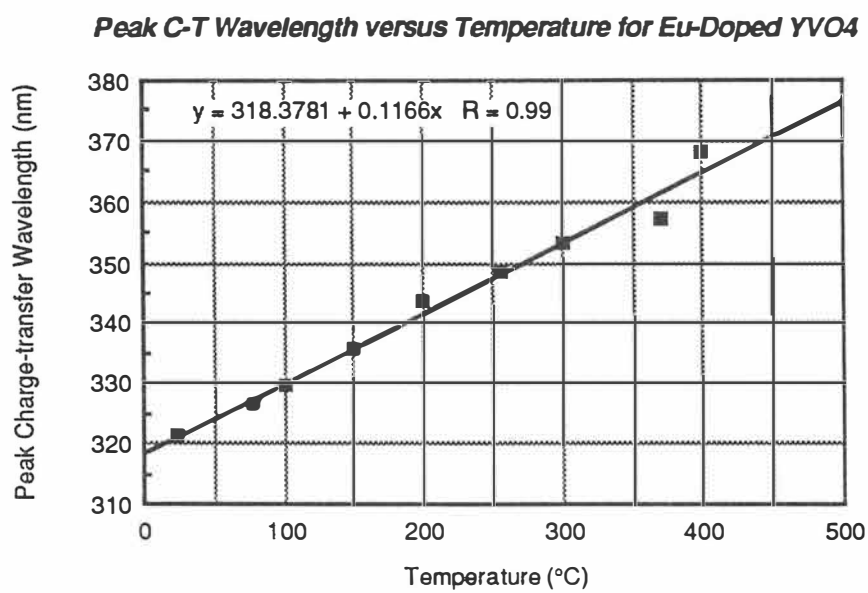
Figure 4-41. Peak charge-transfer wavelength versus temperature for $YVO_4:Eu^{3+}$.

It should be noted in the excitation spectra at elevated temperatures of the Type 2391 phosphor that when the charge-transfer band shifts to the red, it eventually dominates the fluorescence of the atomic excitation peak at 394 nm. Excitation spectra are also presented for Type 1120 YVO_4:Eu^{3+} made within a temperature range of 26.4°C to 350°C. Shown in Figure 4-42 is its excitation spectrum at various temperatures for the 619.0 nm emission line. The absorption band peak wavelength at 26.4°C is located at 310.8 nm, whereas at 350°C, the peak wavelength is found at 342.1 nm, a noticeable change of 31.3 nm in 323.6°C. Again, one of the advantages of these two particular phosphors lies in the fact that their charge-transfer band is located near the 337 nm line and can be used in temperature sensing applications which require a N_2 laser for efficient excitation.

The emission spectrum of Type 2391 YVO_4:Eu^{3+} for excitation at 320 nm is shown in Figure 4-43 for a temperature range of 25°C to 275°C. Several lines of emission are located at 587.3, 595.6, 610.2, 614.9, 618.5, and 638.2 nm. No distinguishable spectral shifts were observed on any of the major emission lines, however it was observed that the relative intensity was sometimes higher at elevated temperatures than that measured at room temperature. It is not known why this occurs.

Figure 4-42. Excitation spectra of europium-doped yttrium vanadate

(Type 1120) at elevated temperatures (619 nm EM).
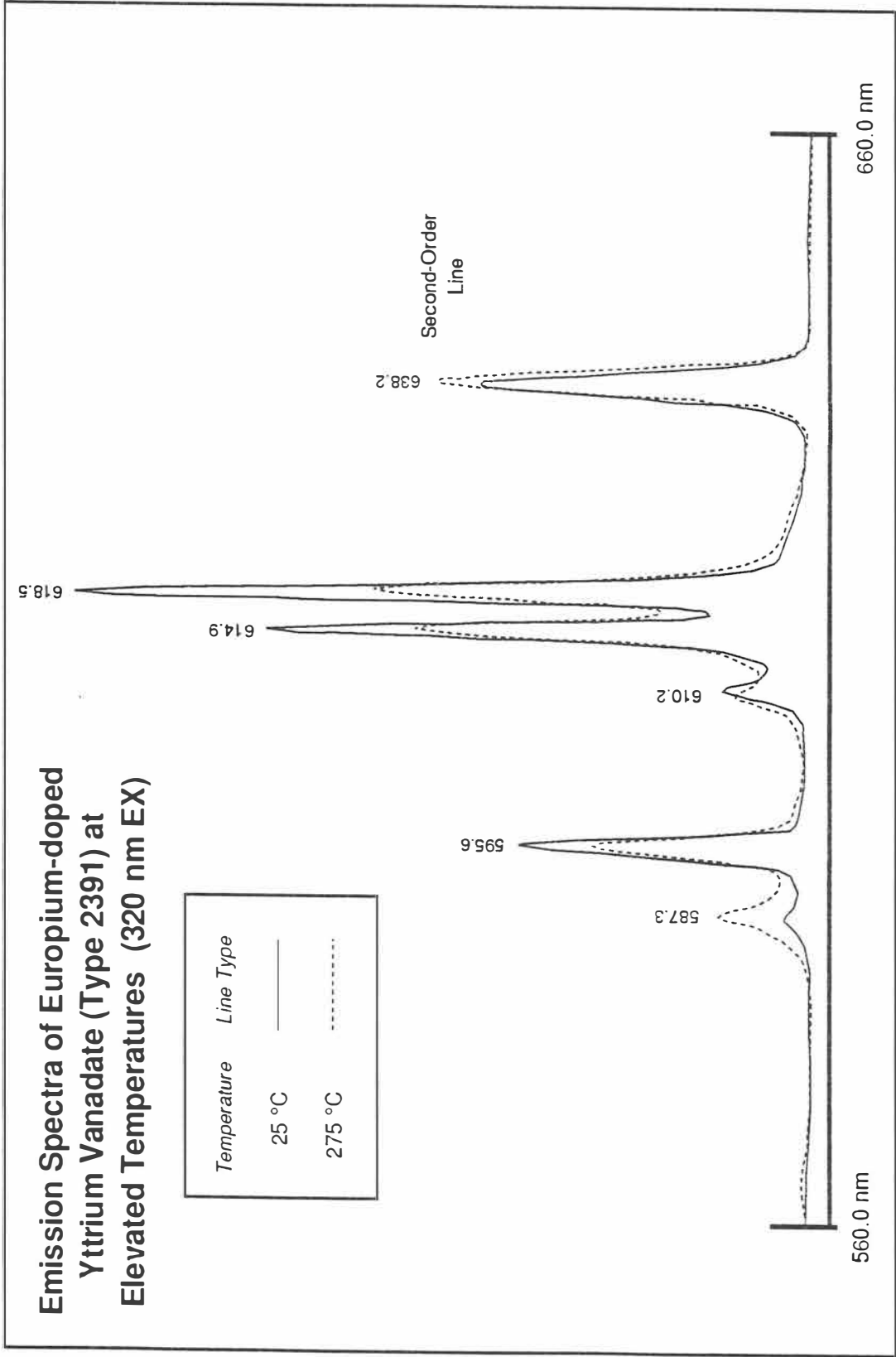
Figure 4-43. Emission spectra of europium-doped yttrium vanadate (Type 2391) at elevated temperatures (320 nm EX).

Europium-doped Barium Phosphate ($Ba_3(PO_4)_2$:Eu^{2+})

Excitation and emission spectra are presented for europium-doped barium phosphate taken within a temperature range of 25°C to 330°C. A room temperature spectrum of $Ba_3(PO_4)_2$:Eu^{2+} are shown in Figure 4-44 and displays the peak position of its charge-transfer band which is located at 355 nm. The observed fluorescence of this phosphor appears blue to the eye and the dopant ion is known to be divalent europium. Figure 4-45 shows the peak emission wavelength positioned at 411 nm when excited by wavelength of 305 nm.

The excitation spectra at various temperatures for the 415.0 nm line of $Ba_3(PO_4)_2$:Eu^{2+} is shown in Figure 4-46. In the excitation spectra, the charge-transfer absorption band shows a slight spectral shift to the red at increasing temperatures. The absorption band peak wavelength at 25°C is found at 355 nm, whereas at 330°C, the peak wavelength is located at 374 nm, a change of 19 nm in 305°C. In addition, the charge-transfer absorption band bandpass wavelength (at FWHM) is measured at 104 nm, 109 nm, 119 nm, and 120 nm for temperatures 25°C, 155°C, 240°C, and 330°C respectively.

An emission spectrum at various temperatures for $Ba_3(PO_4)_2$:Eu^{2+} at 305.0 nm excitation is shown in Figure 4-47. Broadening and spectral shift are also observed. The emission peak wavelength is measured at 31 nm, 38 nm, 42 nm, and 44 nm for temperatures 25°C, 155°C, 240°C, and 330°C respectively. Relative intensities in the emission spectra of this phosphor are still strong at higher temperatures.
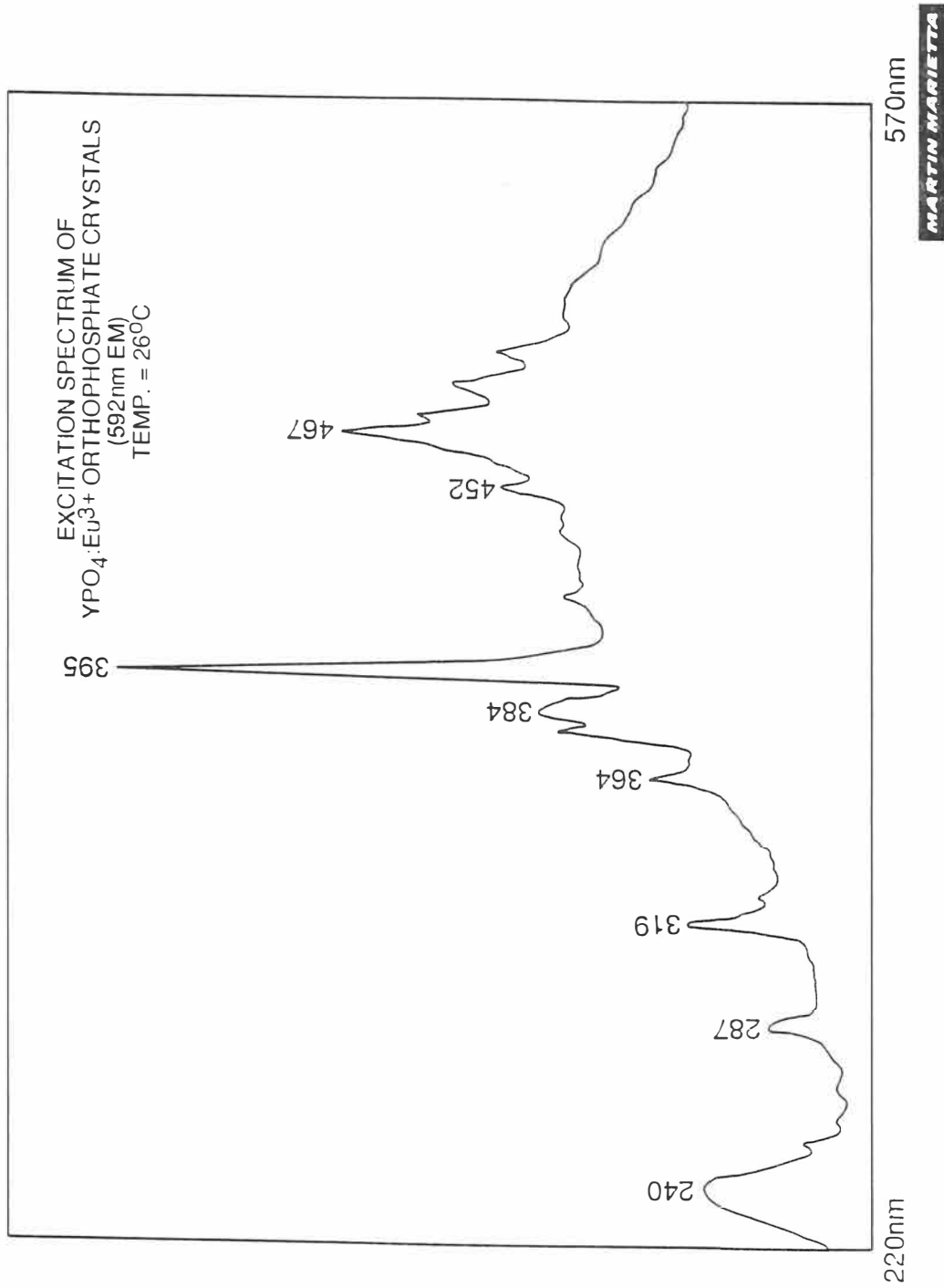
138
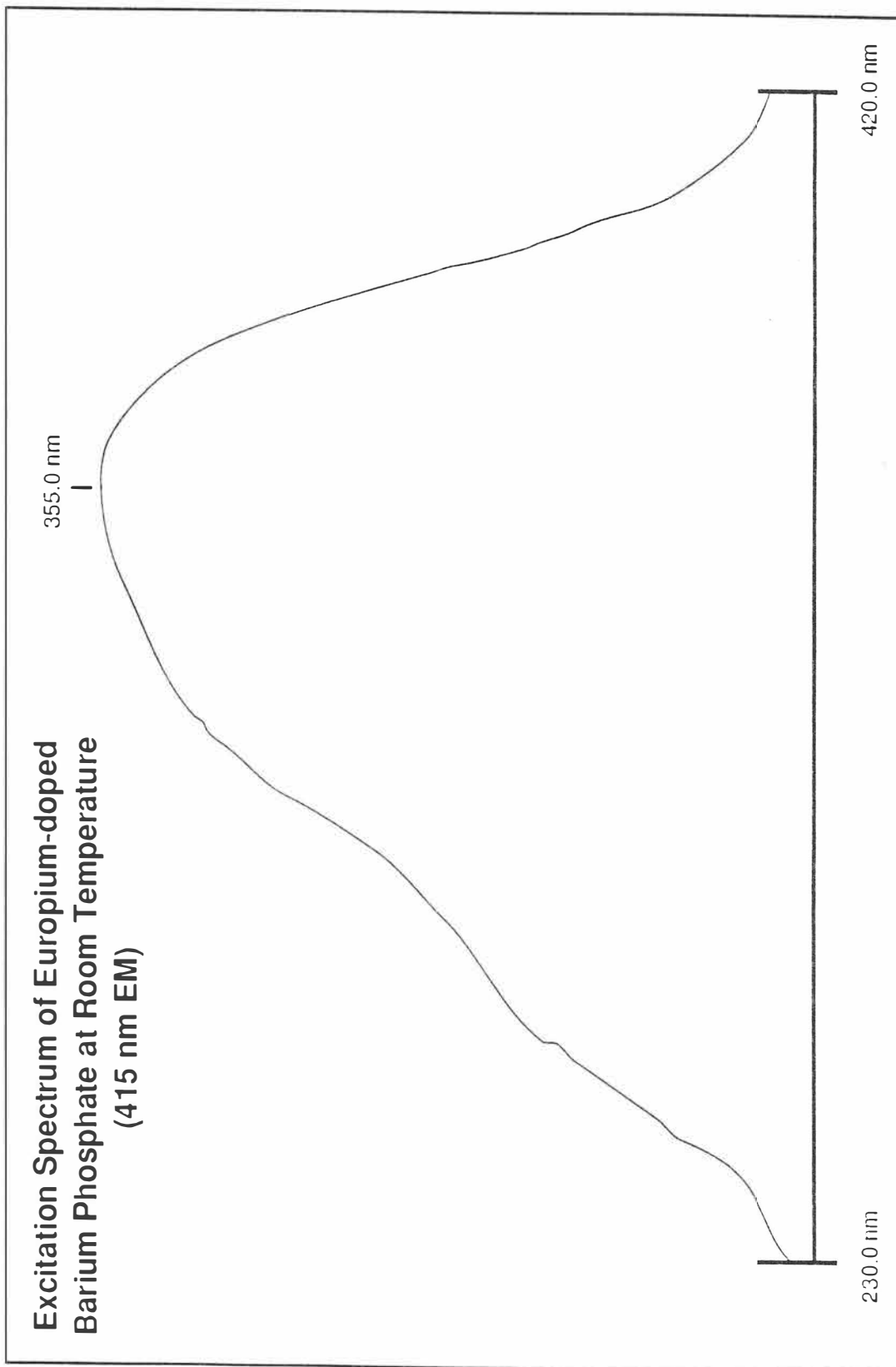
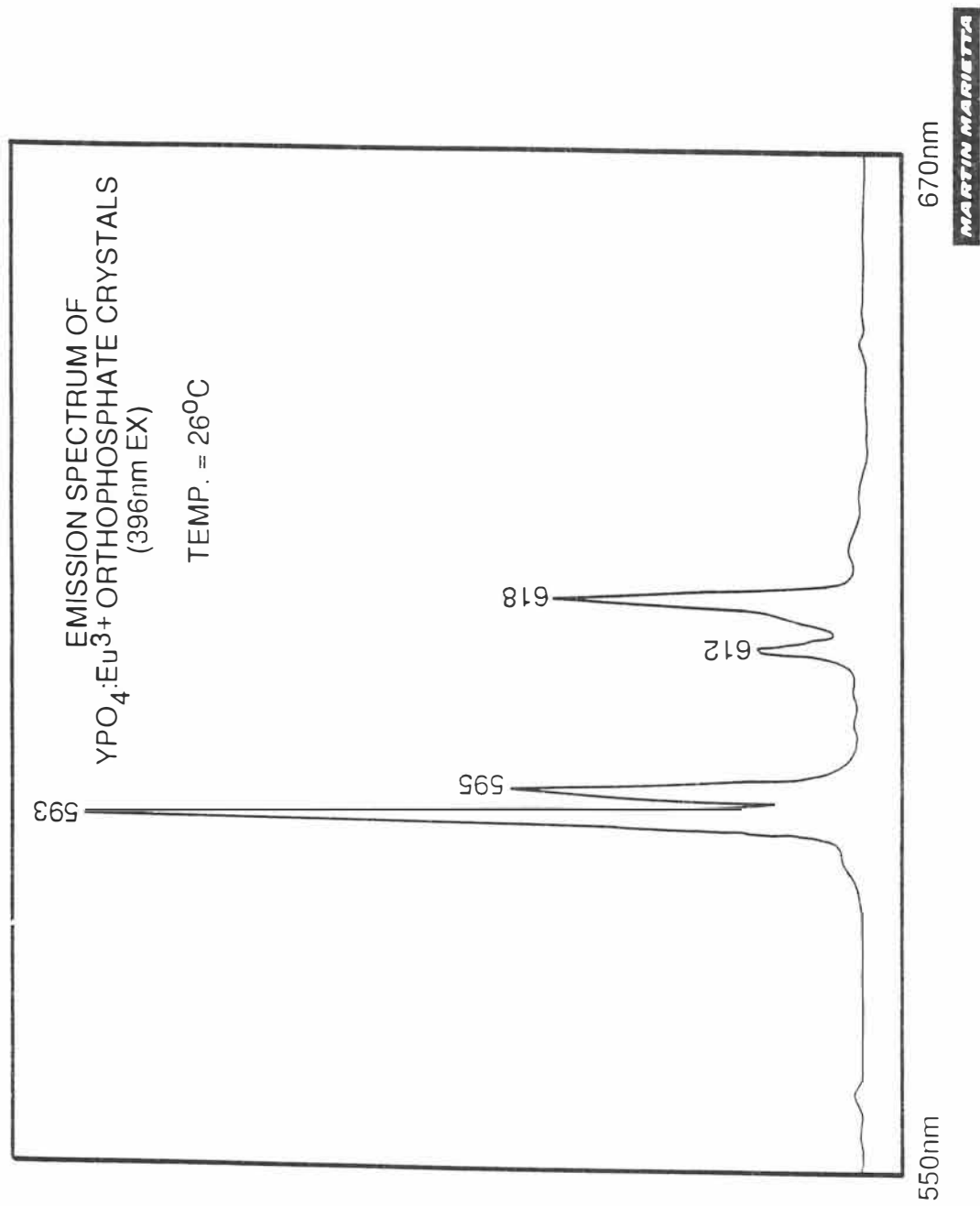Figure 4-44. Excitation spectrum of europium-doped barium phosphate at room temperature (415 nm EM).
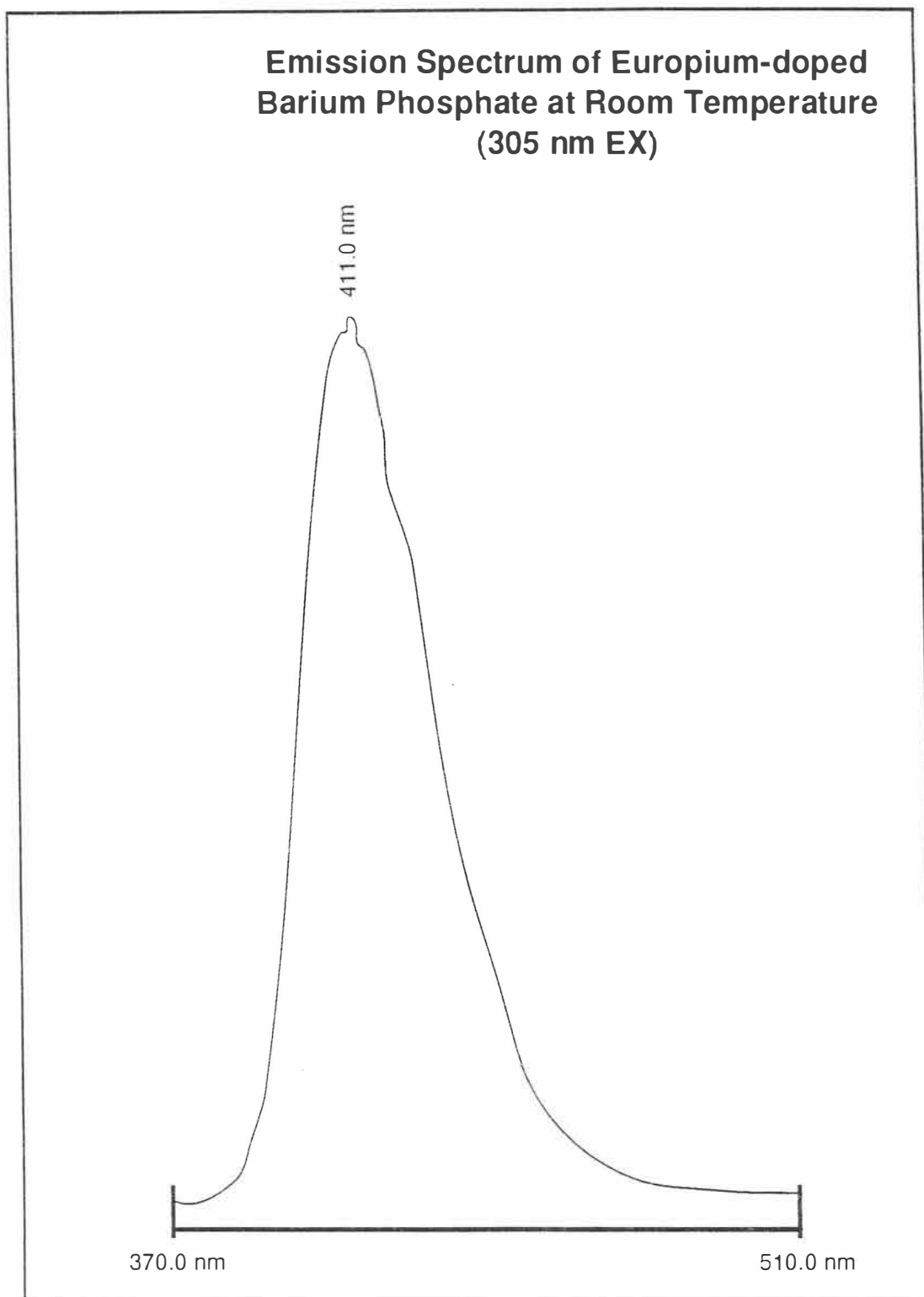
Figure 4-45. Emission spectrum of europium-doped barium phosphate at room temperature (305 nm EX).
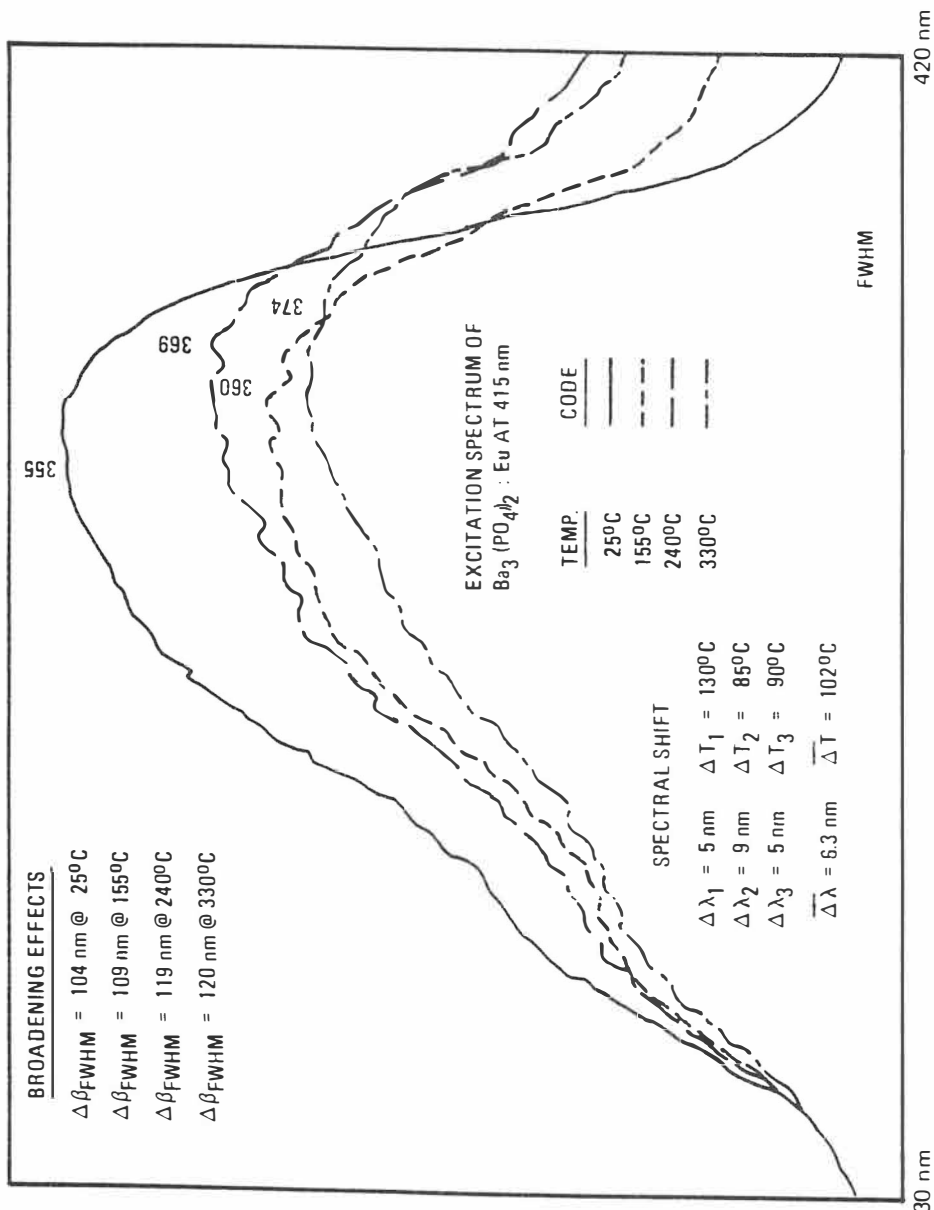
Figure 4-46. Excitation spectra of europium-doped barium phosphate at elevated temperatures (415 nm EM).

SPECTRAL SHIFT INFORMATION

$\Delta\lambda_1 = 3$ nm $\Delta T_1 = 130^oC$

$\Delta\lambda_2 = 4$ nm $\Delta T_2 = 85^oC$

$\Delta\lambda_3 = 5$ nm $\Delta T_3 = 90^oC$

BROADENING EFFECTS

$\Delta\beta_{FWHM} = 31$ nm @ 25^oC

$\Delta\beta_{FWHM} = 38$ nm @ 155^oC

$\Delta\beta_{FWHM} = 42$ nm @ 240^oC

$\Delta\beta_{FWHM} = 44$ nm @ 330^oC

EMISSION SPECTRUM OF
$Ba_3 (PO_4)_2 : Eu$ A T 305 nm

OCT. 20, 1987

TEMP.	CODE
25^oC	——————
155^oC	— — —
240^oC	- - - -
330^oC	—-—-

FWHM

370 nm   510 nm

Figure 4-47. Emission spectrum of europium-doped barium phosphate at elevated temperatures (305 nm EX).

Europium-doped Lanthanum Oxysulfide ($La_2O_2S:Eu^{3+}$)

The excitation spectrum of the 538 nm emission line of $La_2O_2S:Eu^{3+}$ taken at room temperature is shown in Figure 4-48. The peak of the charge-transfer absorption band for this phosphor lies at 340.6 nm. Other less important atomic transition peaks lie at 396.4 and 466.3 nm. The excitation spectrum of the 612 nm emission line of $La_2O_2S:Eu^{3+}$ taken at room temperature is shown in Figure 4-49. The peak of the charge-transfer absorption band for this phosphor lies at 345.4 nm. Other atomic transition peaks are found at 396.0, 466.8 and 538.6 nm. The excitation spectrum of the 619 nm emission line of $La_2O_2S:Eu^{3+}$ taken at room temperature is shown in Figure 4-50. The peak of the charge-transfer absorption band for this phosphor lies at 346.1 nm whereas other atomic transition peaks can be found at 398.0, 469.2 and 540.5 nm.

The room temperature emission spectrum for $La_2O_2S:Eu^{3+}$ at 345 nm excitation is shown in Figure 4-51. Several strong emission lines are seen at 537, 554, 583, 593, 612 and 619 nm. An expanded form of the same room temperature emission spectrum is shown in Figure 4-52 and gives finer resolution to some of the more dominant peaks in the spectrum. Those peaks are located at 536.9, 553.8 and 583.8 nm.

Excitation spectra at elevated temperatures for the 538 nm emission line of $La_2O_2S:Eu^{3+}$ are displayed in Figure 4-53 The peak of the charge-transfer band shifts from roughly 333.2 nm to 335.7 nm, a difference of only 2.5 nm as temperature increased from 25°C to 200°C.

The emission spectra of $La_2O_2S:Eu^{3+}$ for excitation at 350 nm are shown in Figure 4-54 for elevated temperatures. No distinguishable spectral shifts were observed, however it is interesting to note that the spectra show a gradual decrease in intensity of the 592, 612, and 621 nm emission lines as temperature was increased from 22°C to 250°C.
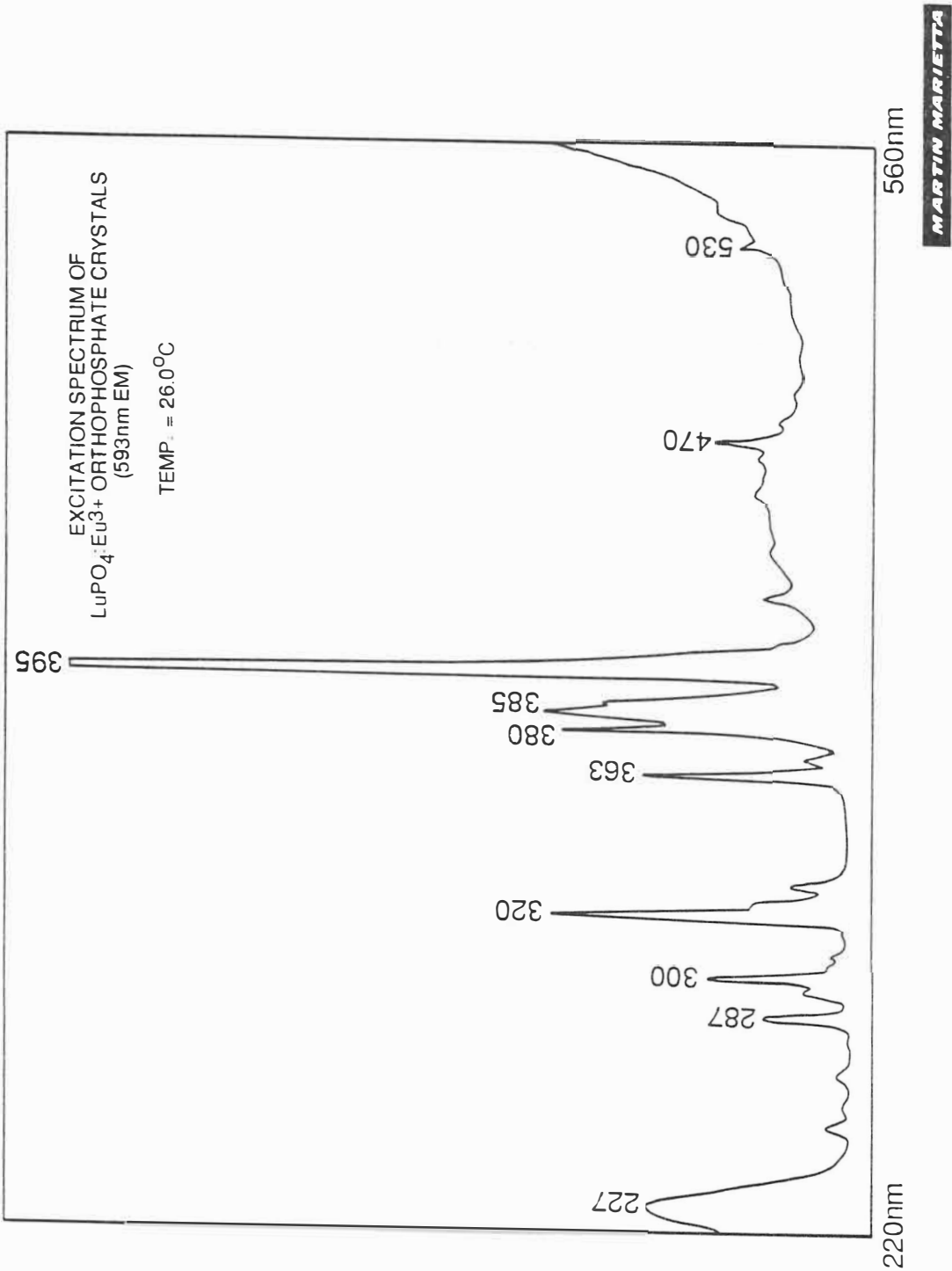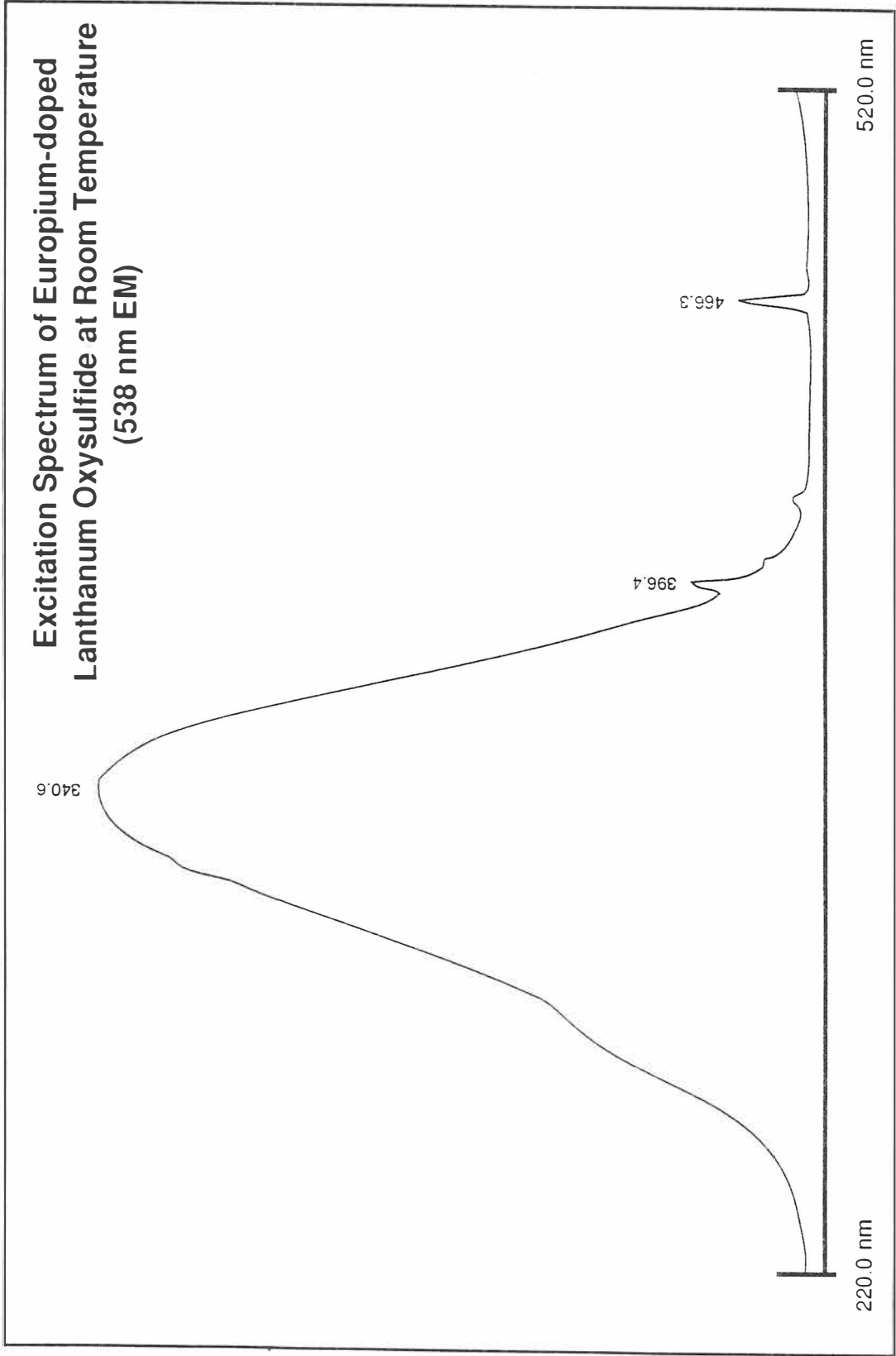
Figure 4-48. Excitation spectrum of europium-doped lanthanum oxysulfide at room temperature (538 nm EM).
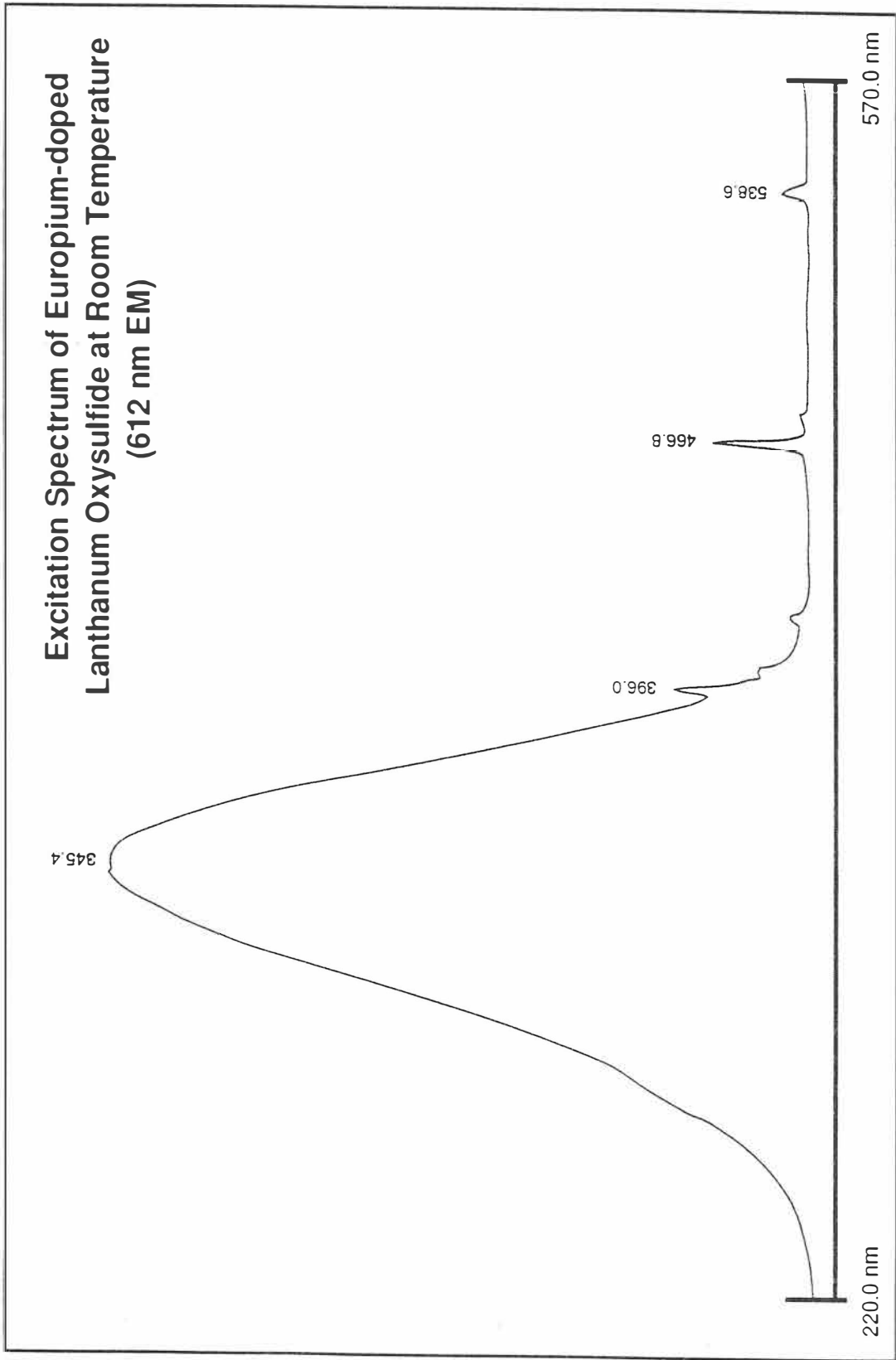
Figure 4-49.   Excitation spectrum of europium-doped lanthanum oxysulfide at room temperature (612 nm EM).

145
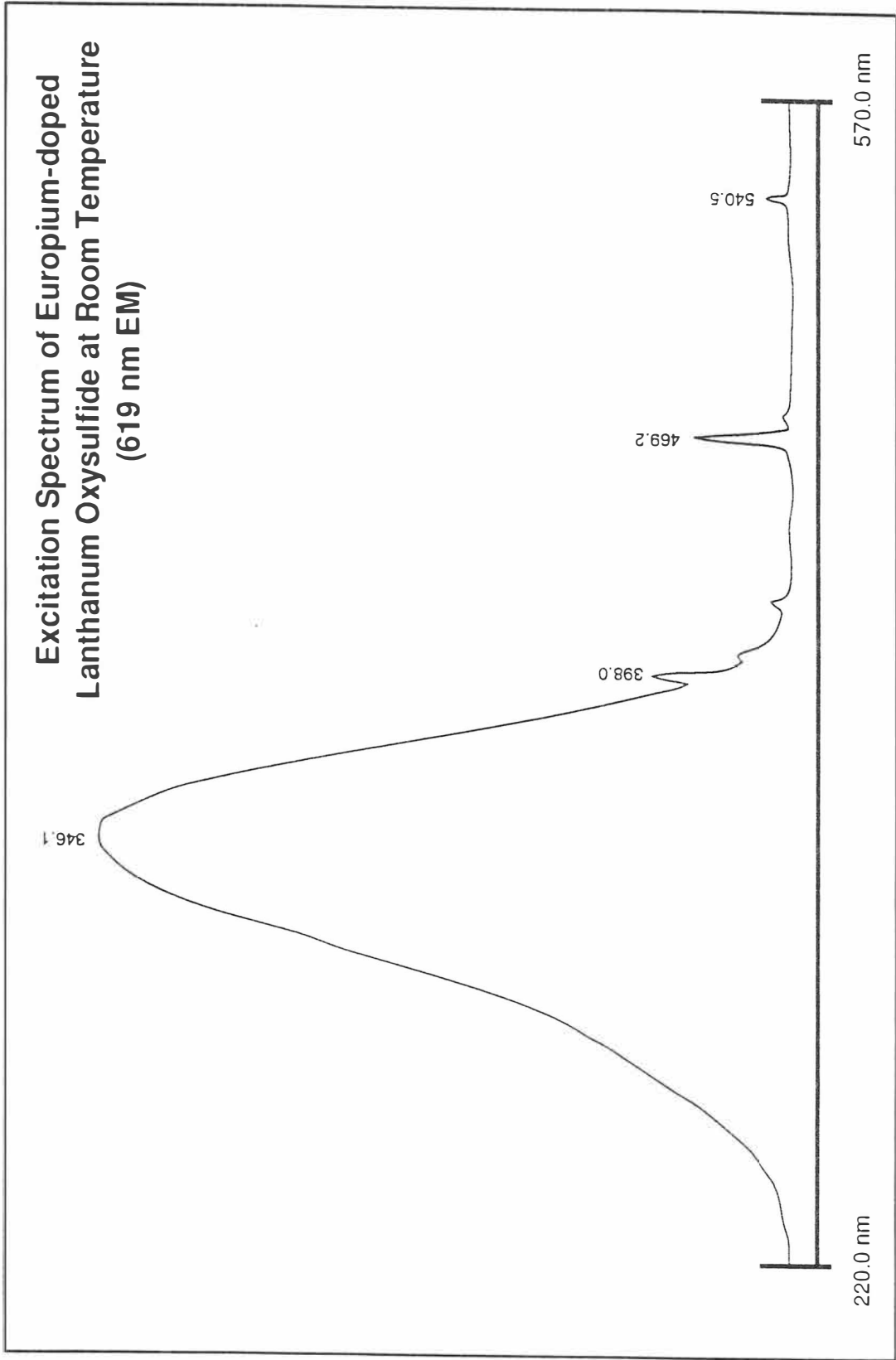
Figure 4-50. Excitation spectrum of europium-doped lanthanum oxysulfide at room temperature (619 nm EM).
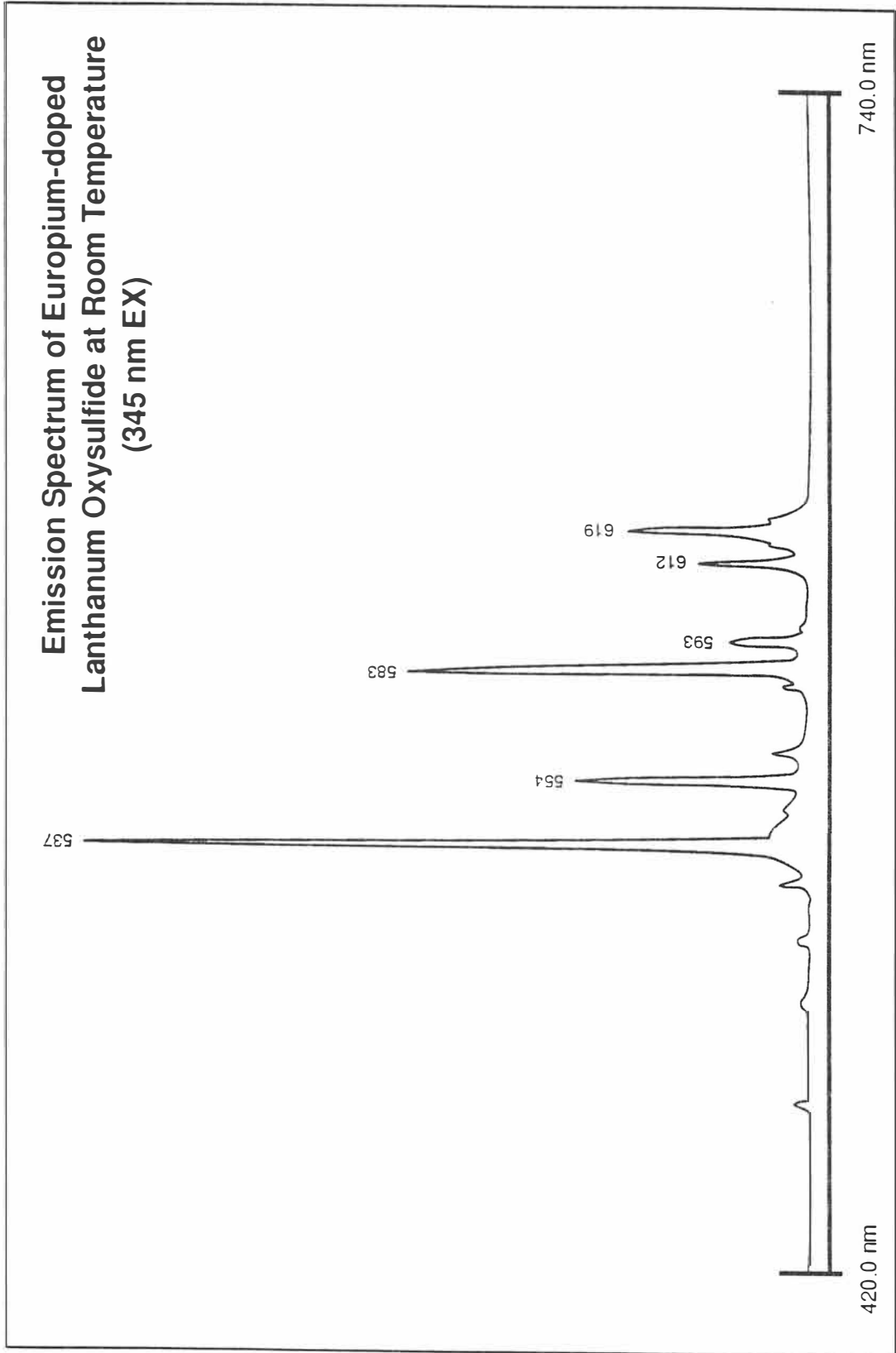
Figure 4-51. Emission spectrum of europium-doped lanthanum oxysulfide at room temperature (345 nm EX).
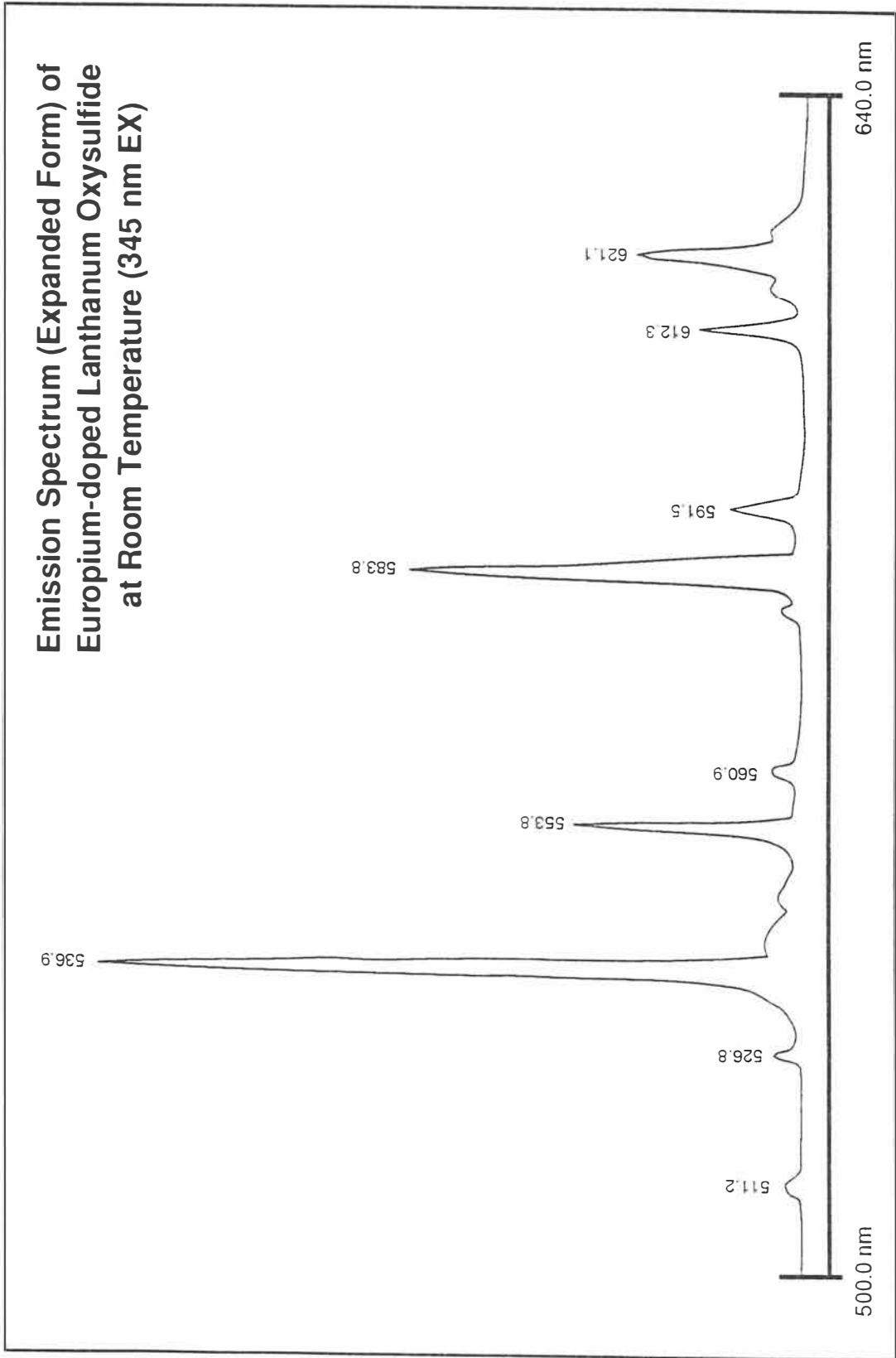
Figure 4-52. Emission spectrum (expanded form) of europium-doped lanthanum oxysulfide at room temperature (345 nm EX).

148
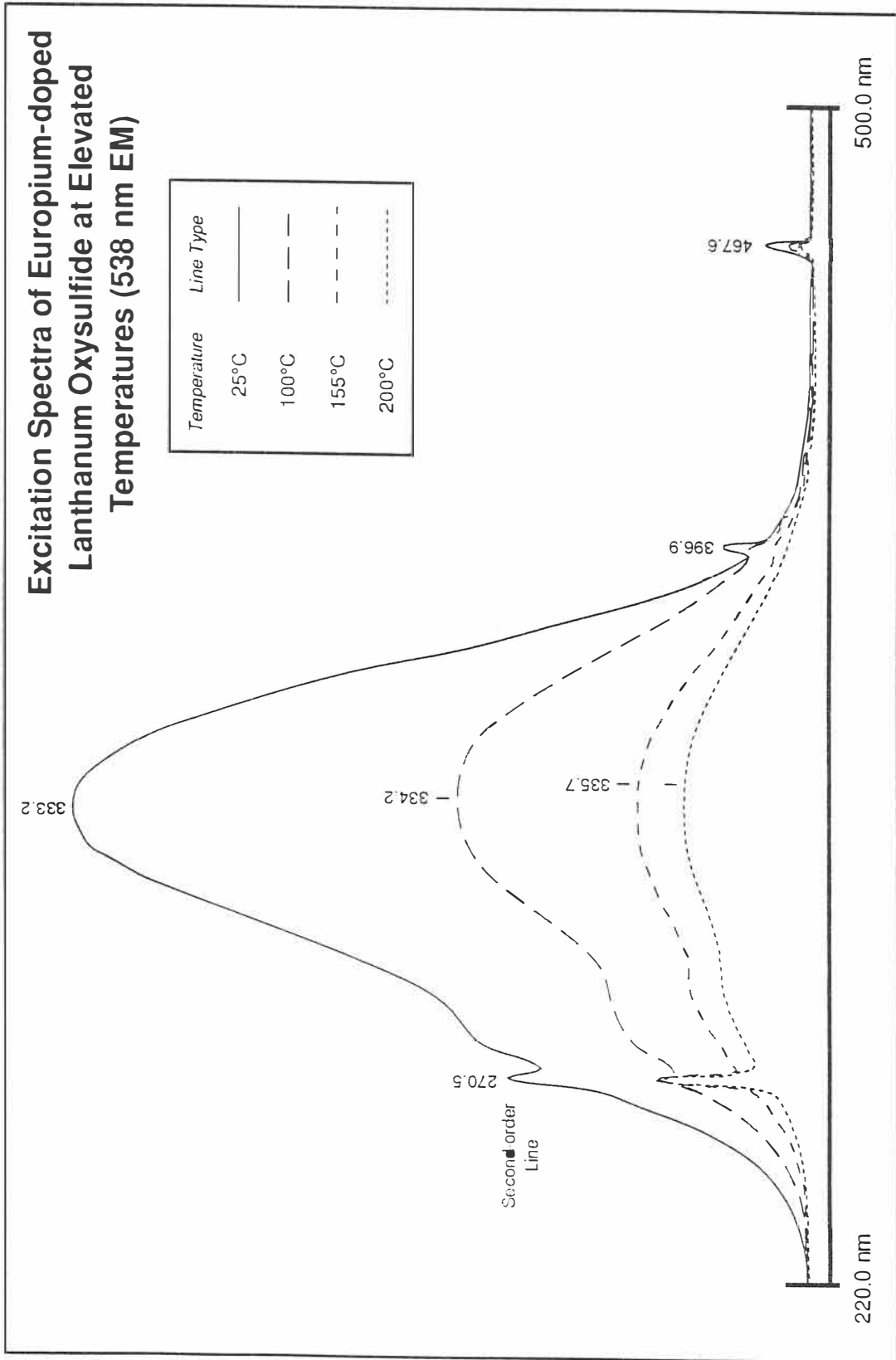
Figure 4-53. Excitation spectra of europium-doped lanthanum oxysulfide at elevated temperatures (538 nm EM).
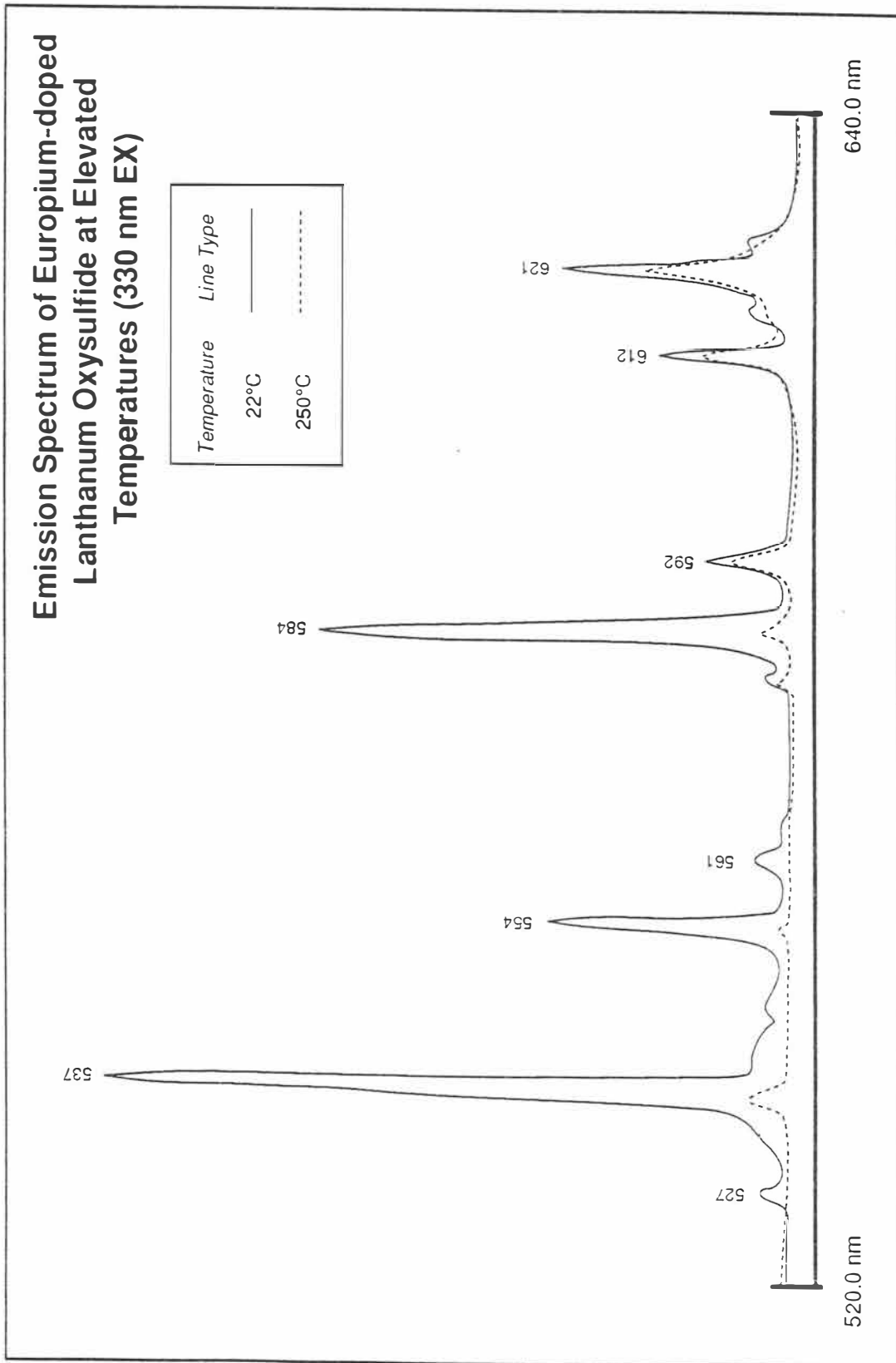
Figure 4-54. Emission spectrum of europium-doped lanthanum oxysulfide at elevated temperatures (330 nm EX).

Europium-doped Yttrium Oxysulfide ($Y_2O_2S:Eu^{3+}$)

Excitation and emission spectra are presented for $Y_2O_2S:Eu^{3+}$ taken at room temperature and at elevated temperatures. The excitation spectrum of the 612 nm emission line of $Y_2O_2S:Eu^{3+}$ taken at room temperature is shown in Figure 4-55. The peak of the charge-transfer absorption band for this phosphor lies at 352.0 nm and another prominent atomic transition line lies at 393.0 nm. Other less important atomic transition peaks lie at 400, 415, 464, 471, 524, and 535 nm. Likewise, the excitation spectrum of the 619 nm emission line of $Y_2O_2S:Eu^{3+}$ taken at room temperature is shown in Figure 4-56. The peak of the charge-transfer absorption band for this phosphor lies at 352.6 nm. Atomic transition lines can be found close to those lines of the spectrum taken at an emission wavelength of 612 nm.

The room temperature emission spectrum for $Y_2O_2S:Eu^{3+}$ at 355 nm excitation is shown in Figure 4-57. Several strong emission lines are seen at 536, 591, 612 and 619 nm while weaker emission lines are found at 468, 495, 512, 554, 580, and 585 nm. An expanded form of the same room temperature emission spectrum is shown in Figure 4-58 and gives finer resolution of some of the major peaks in the spectrum. Those peaks are located at 537.6, 592.2, 613.0, and 622.3 nm.

Excitation spectra at elevated temperatures for the 620 nm emission line of $Y_2O_2S:Eu^{3+}$ are displayed in Figure 4-59. The peak of the charge-transfer band shifts from roughly 349.9 nm to 361.0 nm, a difference of only 11.1 nm as temperature increased from 25.5°C to 200°C. The emission spectra of $Y_2O_2S:Eu^{3+}$ for excitation at 355 nm are shown in Figures 4-60 and 4-61 for discrete temperatures of 25, 105, 200, and 305°C. These spectra show the gradual decrease in intensity as temperature increases. No distinguishable spectral shifts were observed. Figure 4-62 is a compiled version of these spectra measured as a function of temperature.

151
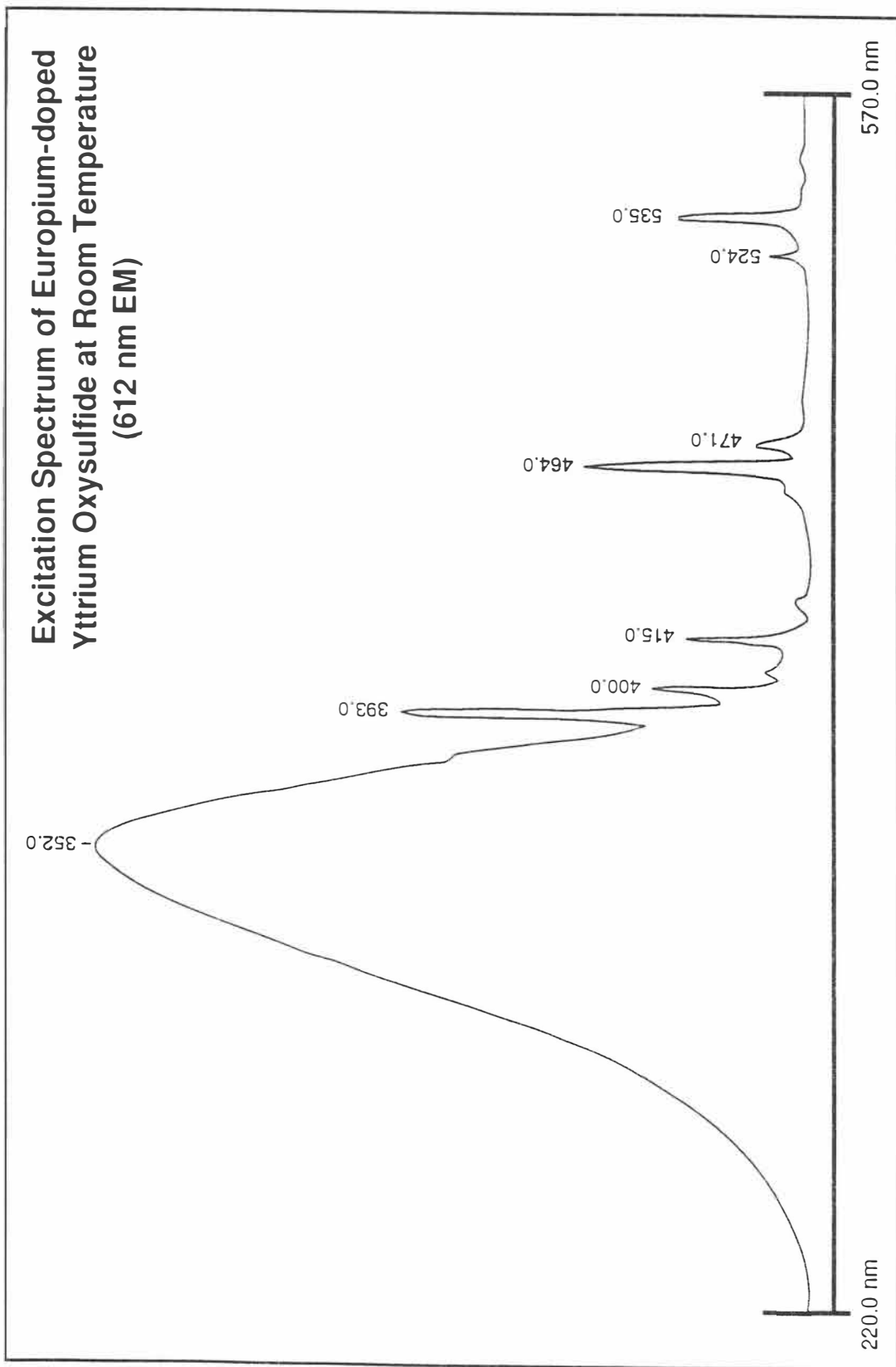
Figure 4-55. Excitation spectrum of europium-doped yttrium oxysulfide at room temperature (612 nm EM).

152
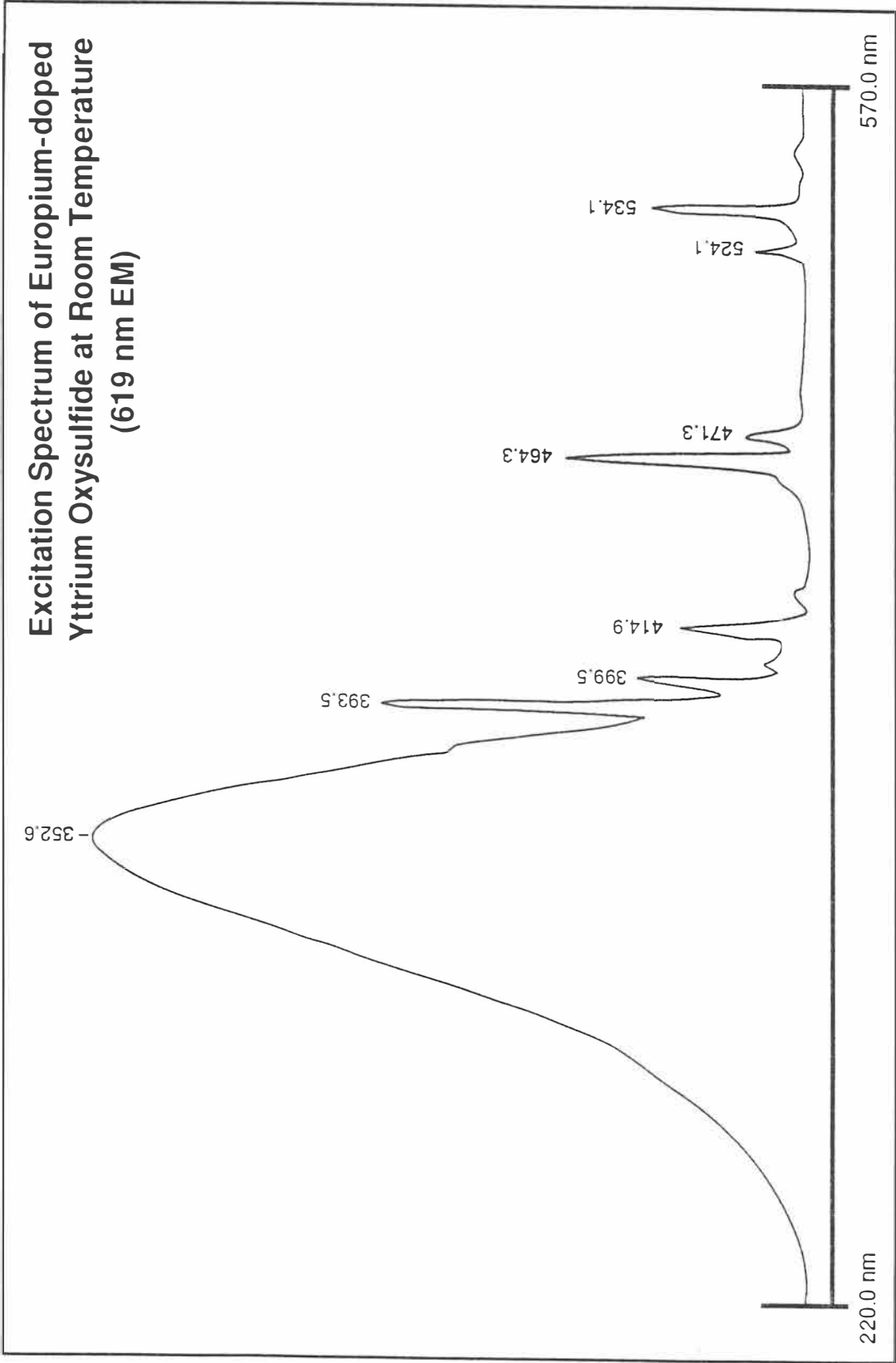
Figure 4-56. Excitation spectrum of europium-doped yttrium oxysulfide at room temperature (619 nm EM).

153
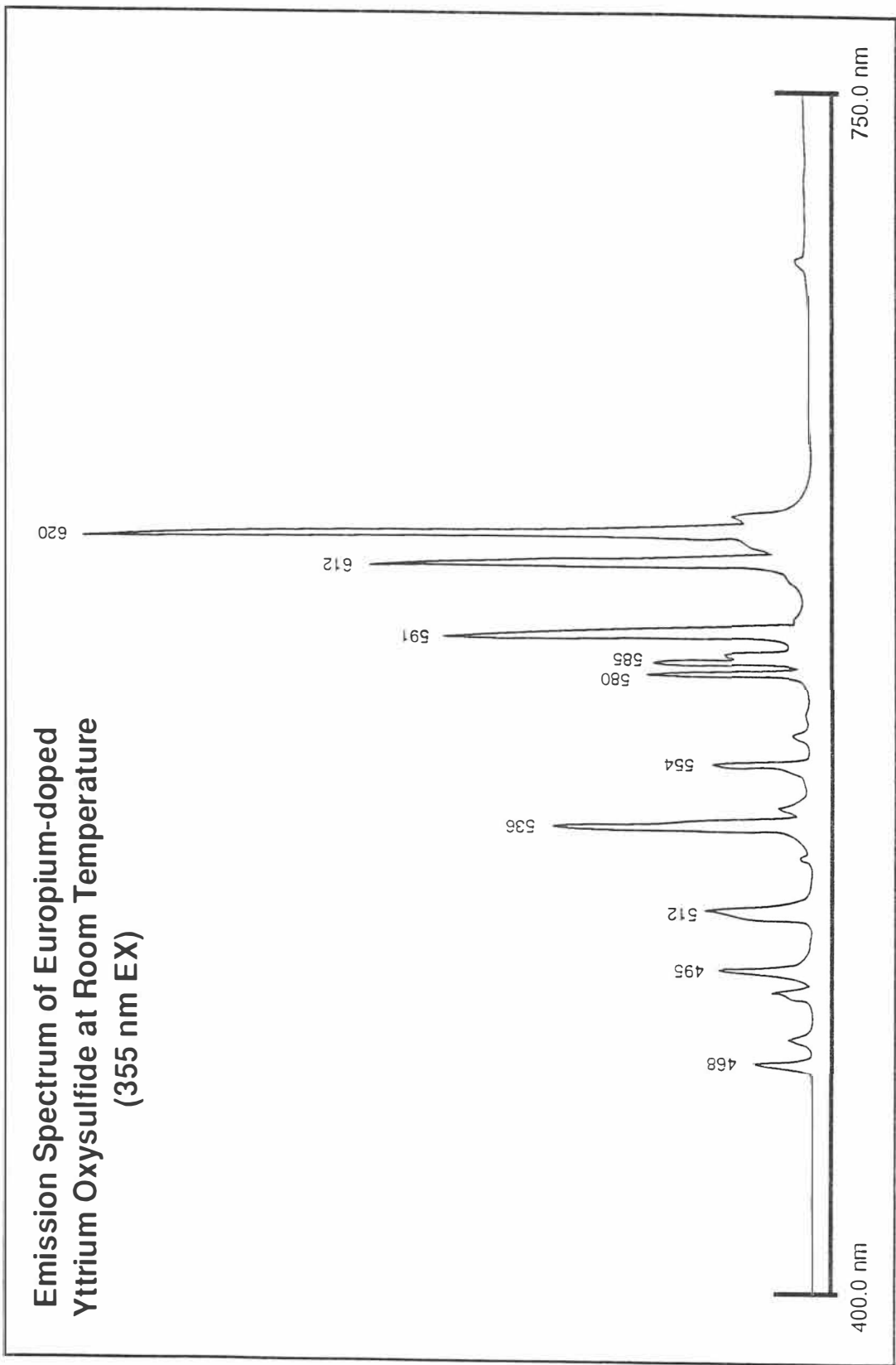
Figure 4-57. Emission spectra of europium-doped yttrium oxysulfide at room temperature (355 nm EX).
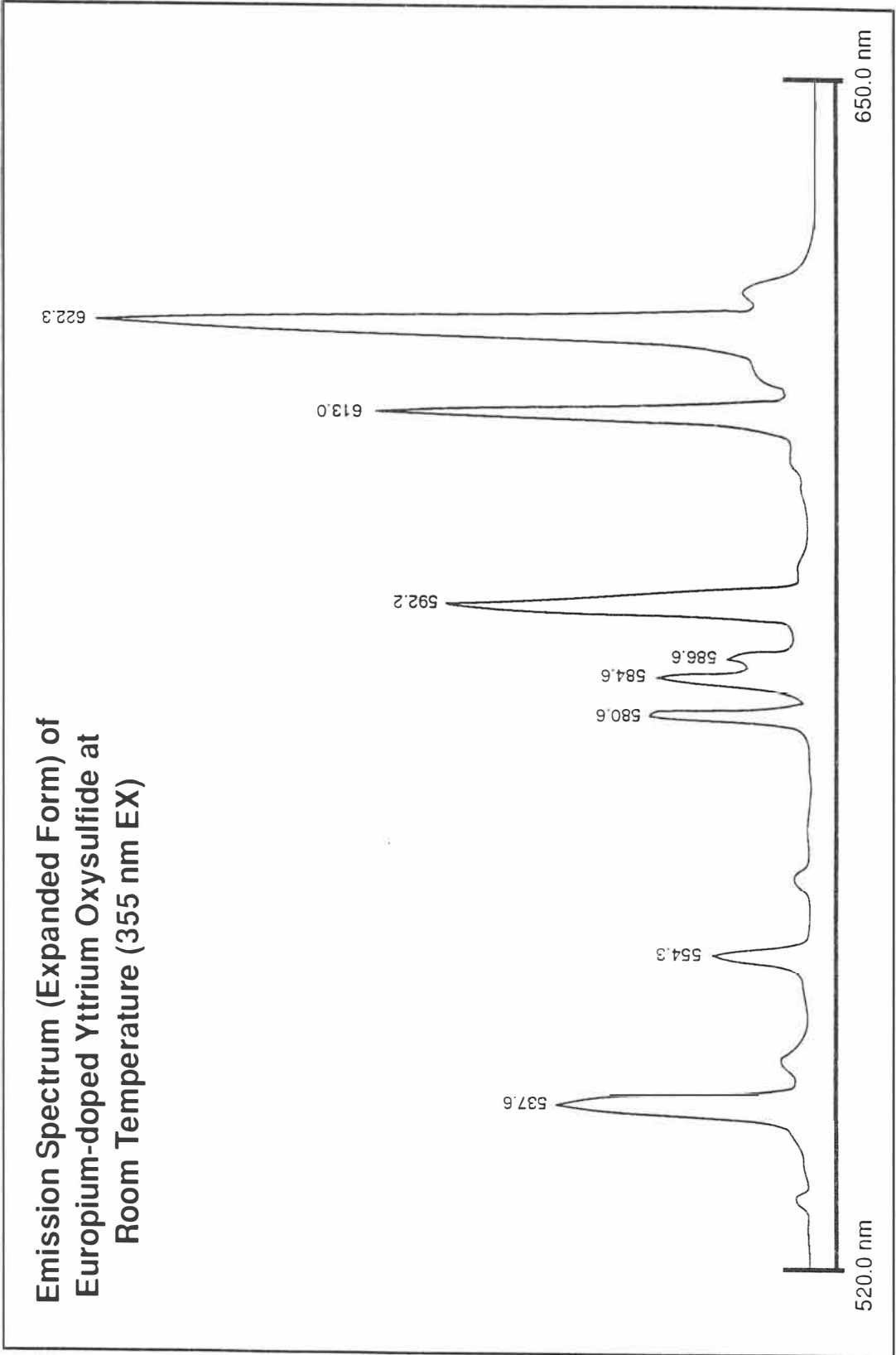
Figure 4-58. Emission spectrum (expanded form) of europium-doped yttrium oxysulfide at room temperature (355 nm EX).

155
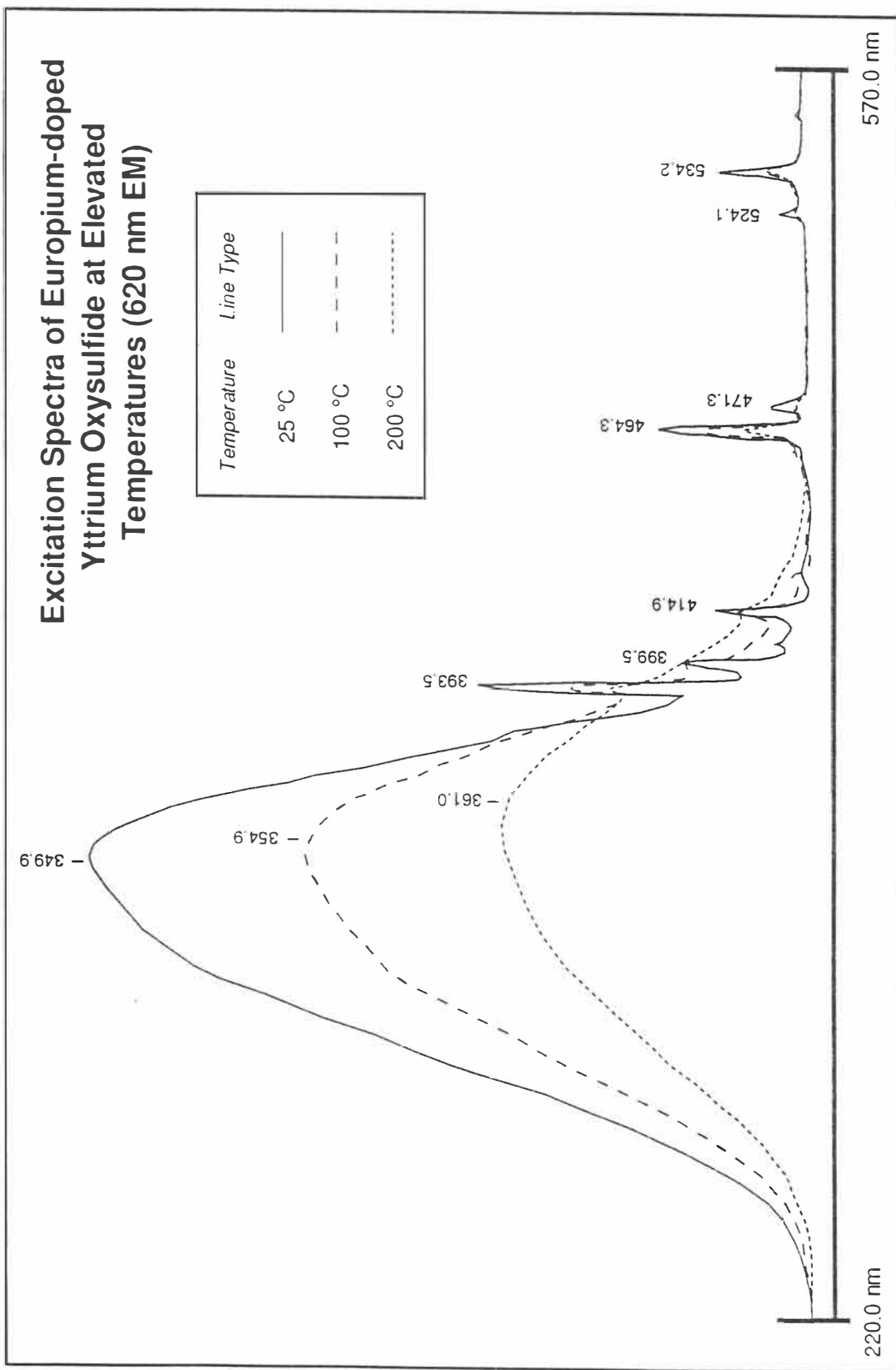
Figure 4-59. Excitation spectrum of europium-doped yttrium oxysulfide at elevated temperatures (620 nm EM).
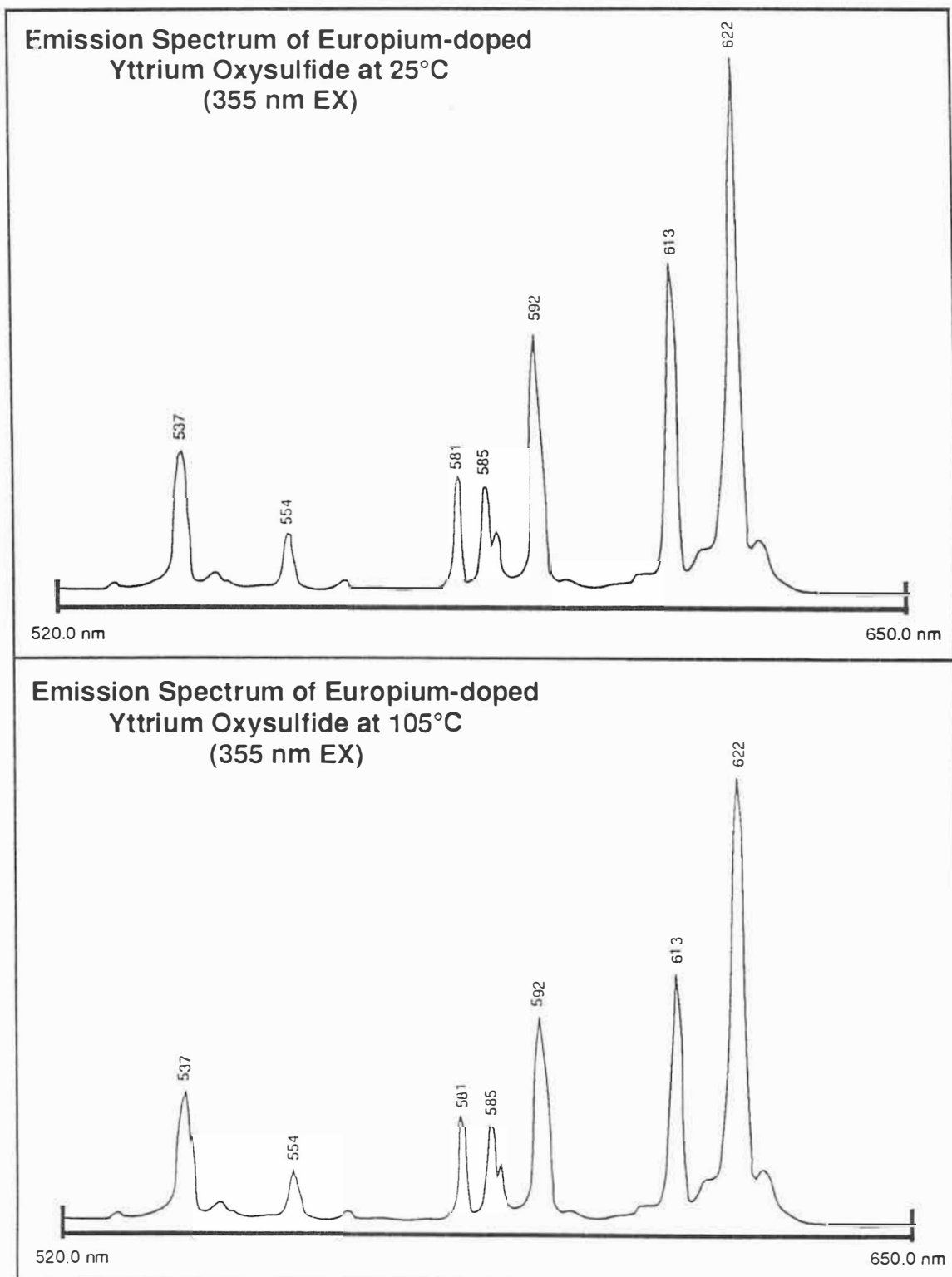
Figure 4-60. Emission spectra of europium-doped yttrium oxysulfide
at 25°C and 105°C (355 nm EX).
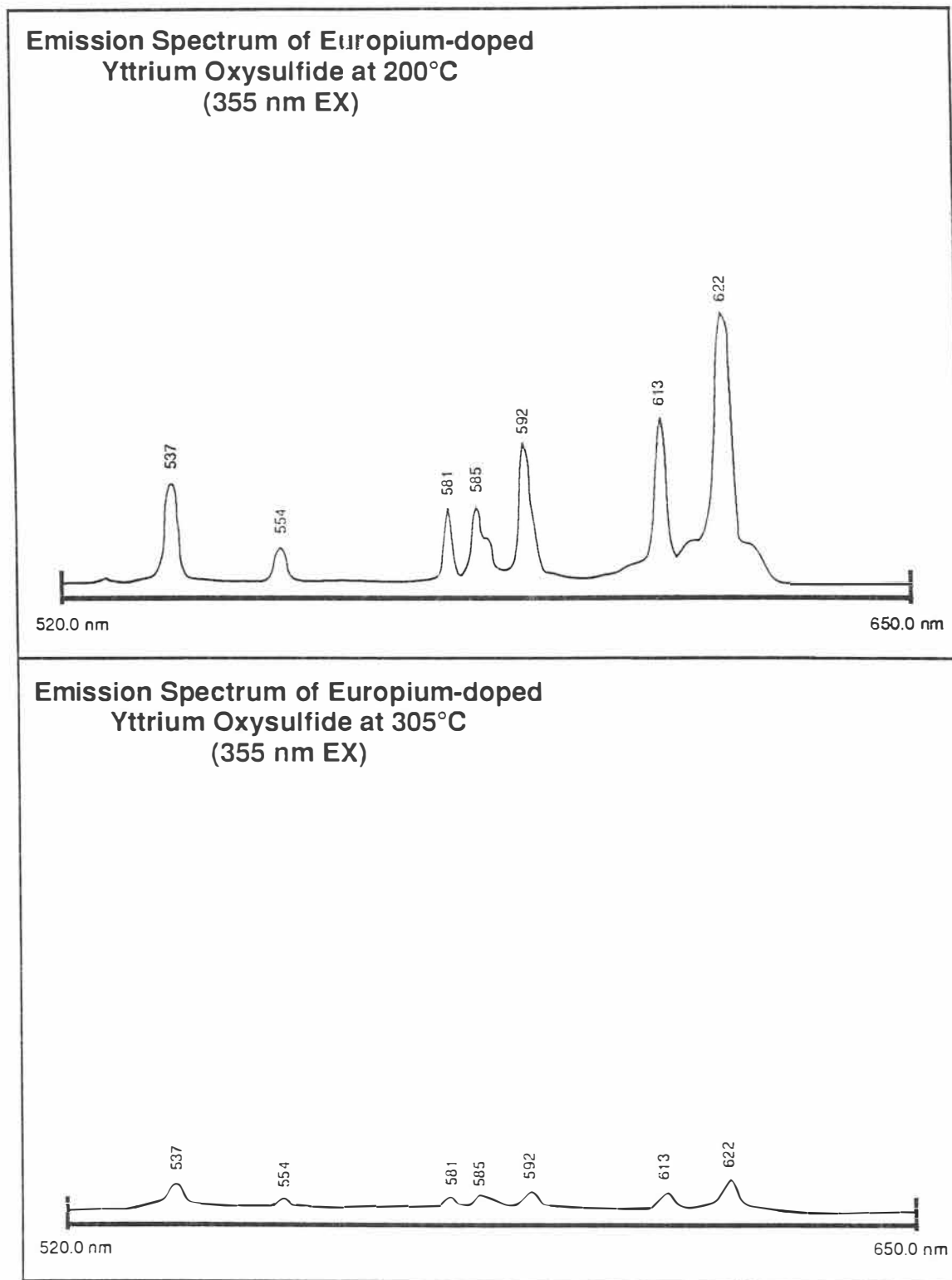
Figure 4-61. Emission spectra of europium-doped yttrium oxysulfide
at 200°C and 305°C (355 nm EX).
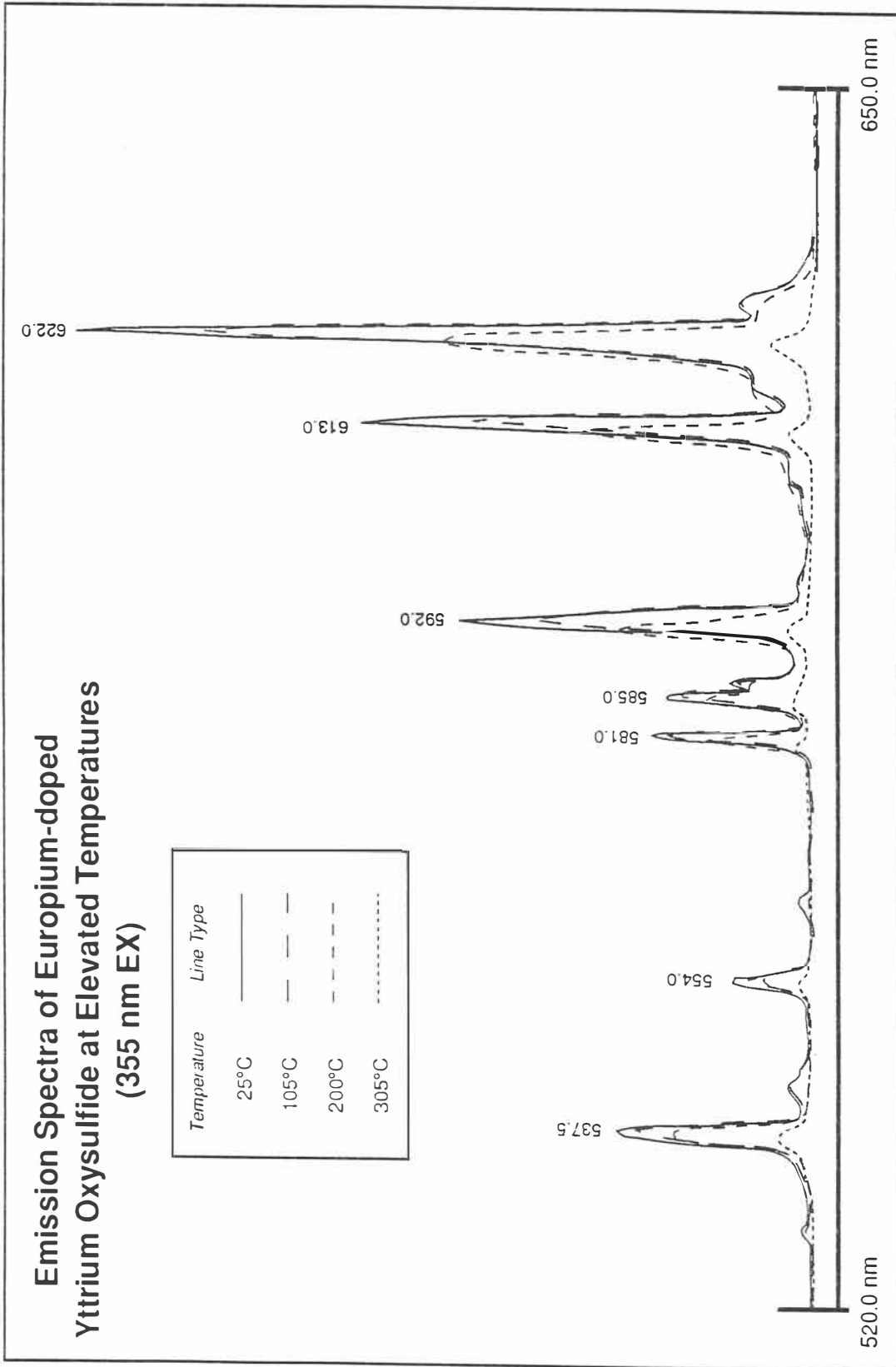
Figure 4-62. Emission spectra of europium-doped yttrium oxysulfide at elevated temperatures (355 nm EX).

Gadolinium-doped Yttrium Oxide (Y$_2$O$_3$:Gd)

Excitation and emission spectra were taken for gadolinium-doped yttrium oxide within a temperature range of 25°C to 335°C. The fluorescence of this phosphor generally yields a bluish color to the eye when excited with an excitation wavelength of approximately 275 nm. The room temperature excitation spectrum for the 315 nm emission line is shown in Figure 4-63 for Y$_2$O$_3$:Gd. Strong absorption lines are observed at 275.6 nm while weaker absorption lines are seen at 248.1 and 255.1 nm. It is uncertain at this time if the observed absorption band is due to a charge-transfer or a ^{5}D state transition and should be further investigated in future research. A room temperature emission spectrum taken at an excitation wavelength of 275 nm is shown in Figure 4-64. Only one strong peak is observed in the spectrum and is located at a peak wavelength of 315.0 nm.

The excitation spectra at various temperatures for the 315 nm line of Y$_2$O$_3$:Gd are shown in Figure 4-65. It was observed that the absorption band showed no significant spectral shift in the excitation spectra as the temperature increased, other than slight shifts due to instrumental errors in the equipment used. Emission spectra at various temperatures for Y$_2$O$_3$:Gd at 275 nm excitation are shown in Figure 4-66. No distinguishable broadening effects or shift in spectral position of the absorption band and atomic emission bands associated with the gadolinium ion were detected. It is also shown that the luminescent intensity of both the absorption band and atomic emission band decreased slightly as the phosphor temperature was increased in both the excitation and emission spectra.
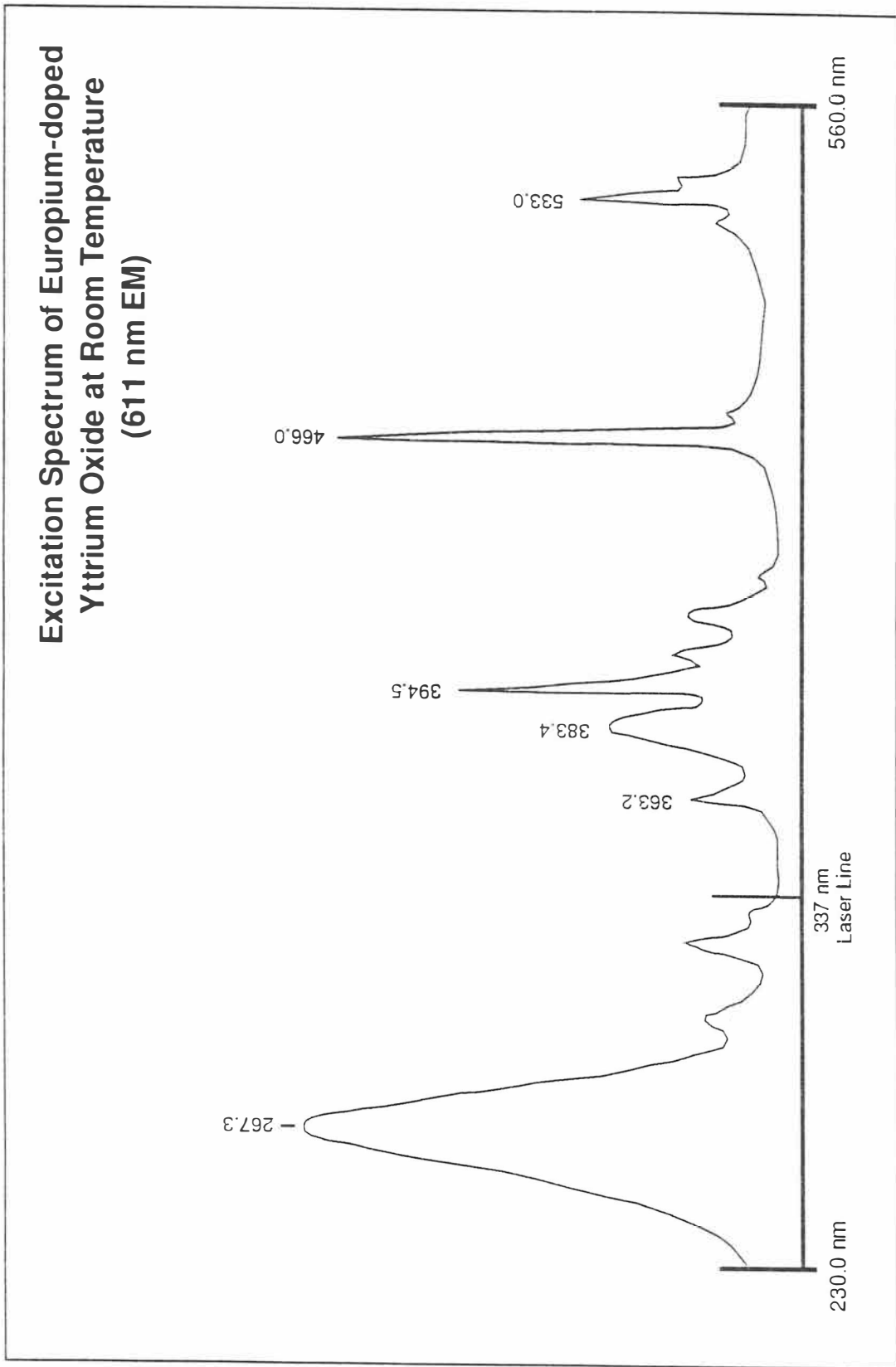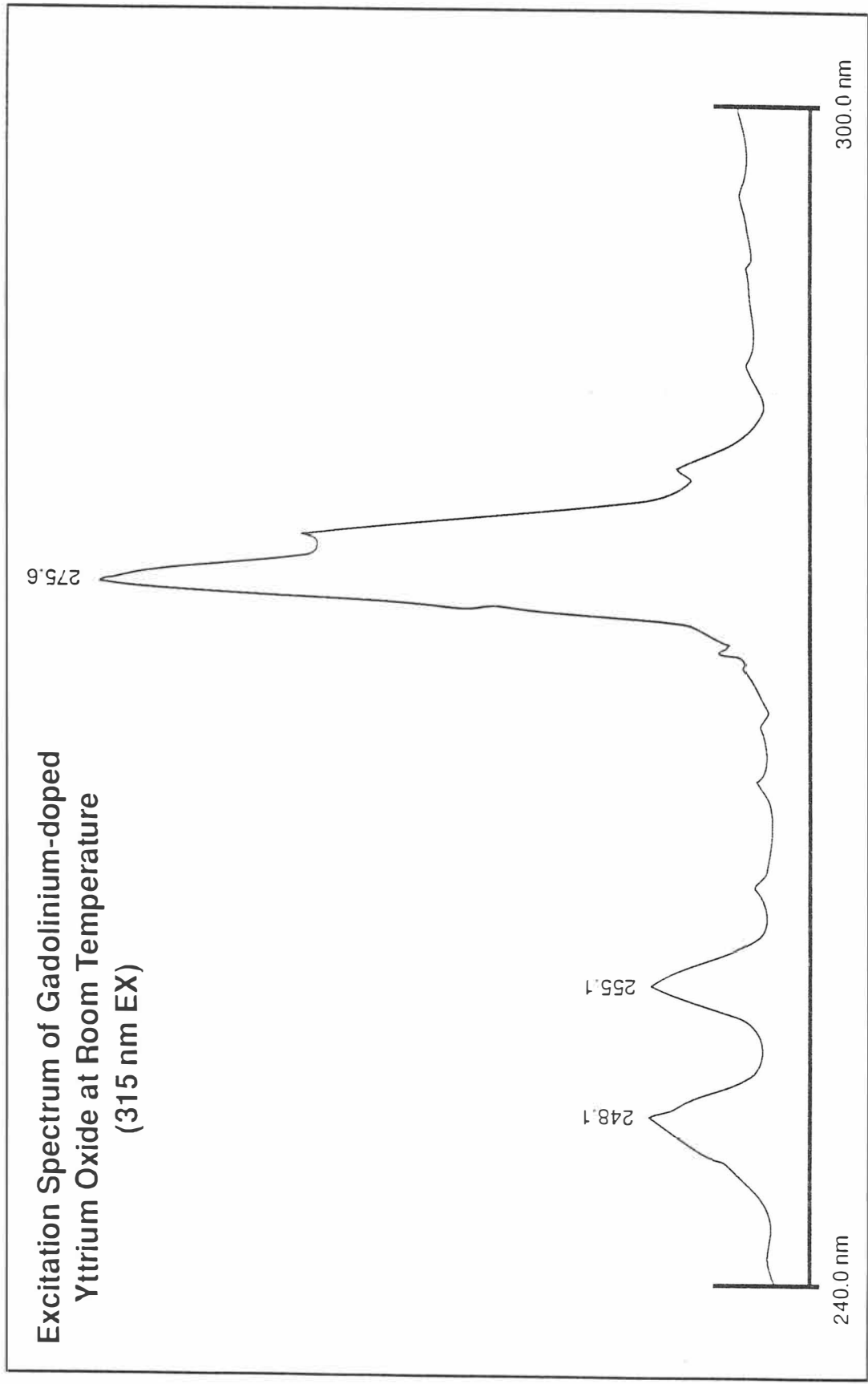
Figure 4-63. Excitation spectrum of gadolinium-doped yttrium oxide at room temperature (315 nm EX).
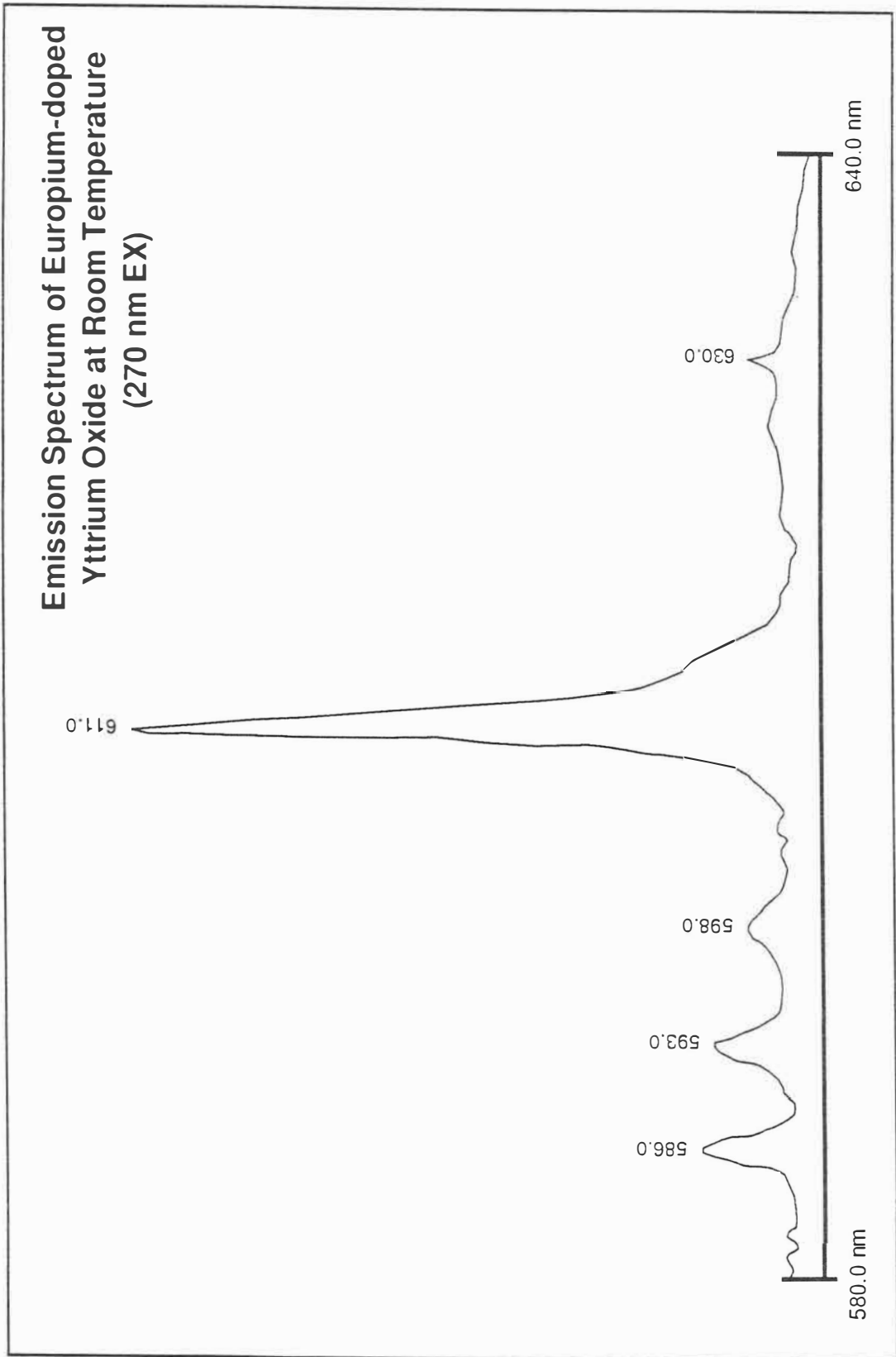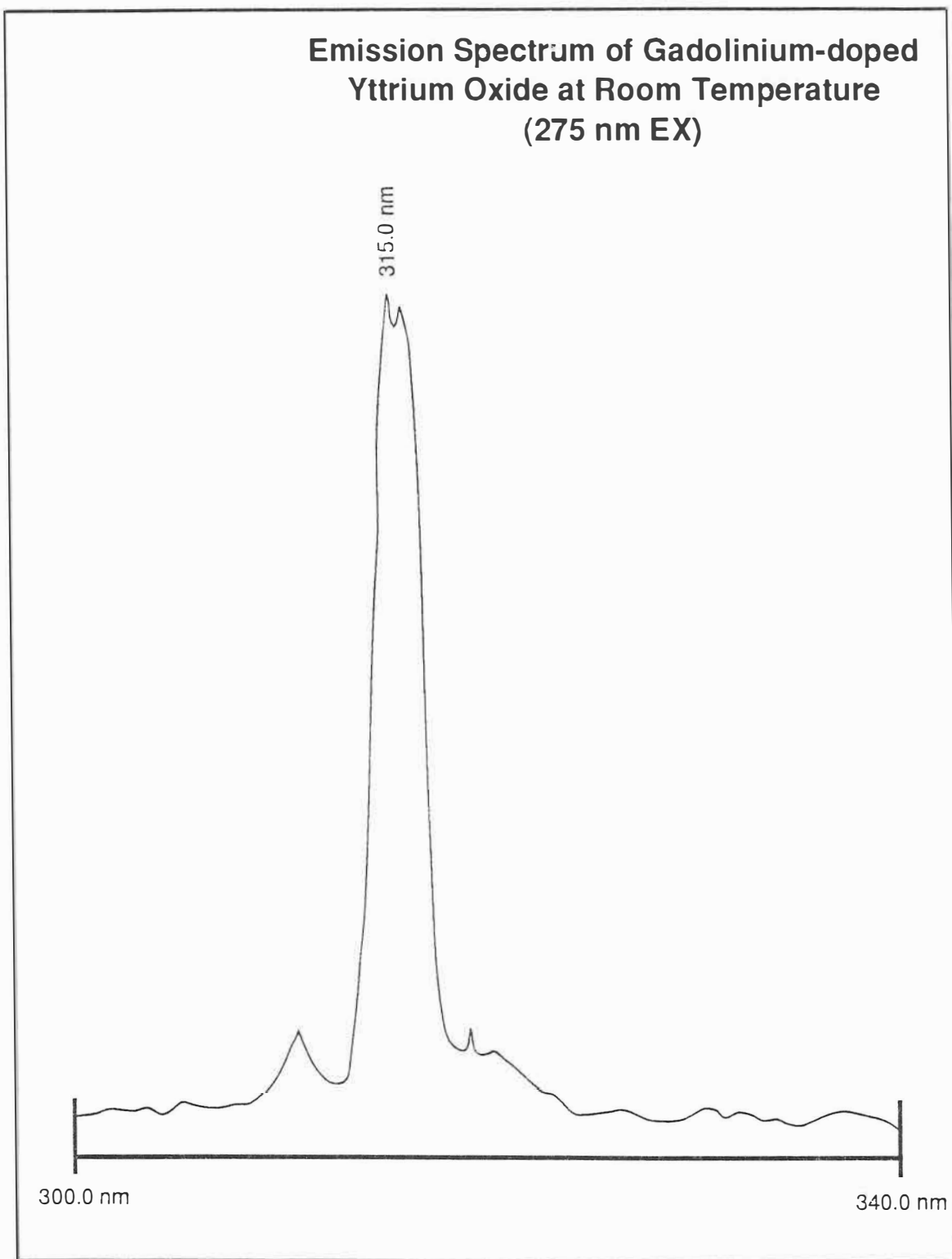
Figure 4-64. Emission spectrum of gadolinium-doped yttrium oxide
at room temperature (275 nm EX).
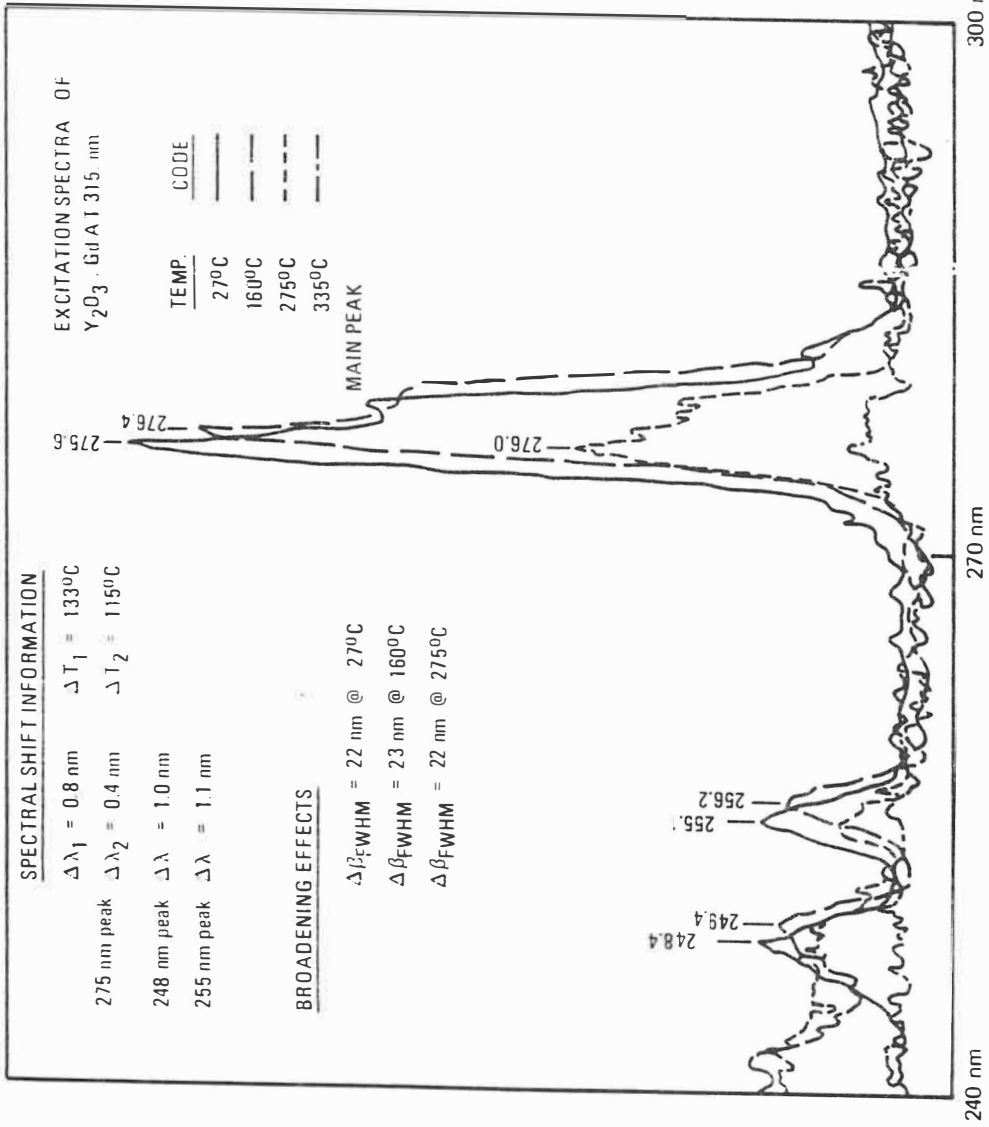
Figure 4-65. Excitation spectrum of gadolinium-doped yttrium oxide at elevated temperatures (315 nm EM).
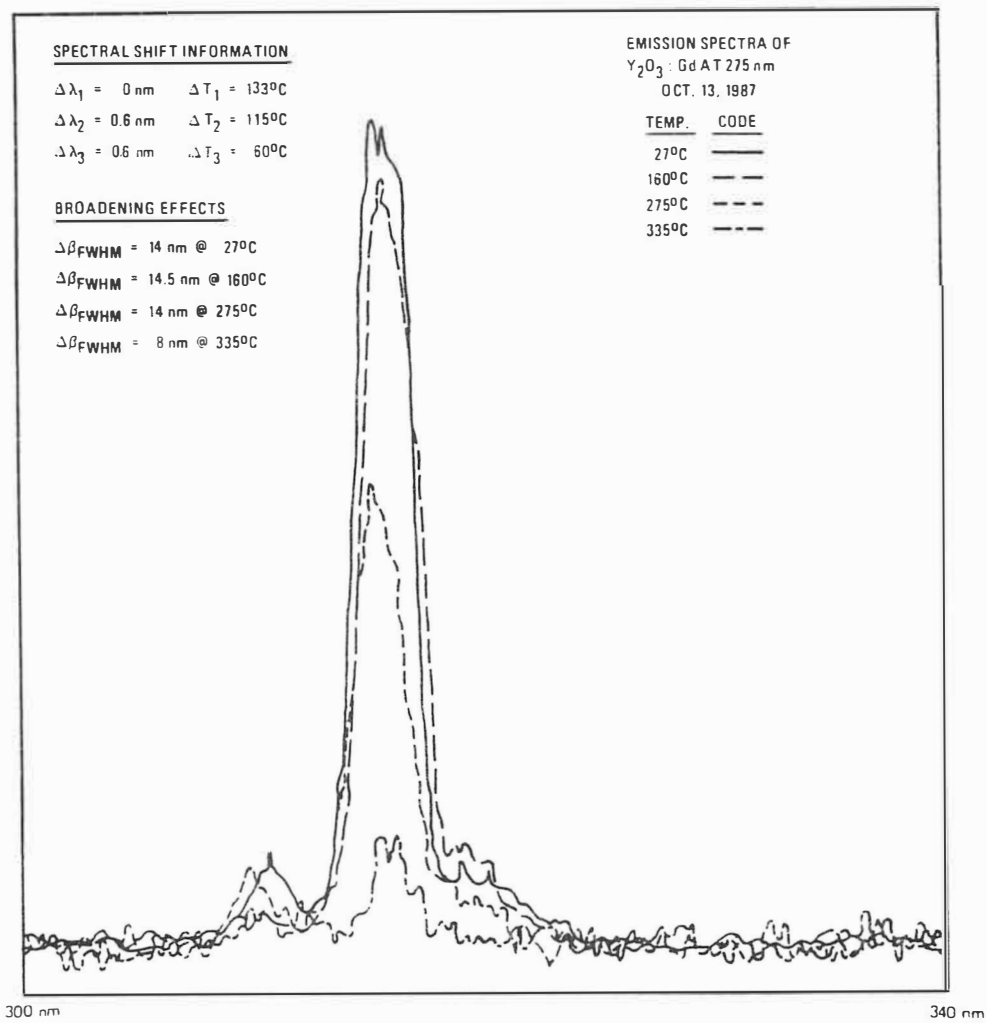
Figure 4-66. Emission spectrum of gadolinium-doped yttrium

oxide at elevated temperatures (275 nm EX).

Manganese-doped Magnesium Fluorogermanate ($Mg_4(F)GeO_6$:Mn)

Excitation and emission spectra are presented for $Mg_4(F)GeO_6$:Mn acquired at room temperature and at elevated temperatures ranging from 25°C to 350°C. The room temperature excitation spectrum of the 628 nm emission line of $Mg_4(F)GeO_6$:Mn is shown in Figure 4-67. The peaks of the two major absorption bands for this phosphor are located at 325.0 and 419.4 nm. An atomic transition peak can be found at 449.3 nm. Likewise, the excitation spectrum of the 655 nm emission line of $Mg_4(F)GeO_6$:Mn taken at room temperature is shown in Figure 4-68. The peaks of the absorption bands for this emission lie at 332.5 and 420.0 nm. An atomic transition line can also be found at 449.6 nm.

The room temperature emission spectrum for $Mg_4(F)GeO_6$:Mn at 325 nm excitation is shown in Figure 4-69. Several strong emission lines are seen at 621.0, 628.0, 647.1 and 654.6 nm while a weaker emission line is found at 637.5 nm. The room temperature emission spectrum for $Mg_4(F)GeO_6$:Mn at 420 nm excitation is shown in Figure 4-70. Similar to the previous spectrum, several strong emission lines are seen at 622.0, 629.0, 648.5 and 6555.0 nm while a weaker emission line is found at 638.0 nm. Figure 4-71 details the intensity peak difference in the emission spectra between excitation at 420 nm as compared to 325 nm.

Excitation spectra at elevated temperatures for the 655 nm emission line of $Mg_4(F)GeO_6$:Mn are displayed in Figure 4-72. There is only a small shift in the peak positions of the absorption bands which more than likely are due to instrumental error. A noticeable decrease in the relative intensity of the peaks was evident. The emission spectra measured as a function of temperature for $Mg_4(F)GeO_6$:Mn under excitation at 420 nm are shown in Figure 4-73. The spectra shows an increase in intensity of the 626 nm line at higher temperatures where the 653 nm line exhibits an intensity reduction.
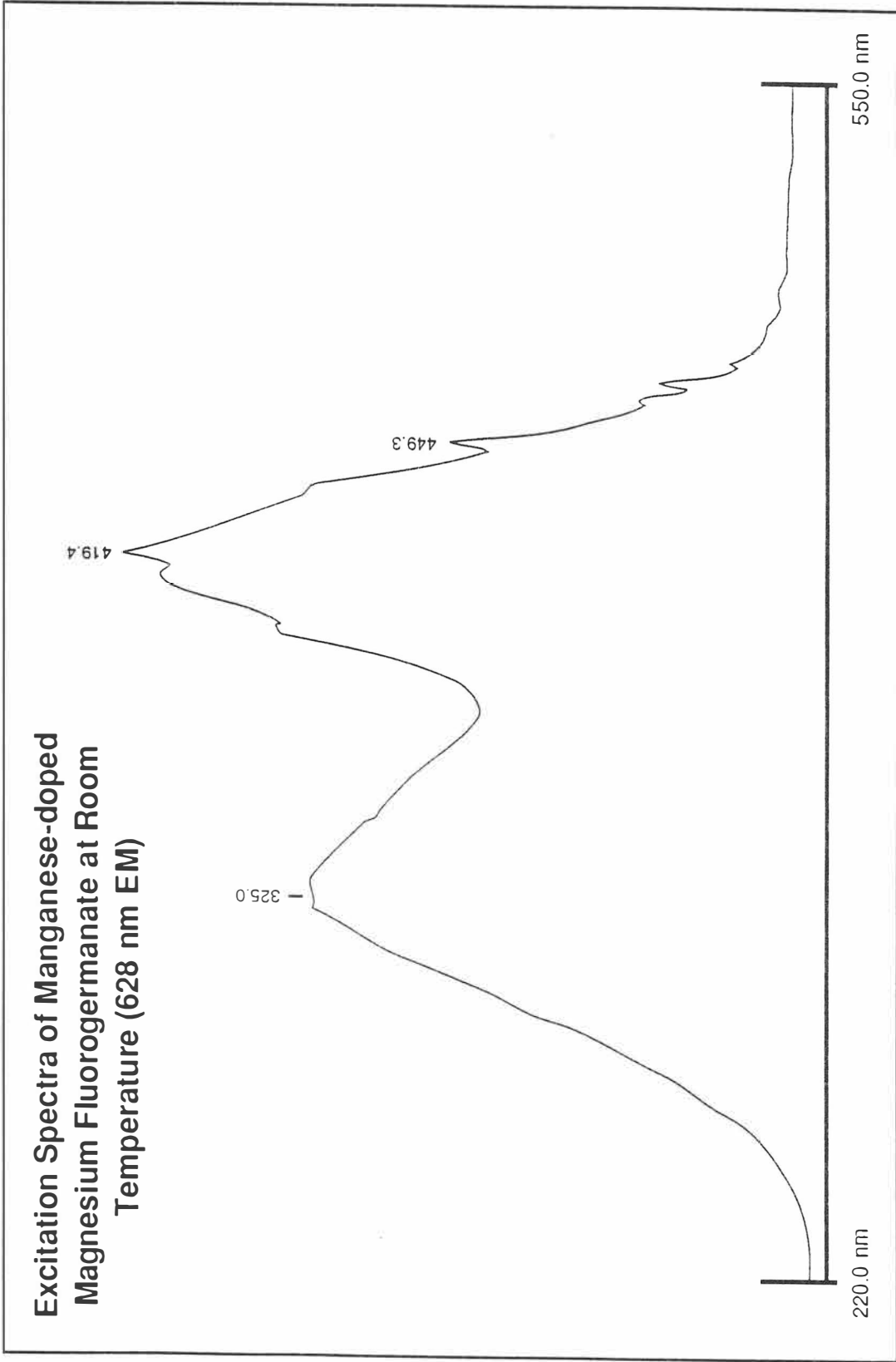
Figure 4-67. Emission spectrum of manganese-doped magnesium fluorogermanate at room temperature (628 nm EM).
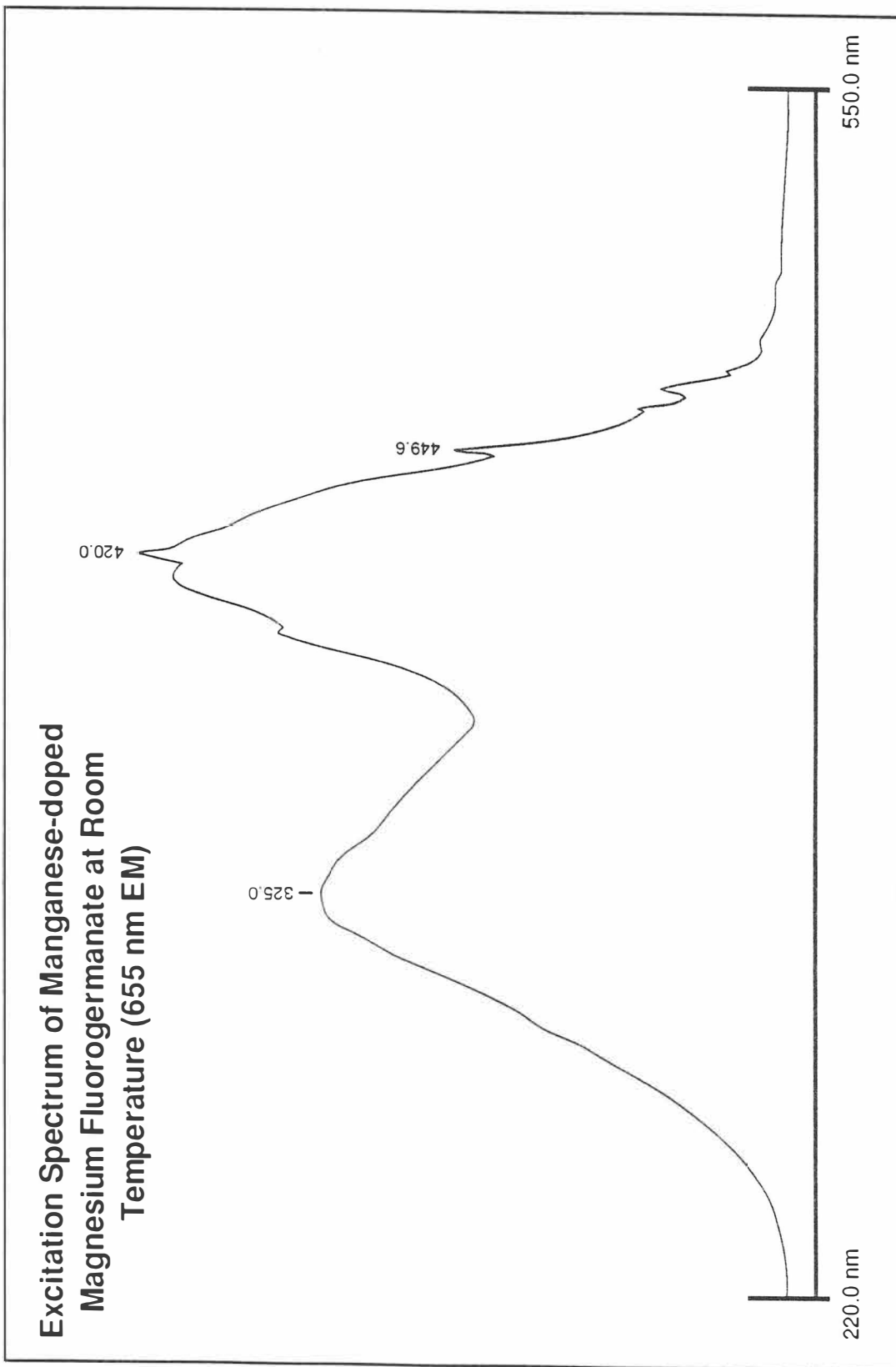
Figure 4-68. Excitation spectrum of manganese-doped magnesium fluorogermanate at room temperature (655 nm EM).

167
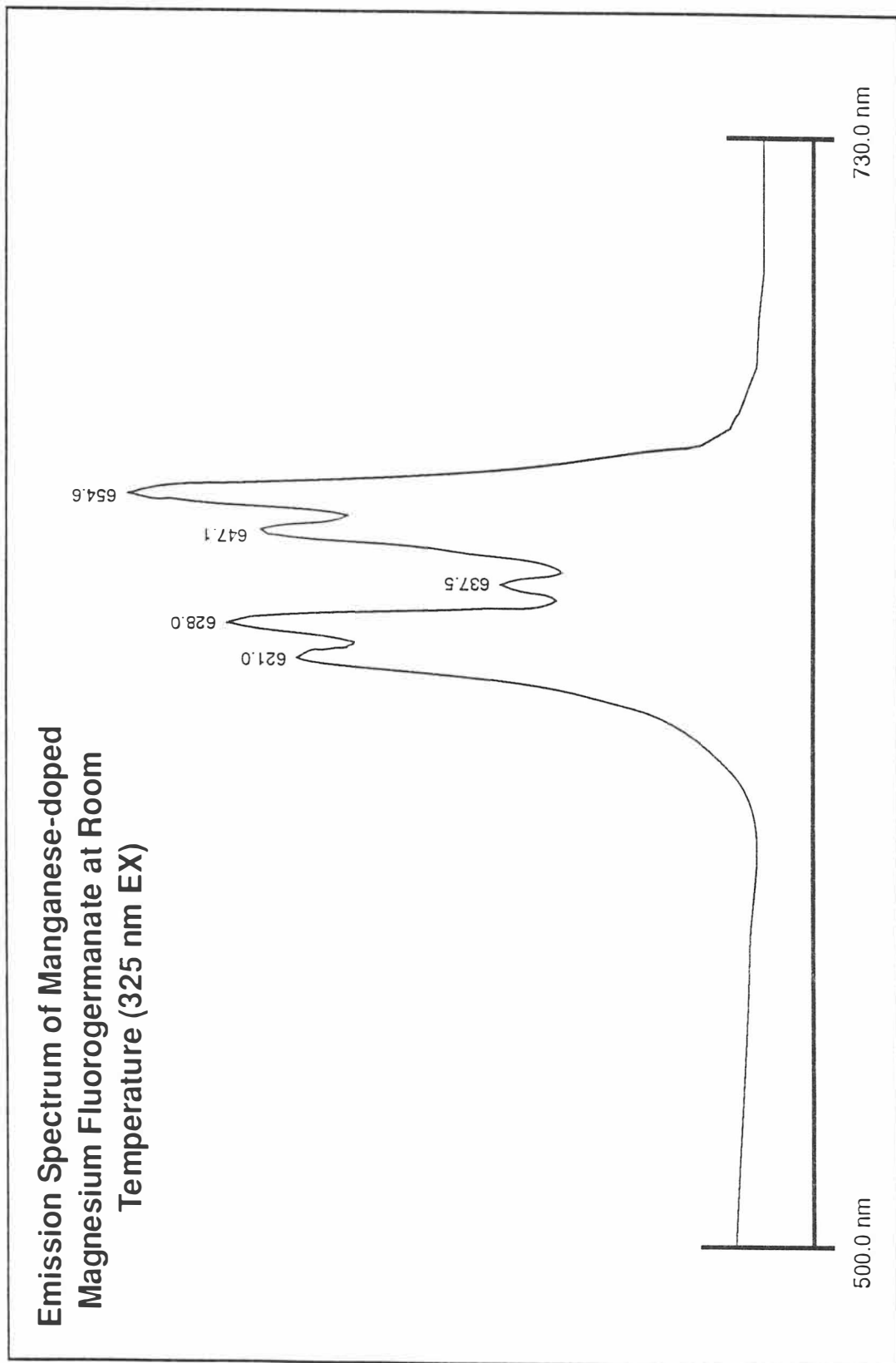
Figure 4-69. Emission spectrum of manganese-doped magnesium fluorogermanate at room temperature (325 nm EX).
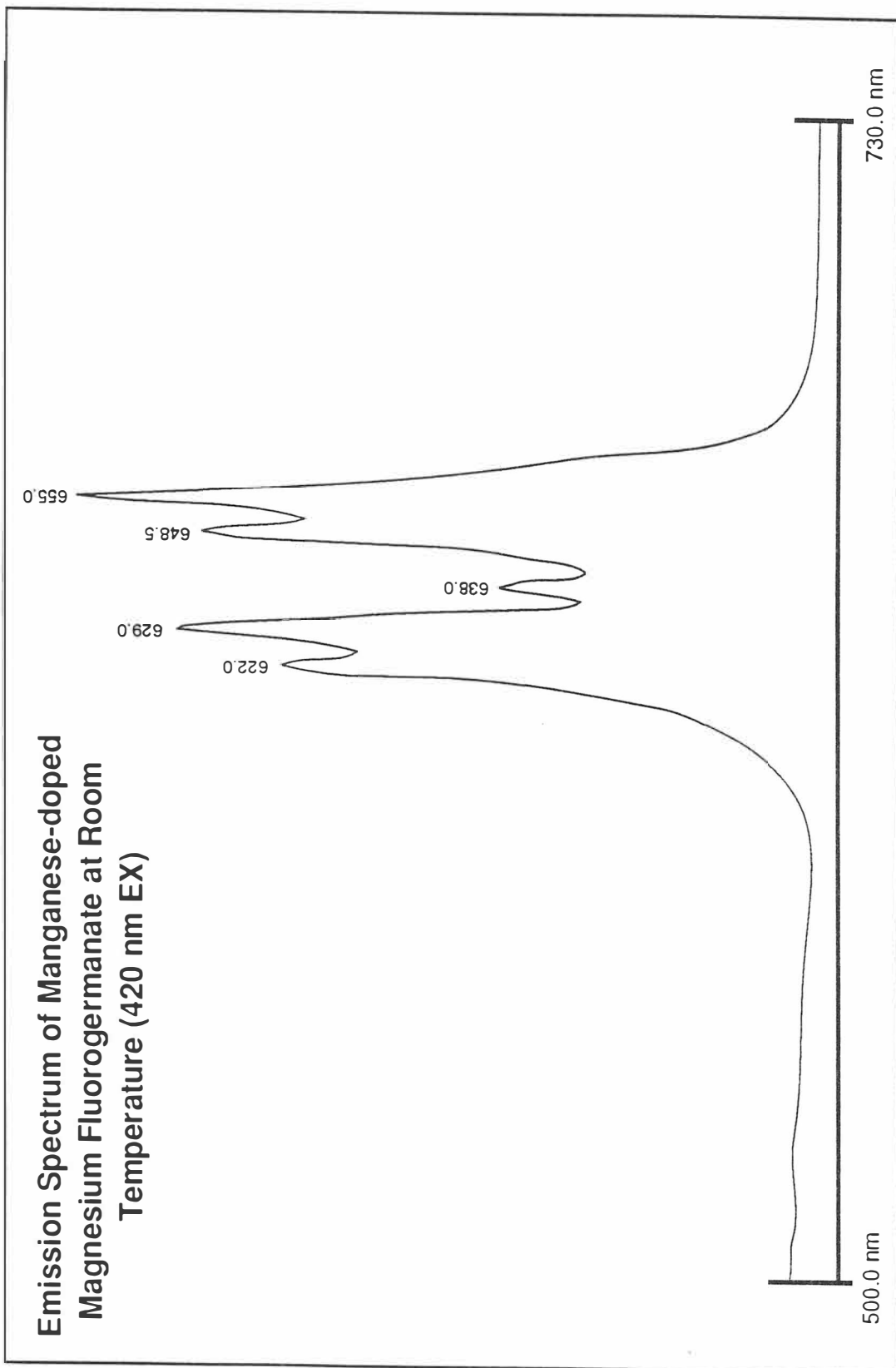
Figure 4-70. Emission spectrum of manganese-doped magnesium fluorogermanate at room temperature (420 nm EX).
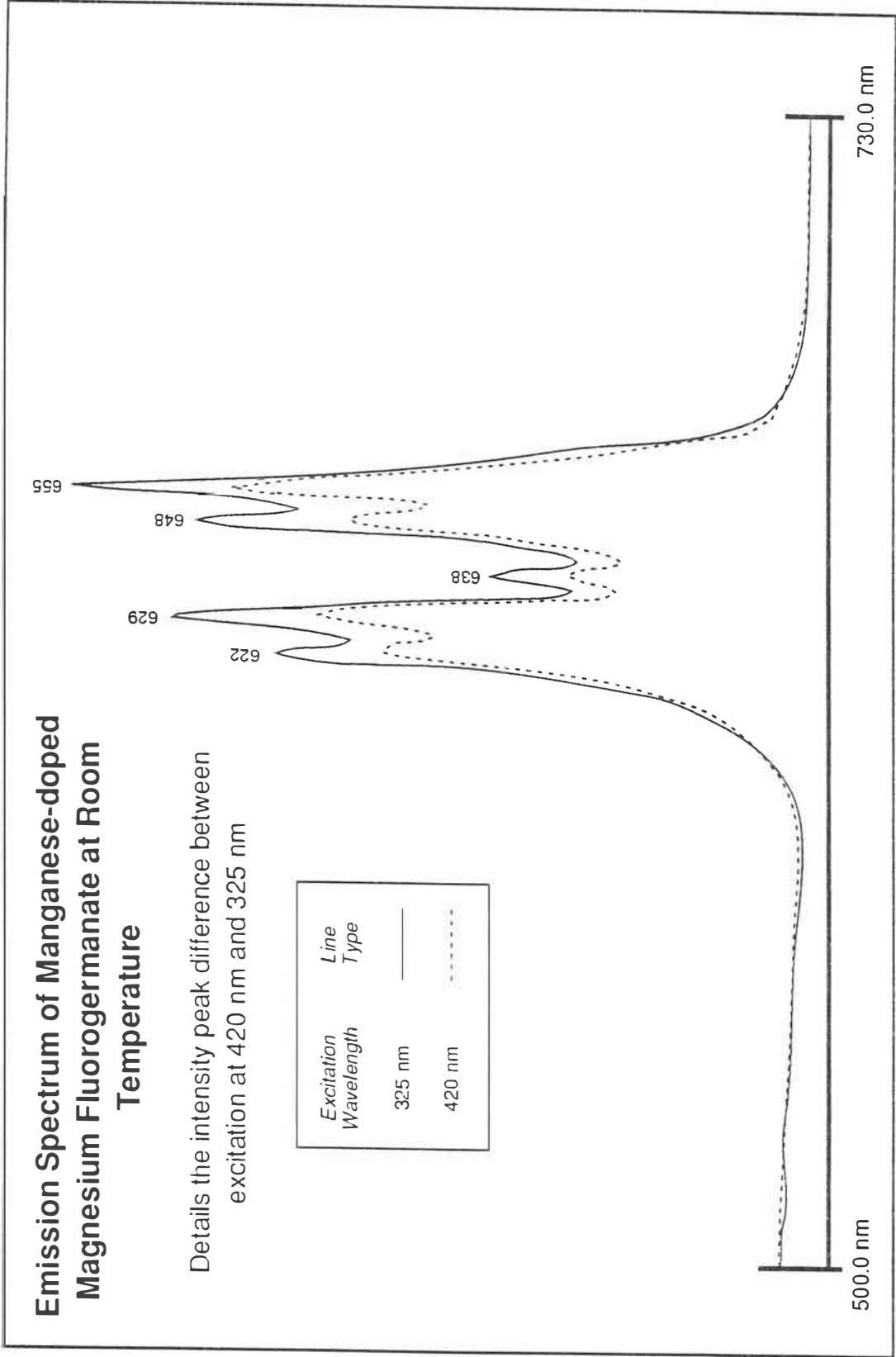
Figure 4-71. Emission spectrum of manganese-doped magnesium fluorogermanate at room temperature (325/420 EX).
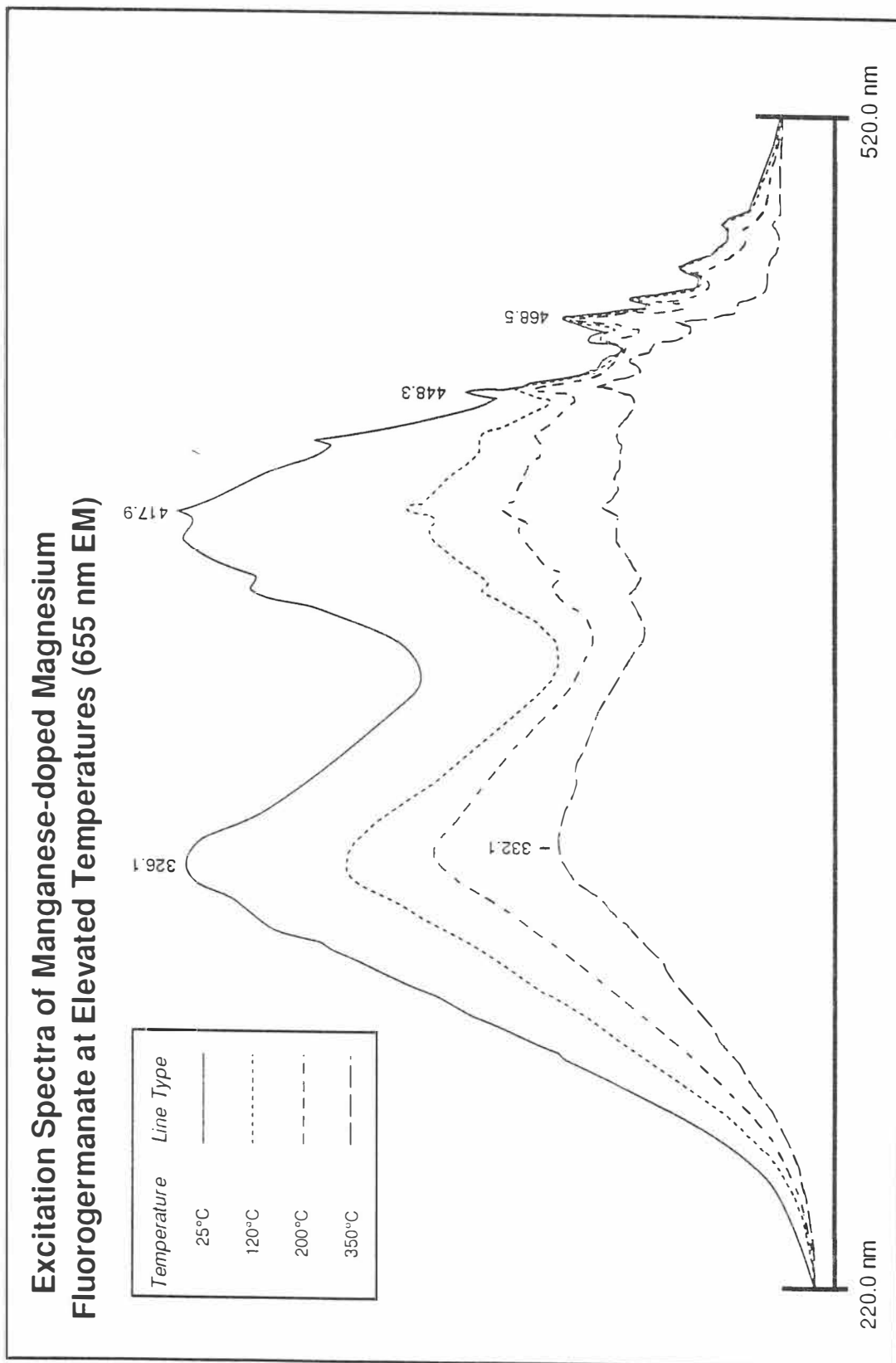
Figure 4-72. Excitation spectra of manganese-doped magnesium fluorogermanate at elevated temperatures (655 nm EM).
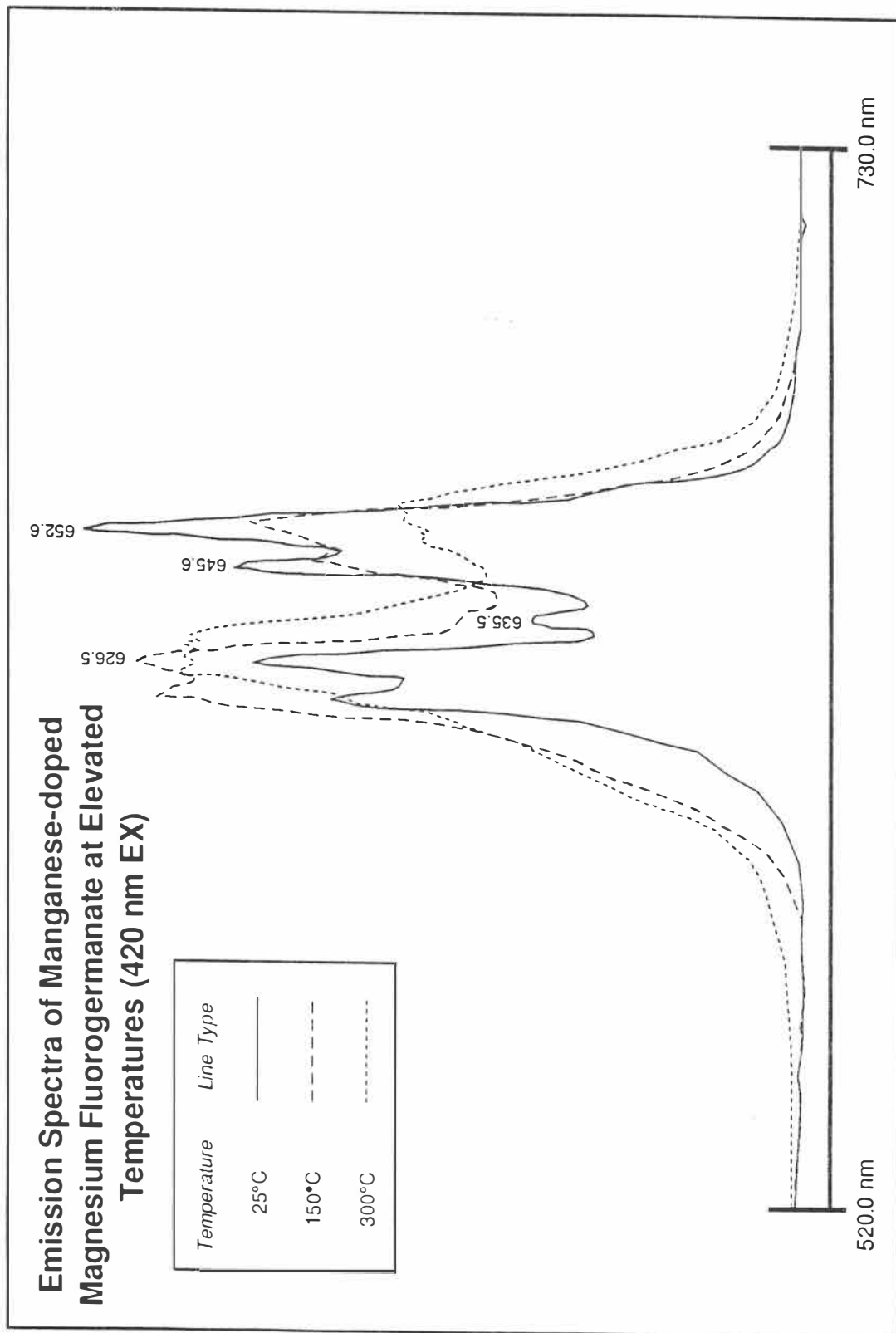
Figure 4-73.   Emission spectrum of manganese-doped magnesium fluorogermanate at elevated temperatures (420 nm EX).

Praseodymium-doped Yttrium Oxysulfide ($Y_2O_2S:Pr$)

Excitation and emission spectra are presented for praseodymium-doped yttrium oxide taken within a temperature range of 20.4°C to 247.7°C. The room temperature excitation spectrum of the 514 nm emission line of $Y_2O_2S:Pr$ is shown in Figure 4-74. The peak of the major absorption band is located at 301.6 nm whereas a smaller, less significant band is located at 266.3 nm. An atomic transition peak can also be found at 468.3 nm.

The room temperature emission spectrum for $Y_2O_2S:Pr$ at 300 nm excitation is shown in Figure 4-75. Two strong emission lines are found in this spectrum and are located at 502.4 and 513.6 nm. Praseodymium-doped phosphors usually exhibit a greenish-yellow color to the eye under stimulation of approximately 300 nm.

Similar to the $Y_2O_3:Gd$ phosphor, it was observed that the absorption band in the excitation spectra showed no significant spectral shift at elevated temperatures. Slight shifting of the emission lines may be due to instrumental error in the spectrophotometer. The excitation spectra at various temperatures for the 514.0 nm line of $Y_2O_2S:Pr$ are shown in Figure 4-76. The origin of the observed absorption band in $Y_2O_2S:Pr$ is unknown.

Emission spectra at various temperatures for $Y_2O_2S:Pr$ at 300.0 nm excitation are shown in Figure 4-77. Again, no distinguishable broadening effects or shift in spectral position of the absorption band and atomic emission bands associated with the praseodymium ion were detected. And furthermore, the luminescent intensity of both the absorption band and atomic emission band decreased significantly at increased temperatures in both the excitation and emission spectra.

173
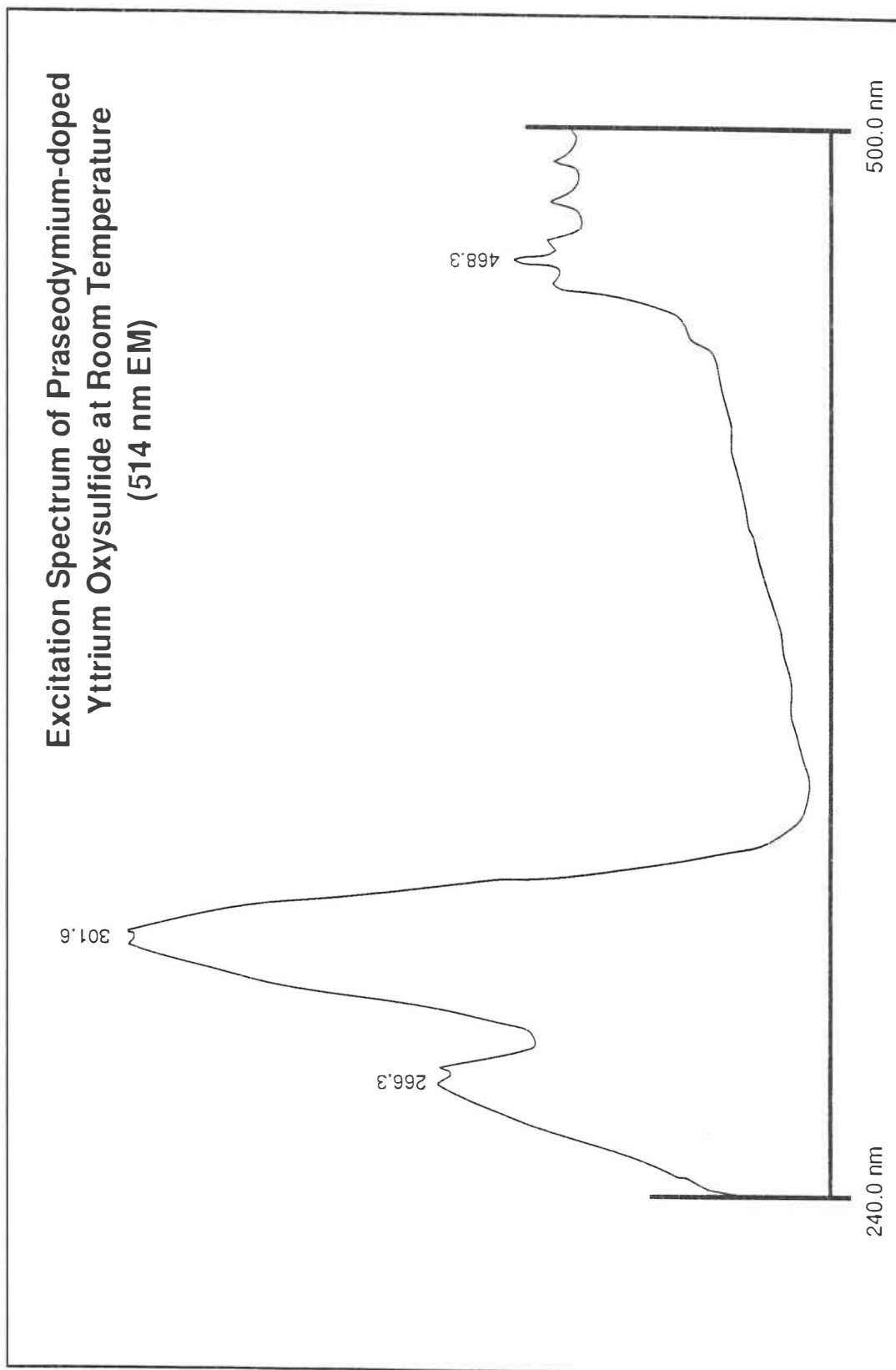
Figure 4-74. Excitation spectrum of praseodymium-doped yttrium oxysulfide at room temperature (514 nm EM).
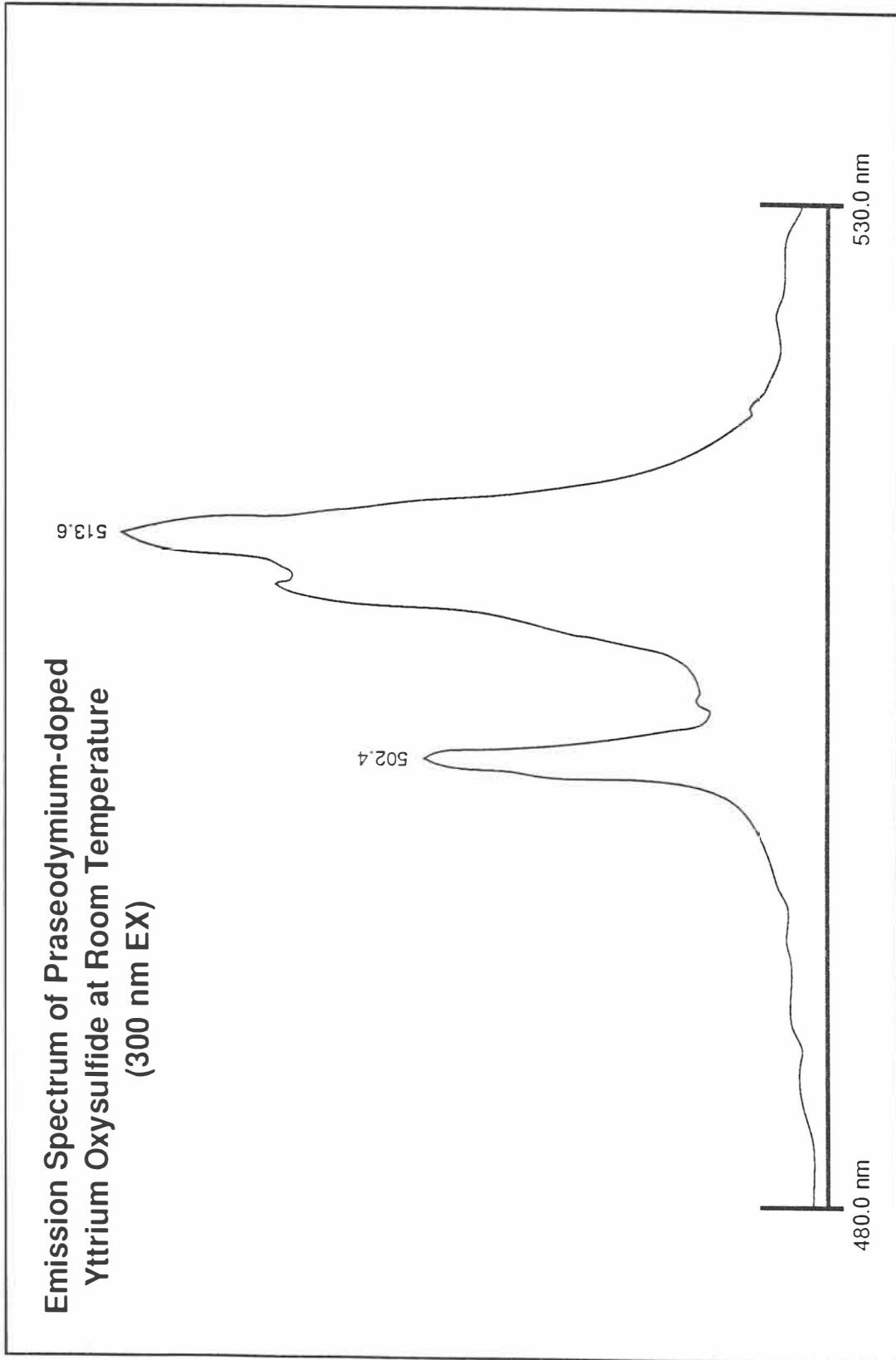
Figure 4-75. Excitation spectrum of praseodymium-doped yttrium oxysulfide at room temperature (300 nm EX).

175
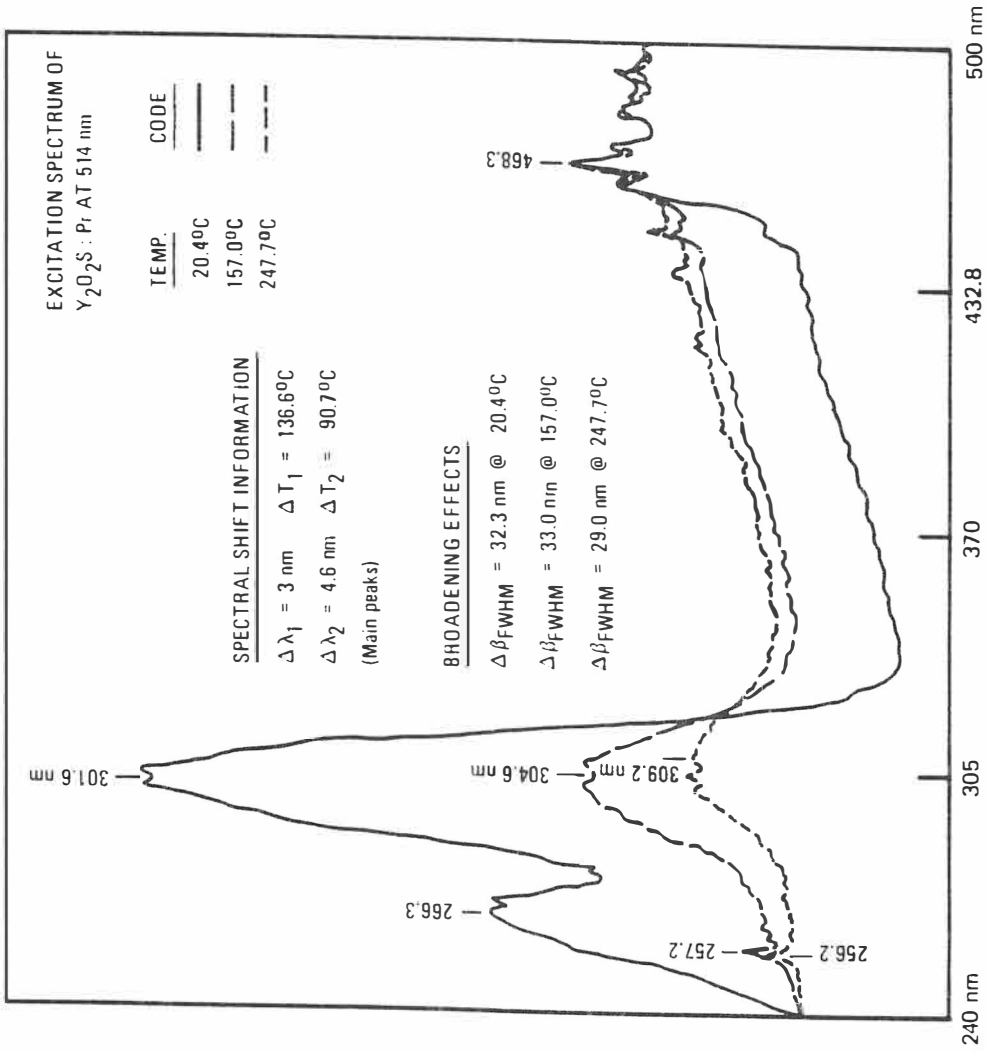
Figure 4-76. Excitation spectra of praseodymium-doped yttrium oxysulfide at elevated temperatures (514 nm EM).

SPECTRAL SHIFT INFORMATION

$\Delta\lambda_1 = 0.3$ nm $\quad \Delta T_1 = 136.6^{\circ}C$

$\Delta\lambda_2 = 0.6$ nm $\quad \Delta T_2 = 90.7^{\circ}C$

BROADENING EFFECTS

$\Delta\beta_{FWHM} = 26$ nm @ $20.4^{\circ}C$

$\Delta\beta_{FWHM} = 35$ nm @ $157.0^{\circ}C$

$\Delta\beta_{FWHM} = 38$ nm @ $247.7^{\circ}C$

EMISSION SPECTRA OF
$Y_2O_2S : Pr$ AT 300 nm

TEMP.	CODE
$20.4^{\circ}C$	——
$157.0^{\circ}C$	- - -
$247.7^{\circ}C$	– – –

513.6

502.4

513.9

514.5

503.4

480 nm 492.5 505 517.5 530 nm
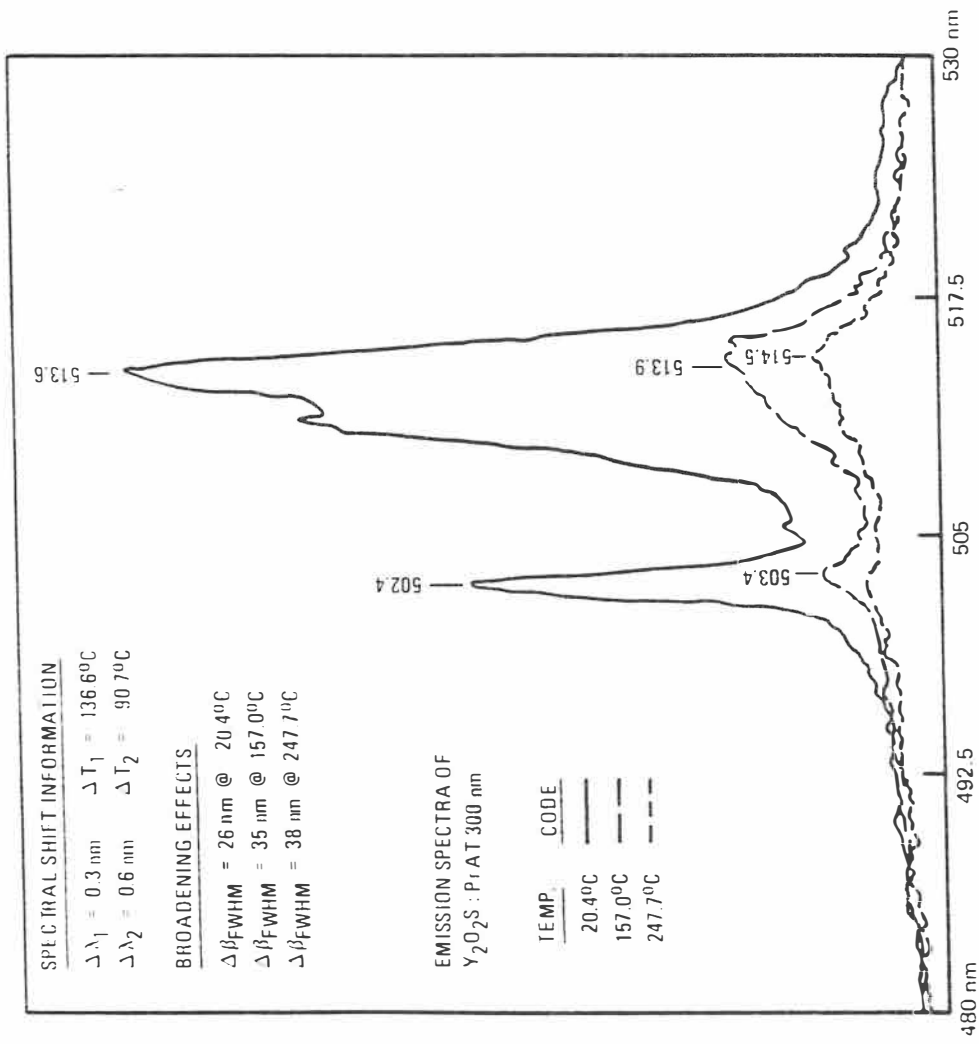
Figure 4-77. Emission spectra of praseodymium-doped yttrium oxysulfide at elevated temperatures (300 nm EX).

Terbium-doped Yttrium Oxysulfide (Y_2O_2S:Tb^{3+})

Excitation and emission spectra are presented for Y_2O_2S:Tb^{3+} measured at room temperature and at elevated temperatures. The excitation spectrum of the 543 nm emission line of Y_2O_2S:Tb^{3+} taken at room temperature is shown in Figure 4-78. A room temperature charge-transfer band is located at a peak wavelength of 290.7 nm. Less intense peaks were observed at 378.5 and 488.7 nm.

Five relatively strong fluorescence lines are found in the Y_2O_2S:Tb^{3+} room temperature emission spectrum under 395 nm excitation and are shown in Figure 4-79. The most intense emission lines are found at 412.9, 416.5, 435.2, 438.2, and 542.6 nm. Other emission lines were observed at 456.3, 468.5, 473.5, 482.6, 487.6, 492.2, 548.2, and 584.5 nm. This emission spectrum is shown in expanded form in Figures 4-80 and 4-81 which covers a range of wavelengths from 400 to 650 nm.

Terbium-doped yttrium oxysulfide also shows a vary slight spectral shift towards the red in its charge-transfer band as temperature is increased. Figure 4-82 displays excitation spectra at elevated temperatures for the 545 nm emission line of Y_2O_2S:Tb^{3+}. The peak position of the charge-transfer absorption band for Y_2O_2S:Tb^{3+} lies at 290.1 nm at room temperature and shifts slightly to 293.2 nm at 200°C. The atomic transition peak at 379.4 shows no significant spectral shift. The emission spectra measured at 25°C and 110°C can be found in Figure 4-83 while the same spectra for temperatures ranging from 150°C to 300°C are shown in Figure 4-84. This basically demonstrates the decrease in relative intensity of Y_2O_2S:Tb^{3+} as a function of temperature. Particular attention should be paid to the strength of the 543 nm line. Figure 4-85 is a compiled version of the emission spectra measured at these same temperatures.

178
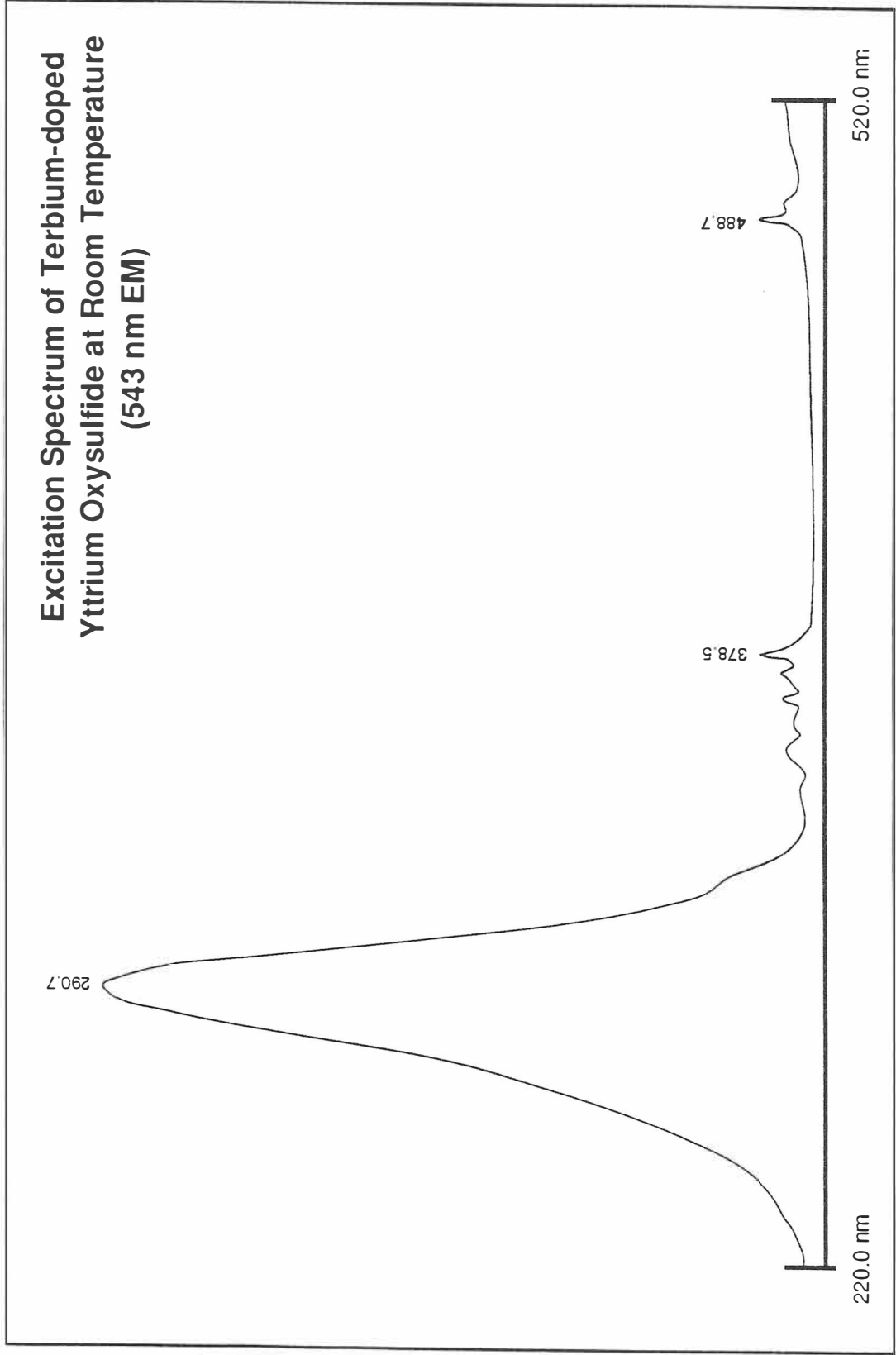
Figure 4-78. Excitation spectrum of terbium-doped yttrium oxysulfide at room temperature (543 nm EM).
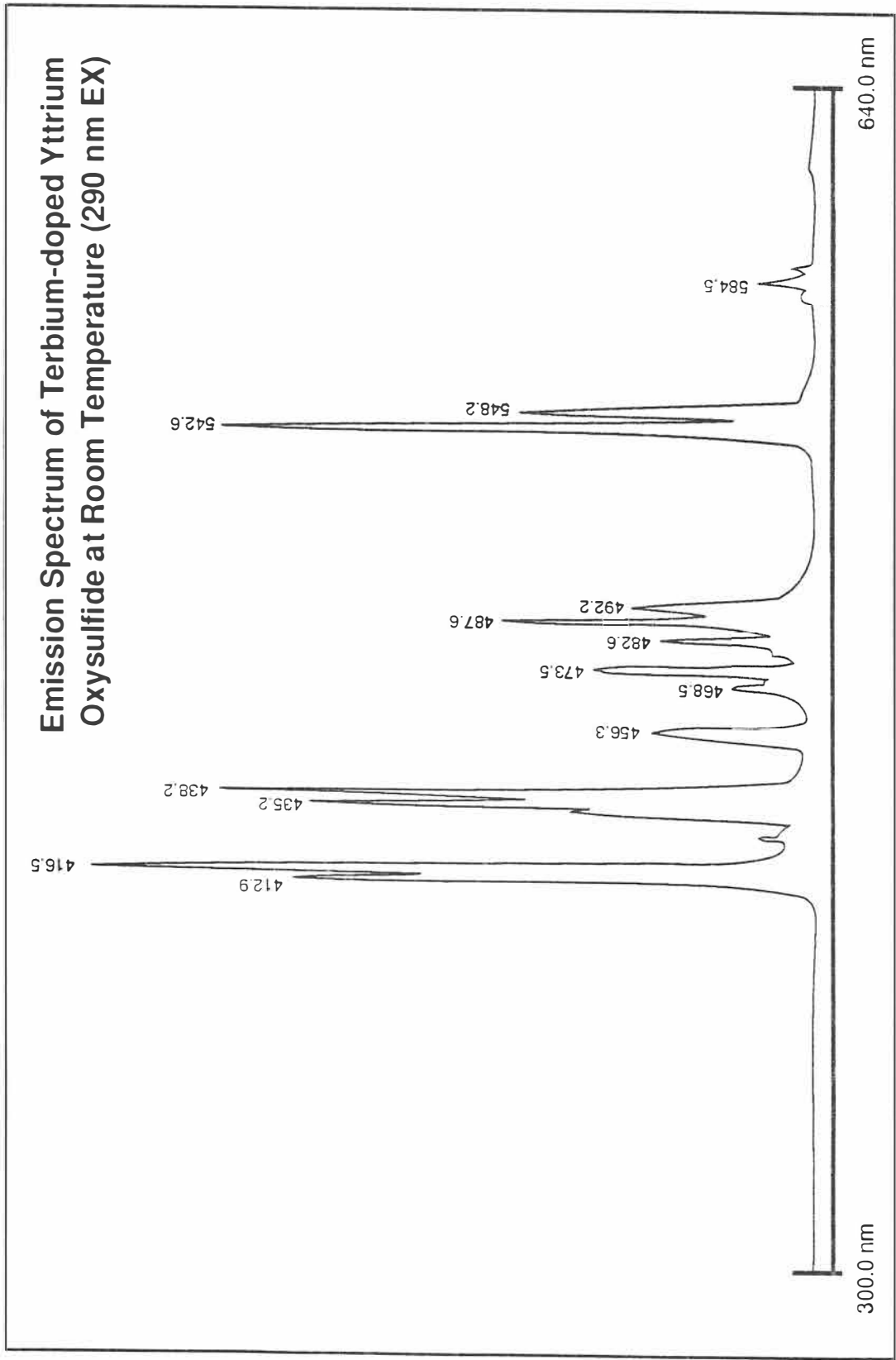
Figure 4-79. Emission spectrum of terbium-doped yttrium oxysulfide at room temperature (290 nm EX).
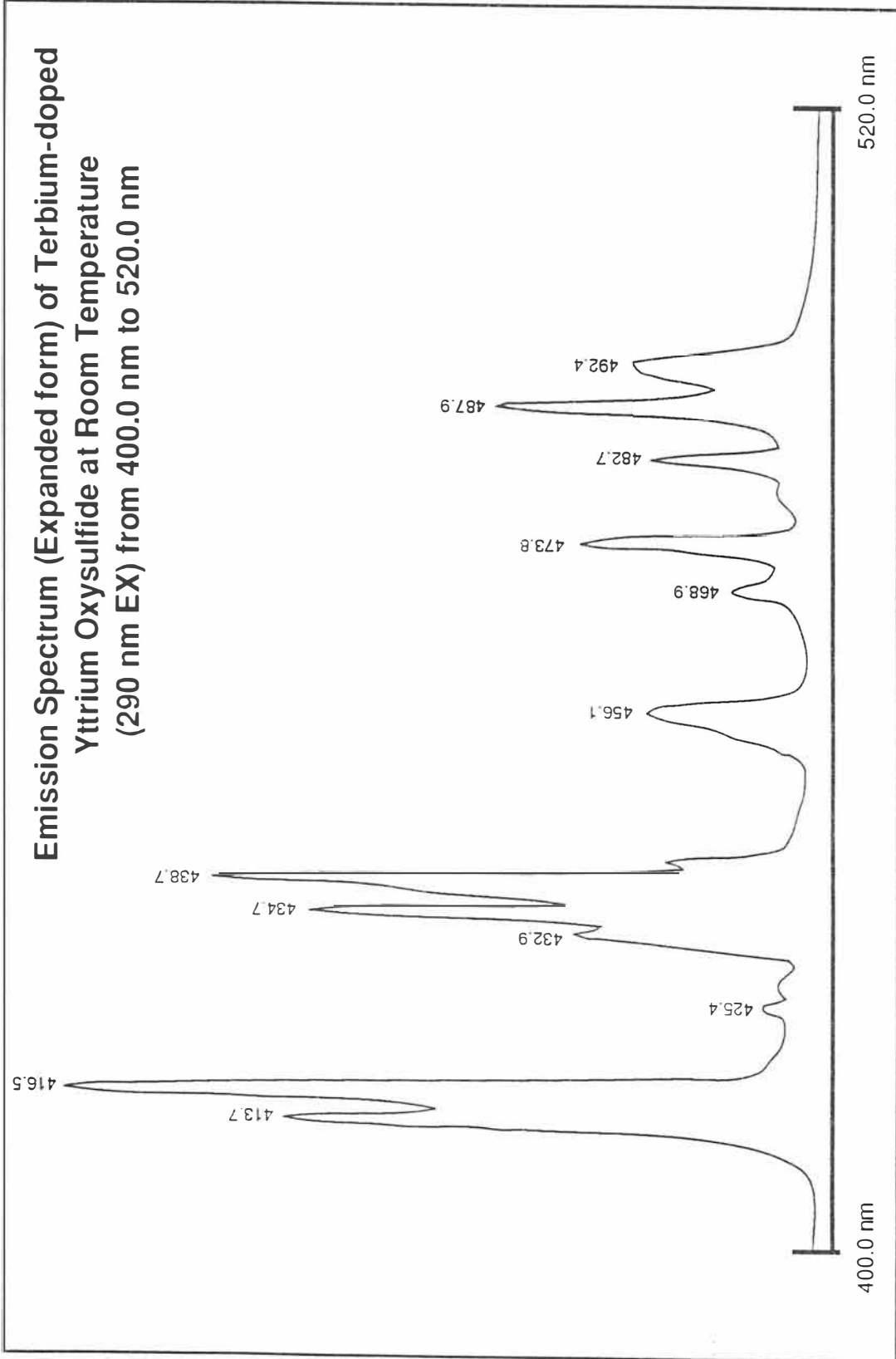
Figure 4-80. Emission spectrum (expanded form) of terbium-doped yttrium oxysulfide at room temperature (290 nm EX) from 400.0 nm to 520.0 nm.

Figure 4-81. Emission spectrum (expanded form) of terbium-doped yttrium oxysulfide at room temperature (290 nm EX) from 520.0 nm to 650.0 nm.
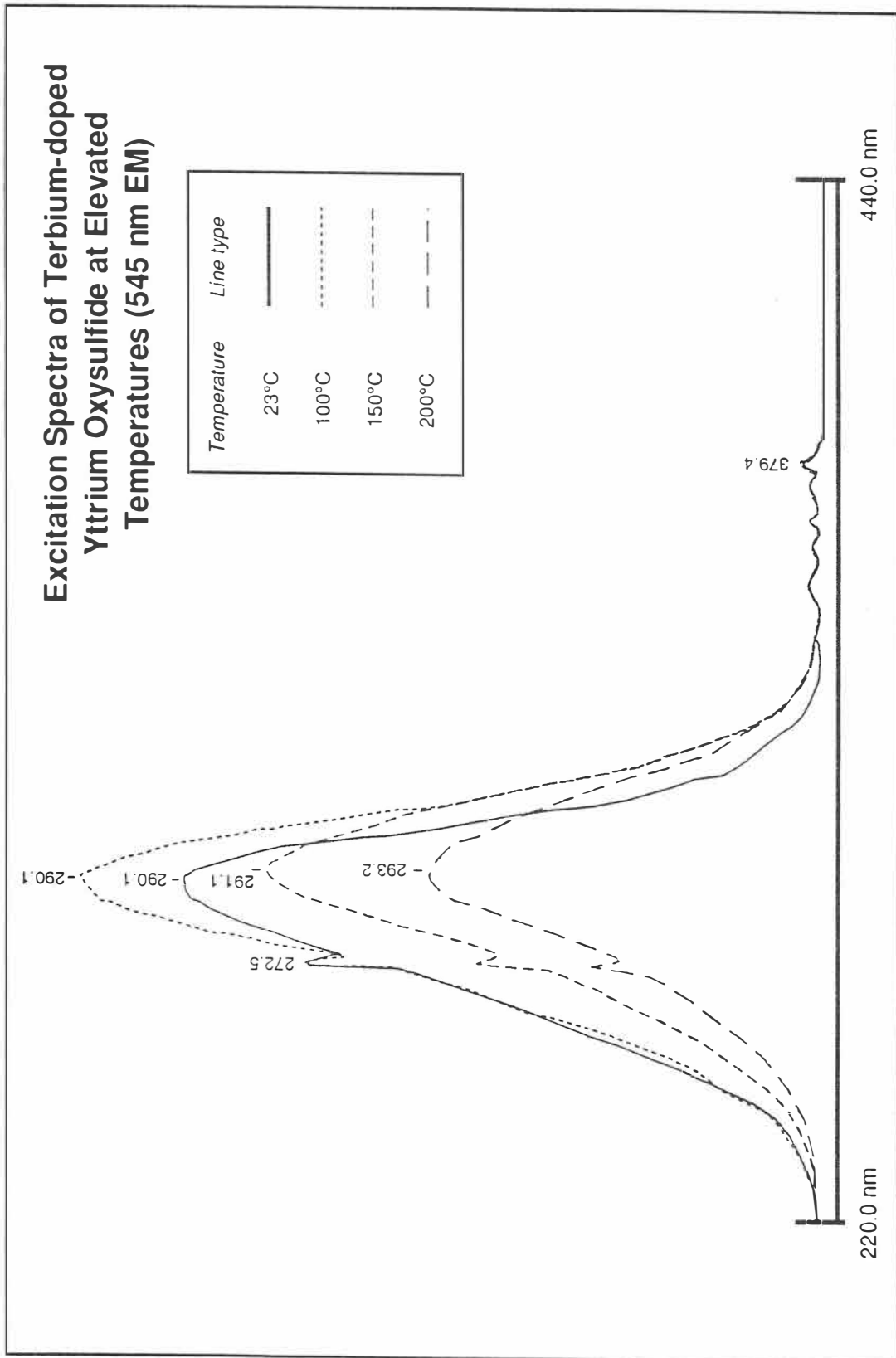
Figure 4-82. Excitation spectra of terbium-doped yttrium oxysulfide at elevated temperature (545 nm EM).
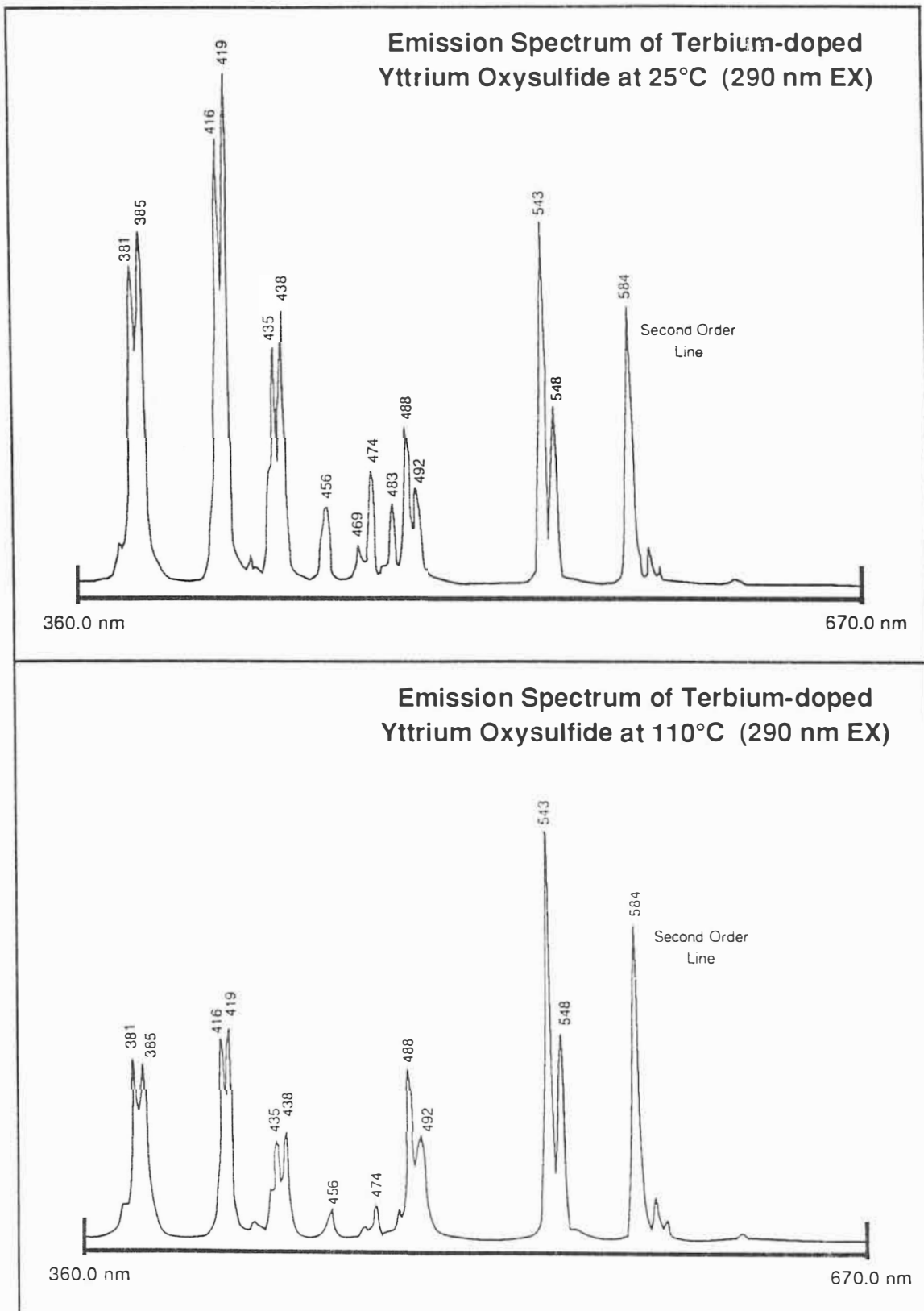
Figure 4-83. Emission spectra of terbium-doped yttrium oxysulfide
at 25°C and 110°C (290 nm EX).

184
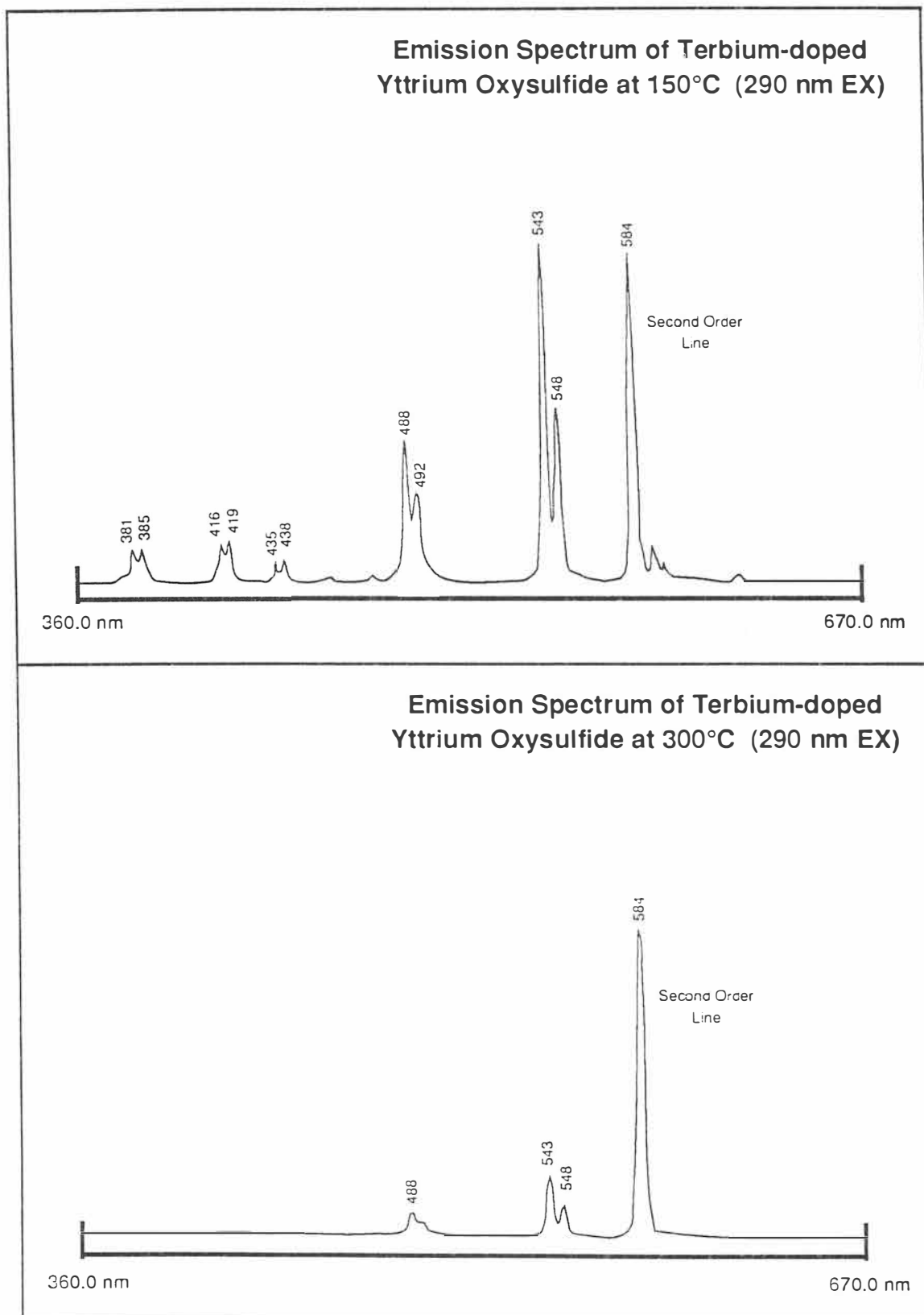
Figure 4-84. Emission spectra of terbium-doped yttrium oxysulfide at 150°C and 300°C (290 nm EX).
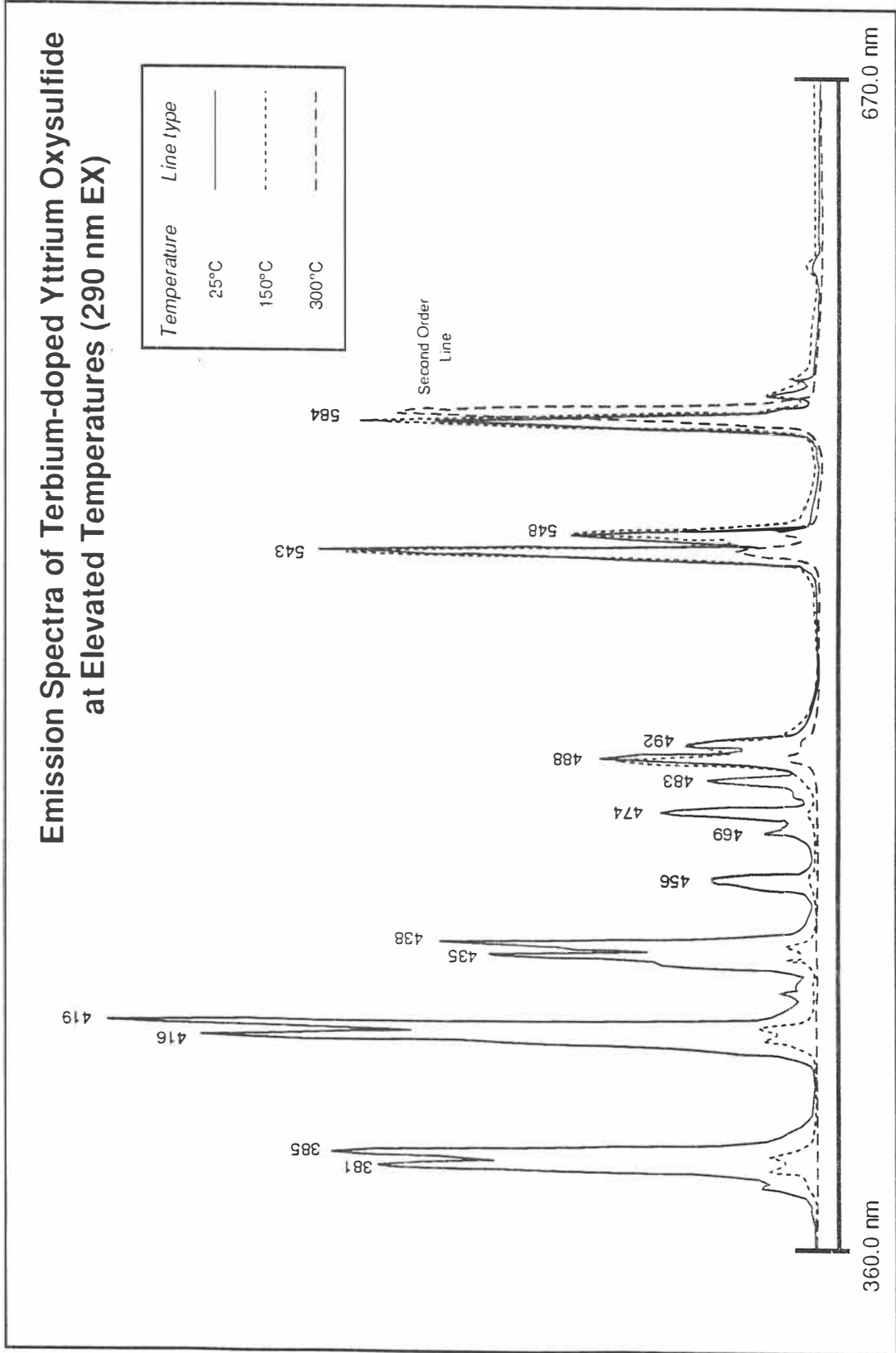
Figure 4-85. Emission spectra of terbium-doped yttrium oxysulfide at elevated temperature (290 nm EX).

Lifetime Decay Measurements

Exponential decay lifetimes of six thermographic phosphors were measured using the experimental configurations and methods described in Chapter 3. The results of these decay measurements have produced lifetime calibration curves for each of the thermographic phosphors tested. Having undergone decay lifetime calibration, these phosphors may someday find application in remote, non-contact, high temperature measurement systems.

Laser excitation of wavelengths near 395 nm were created to stimulate the fluorescence of each orthophosphate crystal sample. In general, all of the europium-doped orthophosphates have room temperature lifetimes near 3200 μsec and in most cases, begin to quench at higher temperatures as compared to europium-doped yttrium oxide. The powder phosphors were stimulated with a nitrogen laser operating at 337 nm. All lifetime measurements for the single crystal were acquired at the Oak Ridge National Laboratory whereas similar measurements for dysprosium-doped yttrium vanadate were produced at the Precision Measurements Laboratory of The University of Virginia. Lifetime data for the europium-doped yttrium oxide thermophosphor are presented for comparison with other accumulated data. Its emission characteristics have been well documented and furthermore it appears to be the current phosphor of choice in high temperature thermometry applications. The data for the europium-doped yttrium oxide phosphor, which is presented here in this section, were taken from experiments performed by Cates and others.[6]

Lifetime measurements are presented on the following pages for $LaPO_4:Eu^{3+}$, $YPO_4:Eu^{3+}$, $LuPO_4:Eu^{3+}$, $LuPO_4:Dy^{3+}$, and $YVO_4:Dy^{3+}$. All lifetime data are presented in tabulated and graphical form. Graphical forms of data presentation are in most cases referred to as lifetime calibration curves. The logarithmic region of the calibration curve is

usually temperature-sensitive. Temperatures are given in degrees centigrade and lifetime values are given in microseconds unless specified other wise. The chapter concludes with a discussion of the results for onset quenching temperature analysis using the CALQUEN program and method.

Europium-doped Lanthanum Phosphate

Lifetime measurements were performed on $LaPO_4:Eu^{3+}$ with the Nd:YAG laser excitation set at 393.1 nm. The decay lifetime data of the 593.8 nm fluorescence line of $LaPO_4:Eu^{3+}$ are presented in Table 4-6 and the calibration curve is shown in Figure 4-86. At room temperature, the recorded lifetime value of $LaPO_4:Eu^{3+}$ is approximately 3265 μsec. Gradually, its decay lifetime decreases in strength to an approximate value of 2000 μsec at 440°C. As the temperature of the phosphor increases, its radiative transitions begin to quench and there is a smooth logarithmic decrease in decay time which begins near a temperature of approximately 500°C and continues to about 700°C.

Europium-doped Yttrium Phosphate

Lifetime measurements were performed on $YPO_4:Eu^{3+}$ with the Nd:YAG laser excitation adjusted to 395.5 nm. The decay lifetime data of the 593.5 nm emission line of $YPO_4:Eu^{3+}$ are presented in Table 4-7 and a calibration curve is shown in Figure 4-87. At room temperature, the recorded value of its lifetime decay is roughly 3139 μsec. Similar to $LaPO_4:Eu^{3+}$, the decay lifetime of $YPO_4:Eu^{3+}$ is gradually reduced in strength to a value of 1900 μsec at 660°C. As the temperature of the phosphor increases, emission quenching begins and there is a smooth logarithmic decrease in decay time which starts at a temperature of approximately 700°C and continues out to nearly 1100°C.

Table 4-6. Lifetime data for europium-doped lanthanum phosphate.

Europium-doped Lanthanum Phosphate	
Temperature ($^{\circ}C$)	Lifetime (μsec)
20.0	3265.0
100.0	3179.0
200.0	3071.0
300.0	2863.0
350.0	2715.0
400.0	2509.0
450.0	1897.0
500.0	1152.0
525.0	547.3
550.0	296.4
575.0	148.2
600.0	86.76
625.0	44.4
650.0	16.31
675.0	11.82
700.0	4.72
750.0	3.57
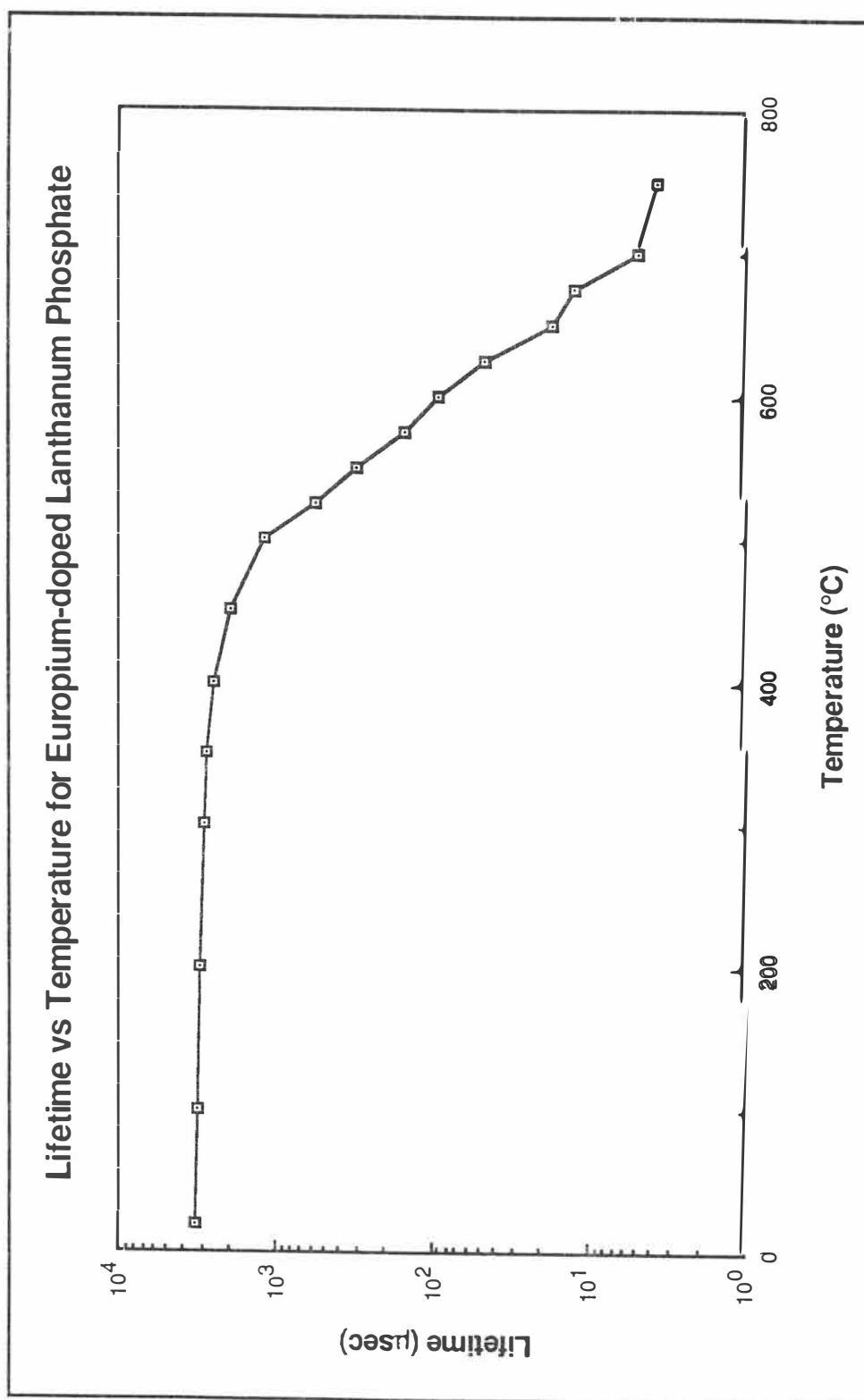
Figure 4-86. Lifetime calibration curve for europium-doped lanthanum orthophosphate.

Table 4-7. Lifetime data for europium-doped yttrium phosphate.

Europium-doped Yttrium Phosphate	
Temperature (°C)	Lifetime (µsec)
20.0	3139.0
100.0	3013.0
200.0	2776.0
300.0	2637.0
400.0	2570.0
500.0	2480.0
600.0	2341.0
660.0	1901.0
700.0	1305.0
725.0	930.2
750.0	584.5
775.0	393.1
800.0	239.8
825.0	146.2
850.0	97.11
900.0	45.7
950.0	28.0
1000.0	5.57
1100.0	1.72
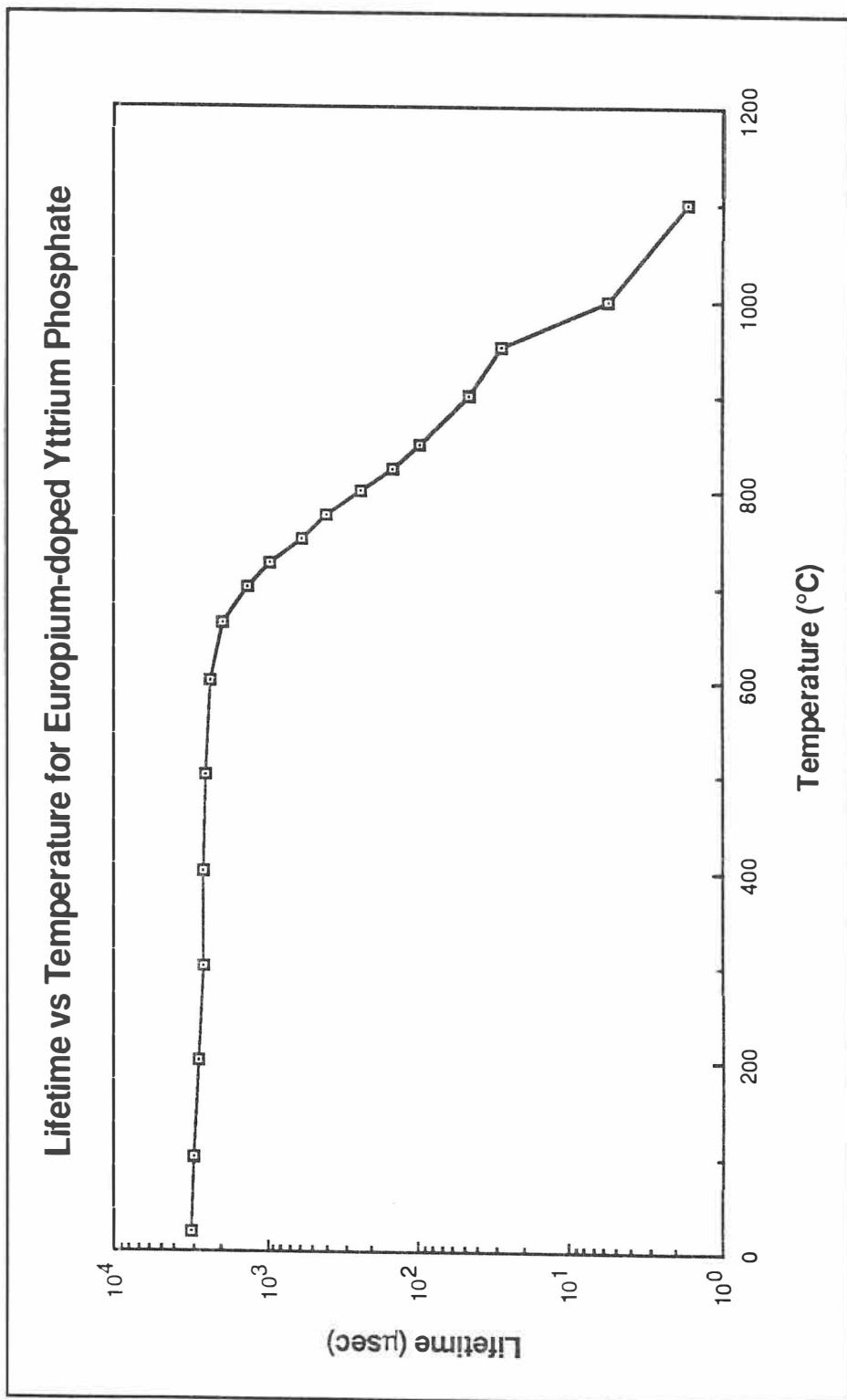
Figure 4-87. Lifetime calibration curve for europium-doped yttrium orthophosphate.

Europium-doped Lutetium Phosphate

Lifetime decay measurements were performed on $LuPO_4:Eu^{3+}$ with the Nd:YAG laser generating an excitation wavelength of 395.4 nm. The decay lifetime data of the 593.5 nm emission line of $LuPO_4:Eu^{3+}$ are listed in Table 4-8 and the calibration curve is shown in Figure 4-88. At room temperature, the recorded value of its lifetime decay is approximately 3125 μsec. Similar to the $LaPO_4:Eu^{3+}$ and $YPO_4:Eu^{3+}$ phosphors, its decay lifetime is slowly reduced in strength from its room temperature point to a value of roughly 1880 μsec at 700°C. As the temperature of the $LuPO_4:Eu^{3+}$ increases, fluorescence quenching starts near 740°C and there is a somewhat smooth logarithmic decrease in decay time which continues out to nearly 1100°C.

During lifetime decay measurements, it is often necessary to continually monitor the logarithm of the signal and check for linearity of its slope. Figures 4-89 and 4-90 show the non-exponential effects of the decay lifetime signals for $LuPO_4:Eu^{3+}$, measured as a function of temperature. This series of oscilloscope photographs displays the acquired fluorescent signals and their corresponding logarithms from 700°C to 1000°C. Typically, below onset quenching temperature, the acquired decay signal is of single exponential form where the slope (or lifetime) of the logarithm can be easily measured. However above the onset quenching temperature, the logarithm of the signal tends to become non-linear and thereby making lifetime analysis much more difficult and less accurate. In the oscilloscope photograph at 700°C, the logarithm of the signal exhibits a linear slope throughout the signal compared to the photograph at 1000°C, where several straight portions of the logarithm can be seen. Oscilloscope photographs were taken for all thermophosphor calibrations to check the non-exponential effects of the signal but were not presented in the thesis documentation.

Table 4-8. Lifetime data for europium-doped lutetium phosphate.

Europium-doped Lutetium Phosphate	
Temperature (°C)	Lifetime (μsec)
26.0	3125.0
300.0	2597.0
600.0	2344.0
650.0	2080.0
700.0	1887.0
750.0	1355.0
800.0	878.9
850.0	413.5
900.0	206.8
950.0	100.0
1000.0	15.98
1050.0	5.86
1100.0	3.399
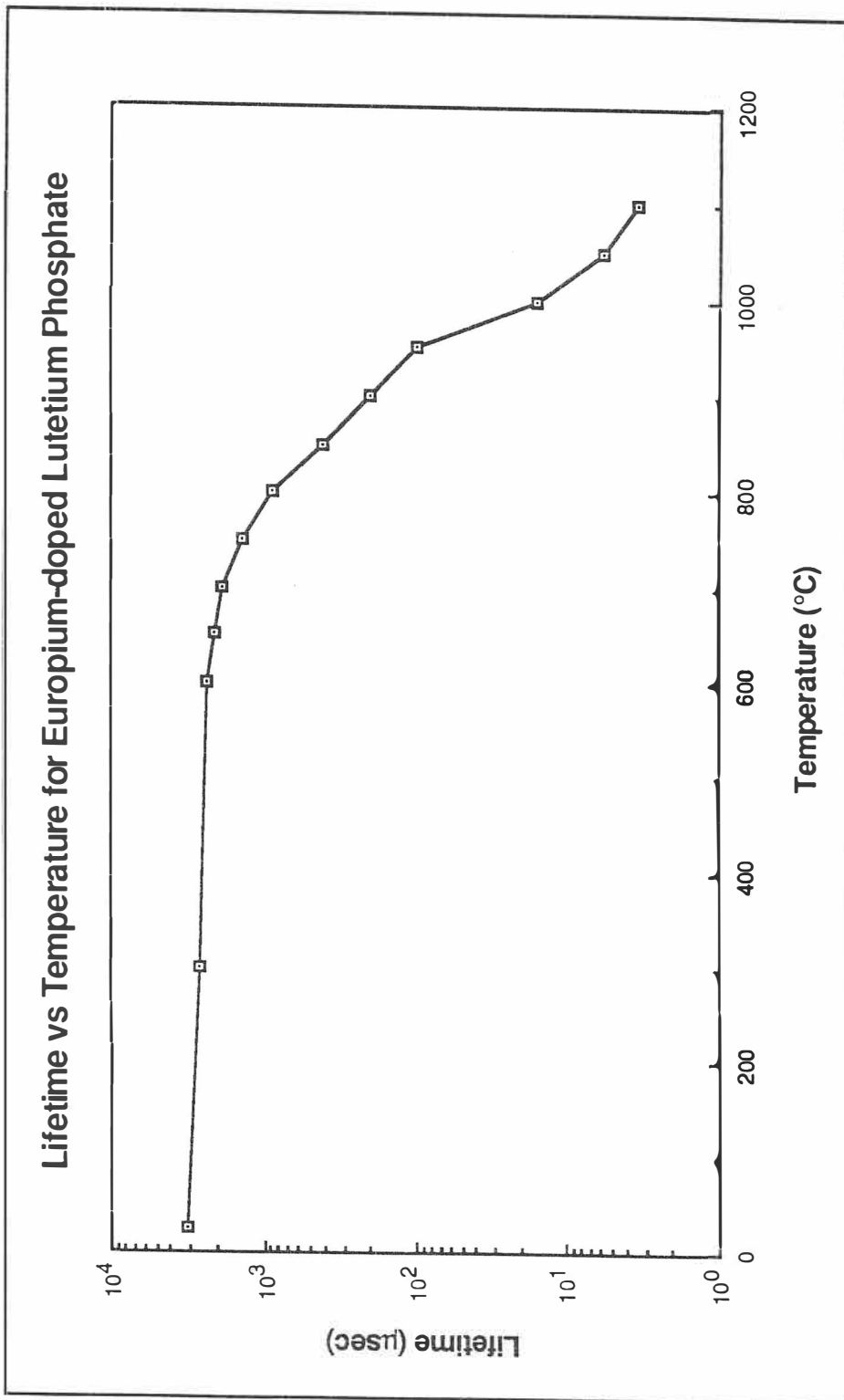
Figure 4-88. Lifetime calibration curve for europium-doped lutetium orthophosphate.
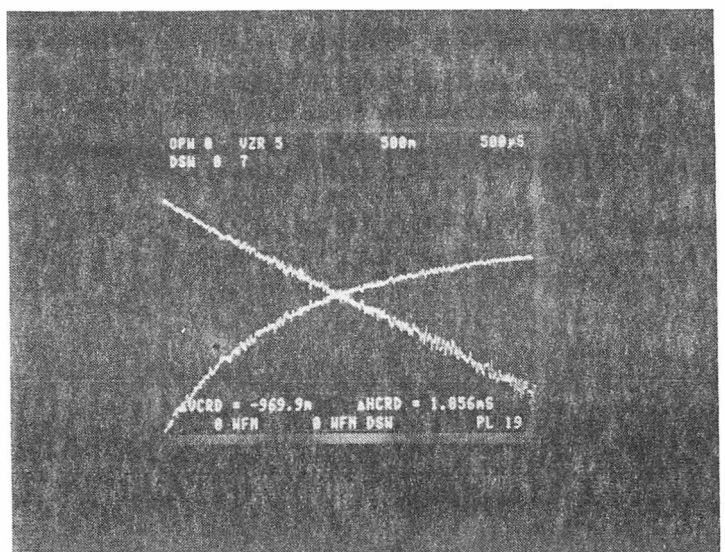
LuPO$_4$:Eu^{3+} TEMP = 700°C τ = 1.887 μs
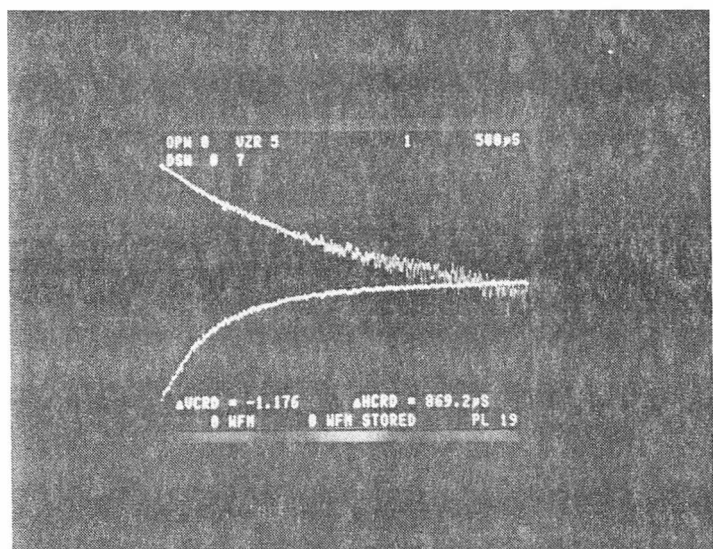
LuPO$_4$:Eu^{3+} TEMP = 800°C τ = 879.9 μs

Figure 4-89. Oscilloscope photographs showing the changing exponential lifetime
decay signal of LuPO$_4$:Eu^{3+} at 700°C and 800°C.

LuPO$_4$:Eu^{3+} TEMP = 900°C τ = 206.8 μs

LuPO$_4$:Eu^{3+} TEMP = 1000°C τ = 15.98 μs
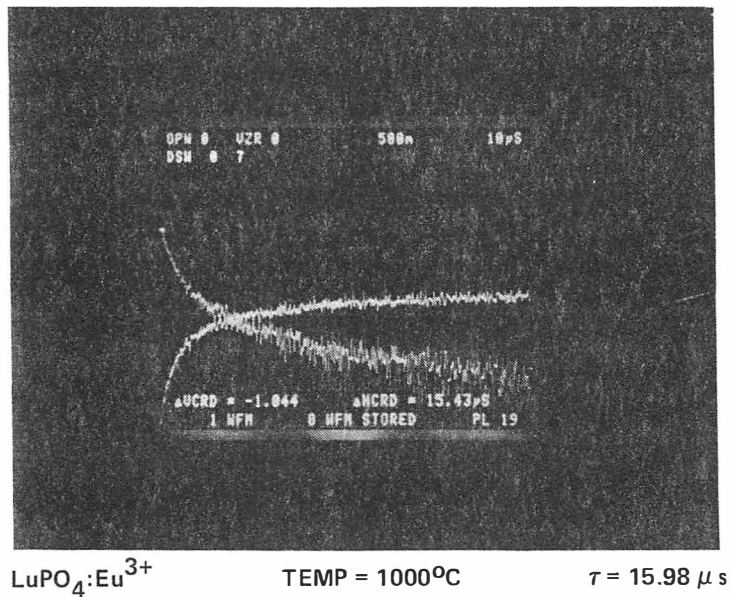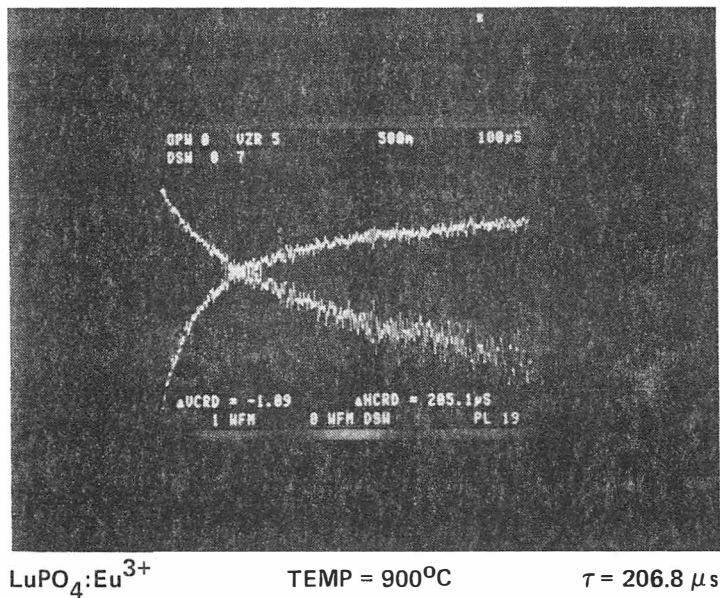
Figure 4-90. Oscilloscope photographs showing the changing exponential lifetime decay signal of LuPO$_4$:Eu^{3+} at 900°C and 1000°C.

Europium-doped Yttrium Oxide

Decay lifetime data of the 611 nm emission line of Y_2O_3:Eu^{3+} are listed in Table 4-9 and its calibration curve is shown in Figure 4-89. At room temperature, the lifetime value is approximately 900 μsec. This phosphor shows a slight rise in lifetime to roughly 1100 μsec at 300°C and then a gradual reduction until quenching takes place at approximately 510°C. A smooth logarithmic decrease in decay time continues out to nearly 1150°C.

Dysprosium-doped Lutetium Phosphate

Lifetime measurements were performed on $LuPO_4$:Dy^{3+} under laser excitation at 397.8 nm. The decay lifetime data of the 574.4 nm fluorescence line of $LuPO_4$:Dy^{3+} are presented in Table 4-10 and a calibration curve is shown in Figure 4-95. At room temperature, the recorded lifetime is approximately 543.0 μsec. Characteristically, it slowly increased in strength in decay lifetime to a maximum value of 610.5 μsec at 700°C. With increasing temperature, the transition began to quench near 900°C. There appears to be a logarithmic decrease in decay time beyond onset quenching temperature however more data are required to fully verify its behavior.

Dysprosium-doped Yttrium Vanadate (YVO_4:Dy^{3+})

Lifetime decay analysis was performed on YVO_4:Dy^{3+} with a nitrogen laser generating an excitation wavelength of 337 nm. The decay lifetime data of the 575.0 nm emission line of YVO_4:Dy^{3+} are listed in Table 4-11 and a calibration curve is shown in Figure 4-96. At room temperature, the recorded lifetime is approximately 160.8 μsec.

Table 4-9. Lifetime data for europium-doped yttrium oxide.

Europium-doped Yttrium Oxide	
Temperature (°C)	Lifetime (μsec)
100.0	900.0
200.0	1000.0
300.0	1100.0
400.0	950.0
450.0	900.0
500.0	850.0
550.0	550.0
600.0	270.0
650.0	115.0
700.0	48.0
750.0	21.0
800.0	10.0
850.0	4.5
900.0	1.9
950.0	1.2
1000.0	0.4
1050.0	0.28
1100.0	0.12
1150.0	0.05
1200.0	0.04
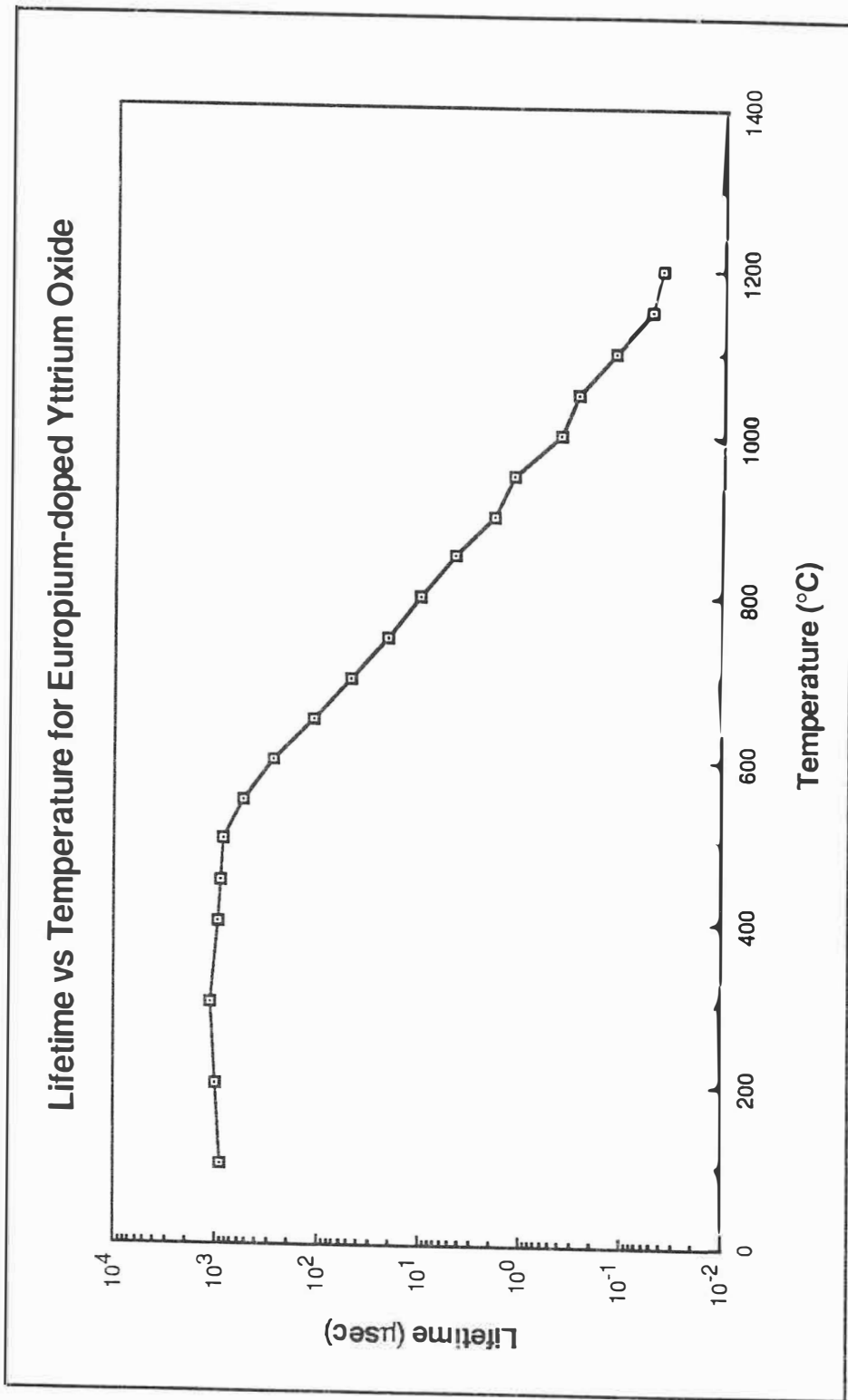
Figure 4-91. Lifetime calibration curve for europium-doped yttrium oxide.

Table 4-10. Lifetime data for dysprosium-doped lutetium phosphate.

Dysprosium-doped Lutetium Phosphate	
Temperature (°C)	Lifetime (μsec)
24.0	543.0
200.0	563.7
300.0	573.8
400.0	620.0
500.0	598.7
600.0	609.9
700.0	610.5
800.0	596.7
900.0	538.0
950.0	475.5
1000.0	411.3
1050.0	336.6
1100.0	171.9
1200.0	95.0
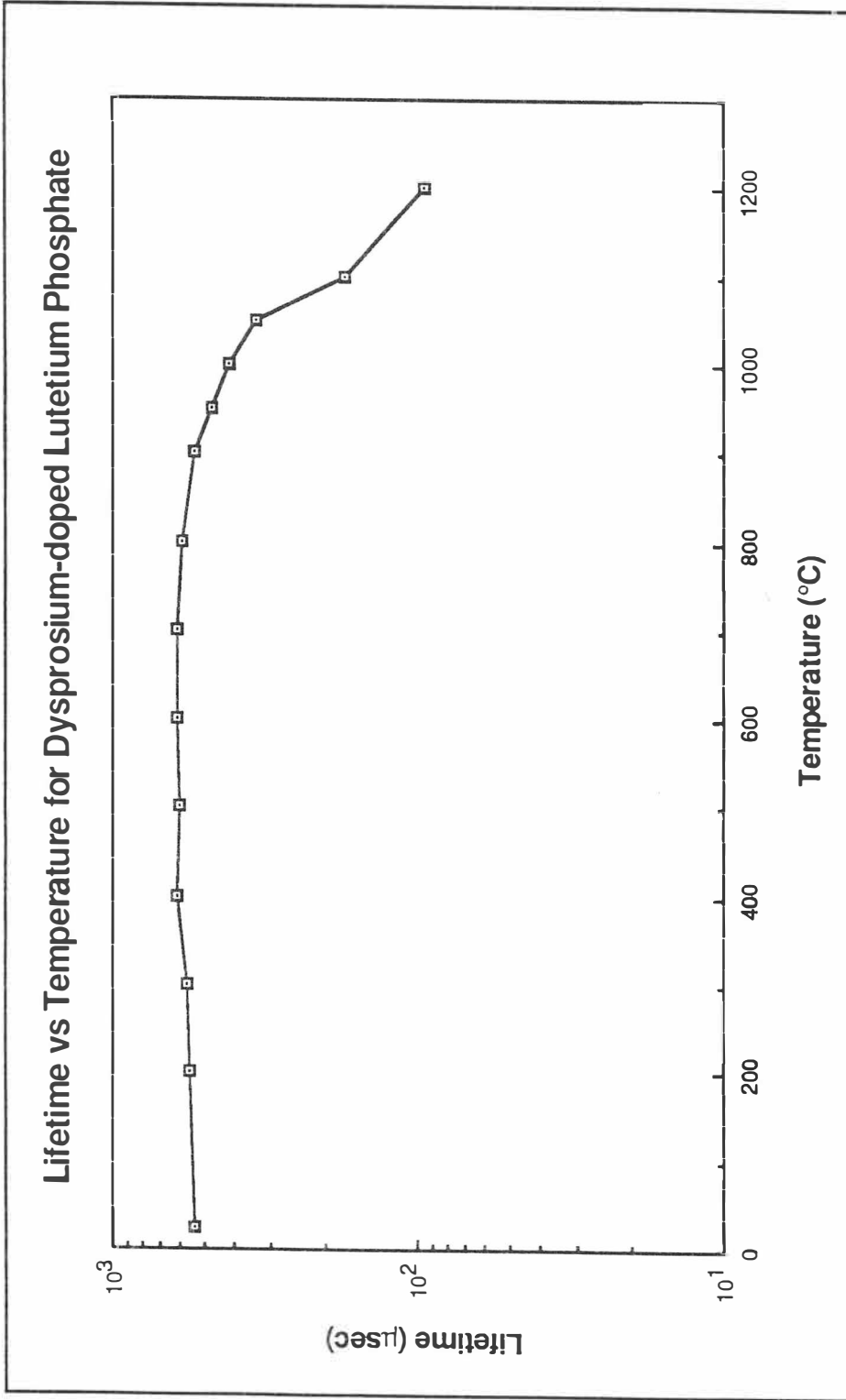
Figure 4-92. Lifetime calibration curve for dysprosium-doped lutetium orthophosphate.

Table 4-11. Lifetime data for dysprosium-doped yttrium vanadate.

Dysprosium-doped Yttrium Vanadate	
Temperature (°C)	*Lifetime (μsec)*
26.0	160.87
150.0	177.17
200.0	167.83
240.0	162.51
300.0	128.71
350.0	50.11
360.0	33.25
370.0	21.88
380.0	14.28
390.0	8.63
400.0	5.82
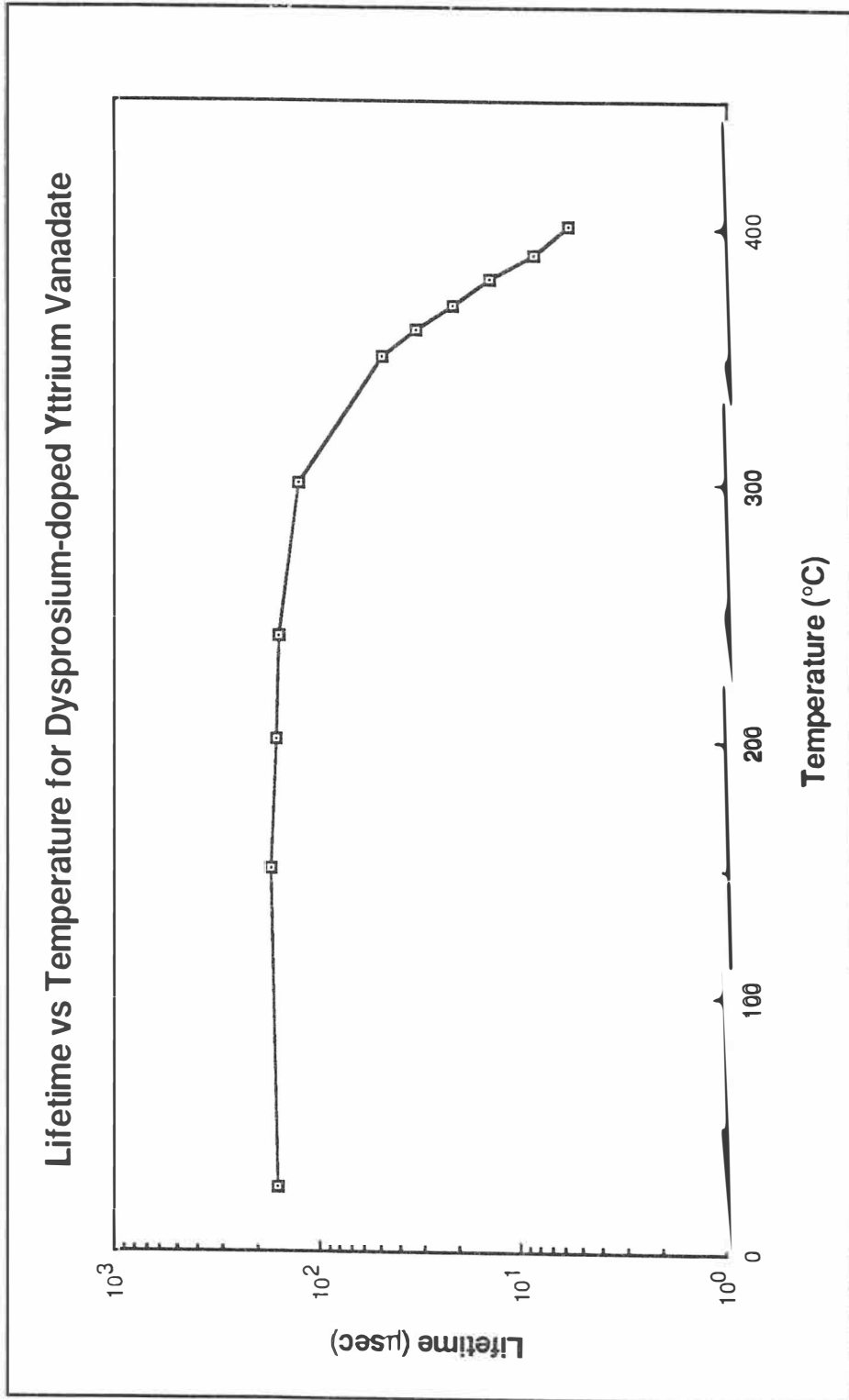
Figure 4-93. Lifetime calibration curve for dysprosium-doped yttrium vanadate.

The lifetime decay of the phosphor slowly increased in strength to a maximum value of 177 μsec at 150°C and then decreases slowly to 129 μsec at 300°C. As temperature increased, the radiative transition began to quench near 305°C. There also appears to be a logarithmic decrease in decay time beyond the onset quenching temperature of this phosphor.

Discussion of the Onset Quenching Temperature

The decay lifetimes of several high temperature thermographic phosphors are compared in the calibration curves of Figure 4-97. The CALQUEN.BAS computer program, written to analyze lifetime calibration data, was used to determine the onset quenching temperature of each phosphor researched. Using the method of line of best-fit, two equations interpolate the lifetime calibration curves of each thermographic phosphor and determine the initial point of temperature dependence. Table 4-12 summarizes the results of the onset quenching temperature analysis for the six thermophosphors.

It is seen that $LuPO_4:Dy^{3+}$ has the highest onset quenching temperature of all the orthophosphates tested. Its onset quenching temperature was calculated as 905.02°C. Proceeding $LuPO_4:Dy^{3+}$, are $LuPO_4:Eu^{3+}$, $YPO_4:Eu^{3+}$, and $LaPO_4:Eu^{3+}$ in which their onset quenching temperatures were found to be 756.5, 668.5, and 461.7°C respectively. Presented again are the cation radii for $LuPO_4:Eu^{3+}$, $YPO_4:Eu^{3+}$, and $LaPO_4:Eu^{3+}$ which measure 0.85, 0.893, and 1.061 Å. It was found that as the cation radius decreases in the europium-doped orthophosphates, their onset quenching temperatures tend to increase. For example, $LuPO_4:Eu^{3+}$, with ionic radius of 0.85 Å and onset quenching temperature of 756.5°C can be compared to $LaPO_4:Eu^{3+}$, with ionic radius of 0.85 Å and onset quenching temperature of 461.7°C.
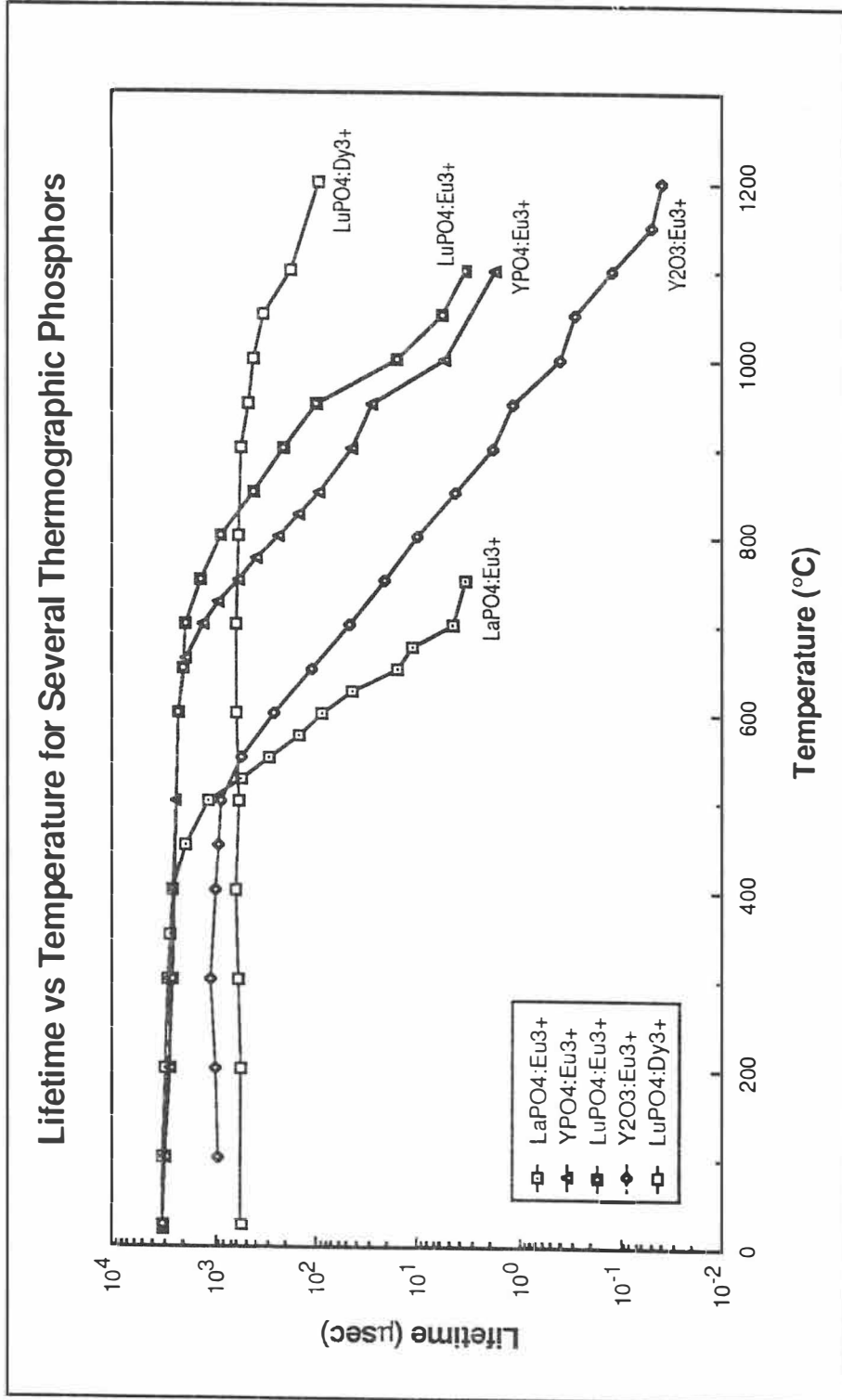
Figure 4-94. Combined lifetime calibration curves for several high temperature thermographic phosphors.

Table 4-12. Onset quenching temperatures of several thermographic phosphors.

Phosphor	Onset Quenching Temperature
Europium-doped Lanthanum Phosphate	461.6932 °C
Europium-doped Yttrium Phosphate	668.4855 °C
Europium-doped Lutetium Phosphate	756.5296 °C
Europium-doped Yttrium Oxide	506.9153 °C
Dysprosium-doped Lutetium Phosphate	905.0262 °C
Dysprosium-doped Yttrium Vanadate	304.9198 °C

With this observation in mind, it is probable that an europium-doped scandium phosphate crystal phosphor should yield an even higher onset quenching temperature since its cation radius is approximately 0.73 Å   This cation radius is much smaller than other europium-doped orthophosphates tested. This hypothesis may also be extended to other phosphors whose host cation radius is as small when compared to the cation radii of phosphors researched in this work.

CHAPTER V

SUMMARY AND CONCLUSION

Some of the emission properties of thermographic phosphors were measured because of their potential use in high temperature sensing applications. Specifically, the role of the charge-transfer state in the host/dopant crystal lattice and its relationship to thermophosphor emission properties was discussed. An experimental study of the excitation and emission spectra measured as a function of increasing temperature of fifteen phosphors was reported. In addition to spectral experiments, the emission decay times of these phosphors were measured. These lifetime decay plots are calibrations for use in remote thermographic measurement applications. Experimental errors, complications and corrections for the fluorescence spectrophotometer and lifetime decay configurations were presented. And finally, a computer program was developed to help clarify the onset quenching temperature point given a lifetime calibration curve. The intersection of the two lines that interpolate the lifetime data is defined as the onset quenching temperature point.

Several conclusions can be drawn from these research efforts and are listed in the paragraphs that follow:

a. In the excitation spectra taken from room temperature to approximately 400°C, the phosphors $Y_2O_3:Eu^{3+}$, $YVO_4:Eu^{3+}$, $Ba_3(PO_4)_2:Eu^{2+}$, $LaPO_4:Eu^{3+}$, $LuPO_4:Eu^{3+}$, $YPO_4:Eu^{3+}$, $YVO_4:Dy^{3+}$, $Y_2O_2S:Eu^{3+}$, and $Y_2O_2S:Tb^{3+}$ exhibit a

significant temperature-dependent spectral shift towards the red in their charge-transfer absorption bands. In general, it was observed in the several of the europium-doped phosphors that this shift is linearly as temperature increases.

b. The peak position of the charge transfer band in the europium-doped orthophosphate crystals is located at higher energies or deeper into the ultraviolet as the cation radius of the host crystal lattice decreases.

c. It is found that in the europium-doped orthophosphate crystals, the onset quenching temperature increases with a decrease in host cation radius. This phenomenon was observed in the lifetime calibration curves of $LaPO_4:Eu^{3+}$, $LuPO_4:Eu^{3+}$, and $YPO_4:Eu^{3+}$.

d. The orthophosphate crystals have the highest onset quenching temperatures of any of the thermophosphors that have been characterized to date. In particular, dysprosium-doped lutetium phosphate has an onset quenching temperature of approximately 905°C. The orthophosphate crystals $YPO_4:Eu^{3+}$ and $LuPO_4:Eu^{3+}$ were also found to have high onset quenching temperatures, 668.49°C and 756.53°C respectively.

e. The orthophosphate crystals may prove to be the phosphors of choice for high temperature sensing applications ranging from 700°C to 1400°C based on experimental data.

Future Research and Experimental Suggestions

The original intent of this thesis research was to investigate the spectra of powder and orthophosphate phosphors measured as a function of temperature and to obtain lifetime decay calibration for several thermophosphors. However this work has opened many new doors for future experimentation and research projects to further elucidate characteristics of emission properties and high temperature measurement applications of thermographic phosphors. There are many more questions to be asked and answered with respect to this work. Different experiments and methods can be used, and slight variations of past spectra and lifetime experiments can be performed to further verify the results presented in this thesis. For example, the spectral experiments can be done at higher wavelength resolution while lifetime decay measurements can be performed with greater accuracy and precision. On the following pages are details of comments and suggestion for improvements to past experimentation and ideas for future experiments related to the characterization of high temperature thermophosphors.

Background blackbody radiation effects on the photomultiplier tube can be a real problem in the measurement of spectra or lifetime decay at temperatures above 600°C. Similarly, thermal leakage near the optics and front surface area of the photomultiplier tube in the housing of the fluorescence spectrophotometer can possibly increase its dark current output at higher temperatures and drastically effect the results of the experiment. Therefore, several suggestions are in order. One can connect an ammeter in series with the output of the photomultiplier tube to measure and verify its output dark current as temperature increases and then compare the acquired current to the manufacturers specifications, if they are available. Most photomultiplier tubes have a range where certain dark currents are usable. This procedure should be done with no optical radiation

incident to the photomultiplier tube. The dark current should remain constant as the temperature of the oven is increased or as the area around the photomultiplier tube is heated. It may be necessary to cool the photomultiplier tube with liquid nitrogen in an attached surrounding chamber or to use an internally-mounted fan to circulate and cool the air near the photomultiplier tube housing. Another way to help reduce the thermal leakage from the oven in the spectrophotometer housing would be to use a ceramic material with greater insulating properties. This way less heat would affect the photomultiplier tube dark current and nearby optics.

Future research of excitation spectra measured at elevated temperatures may include the measurement of the spectra at higher resolution. With the use of the pulsed Nd:YAG pump laser, a tunable dye laser and a large variety of available dyes, a researcher may be able to obtain a high resolution excitation (and emission) spectra measured as a function of temperature. Since the Quanta Ray dye laser has a stepper motor attached to the diffraction grating, additional electronic control circuitry can be used to pulse the motor thus achieving a range of excitation wavelengths. A monochromator can be used to select the emission wavelength and its photomultiplier tube output would connect to a chart recorder to acquire an excitation scan. Similarly an emission scan could be acquired by first selecting an excitation line from the laser and using the built-in stepper motor on the monochromator to rotate the emission grating. Several electronic circuits and stepper motor controllers are available for the Quanta Ray dye laser unit. Since the phosphor sample would be placed in the Linberg oven, excitation and emission spectra have the potential to be measured at temperatures ranging from 400 to 1200 °C with much higher resolution. Accuracy of these spectra would be closer to ±1 Angstrom as compared to ±20 Angstrom (±2 nm) using the spectrophotometer. This type of measurement system, using the tunable dye laser in conjunction with the monochromator may help reduce the

background blackbody radiation, since it is a pulsed measuring system as opposed to a continuous measuring system. The photomultiplier tube in the case of the pulsed measuring system would only "see" the fluorescence when the laser is pulsed and the blackbody would therefore be a smaller part of the total acquired signal.

Another experimental lifetime decay calibration system could possibly be configured with a liquid crystal display (LCD) optical window to help reduce the blackbody radiation. The LCD widow, when placed in front of the monochromator or before the photomultiplier tube, can be synchronized with the timing of the laser trigger to open only during the emission of fluorescence from the phosphor sample. The overall pulse width of the timing window can be adjusted with a pulse delay generator. The properties of a usable LCD window would include high optical transmission with no absorption of fluorescence and a very fast rise and fall time such that the window could be synchronized to the 10 Hz pulse rate of the Nd:YAG laser trigger. Another technique similar to the LCD optical window may include the use of mechanical choppers to produce the same effect of reducing acquired blackbody background emission. One may even choose to experiment with a hybrid configuration coupling the LCD window along with the mechanical chopper.

All of the high temperature lifetime measurements performed in this thesis were constrained to the upper temperature limits of the Linberg oven. This oven has a maximum temperature output of approximately 1200°C. Since the Oak Ridge National laboratory facility has ovens that achieve internal temperatures to 1700°C, it is suggested that lifetime decay measurements be performed within the range of 1200°C to 1700°C. In particular, the lifetimes of the orthophosphates $LuPO_4:Eu^{3+}$, $YPO_4:Eu^{3+}$, and $LuPO_4:Dy^{3+}$, and the powder $Y_2O_3:Eu^{3+}$ should be characterized above 1200°C until their fluorescence is entirely quenched. Other phosphors, both powders and single

crystals can be investigated for higher temperatures. Special attention and care should be given to the lifetime measurements above the onset quenching temperature point so that more accurate data may be acquired in the temperature sensing region of the calibration curve. Once again, care must be taken to reduce the blackbody radiation generated by the ovens at these higher temperatures.

Another addition to past experimentation would be a thorough analysis of temperature cycling phenomena associated with lifetime measurements. As mentioned previously in this thesis, the need for this data will be most useful to applications which utilize the thermophosphor technique. There are many factors involved in the fluorescence process, and small variations is the ion/dopant concentration or physical and chemical changes in the phosphor structure can change the phosphor's temperature dependence slightly or even drastically. Temperature cycling experiments would provide important data that may determine the useful life of a thermophosphor in a high temperature environment and would generate information related to the reproducibility of the lifetime decay and temperature measurement.

It may become necessary to further understand the chemical composition of the thermophosphors used in high temperature measurements and therefore a complete and thorough chemical analysis of certain phosphors should be undertaken. Phosphor manufacturers usually don't list complete chemical constituents of their products due partially to proprietary protection. The researcher may find that impurities in commercially-manufactured phosphors have an effect on spectral or lifetime measurements since it is known that these unwanted or unknown impurities do affect the spectral properties. Several techniques such as x-ray diffraction, electron spectrometry for chemical analysis (ESCA) and other similar methods can be used to determine phosphor binding energies, elemental composition, and purity. Continued collaborative

efforts with the Solid State Division of Oak Ridge National Laboratory can further provide custom-grown, high-purity powder and crystal phosphors for use in future research and development of high temperature thermophosphor experiments. Bonding techniques and methods, specifically for orthophosphate crystals, need further investigation for potential use in thermophosphor applications.

To further elucidate the lifetime decay measurements, it may be interesting to develop a reflectance experiment where the intensity ratio of two emission lines is measured as a function of temperature. Although the lifetime technique has been thoroughly investigated and is most reliable, this reflectance experiment may generate data which can be compared to lifetime measurements as an alternate method of checking experimental calibration and consistency. This experiment can be performed by selecting two dominant emission lines in a phosphor, one being temperature-dependent and the other not being temperature-dependent and measuring the ratio of the intensities of the two lines as the temperature is increased. Other possible advantages of reflectance-based thermometry are that it may work at higher temperatures and may enable transient measurements to be made.

Several orthophosphate crystals in particular should be investigated and characterized as soon as possible. Europium-doped scandium phosphate should be thoroughly characterized for lifetime decay along with its excitation and emission spectra measured as a function of increasing temperature. As mentioned in previous chapters, since the ionic radius of the scandium host is smaller than that of lutetium and yttrium (although these three crystals maintain the same crystal structure), one should find that the charge-transfer band of scandium phosphate lies deep in the ultraviolet or at higher energies in the phosphor's excitation spectra. Because of this factor, scandium phosphate should thus yield a higher onset quenching temperature than the onset

quenching temperatures observed in yttrium and lutetium phosphate. Using the same experimental configurations detail in this work, scandium phosphate can and should be fully characterized and investigated for these phenomena.

Dysprosium-doped yttrium and scandium phosphate phosphors are available and are in need of spectral and lifetime characterization. Since dysprosium-doped lutetium phosphate has been characterized, it would be of interest to investigate the effects of the variable host cation radii of dysprosium-doped yttrium and scandium phosphate with respect to the onset quenching temperature and spectral shift of the excitation spectra. It is possible that the dysprosium-doped orthophosphate phosphors may parallel the cation host radius theory as was observed in the europium-doped orthophosphate phosphors. Hence it may be observed that dysprosium-doped lutetium phosphate could have a higher onset quenching temperature than that of dysprosium-doped yttrium phosphate if the theory holds true.

It may be of interest to perform spectral and lifetime experiments on a phosphor with variable dopant levels or dopant concentration. Since dopant concentration tends to increase the fluorescent intensity of phosphors in most cases, the effect of this variable should be observed in the excitation and emission spectra and lifetime decay measurements. In addition to varying the dopant concentration of the phosphor, it would be of interest to vary the phosphor particle size while holding the dopant concentration constant. It may be possible that the varying particle size of the phosphor may change the host-dopant coupling or shift the charge-transfer band to lower or higher energies. If this is found to be true, researchers can design phosphors to meet specific temperature sensing regions simply by varying the particle size and consequently relocating the charge-transfer energy location. Hence one can develop "tunable thermographic phosphors", if such terminology is applicable. The possibilities for creating and

constructing usable thermophosphors could then be multiplied.

In addition to the europium- and dysprosium-doped orthophosphates, a large variety of other rare-earth activated orthophosphate crystals developed by the ORNL Solid State Division are available to the thermophosphor program. Lifetime decay and excitation and emission spectra can be measured at both room and elevated temperatures to further characterize the phosphors. Some of these single crystals may someday find potential application in high or possibly low temperature measurements. These meticulous and sometimes laborious research efforts simply must be continued in search of an optimum and potentially useful phosphor material.

LIST OF REFERENCES

LIST OF REFERENCES

[1]   Pringsheim, P. and M. Vogel, Luminescence of Liquids and Solids and its Practical Applications, (Interscience Publishers, Inc., New York 1946) pp.12-13.

[2]   Cates, M.R., et al., *"Remote Thermometry of Moving Surfaces of Laser-Induced Fluorescence of Surface-Bonded Phosphors,"* Proceedings of the International Congress on Applications of Lasers and Electro-optics. (1983).

[3]   Allison, S.W., M.R. Cates, M.B. Scudiere, H.T. Bentley III, H. Borella, and B. Marshall, *"Remote Thermometry in a Combustion Environment Using the Phosphor Technique,"* Proceedings of the Society of Photo-Optical Instrumentation Engineers. Vol. 788, (1987).

[4]   Noel, B.W., et al., *"Proposed Laser-Induced Fluorescence Method for Remote Thermometry in Turbine Engines,"* Journal of Propulsion and Power, Vol. 2, No. 6, p.565. (1986).

[5]   Cates, M.R., et al., *Applications of Pulsed-Laser Techniques and Thermographic Phosphors to Dynamic Thermometry of Rotating Surfaces*, Proceedings of the International Congress on Applications of Lasers and Electro-optics., (1984).

[6]   Cates, M.R., et al., *Laser-Induced Fluorescence of Europium-doped Yttrium Oxide for Remote High-Temperature Thermometry*, Proceedings of the International Congress on Applications of Lasers and Electro-optics, (1985).

[7]   M.S. Elmanharawy, et al., *"Spectra of Europium-Doped Yttrium Oxide and Yttrium Vanadate Phosphors,"* Czech. Journal of Physics., B28: pp. 1164-1173, (1978).

[8]   H. Kusama, et al., *"Line Shift Method for Phosphor Temperature Measurements,"* Japanese Journal of Applied Physics., Vol. 15, No. 12: pp. 2349-2358., (December 1976).

[9]   K.A. Wickersheim and R.A. Lefeuer, *"Luminescent Behavior of the Rare Earths in Yttrium Oxide and Related Hosts,"* Journal of the Electrochemical Society., Vol. 111, No.1:45-51 (1964).

[10]   Bugos,A.R.,et al., *"Emission Properties of Phosphors for High Temperature Sensor Applications,"* Proceedings of the Institute of Electrical and Electronic Engineers (IEEE) Southeast Conference., (April 1988).

[11]   Bugos,A.R.,et al., *"Emission Properties of Europium-doped Lanthanum and Lutetium Orthophosphate Crystals for use in High Temperature Sensor Applications,"* Proceedings of the Institute of Electrical and Electronic Engineers (IEEE) Southeast Conference., (April 1989).

[12]   Siegman, A.E., Lasers, (University Science Books, Mill Valley, CA, 1986).

[13]   Peatman, W.C., *Luminescence in $Y_2O_3:Eu^{3+}$ and $Y_2O_2S:Eu^{3+}$ Phosphors,* University of Virginia Master's Thesis, (1987).

[14]   Goldberg, P., Luminescence of Inorganic Solids, (Academic Press, New York, 1966), pp. 484-5.

[15]   Struck, C.W. and W.H. Fonger, *Dissociation of $Eu3^+$ Charge-Transfer State in Y_2O_2S and La_2O_2S into Eu^{2+} and a Free Hole,* Physical Review B, Vol. 4, No.1, pp. 22-34. (July 1971).

[16]   Ozawa, L., *Excitation into Charge Transfer Band of Y_2O_2S:Eu*, Electrochemical Society Technical Note, Vol. 128, No. 11 (1981).

[17]   Struck, C.W. and W.H. Fonger, *"Role of the Charge-Transfer States in Feeding and Thermally Emptying the ^5D States of Eu^{3+} in Y_2O_2S and La_2O_2S,"* Journal of Luminescence, Vol. 1, No.2, pp. 456-469. (1970).

[18]   Struck, C.W. and W.H. Fonger, *"$Eu^{3+}\,^5D$ Resonance Quenching to the Charge-Transfer States in Y_2O_2S, La_2O_2S, and LaOCl,"* Journal of Chemical Physics, Vol. 52, No.12, pp. 6364-6372. (1970).

[19]   Haake, C.H., *"The Significance of the Temperature Dependence of Fluorescence Intensity,"* Journal of The Electrochemical Society, Vol. 108, No. 1, pp. 78-82. (January 1961).

[20]   Ropp, R.C. and B. Carroll, *"Charge-Transfer and ^5D States of the Trivalent Rare-Earths,"* The Journal of Physical Chemistry, Vol. 81, No. 17, (1977).

[21]   Hoefdraad, H.E., *"The Charge-Transfer Absorption Band of Eu^{3+} in Oxides,"* Journal of Solid State Chemistry, Vol. 15, pp. 175-177 (1975).

[22]   Blasse, G., *"Thermal Quenching of Characteristic Fluorescence,"* The Journal of Chemical Physics, Vol. 51, No. 8, pp. 3529-3530 (1969).

[23]   Sylvania Chemicals and Metals Division, *Technical Information Bulletins*, GTE Products Corporation, Chemical and Metallurgical Division, Towanda, PA 18848 (Dec. 1986).

[24]   Sylvania Chemicals and Metals Division, *Inorganic Phosphors and Related Chemicals - A Reference*, GTE Products Corporation, Chemical and Metallurgical Division, Towanda, PA 18848 (Feb. 1988).

[25] L.A.Boatner, G.W. Beall, M.M. Abraham, C.B. Finch, R.J. Floran, P.G. Huray, M. Rappaz, *Lanthinide Orthophosphates for the Primary Immobilization of Actinide Wastes*, Management of Alpha-contaminated Wastes, International Atomic Energy Agency (1981).

[26] L.A.Boatner, M.M. Abraham, and M. Rappaz, *The Characterization of Nuclear Waste Forms by EPR Spectroscopy*, Scientific Basis for Nuclear Waste Management, Vol. 3 (Plenum Publishing Corporation, 1981).

[27] D.F. Mullica, W.O. Milligan, D.A. Grossie, G.W. Beall and L.A.Boatner, *Ninefold Coordination in LaPO$_4$: Pentagonal Interpenetrating Tetrahedral Polyhedron*, Inorganica Chimica Acta, No. 60:pp.39-43 (1982).

[28] W.O. Milligan, D.F. Mullica, G.W. Beall and L.A.Boatner, *Structural Investigations of YPO$_4$, ScPO$_4$, and LuPO$_4$*, Inorganica Chimica Acta, No. 60:pp.39-43 (1982).

[29] M.M. Abraham, L.A. Boatner, J.O.Ramey, and M Rappaz, *An EPR Study of Rare-earth Impurities in Single Crystals of the Zircon-structure Orthophosphates ScPO$_4$, YPO$_4$, and LuPO$_4$*, J. Chem. Phys. 78(1), pp.3-10 (Jan. 1983).

[30] Heinz Kohler, *Statistics for Business and Economics*, Scott Foresman and Co., Glenview, Illinois, (1988). pp. 91-113.

[31] Gillies, G.T., *Noncontact Thermometry via Laser Pumped, Thermographic Phosphors: Characterization of Systematic Errors and Industrial Applications.* Proceedings of the International Conference on Applications of Lasers and Electro-optics (ICALEO 87), November 1987.

[32] Dowell, L.J., *A Comprehensive Error Analysis of a Phosphor Thermography System,* University of Virginia Master's Thesis (1987).

[33]   Lutz, W.N., *A Computer Aided Data Acquisition System for use in High Temperature Furnace Calibration*, University of Virginia Master's Thesis (1987).

[34]   O'Flaherty, B., *"Advantages of Temperature Stabilization of Photomultipliers During Fluorescence Detection,"* American Laboratory, pp. 22-24. Oct. 1988.

[35]   Dence, Thomas P., *Solving Math Problems in BASIC*, Tab Books, Inc.,1983, Blue Ridge Summit, PA. pp. 333-340.

[36]   Blasse, G., Handbook on the Physics and Chemistry of Rare Earths, (North-Holland Publishing Co., Holland, 1979), pp. 237-274.

APPENDICES

APPENDIX A
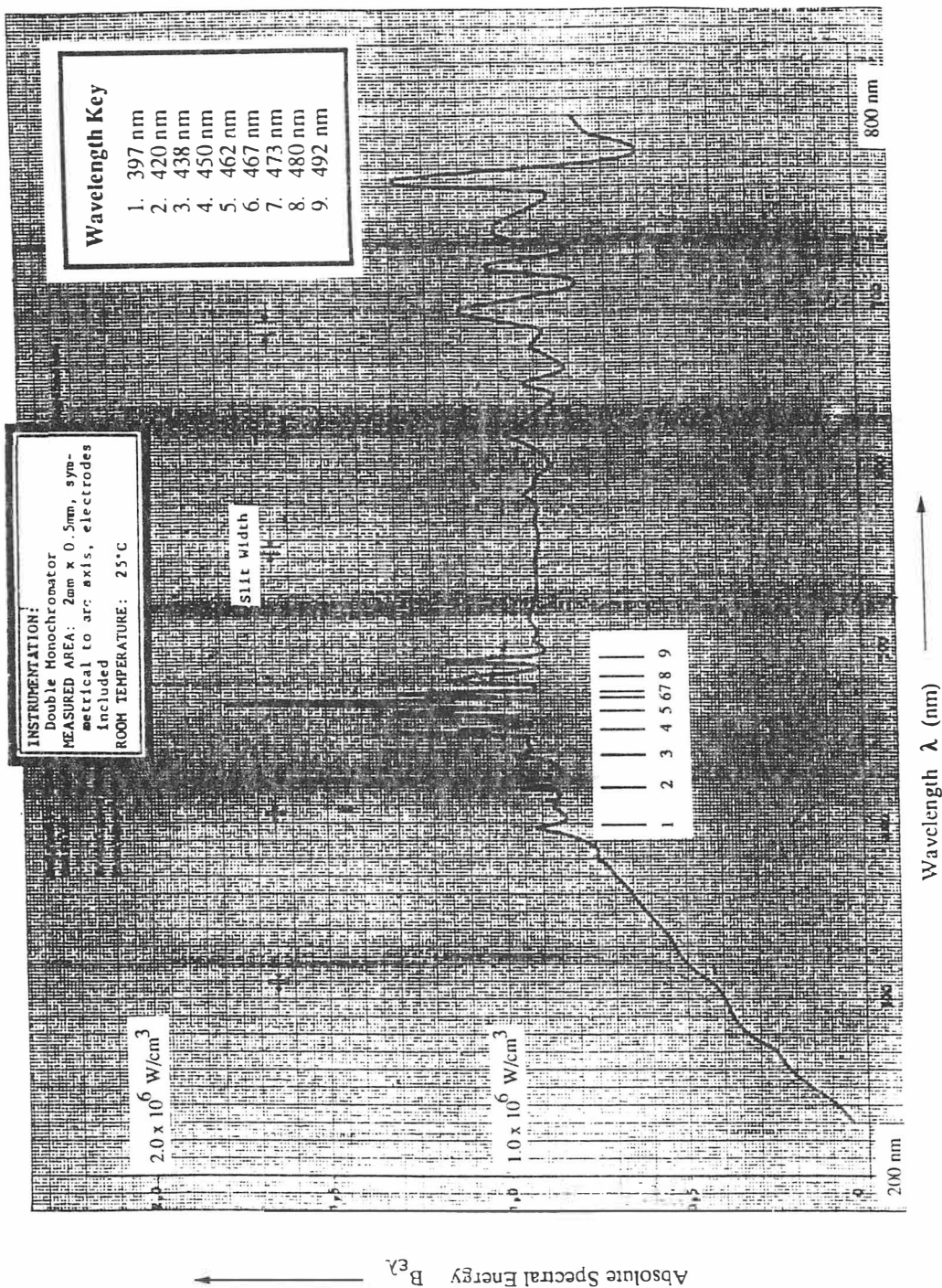
Spectral radiant distribution of the OSRAM xenon high-pressure lamp XBO 150 watts

APPENDIX B

A listing of a Tektronix 7854 oscilloscope program used for analyzing the lifetime value of an exponential fluorescence signal.

EXP.PRO

```
LNN 0 0 NEXT
VMDL HMDB NEXT
BOTH NEXT
100 AVG NEXT
9 >WFM NEXT
LNN 0 1 NEXT
STOP NEXT
100 AVG NEXT
8 >WFM NEXT
0 WFM  9 WFM -  NEXT
7 >WFM NEXT
7 WFM NEXT
0.6 SMOOTH NEXT
CRS1 NEXT
STOP NEXT
VCRD NEXT
2.718 / NEXT
STOP NEXT
CRS2-1  NEXT
STOP NEXT
1  LBL GOTO NEXT
```

APPENDIX C

```
10      REM ********************************************************************
20      REM ***                                                            ***
30      REM ***        This program will determine the onset quenching temperature    ***
40      REM ***        of a thermographic phosphor from the analysis of its lifetime   ***
50      REM ***        calibration curve.  The analysis uses linear regression and     ***
60      REM ***        a best-fit line to the calibration curve. The intersection of   ***
70      REM ***        the two lines is defined as the onset quenching temperature.    ***
80      REM ***                                                            ***
90      REM ***                       Alan R. Bugos                        ***
100     REM ***                                                            ***
110     REM ***              Oak Ridge National Laboratory                 ***
120     REM ***                                                            ***
130     REM ***                       January 1989                        ***
140     REM ***                                                            ***
150     REM ***                                                            ***
160     REM ********************************************************************
170     REM ***                                                            ***
180     REM ***              CALQUEN.BAS  Version 1.00                     ***
190     REM ***                                                            ***
200     REM ********************************************************************
210     REM
220     REM
230     REM ********************************************************************
240     REM ***                                                            ***
250     REM ***            Setting up the Screen Graphics Routine          ***
260     REM ***                                                            ***
270     REM ********************************************************************
280     REM
290     REM
300         CLS:SCREEN 2:CLS:FOR T=1 TO 700 STEP 5
310         LINE (0,0)-(T,200),4
320         IF T>200 THEN LINE (0,0)-(T-200,200),0 ELSE 330
330         NEXT T
340         CLS:SC=4:FOR T = 700 TO 1 STEP -7
350         LINE (0,0)-(T,200),SC
360         NEXT T:FOR D=1 TO 1000:NEXT D:CLS:SCREEN 0
370     REM
380     REM
390     REM ********************************************************************
400     REM ***                                                            ***
410     REM ***                Beginning of the Main Program              ***
420     REM ***                                                            ***
430     REM ********************************************************************
440     REM
```

```
450   REM
460   REM ***************   Define variables, parameters, and other values   ***************
470   REM
480       KEY OFF:CLS:DEFSTR S
490       DIM X1(100), Y1(100), XX(100), YY(100), XY(100)
500       DIM M(30), B(30), D1(100), D2(100), X2(100),Y2(100)
510       DIM Y1A(100), Y2A(100)
520       XSUM = 0:YSUM = 0:XXSUM = 0:YYSUM = 0:XYSUM = 0
530   REM
540   REM *************   Display the first screen and link the HELP program   *************
550   REM
560       CLS:COLOR 9
570       LOCATE 3,6:FOR P = 1 TO 35:PRINT "**";:NEXT P
580       LOCATE 4,6:FOR P = 1 TO 35:PRINT "**";:NEXT P:COLOR 13
590   REM
600   REM ********************************************************************
610   REM ***                                                            ***
620   REM ***          Screen Data and Routine for the Main Menu         ***
630   REM ***                                                            ***
640   REM ********************************************************************
650   REM
660       LOCATE 6,15:PRINT"Welcome to CALQUEN.BAS, a program which approximates
670       LOCATE 7,15:PRINT"the onset quenching temperature of a thermographic
680         LOCATE 8,15:PRINT"phosphor given its temperature and lifetime calib-
690         LOCATE 9,15:PRINT"ration data.":COLOR 9
700         LOCATE 11,6:FOR P = 1 TO 35:PRINT "**";:NEXT P
710         LOCATE 12,6:FOR P = 1 TO 35:PRINT "**";:NEXT P:COLOR 12
720         LOCATE 14,15:PRINT"****************** Main Menu ******************
730       COLOR 11
740         LOCATE 16,20:PRINT"1.)   Help
750         LOCATE 17,20:PRINT"2.)   Load Data Manually (Sequential Input)
760         LOCATE 18,20:PRINT"3.)   Load External Data Files
770         LOCATE 19,20:PRINT"4.)   Quit":COLOR 10
780         LOCATE 21,20,1:PRINT"     What is your selection?";:S$= INPUT$(1)
790       IF INSTR("1234",S$) THEN K = VAL(S$) ELSE 780
800       ON K GOTO 830,1070,2840,940
810   REM
820   REM
830   REM ********************************************************************
840   REM ***                                                            ***
850   REM ***            Linking the CALHELP.BAS program                 ***
860   REM ***            for help and introduction information           ***
870   REM ***                                                            ***
880   REM ********************************************************************
890   REM
900   REM
910       COMMON ALL:CHAIN "CALHELP.BAS"
920   REM
930   REM
940   REM ********************************************************************
950   REM ***                                                            ***
```

```
960    REM ***                    Quitting the CALQUEN.BAS program              ***
970    REM ***                      and returning back to DOS.                  ***
980    REM ***                                                                  ***
990    REM *****************************************************************************
1000   REM
1010   REM
1020       CLS:FOR T = 1 TO 2000:NEXT T:BEEP:COLOR 10
1030       LOCATE 12,15:PRINT"*********   Leaving CALQUEN.BAS   *********"
1040       FOR T = 1 TO 10000:NEXT T:CLS:END
1050   REM
1060   REM
1070   REM *****************************************************************************
1080   REM ***                                                                  ***
1090   REM ***                 Routine for manual sequential data input          ***
1100   REM ***                                                                  ***
1110   REM *****************************************************************************
1120   REM
1130   REM
1140       CLS:BEEP:COLOR 9
1150       FOR P=1 TO 38:PRINT"**";:NEXT P:COLOR 12
1160         LOCATE 3,22:PRINT"********* Phosphor Name *********":COLOR 10
1170         LOCATE 7,9:INPUT"What is the name of the phosphor? ",PHOSNAME$:COLOR 11
1180         LOCATE 22,16:PRINT"********* PRESS ANY KEY TO CONTINUE *********"
1190       RET$=INPUT$(1):FOR T = 1 TO 5000:NEXT T
1200   REM
1210   REM
1220       CLS:BEEP:COLOR 9
1230       FOR P=1 TO 38:PRINT"**";:NEXT P:COLOR 12
1240         LOCATE 3,22:PRINT"****** Temperature Scale *****":COLOR 10
1250         LOCATE 7,9:INPUT"What are the temperature units <C or F>? ",DG$:COLOR 11
1260         LOCATE 22,16:PRINT"********* PRESS ANY KEY TO CONTINUE *********"
1270       RET$=INPUT$(1):FOR T = 1 TO 5000:NEXT T
1280   REM
1290   REM
1300       CLS:BEEP:COLOR 9
1310       FOR P=1 TO 38:PRINT"**";:NEXT P:COLOR 12
1320         LOCATE 3,22:PRINT"******* Manual Data Input *******":COLOR 11
1330         LOCATE 5,9:PRINT"Data Input for Calibration Line 1":COLOR 13
1340         LOCATE 7,9:INPUT"Number of Data Points for Line 1: ", N1
1350       FOR M = 1 TO N1:COLOR 10
1360       LOCATE 10,9:PRINT"Temp. point";M;:INPUT"   : ",X1(M)
1370       IF X1(M)<=0 THEN GOSUB 1460:GOTO 1360
1380       LOCATE 11,9:PRINT"Lifetime point";M;:INPUT": ",Y1A(M)
1390       IF Y1A(M)<=0 THEN GOSUB 1460:GOTO 1380
1400         LOCATE 10,9:PRINT"Temp. point";M;"   :              "
1410         LOCATE 11,9:PRINT"Lifetime point";M;":            "
1420       BEEP:NEXT M:COLOR 11:GOTO 1560
1430   REM
1440   REM *****************************************************************************
1450   REM ***                                                                  ***
1460   REM ***                    Less than zero input subroutine                ***
```

```
1470  REM ***                                                          ***
1480  REM ************************************************************************
1490  REM
1500       COLOR 13
1510       LOCATE 14,9:PRINT"Value must be greater than zero!":BEEP:COLOR 10
1520       FOR T=1 TO 10000:NEXT T:LOCATE 14,9:PRINT STRING$(50," ")
1530       RETURN
1540  REM
1550  REM
1560       LOCATE 14,9:PRINT"Number of data points input for Line 1: ";N1:COLOR 12
1570       LOCATE 20,10:PRINT"***** Press any key to verify data for Line 1  *****
1580       RET$=INPUT$(1):FOR T = 1 TO 1500:NEXT T:CLS:COLOR 9
1590       LOCATE 3,12:PRINT"************** DATA FOR LINE 1  ***************"
1600       PRINT:COLOR 10:FOR M = 1 TO N1
1610       PRINT" Temp:";X1(M),"Lifetime:";Y1A(M)
1620       NEXT M:COLOR 11
1630       PRINT:INPUT"Is your data correct?  [Y or N]: ",ANS$
1640       IF ANS$="Y" OR ANS$="y" THEN 1680 ELSE 1100
1650  REM
1660  REM ************************************************************************
1670  REM ***                                                          ***
1680  REM ***                 Writing data to an external file          ***
1690  REM ***                                                          ***
1700  REM ************************************************************************
1710  REM
1720  REM   LINE1.DAT  Data file for the raw data of the 1st calibration line
1730  REM
1740  REM
1750       CLS
1760       LOCATE 4,4:PRINT"This data will be stored on disk in filename:":COLOR 13
1770       LOCATE 4,50:PRINT" LINE1.DAT ":COLOR 11
1780       LOCATE 4,62:PRINT"for future use.":COLOR 10
1790       LOCATE 22,18:PRINT"******** PRESS ANY KEY TO CONTINUE ********"
1800       RET$=INPUT$(1):BEEP:FOR T = 1 TO 1000:NEXT T:CLS
1810       OPEN "LINE1.DAT" FOR OUTPUT AS #1:FOR M = 1 TO N1
1820       PRINT#1,X1(M),Y1A(M):NEXT M:CLOSE #1
1830  REM
1840  REM ************************************************************************
1850  REM ***                                                          ***
1860  REM ***                 End of Calibration Line 1 Input           ***
1870  REM ***                                                          ***
1880  REM ************************************************************************
1890  REM
1900  REM
1910       CLS:BEEP:COLOR 9
1920       FOR P=1 TO 38:PRINT"**";:NEXT P:PRINT:COLOR 12
1930          LOCATE 3,22:PRINT"******* Manual Data Input *******":COLOR 11
1940          LOCATE 5,9:PRINT"Data Input for Calibration Line 2":COLOR 13
1950          LOCATE 7,9:INPUT"Number of Data Points for Line 2: ", N2
1960       FOR M = 1 TO N2:COLOR 10
1970       LOCATE 10,9:PRINT"Temp. point";M;:INPUT"  : ",X2(M)
```

```
1980       F X2(M)<=0 THEN GOSUB 2040:GOTO 1970
1990       LOCATE 11,9:PRINT"Lifetime point";M;:INPUT": ",Y2A(M)
2000       IF Y2A(M)<=0 THEN GOSUB 2040:GOTO 1990
2010         LOCATE 10,9:PRINT"Temp. point";M;"  :            "
2020         LOCATE 11,9:PRINT"Lifetime point";M;":          "
2030       BEEP:NEXT M:COLOR 11:GOTO 2150
2040 REM
2050 REM ****************************************************************
2060 REM ***                                                         ***
2070 REM ***              Less than zero input subroutine            ***
2080 REM ***                                                         ***
2090 REM ****************************************************************
2100 REM
2110       COLOR 13
2120       LOCATE 14,9:PRINT"Value must be greater than zero!":BEEP:COLOR 10
2130       FOR T=1 TO 10000:NEXT T:LOCATE 14,9:PRINT STRING$(50," ")
2140       RETURN
2150       LOCATE 14,9:PRINT"Number of Data Points Input for Line 2: ";N2:COLOR 12
2160       LOCATE 20,10:PRINT"****** Press Any Key to Verify Data for Line 2 ******
2170       RET$=INPUT$(1):BEEP:FOR T = 1 TO 1500:NEXT T:CLS:COLOR 9
2180       LOCATE 3,12:PRINT"************** DATA FOR LINE 2 ***************"
2190       PRINT:COLOR 10:FOR M = 1 TO N2
2200       PRINT" Temp:";X2(M),"Lifetime:";Y2A(M)
2210       NEXT M:COLOR 11
2220       PRINT:INPUT"Is your data correct?  [Y or N]: ",ANS$
2230       IF ANS$="Y" OR ANS$="y" THEN 2240 ELSE 1910
2240 REM
2250 REM
2260 REM ****************************************************************
2270 REM ***                                                         ***
2280 REM ***              Writing data to an external file           ***
2290 REM ***                                                         ***
2300 REM ****************************************************************
2310 REM
2320 REM   LINE2.DAT  Data file for the raw data of the 2nd calibration line
2330 REM
2340 REM
2350       CLS
2360         LOCATE 4,4:PRINT"This data will be stored on disk in filename:":COLOR 13
2370         LOCATE 4,50:PRINT" LINE2.DAT ":COLOR 11
2380         LOCATE 4,62:PRINT"for future use.":COLOR 10
2390         LOCATE 22,18:PRINT"******** PRESS ANY KEY TO CONTINUE ********"
2400       RET$=INPUT$(1):BEEP:FOR T = 1 TO 1000:NEXT T:CLS
2410       OPEN "LINE2.DAT" FOR OUTPUT AS #2:FOR M = 1 TO N2
2420       PRINT#2,X2(M),Y2A(M):NEXT M:CLOSE #2
2430 REM
2440 REM
2450 REM ****************************************************************
2460 REM ***                                                         ***
2470 REM ***              End of Calibration Line 2 Input            ***
2480 REM ***                                                         ***
```

```
2490  REM **********************************************************************
2500  REM ***                                                               ***
2510  REM ***          Printing the raw data on the line printer            ***
2520  REM ***              and continuing the calculations.                 ***
2530  REM ***                                                               ***
2540  REM **********************************************************************
2550  REM
2560  REM
2570      CLS:COLOR 9:PRINT:PRINT
2580      FOR P = 1 TO 38:PRINT "**";:NEXT P:COLOR 10
2590      LOCATE 7,15:PRINT"The raw data has been stored in the following files:"
2600      COLOR 13:LOCATE 9,35:PRINT"LINE1.DAT":LOCATE 10,35:PRINT"LINE2.DAT"
2610      COLOR 10
2620         LOCATE 13,15:PRINT "Select an option:":COLOR 11
2630         LOCATE 15,20:PRINT "1.)  Continue with calculations"
2640         LOCATE 16,20:PRINT "2.)  Print Raw Data Files
2650         LOCATE 17,20:PRINT "3.)  Quit the program":COLOR 10
2660         LOCATE 19,15:PRINT" What is your selection?":S$=INPUT$(1)
2670      IF INSTR("123",S$) THEN K = VAL(S$) ELSE 2660
2680      ON K GOTO 4920,2720,940
2690  REM
2700  REM **********************************************************************
2710  REM ***                                                               ***
2720  REM ***                    Printing the raw data                      ***
2730  REM ***                                                               ***
2740  REM **********************************************************************
2750  REM
2760  REM
2770      LPRINT:LPRINT:
2780      LPRINT"Raw Data for Calibration Line 1 and Line 2":LPRINT:LPRINT
2790        FOR N = 1 TO N1:LPRINT"Temp. =";X1(N),"Lifetime = ";Y1A(N):NEXT N
2800        FOR M = 1 TO N2:LPRINT"Temp. =";X2(M),"Lifetime = ";Y2A(M)
2810      NEXT M:LPRINT:LPRINT:LPRINT"End of Data":GOTO 2570
2820  REM
2830  REM
2840  REM **********************************************************************
2850  REM ***                                                               ***
2860  REM ***           Routines for reading in calibration data            ***
2870  REM ***                 from an external data file.                   ***
2880  REM ***                                                               ***
2890  REM **********************************************************************
2900  REM
2910  REM
2920      CLS:BEEP:COLOR 9
2930      FOR P=1 TO 38:PRINT"**";:NEXT P:COLOR 12
2940        LOCATE 3,22:PRINT"********* Phosphor Name *********":COLOR 10
2950        LOCATE 7,9:INPUT"What is the name of the phosphor? ",PHOSNAME$:COLOR 11
2960        LOCATE 22,16:PRINT"********* PRESS ANY KEY TO CONTINUE *********"
2970      RET$=INPUT$(1):FOR T = 1 TO 5000:NEXT T
2980  REM
2990  REM
```

```
3000      CLS:BEEP:COLOR 9
3010      FOR P=1 TO 38:PRINT"**";:NEXT P:COLOR 12
3020        LOCATE 3,22:PRINT"***** Temperature Scale *****":COLOR 10
3030        LOCATE 7,9:INPUT"What are the temperature units <C or F>? ",DG$:COLOR 11
3040        LOCATE 22,16:PRINT"********* PRESS ANY KEY TO CONTINUE **********"
3050      RET$=INPUT$(1):FOR T = 1 TO 5000:NEXT T
3060 REM
3070 REM
3080 REM ***************************************************************
3090 REM ***                                                        ***
3100 REM ***                  External Data File Menu               ***
3110 REM ***                                                        ***
3120 REM ***************************************************************
3130 REM
3140 REM
3150      CLS:COLOR 9:LOCATE 3,6:FOR P = 1 TO 35:PRINT"**";:NEXT P:COLOR 12
3160        LOCATE 5,23:PRINT"Loading Data From An External Data File":COLOR 10
3170        LOCATE 7,9:PRINT "Select an Option:":COLOR 11
3180        LOCATE 9,12:PRINT"1.)  Read Data Files for Line 1 and Line 2"
3190        LOCATE 10,12:PRINT"2.)  Return to the Main Menu"
3200        LOCATE 11,12:PRINT"3.)  Quit the program":COLOR 10
3210        LOCATE 15,12:PRINT"What is your selection?";:E$=INPUT$(1)
3220      IF INSTR("123",E$) THEN K=VAL(E$) ELSE 3210
3230      ON K GOTO 3280,540,940
3240 REM
3250 REM
3260 REM ***************************************************************
3270 REM ***                                                        ***
3280 REM ***              Reading the External Data Files           ***
3290 REM ***                                                        ***
3300 REM ***************************************************************
3310 REM ***                                                        ***
3320 REM ***           Data for LINE 1 of the Calibration Curve     ***
3330 REM ***                                                        ***
3340 REM ***************************************************************
3350 REM
3360 REM
3370      CLS:COLOR 9:LOCATE 3,6:FOR P = 1 TO 35:PRINT"**";:NEXT P:COLOR 12
3380        LOCATE 5,23:PRINT"Loading Data From an External Data File":COLOR 10
3390        LOCATE 7,10:PRINT"Do you want to inspect the files on disk? <Y or N>";
3400      A$=INPUT$(1):PRINT:PRINT:IF A$="y" OR A$="Y" THEN FILES ELSE 3460
3410      COLOR 11
3420      LOCATE 22,16:PRINT"********* PRESS ANY KEY TO CONTINUE **********"
3430      RET$=INPUT$(1):FOR T = 1 TO 5000:NEXT T
3440 REM
3450 REM
3460      J = 1:ERRORCHK = 0
3470      CLS:COLOR 9:LOCATE 3,6:FOR P = 1 TO 35:PRINT"**";:NEXT P:COLOR 12
3480      LOCATE 5,23:PRINT"Loading Data From an External Data File":COLOR 10
3490      LOCATE 7,9:PRINT "What is the filename and extension for Line 1?"
3500      COLOR 11:LOCATE 9,20:PRINT "Example:  TEST.DAT":COLOR 10
```

```
3510       ON ERROR GOTO 6500
3520       LOCATE 11,9:INPUT"Filename:  ", FI$
3530       OPEN FI$ FOR INPUT AS #1:COLOR 13
3540       LOCATE 14,26:PRINT"***** Reading Data File 1 ******"
3550          FOR T= 1 TO 4000:NEXT T:CLS
3560          FOR P=1 TO 38:PRINT"**";:NEXT P:PRINT:COLOR 11:PRINT
3570       PRINT " No.      Temp.     Lifetime":PRINT
3580       IF EOF(1) THEN CLOSE #1:GOTO 3620
3590          INPUT#1, X1(J),Y1A(J)
3600          PRINT TAB(3) J,X1(J),Y1A(J)
3610          J = J + 1:GOTO 3580
3620       COLOR 10:LOCATE 20,22:PRINT"   ***** End of Data 1 *****"
3630       SOUND 500,5:FOR T=1 TO 2000:NEXT T:SOUND 500,7
3640       COLOR 11
3650       LOCATE 23,16:PRINT"********* PRESS ANY KEY TO CONTINUE **********"
3660       RET$=INPUT$(1):FOR T = 1 TO 5000:NEXT T
3670 REM
3680 REM
3690 REM ******************************************************************
3700 REM ***                                                          ***
3710 REM ***               End of External Data for LINE 1             ***
3720 REM ***                                                          ***
3730 REM ******************************************************************
3740 REM ***                                                          ***
3750 REM ***          Data for LINE 2 of the Calibration Curve         ***
3760 REM ***                                                          ***
3770 REM ******************************************************************
3780 REM
3790 REM
3800       CLS:COLOR 9:LOCATE 3,6:FOR P = 1 TO 35:PRINT"**";:NEXT P:COLOR 12
3810       LOCATE 5,23:PRINT"Loading Data From an External Data File":COLOR 10
3820       LOCATE 7,10:PRINT"Do you want to inspect the files on disk? <Y or N>";
3830       A$=INPUT$(1):PRINT:PRINT:IF A$="y" OR A$="Y" THEN FILES ELSE 3890
3840       COLOR 11
3850       LOCATE 22,16:PRINT"********* PRESS ANY KEY TO CONTINUE **********"
3860       RET$=INPUT$(1):FOR T = 1 TO 5000:NEXT T
3870 REM
3880 REM
3890       L = 1:ERRORCHK = 1
3900       CLS:COLOR 9:LOCATE 3,6:FOR P = 1 TO 35:PRINT"**";:NEXT P:COLOR 12
3910       LOCATE 5,23:PRINT"Loading Data From an External Data File":COLOR 10
3920       LOCATE 7,9:PRINT "What is the filename and extension for Line 2?"
3930       COLOR 11:LOCATE 9,20:PRINT "Example:  TEST2.DAT":COLOR 10
3940       ON ERROR GOTO 6500
3950       LOCATE 11,9:INPUT"Filename:  ", FFI$
3960       OPEN FFI$ FOR INPUT AS #1:COLOR 13
3970       LOCATE 14,26:PRINT"***** Reading Data File 2  *****"
3980          FOR T= 1 TO 8000:NEXT T:CLS
3990          FOR P=1 TO 38:PRINT"**";:NEXT P:PRINT:COLOR 11:PRINT
4000       PRINT " No.      Temp.     Lifetime":PRINT
4010       IF EOF(1) THEN CLOSE #1:GOTO 4050
```

```
4020          INPUT#1, X2(L),Y2A(L)
4030           PRINT TAB(3) L,X2(L),Y2A(L)
4040       L = L + 1:GOTO 4010
4050       COLOR 10:LOCATE 20,22:PRINT"  ***** End of Data 2 *****"
4060       SOUND 500,5:FOR T=1 TO 2000:NEXT T:SOUND 500,7
4070       COLOR 11
4080       LOCATE 23,16:PRINT"********* PRESS ANY KEY TO CONTINUE **********"
4090       RET$=INPUT$(1):FOR T = 1 TO 5000:NEXT T
4100  REM
4110  REM
4120  REM ***********************************************************************
4130  REM ***                                                               ***
4140  REM ***              End of External Data for LINE 2                  ***
4150  REM ***                                                               ***
4160  REM ***********************************************************************
4170  REM ***                                                               ***
4180  REM ***              Printing out the data read in from a file        ***
4190  REM ***              and setting up the date verification menu.       ***
4200  REM ***                                                               ***
4210  REM ***********************************************************************
4220  REM
4230  REM
4240       N1 = J-1:N2 = L-1
4250       CLS:COLOR 9:LOCATE 3,6:FOR P = 1 TO 35:PRINT"**";:NEXT P
4260          LOCATE 4,6:FOR P = 1 TO 35:PRINT"**";:NEXT P:COLOR 12
4270          LOCATE 9,15:PRINT "EXTERNAL DATA VERIFICATION":COLOR 11
4280          LOCATE 13,15:PRINT "Select an option:":COLOR 11
4290          LOCATE 15,20:PRINT "1.) Continue with calculations"
4300          LOCATE 16,20:PRINT "2.) Verify Line 1 data on the screen"
4310          LOCATE 17,20:PRINT "3.) Verify Line 2 data on the screen"
4320          LOCATE 18,20:PRINT "4.) Print both data files on the printer"
4330          LOCATE 19,20:PRINT "5.) Quit the program":COLOR 10
4340          LOCATE 22,15:PRINT" What is your selection?":P$=INPUT$(1)
4350       IF INSTR("12345",P$) THEN I = VAL(P$) ELSE 4340
4360       ON ERROR GOTO 4370
4370       ON I GOTO 4920,4400,4550,4710,940
4380  REM
4390  REM
4400  REM ***********************************************************************
4410  REM ***                                                               ***
4420  REM ***              Line 1 data printed to the screen                ***
4430  REM ***                                                               ***
4440  REM ***********************************************************************
4450  REM
4460  REM
4470       CLS:COLOR 10
4480       PRINT TAB(21)"******  DATA FOR LINE 1  ******":PRINT:PRINT
4490       N1 = J-1:N2 = L-1:COLOR 11
4500       FOR N = 1 TO N1:PRINT"Temp. =";X1(N),"Lifetime = ";Y1A(N):NEXT N
4510       PRINT:PRINT:PRINT"End of Data":COLOR 12
4520       LOCATE 22,16:PRINT"********* PRESS ANY KEY TO CONTINUE **********"
```

```
4530      RET$=INPUT$(1):FOR T = 1 TO 5000:NEXT T:GOTO 4180
4540 REM
4550 REM
4560 REM ***************************************************************
4570 REM ***                                                         ***
4580 REM ***              Line 2 data printed to the screen          ***
4590 REM ***                                                         ***
4600 REM ***************************************************************
4610 REM
4620 REM
4630      CLS:COLOR 10
4640      PRINT TAB(21) "******  DATA FOR LINE 2  ******":PRINT:PRINT
4650      N1 = J-1:N2 = L-1:COLOR 11
4660      FOR M = 1 TO N2:PRINT"Temp. =";X2(M),"Lifetime = ";Y2A(M)
4670      NEXT M:PRINT:PRINT:PRINT"End of Data":COLOR 12
4680      LOCATE 22,16:PRINT"********* PRESS ANY KEY TO CONTINUE **********"
4690      RET$=INPUT$(1):FOR T = 1 TO 5000:NEXT T:GOTO 4180
4700 REM
4710 REM
4720 REM ***************************************************************
4730 REM ***                                                         ***
4740 REM ***      Printing the data for Lines 1 and 2 to the line printer ***
4750 REM ***                                                         ***
4760 REM ***************************************************************
4770 REM
4780 REM
4790      LPRINT:LPRINT:
4800      LPRINT"Raw Data for Calibration Line 1 and Line 2":LPRINT:LPRINT
4810      N1 = J:N2 = L
4820        FOR N = 1 TO N1-1:LPRINT"Temp. =";X1(N),"Lifetime = ";Y1A(N):NEXT N
4830        FOR M = 1 TO N2-1:LPRINT"Temp. =";X2(M),"Lifetime = ";Y2A(M)
4840      NEXT M:LPRINT:LPRINT:LPRINT"End of Data":GOTO 4180
4850 REM
4860 REM
4870 REM ***************************************************************
4880 REM ***                                                         ***
4890 REM ***                                                         ***
4900 REM ******************* PROGRAM CALCULATIONS    ********************
4910 REM ***                                                         ***
4920 REM ***            Calculating least-fit values and constants   ***
4930 REM ***                                                         ***
4940 REM ***************************************************************
4950 REM
4960 REM
4970      FOR A = 1 TO N1:LET Y1(A) = LOG(Y1A(A)):NEXT A
4980      FOR A = 1 TO N2:LET Y2(A) = LOG(Y2A(A)):NEXT A
4990 REM
5000 REM
5010 REM ***************************************************************
5020 REM ***                                                         ***
5030 REM ***              Performing calculations for the Line 1     ***
```

```
5040  REM ***                                                              ***
5050  REM ********************************************************************
5060  REM
5070  REM
5080        XSUM = 0:YSUM = 0:XXSUM = 0:YYSUM = 0:XYSUM = 0
5090        FOR A = 1 TO N1
5100           XSUM = X1(A) + XSUM
5110           YSUM = Y1(A) + YSUM
5120           XX(A) = X1(A) * X1(A):XXSUM = XX(A) + XXSUM
5130           YY(A) = Y1(A) * Y1(A):YYSUM = YY(A) + YYSUM
5140           XY(A) = X1(A) * Y1(A):XYSUM = XY(A) + XYSUM
5150        NEXT A
5160  REM
5170  REM ********************************************************************
5180  REM ***                                                              ***
5190  REM ***          Calculating linear regression parameters for Line 1  ***
5200  REM ***                                                              ***
5210  REM ********************************************************************
5220  REM
5230        M1 = (N1*XYSUM - XSUM*YSUM)/(N1*XXSUM - XSUM*XSUM)
5240        B1 = (YSUM*XXSUM - XSUM*XYSUM)/(N1*XXSUM - XSUM*XSUM)
5250  REM
5260  REM ********************************************************************
5270  REM ***                                                              ***
5280  REM ***              End of calculations for Line 1                  ***
5290  REM ***                                                              ***
5300  REM ********************************************************************
5310  REM
5320  REM
5330  REM
5340  REM ********************************************************************
5350  REM ***                                                              ***
5360  REM ***          Performing calculations for the Line 2              ***
5370  REM ***                                                              ***
5380  REM ********************************************************************
5390  REM
5400        XSUM = 0:YSUM = 0:XXSUM = 0:YYSUM = 0:XYSUM = 0
5410        FOR A = 1 TO N2
5420           XSUM = X2(A) + XSUM
5430           YSUM = Y2(A) + YSUM
5440           XX(A) = X2(A) * X2(A):XXSUM = XX(A) + XXSUM
5450           YY(A) = Y2(A) * Y2(A):YYSUM = YY(A) + YYSUM
5460           XY(A) = X2(A) * Y2(A):XYSUM = XY(A) + XYSUM
5470        NEXT A
5480  REM
5490  REM ********************************************************************
5500  REM ***                                                              ***
5510  REM ***          Calculating linear regression parameters for Line 1  ***
5520  REM ***                                                              ***
5530  REM ********************************************************************
5540  REM
```

```
5550      M2 = (N2*XYSUM - XSUM*YSUM)/(N2*XXSUM - XSUM*XSUM)
5560      B2 = (YSUM*XXSUM - XSUM*XYSUM)/(N2*XXSUM - XSUM*XSUM)
5570 REM
5580 REM ***************************************************************
5590 REM ***                                                        ***
5600 REM ***              End of calculations for Line 2            ***
5610 REM ***                                                        ***
5620 REM ***************************************************************
5630 REM
5640 REM ***************************************************************
5650 REM ***                                                        ***
5660 REM ***           Solving the 2x2 determinant to find          ***
5670 REM ***             the onset quenching temperature            ***
5680 REM ***                                                        ***
5690 REM ***************************************************************
5700 REM
5710 REM ***************************************************************
5720 REM ***                                                        ***
5730 REM ***            Solving for the temperature point TMP       ***
5740 REM ***                                                        ***
5750 REM ***************************************************************
5760 REM
5770      TMP = (B2 - B1)/(M1 - M2)
5780 REM
5790 REM ***************************************************************
5800 REM ***                                                        ***
5810 REM ***             Solving for the lifetime point LTP         ***
5820 REM ***                                                        ***
5830 REM ***************************************************************
5840 REM
5850      LTP = ((B1*-M2) - (B2*-M1))/(M1 - M2)
5860 REM
5870 REM ***************************************************************
5880 REM ***                                                        ***
5890 REM ***        Printing the results of the calculations to the screen  ***
5900 REM ***                                                        ***
5910 REM ***************************************************************
5920 REM
5930      CLS:COLOR 9:FOR T = 1 TO 5000:NEXT T
5940      FOR P=1 TO 38:PRINT"**";:NEXT P:PRINT:COLOR 26
5950         LOCATE 12,25:PRINT"Performing Calculations ...."
5960      FOR T = 1 TO 15000:NEXT T:BEEP:CLS:COLOR 9
5970      FOR P=1 TO 38:PRINT"**";:NEXT P:PRINT:COLOR 11
5980         LOCATE 4,25:PRINT"Results of the Calculations":COLOR 10
5990         LOCATE 10,15:PRINT"Thermographic Phosphor:":COLOR 13
6000         LOCATE 10,40:PRINT PHOSNAME$:COLOR 10
6010         LOCATE 12,15:PRINT "The Onset Quenching Temperature:":COLOR 13
6020         LOCATE 12,48:PRINT TMP:COLOR 10
6030         LOCATE 12,60:PRINT "degrees "+DG$:COLOR 12
6040         LOCATE 21,16:PRINT"********              ********"
6050         LOCATE 23,16:PRINT"********              ********"
```

```
6060        COLOR 11
6070        LOCATE 21,26:PRINT"Press P to print the results"
6080        LOCATE 23,26:PRINT"or any other key to continue"
6090        RET$ =INPUT$(1):IF RET$="p" OR RET$ ="P" THEN 6130
6100        BEEP:FOR T = 1 TO 1000:NEXT T:CLS:GOTO 540
6110  REM
6120  REM
6130  REM ********************************************************************
6140  REM ***                                                           ***
6150  REM ***         Printing the results of the calculations to the line printer    ***
6160  REM ***                                                           ***
6170  REM ********************************************************************
6180  REM
6190  REM
6200        CLS:COLOR 9:FOR P=1 TO 38:PRINT"**";:NEXT P:COLOR 11
6210        LOCATE 4,25:PRINT"***  PRINTING ROUTINE  ***":COLOR 26:BEEP
6220        LOCATE 11,21:PRINT"Make sure your printer is turned on!":COLOR 11
6230        LOCATE 22,16:PRINT"********* PRESS ANY KEY TO CONTINUE *********"
6240        RET$=INPUT$(1):FOR T = 1 TO 5000:NEXT T
6250        CLS:COLOR 9:FOR P = 1 TO 38:PRINT"**";:NEXT P:COLOR 26
6260        LOCATE 12,23:PRINT"Printing Data and Results...":COLOR 13
6270        FOR P = 1 TO 35:LPRINT"**";:NEXT P
6280        LPRINT:LPRINT:
6290        LPRINT TAB(4) "Thermographic Phosphor:  ";PHOSNAME$:LPRINT
6300        LPRINT TAB(4) "Data for Calibration Line 1":LPRINT
6310        FOR N=1 TO N1:LPRINT TAB(7) "Temp. =";X1(N),"Lifetime = ";Y1A(N):NEXT N
6320        LPRINT:LPRINT TAB(4) "Data for Calibration Line 2":LPRINT
6330        FOR M=1 TO N2:LPRINT TAB(7) "Temp. =";X2(M),"Lifetime = ";Y2A(M)
6340        NEXT M:LPRINT:LPRINT:LPRINT
6350        LPRINT TAB(4) "Onset Quenching Temperature: ";TMP;" degrees C":LPRINT
6360        LPRINT:FOR P = 1 TO 35:LPRINT"**";:NEXT P:LPRINT:LPRINT:LPRINT
6370        LOCATE 12,23:PRINT" Returning to Main Menu .....":GOSUB 6400
6380        GOSUB 6400:GOSUB 6400:GOTO 530
6390  REM
6400  REM ********************************************************************
6410  REM ***                                                           ***
6420  REM ***                     Timing Subroutine                     ***
6430  REM ***                                                           ***
6440  REM ********************************************************************
6450  REM
6460        FOR T = 1 TO 6000:NEXT T:BEEP:RETURN
6470        END
6480  REM
6490  REM ********************************************************************
6500  REM ***                                                           ***
6510  REM ***                 Error Trapping Subroutine                 ***
6520  REM ***                                                           ***
6530  REM ********************************************************************
6540  REM
6550        COLOR 11:PRINT:BEEP
6560        IF ERR = 53 THEN PRINT TAB(6)"The file was not found"
```

```
6570        FOR T = 1 TO 7000:NEXT T
6580        IF ERRORCHK = 0 THEN RESUME 3460
6590        IF ERRORCHK = 1 THEN RESUME 3890
6600   REM
6610   REM *************************************************************************
6620   REM ***                                                                 ***
6630   REM ***                    End of Error Trapping Subroutine             ***
6640   REM ***                                                                 ***
6650   REM *************************************************************************
6660   REM
6670        END
6680   REM
6690   REM *************************************************************************
6700   REM ***                                                                 ***
6710   REM ***                    End of Program (CALQUEN.BAS)                 ***
6720   REM ***                                                                 ***
6730   REM *************************************************************************


10        REM *************************************************************************
20        REM ***                                                                 ***
30        REM ***                    Help file for CALQUEN.BAS                    ***
40        REM ***                                                                 ***
50        REM ***        This file is linked to the main program and is used      ***
60        REM ***        specifically for help and program information.           ***
70        REM ***                                                                 ***
80        REM ***                                                                 ***
90        REM ***                         Alan R. Bugos                           ***
100       REM ***                                                                 ***
110       REM ***                  Oak Ridge National Laboratory                  ***
120       REM ***                                                                 ***
130       REM ***                         January 1989                            ***
140       REM ***                                                                 ***
150       REM *************************************************************************
160       REM ***                                                                 ***
170       REM ***                  CALHELP.BAS Version 1.00                        ***
180       REM ***                                                                 ***
190       REM *************************************************************************
200       REM ***                                                                 ***
210       REM ***                      Screen 1 Information                        ***
220       REM ***                                                                 ***
230       REM *************************************************************************
240       REM
250           CLS:COLOR 9:PRINT
260           FOR P = 1 TO 38:PRINT"**";:NEXT P:PRINT
270           FOR P = 1 TO 38:PRINT"**";:NEXT P:PRINT:PRINT:COLOR 13
280           LOCATE 5,19:PRINT "Welcome to the Help File for CALQUEN.BAS":COLOR 10
290           LOCATE 9,7:PRINT "This program was written to find the onset quenching temperature"
300           LOCATE 10,7:PRINT "of a thermographic phosphor given its calibration data curve."
310           LOCATE 12,7:PRINT
320           GOSUB 1380
```

```
330    REM
340    REM ************************************************************************
350    REM ***                                                                 ***
360    REM ***                       Screen 2 Information                      ***
370    REM ***                                                                 ***
380    REM ************************************************************************
390    REM
400        COLOR 10
410        FOR R = 22 TO 6 STEP -1:LOCATE R,1:PRINT STRING$(79,32):NEXT R
420        LOCATE 9,7:PRINT "The analysis uses a best-fit line interpolation on two lines"
430        LOCATE 10,7:PRINT "of the calibration curve.  The program will perform the linear"
440        LOCATE 11,7:PRINT "interpolation on the two lines and then determine the intersection"
450        LOCATE 12,7:PRINT "of these lines.  We define this intersection point to be the"
460        LOCATE 13,7:PRINT "onset quenching temperature of the thermographic phosphor."
470        GOSUB 1380
480    REM
490    REM ************************************************************************
500    REM ***                                                                 ***
510    REM ***                       Screen 3 Information                      ***
520    REM ***                                                                 ***
530    REM ************************************************************************
540    REM
550        COLOR 10
560        FOR R = 22 TO 6 STEP -1:LOCATE R,1:PRINT STRING$(79,32):NEXT R
570        LOCATE 9,7 :PRINT"Using this menu-driven program is rather easy.  It is recommended
580        LOCATE 10,7:PRINT"that you have the calibration curve of the thermophosphor
590        LOCATE 11,7:PRINT"available so that you may get a rough idea as to how to input the
600        LOCATE 12,7:PRINT"Line 1 and Line 2 data.  On the calibration curve, find the knee
610        LOCATE 13,7:PRINT"or breaking point and separate the two individual lines of the"
620        LOCATE 14,7:PRINT"curve from there."
630        GOSUB 1380
640    REM
650    REM ************************************************************************
660    REM ***                                                                 ***
670    REM ***                       Screen 4 Information                      ***
680    REM ***                                                                 ***
690    REM ************************************************************************
700    REM
710        COLOR 10
720        FOR R = 22 TO 6 STEP -1:LOCATE R,1:PRINT STRING$(79,32):NEXT R
730        LOCATE 9,7 :PRINT"You have the option to either input data manually or you can access
740        LOCATE 10,7:PRINT"an ASCII data (text) file from a disk.  If you input data manually,
750        LOCATE 11,7:PRINT"you will have the option to save it for later use.  Make sure the
760        LOCATE 12,7:PRINT"data are broken into two separate lines and are stored as two"
770        LOCATE 13,7:PRINT"separate files.  You also have the option to verify and print"
780        LOCATE 14,7:PRINT"data and results on a line printer.
790        GOSUB 1380
800    REM
810    REM ************************************************************************
820    REM ***                                                                 ***
830    REM ***                       Screen 5 Information                      ***
```

```
840   REM ***                                                              ***
850   REM *********************************`**********************************
860   REM
870        COLOR 10
880        FOR R = 22 TO 6 STEP -1:LOCATE R,1:PRINT STRING$(79,32):NEXT R
890        LOCATE 8,7 :PRINT"If you input your data manually, the two lines will be stored
900        LOCATE 9,7:PRINT"on the active disk as LINE1.DAT and LINE2.DAT. Make sure the
units
910        LOCATE 11,7:PRINT"are consistent, i.e. temperature in degrees C or F and lifetime are"
920        LOCATE 12,7:PRINT"all in usec or milliseconds.  Be sure to use the RENAME command"
930        LOCATE 13,7:PRINT"in DOS to rename the filenames for these lines.  An example of"
940        LOCATE 14,7:PRINT"this command is as follows:":COLOR 9
950        LOCATE 16,24:PRINT"RENAME LINE1.DAT YPO4EU1.DAT"
960        GOSUB 1380
970   REM
980   REM ********************************************************************
990   REM ***                                                              ***
1000  REM ***                  Screen 6 Information                        ***
1010  REM ***                                                              ***
1020  REM ********************************************************************
1030  REM
1040       COLOR 10
1050       FOR R = 22 TO 6 STEP -1:LOCATE R,1:PRINT STRING$(79,32):NEXT R
1060       LOCATE 9,7 :PRINT"You may also want to create external data files using EDLIN,"
1070       LOCATE 10,7:PRINT"a DOS Line Editor or a wordprocessor such as WordPerfect."
1080       LOCATE 11,7:PRINT"Make sure the wordprocessor saves the data file as a DOS text"
1090       LOCATE 12,7:PRINT"file.  Remember to create two individual data files for each"
1100       LOCATE 13,7:PRINT"line of the calibration curve."
1110       GOSUB 1380
1120  REM
1130  REM

1140  REM ********************************************************************
1150  REM ***                                                              ***
1160  REM ***                  Screen 7 Information                        ***
1170  REM ***                                                              ***
1180  REM ********************************************************************
1190  REM
1200       COLOR 10
1210       FOR R = 22 TO 6 STEP -1:LOCATE R,1:PRINT STRING$(79,32):NEXT R
1220       LOCATE 9,7 :PRINT"If you have any questions or comments concerning this program"
1230       LOCATE 10,7:PRINT"or method of onset quenching temperature analysis for thermo-
1240       LOCATE 11,7:PRINT"graphic phosphors, please contact:":COLOR 11
1250       LOCATE 13,22:PRINT"Alan R. Bugos or Stephen W. Allison":COLOR 10
1260       LOCATE 14,25:PRINT"Applied Technology Division
1270       LOCATE 15,25:PRINT"Oak Ridge National Laboratory
1280       LOCATE 16,25:PRINT"MS 7280, Building K-1220
1290       LOCATE 17,25:PRINT"Oak Ridge, Tennessee  37831
1300       LOCATE 18,25:PRINT"Phone: (615) 576-2821 or
1310       LOCATE 19,25:PRINT"      (615) 576-2726
1320       GOSUB 1380
```

```
1330        GOTO 1550
1340 REM
1350 REM
1360 REM ********************************************************************
1370 REM ***                                                            ***
1380 REM ***                    Continue Subroutine                     ***
1390 REM ***                                                            ***
1400 REM ********************************************************************
1410 REM
1420        COLOR 12
1430        LOCATE 23,20:PRINT"*****  PRESS ANY KEY TO CONTINUE  *****":COLOR 11
1440        LOCATE 23,27:PRINT"PRESS ANY KEY TO CONTINUE":RET$=INPUT$(1)
1450        BEEP:GOSUB 1490:COLOR 10:RETURN
1460 REM
1470 REM ********************************************************************
1480 REM ***                                                            ***
1490 REM ***                     Timing Subroutine                      ***
1500 REM ***                                                            ***
1510 REM ********************************************************************
1520 REM
1530        FOR T = 1 TO 2000:NEXT T:RETURN
1540 REM
1550 REM ********************************************************************
1560 REM ***                                                            ***
1570 REM ***          Linking the help routine back to the Main Program ***
1580 REM ***                                                            ***
1590 REM ********************************************************************
1600 REM
1610        CLS:COLOR 30
1620        LOCATE 12,25:PRINT" Returning to the main program ...."
1630        COMMON ALL:CHAIN "calquen.bas",400:END
1640 REM
1650 REM ********************************************************************
1660 REM ***                                                            ***
1670 REM ***                End of Program (CALHELP.BAS)                ***
1680 REM ***                                                            ***
1690 REM ********************************************************************
```

VITA

Alan Ronald Bugos was born in Pittsburgh, Pennsylvania on January 15, 1960 to Ronald and Shirley Bugos. After graduating from Oak Ridge High School, Oak Ridge,Tennessee in 1978, he attended the University of Tennessee at Knoxville, enrolled in the Engineering Physics Department. In 1982 and 1983, he won first place awards for engineering research projects entered in Engineer's Day competition. He received his Bachelor of Science degree in Engineering Physics in June of 1983.

Upon graduation, he entered the United States Peace Corps and served as a volunteer in Fiji , a small island country in the South Pacific. During his two year stay in Fiji, he taught Physics and Appropriate Technology at a rural Fijian secondary school and was involved in the construction and improvement of rural village water supplies and in the use of photovoltaics for battery charging and pumping water. He helped to implement a village technology curriculum into the Fijian school system which prepared students not going on to higher education to help improve conditions within their villages. He is fluent in the Fijian language.

Immediately following his Peace Corps experience, he returned to the United States and entered graduate school in the Department of Electrical and Computer Engineering at the University of Tennessee, Knoxville. During his studies, he served the Department as a graduate teaching assistant, teaching laboratory classes in Electro-optics, Plasma Science, and Small Computer Systems. With a strong interest in electro-optics, he wrote and published a laboratory manual for the electro-optics laboratory at UTK which he primary taught as a graduate teaching assistant. In June of 1987, he also accepted a graduate research assistantship with the Enrichment Technologies Applications Center at

the Oak Ridge National Laboratory in Oak Ridge, Tennessee where he researched thermographic phosphors for high temperature sensor applications.

He is a member of Eta Kappa Nu, the Institute of Electrical and Electronic Engineers, the American Institute of Aeronautics and Astronautics, the Society of Photo-Optical Instrumentation Engineers, and the American Solar Energy Society.